THE

LONDON, EDINBURGH, AND DUBLIN

PHILOSOPHICAL MAGAZINE

AND

JOURNAL OF SCIENCE.

[SEVENTH SERIES.]

OCTOBER 1932.

LXII. *The Viscosity of Strong Electrolyte Solutions according to Electrostatic Theory.* *By* H. FALKENHAGEN, *University of Cologne, Germany, and* E. L. VERNON, *Department of Physical Chemistry, University of Wisconsin, Madison, Wisconsin* *.

1. INTRODUCTION.

EXPERIMENTAL work has been done on the viscosity of solutions of strong electrolytes, but in much of it the concentrations have been too high for consideration according to the Debye theory. An account of some of the earlier work has been given by Jones and Dole †, who also determined empirically from their own measurements that the relative viscosity $\frac{\eta_\gamma}{\eta_0}$ of solutions of strong electrolytes depends on the concentration as follows:

$$\frac{\eta_\gamma}{\eta_0} = 1 + A\sqrt{\gamma} + B\gamma, \quad . \quad . \quad . \quad . \quad . \quad (1)$$

where η_γ is the coefficient of viscosity at molar concentration, γ, η_0 is the coefficient of viscosity at zero concentration, and A and B are constant for a given electrolyte.

This work suggested ‡ the development of a formula for

* Communicated by Professor P. Debye.

† G. Jones and M. Dole, J. A. C. S. li. p. 2950 (1929).

‡ H. Falkenhagen and M. Dole, *Zs. f. Physik. Chem.* B. vi. p. 159 (1929).

the constant A from electrostatic theory. This was done successfully for the very special case of binary electrolytes with ions of equal mobilities *. Later Falkenhagen extended the discussion, giving the solution for the general case and applying it to the special case of binary electrolytes †. This paper will give the connexion between the problem of viscosity and the general case of electrolyte solutions, will outline the solution of the problem, and will apply the solution to the general case of any electrolyte.

2. Statement of the Problem.

In a solution of an electrolyte which is completely dissociated the ions are not distributed entirely at random, as in the case of neutral particles such as are treated in the kinetic theory of an ideal gas. There is instead an ionic "atmosphere" around each ion which is composed of ions of all types and is equal to and opposite in charge to the charge of the central ion. Or, due to Coulomb forces of interionic attraction, there is always a greater probability of finding an ion of opposite charge at a certain distance from the central ion than of finding an ion of like charge at the same distance from the central ion. As the ion is inseparable from its atmosphere, in problems involving ionic forces it is necessary to determine a function which will represent the distribution of ions around a central ion.

In this problem of viscosities, as in all problems concerning strong electrolytes, we shall obtain such a distribution function, f_{ij}, which indicates the distribution of ions of type j in the vicinity of an ion of type i. How will the lamellar velocities affect this distribution of the ions? In viscosity problems we consider the liquid moving along parallel planes, always in the same direction, with the velocity along each plane proportional to the distance from some fixed plane. The motion in each plane relative to adjoining planes exerts a shearing force per unit area of amount η_0 times the gradient of velocity measured in a direction perpendicular to the planes. This quantity η_0 is the coefficient of viscosity of the pure liquid ‡. When the liquid contains a dissolved electrolyte there will be added to the original shearing force

* H. Falkenhagen and M. Dole, *Physik. Z.* xxx. p. 611 (1929).

† H. Falkenhagen, *Physik. Z.* xxxii. p. 745 (1931).

‡ It is of interest to note that the theoretical problem of viscosity of pure liquids has been attempted many times by mathematicians and physicists, but because of a lack of knowledge of the forces between the particles of the liquid it has never been solved.

another force due to distortion of the ionic atmosphere, which is what we must calculate.

The distribution functions f_{ij} can be related to the velocities by the continuity equation in the sense of hydrodynamics and solved as a function of space coordinates proportional to the velocity gradient. The electric densities, Π_i, the functions representing distribution of electric charge, may be expressed in terms of the distribution functions f_{ij}, and the shearing forces involved in distortion of equilibrium configurations may be calculated. The components of all the forces exerted on the ions, acting on one square centimetre parallel to the planes of shear, will be shown to be equal to a constant times the velocity gradient. This constant is, by the definition of viscosity, the correction due to ionic attraction which must be added to the coefficient of viscosity, η_0, of the pure solvent.

First we shall discuss the distribution functions f_{ij}, showing how they may be derived and indicating their significance in other problems.

3. The Distribution Functions f_{ij}.

(a) *Special Case of Random Distribution.*

Take the elements of volume dS_P and dS_Q at the points $P(x_P, y_P, z_P)$ and $Q(x_Q, y_Q, z_Q)$ fixed in space and consider ions of types $1 \ldots i \ldots s$ of concentrations $n_1 \ldots n_i \ldots n^s$ expressed in ions per cubic centimetre. If t_i is the time an ion of type i is in dS_P during the total time t, the probability of finding an ion of type i in dS_P during the time t is

$$\frac{t_i}{t} = n_i \, dS_P. \quad . \quad . \quad . \quad . \quad . \quad . \quad (2)$$

Similarly the probability of finding an ion of type j in dS_Q during the time t is

$$\frac{t_j}{t} = n_j \, dS_Q. \quad . \quad . \quad . \quad . \quad . \quad . \quad (2')$$

The probability of the event of an ion of type i being in dS_P at the same time that an ion of type j is in dS_Q is then the product of the probabilities (2) and (2'). If t_{ij} is the interval of time during the time t when an ion i is in dS_P while an ion j is in dS_Q, the probability is

$$\frac{t_{ij}}{t} = n_i n_j \, dS_P \, dS_Q. \quad . \quad . \quad . \quad . \quad . \quad (3)$$

Write

$$f_{ij}^0 = n_i n_j, \quad . \quad . \quad . \quad . \quad . \quad . \quad . \quad (4)$$

where f_{ij}^0 is the distribution function for the ions j in the neighbourhood of an i-ion when no consideration is taken of interionic forces, or the distribution is irregular. We see from (4) the significance of the f_{ij}^0 which are thus connected with the concentrations of the ions i and j. As the system is in equilibrium, we may write

$$f_{ij}^0 = f_{ji}^0 = n_i n_j = n_j n_i. \quad . \quad . \quad . \quad . \quad . \quad (5)$$

(b) *Case of no External Forces.*

From electrostatic theory we know that a particle with a charge ϵ in a medium with dielectric constant D has around it an electric field for which the potential ψ at a point a distance r from the charge is

$$\psi = \frac{1}{D}\frac{\epsilon}{r}. \quad . \quad . \quad . \quad . \quad . \quad . \quad . \quad . \quad (6)$$

If the medium is a liquid in which are distributed the ions of an electrolyte, the potential ψ_i^{I} which the ionic atmosphere of an i-ion of charge e_i in $d\mathrm{S_P}$ produces upon ions of type j in $d\mathrm{S_Q}$ may be obtained by application of the Poisson equation and the Maxwell-Boltzmann principle. The potential ψ_i^{I} results in an electric field strength $\mathbf{E}_i$ at $d\mathrm{S_Q}$ which is defined by

$$\mathbf{E}_i = -\frac{d\psi_i^{\mathrm{I}}}{dr}, \quad . \quad . \quad . \quad . \quad . \quad . \quad . \quad (7)$$

or more completely,

$$\mathbf{E}_i = -\mathrm{grad}_{\mathrm{Q}}\,\psi_i^{\mathrm{I}} = -\left(\mathbf{i}\frac{\partial}{\partial x_{\mathrm{Q}}} + \mathbf{j}\frac{\partial}{\partial y_{\mathrm{Q}}} + \mathbf{k}\frac{\partial}{\partial z_{\mathrm{Q}}}\right)\psi_i^{\mathrm{I}}. \quad (7')$$

The electric forces are

$$\mathbf{K}_i = e_j\mathbf{E}_i = -e_j\,\mathrm{grad}_{\mathrm{Q}}\,\psi_i^{\mathrm{I}}, \quad . \quad . \quad . \quad . \quad (8)$$

$$\mathbf{K}_j = e_i\mathbf{E}_j = -e_i\,\mathrm{grad}_{\mathrm{P}}\,\psi_j^{\mathrm{I}}, \quad . \quad . \quad . \quad . \quad (8')$$

where $\mathbf{K}_i$ resp. $\mathbf{K}_j$ are the forces exerted by i-ions resp. j-ions upon j-ions resp. i-ions. The collection of charges sets up an electric field, and if we consider all points in this field having the same potential, an equipotential surface is formed. By Gauss's theorem the flux through an element of area $d\sigma$ is the total charge times $d\omega$ divided by the dielectric constant of the medium where $d\omega$ is an element of solid angle. The total flux through the whole surface is the integral of this, or 4π times the total quantity of electricity within the

surface divided by the dielectric constant. If we apply this theorem to an element of volume, we obtain

$$\begin{aligned}\mathrm{div}_Q \mathbf{E}_i &= -\mathrm{div}_Q \,\mathrm{grad}_Q \psi_i^{\mathrm{I}} = -\nabla_Q^2 \psi_i^{\mathrm{I}} \\ &= -\left(\frac{\partial^2}{\partial x_Q^2} + \frac{\partial^2}{\partial y_Q^2} + \frac{\partial^2}{\partial z_Q^2}\right)\psi_i^{\mathrm{I}} = \frac{4\pi}{\mathrm{D}}\Pi_i.\end{aligned}$$

This leads to the familiar form of Poisson's differential equations

$$\nabla_Q^2 \psi_i^{\mathrm{I}} = -\frac{4\pi}{\mathrm{D}}\Pi_i, \quad \ldots\ldots (9)$$

$$\nabla_P^2 \psi_j^{\mathrm{I}} = -\frac{4\pi}{\mathrm{D}}\Pi_j, \quad \ldots\ldots (9')$$

where Π_i is the density of charges around an ion of type i.

From the section on irregular distribution we can write, for an ion of type i, the density of electric charges due to ions of type j as

$$\pi_j = n_j e_j = \frac{n_i n_j}{n_i} e_j = \frac{f_{ij}^0}{n_i} e_j. \quad \ldots\ldots (10)$$

Equation (10) gives us an indication of the correct form, which we may write

$$\pi_j = \frac{f_{ij}^{\mathrm{I}}}{n_i} e_j, \quad \ldots\ldots (11)$$

where f_{ij}^{I} is the function showing distribution of ions of type j in the vicinity of an ion of type i when interionic forces are included, but there are no external forces. Then the density in the neighbourhood of ions of type i for ions of all types is

$$\Pi_i = \sum_j \pi_j = \frac{1}{ni} \sum_j f_{ij}^{\mathrm{I}} e_j, \quad \ldots\ldots (12)$$

and that the density in the neighbourhood of ions of type j is

$$\Pi_j = \sum_i \pi_i = \frac{1}{n_j} \sum_i f_{ji}^{\mathrm{I}} e_i. \quad \ldots\ldots (12')$$

Poisson's equations become

$$\nabla_Q^2 \psi_i^{\mathrm{I}} = -\frac{4\pi}{\mathrm{D}} \frac{1}{n_i} \sum_j f_{ij}^{\mathrm{I}} e_j, \quad \ldots\ldots (13)$$

$$\nabla_P^2 \psi_j^{\mathrm{I}} = -\frac{4\pi}{\mathrm{D}} \frac{1}{n_j} \sum f_{ji}^{\mathrm{I}} e_i. \quad \ldots\ldots (13')$$

It is now necessary to determine how the distribution functions f_{ij}^0 are modified by the potential ψ_i^{I}. With no interionic forces, when an ion of type i is in $d\mathrm{S_P}$, the chances of ions of types i or j entering $d\mathrm{S_Q}$ depend only upon the numbers of each type present. But ions of type i have an ionic atmosphere producing the potential ψ_i^{I}. The work necessary to bring a j-ion from infinity to $d\mathrm{S_Q}$ is then $e_j\psi_i^{\mathrm{I}}$, while an ion of type i requires the potential energy $e_i\psi_j^{\mathrm{I}}$ to be brought from infinity to $d\mathrm{S_P}$. According to the Boltzmann principle the ionic distribution f_{ij}^{I} of j-ions in $d\mathrm{S_Q}$ near an i-ion depends upon the exponential of the ratio of potential energy $-e_j\psi_i^{\mathrm{I}}$ to $k\mathrm{T}$, and similarly for i-ions. Then we have

$$f_{ij}^{\mathrm{I}} = \mathrm{B}_i e^{-\frac{e_j\psi_i^{\mathrm{I}}}{k\mathrm{T}}}, \quad f_{ji}^{\mathrm{I}} = \mathrm{B}_j e^{-\frac{e_i\psi_j^{\mathrm{I}}}{k\mathrm{T}}}, \quad . \quad . \quad (14)$$

where k is the Boltzmann constant ($k = 1{\cdot}37 \times 10^{-16}$ ergs/degree), T is the absolute temperature, and B_i and B_j are quantities which must yet be evaluated.

When interionic forces do not act, or as $\psi_i^{\mathrm{I}} \to 0$, $f_{ij}^{\mathrm{I}} \to f_{ij}^0$, then

$$\lim_{\psi_i^{\mathrm{I}} \to 0} f_{ij}^{\mathrm{I}} = \lim_{\psi_i^{\mathrm{I}} \to 0} \mathrm{B}_i e^{-\frac{e_j\psi_i^{\mathrm{I}}}{k\mathrm{T}}} = f_{ij}^0 = \mathrm{B}_i = n_i n_j.$$

Similarly

$$\mathrm{B}_j = n_j n_i,$$

and we have

$$f_{ij}^{\mathrm{I}} = n_i n_j e^{-\frac{e_j\psi_i^{\mathrm{I}}}{k\mathrm{T}}}, \quad f_{ji}^{\mathrm{I}} = n_j n_i e^{-\frac{e_i\psi_j^{\mathrm{I}}}{k\mathrm{T}}} \quad . \quad . \quad . \quad (15)$$

When the concentrations are taken as small, we may write a series approximation for the exponentials in (15) and obtain

$$f_{ij}^{\mathrm{I}} = n_i n_j \left(1 - \frac{e_j\psi_i^{\mathrm{I}}}{k\mathrm{T}}\right), \quad . \quad . \quad . \quad . \quad (16)$$

$$f_{ji}^{\mathrm{I}} = n_j n_i \left(1 - \frac{e_i\psi_j^{\mathrm{I}}}{k\mathrm{T}}\right). \quad . \quad . \quad . \quad . \quad (16')$$

Placing (16) and (16′) in the Poisson equations (13) and (13′), we have

$$\nabla_{\mathrm{Q}}^2\psi_i^{\mathrm{I}} = -\frac{4\pi}{\mathrm{D}}\frac{1}{n_i}\sum_j f_{ij}^{\mathrm{I}} e_j = -\frac{4\pi}{\mathrm{D}}\sum_j n_j e_j + \frac{4\pi}{\mathrm{D}k\mathrm{T}}\sum_j n_j e_j^2 \psi_i^{\mathrm{I}}, \quad . \quad . \quad . \quad (17)$$

$$\nabla_{\mathrm{P}}^2\psi_j^{\mathrm{I}} = -\frac{4\pi}{\mathrm{D}}\frac{1}{n_j}\sum_i f_{ji}^{\mathrm{I}} e_i = -\frac{4\pi}{\mathrm{D}}\sum_i n_i e_i + \frac{4\pi}{\mathrm{D}k\mathrm{T}}\sum_i n_i e_i^2 \psi_j^{\mathrm{I}}. \quad . \quad . \quad . \quad (17')$$

Since

$$\sum_j n_j e_j = 0$$

is the condition for electric neutrality in the solution as a whole, we have for ψ_i^{I} from (17) and (17′)

$$\nabla_{\mathrm{Q}}^2 \psi_i^{\mathrm{I}} = \kappa^2 \psi_i^{\mathrm{I}} : \nabla_{\mathrm{P}}^2 \psi_j^{\mathrm{I}} = \kappa^2 \psi_j^{\mathrm{I}}, \quad . \quad . \quad (18)$$

where

$$\kappa^2 = \frac{4\pi}{\mathrm{D}\,k\mathrm{T}} \sum_j n_j e_j^2. \quad . \quad . \quad . \quad . \quad . \quad (19)$$

These equations (18) are the fundamental equations of Debye and Hückel *, who gave as solutions

$$\psi_i^{\mathrm{I}} = \frac{e_i}{\mathrm{D}} \frac{e^{-\kappa r}}{r} : \quad \psi_j^{\mathrm{I}} = \frac{e_j}{\mathrm{D}} \frac{e^{-\kappa r}}{r}. \quad . \quad . \quad . \quad (20)$$

The quantity $\frac{1}{\kappa}$ defined in (19) is that property of the ionic atmosphere which is said to describe the "thickness," $\frac{1}{\kappa}$ having the dimensions of length. It is a measure of the distance from the ion at which the potential has decreased nearly to $1/e$ of its value as a result of the surrounding atmosphere, and is thus a probable distance which varies with the square root of the concentration in the case of a simple electrolyte.

If we make use of equations (20), the final form for the distribution functions f_{ij}^{I} from (16) and (16′) is the expression

$$f_{ij}^{\mathrm{I}} = n_i n_j \left(1 - \frac{e_i e_j}{\mathrm{D}\,k\mathrm{T}} \frac{e^{-\kappa r}}{r}\right), \quad f_{ij}^{\mathrm{I}} = f_{ji}^{\mathrm{I}}. \quad . \quad (21)$$

The functions f_{ij}^{I} represent a "probability density," a probable distribution of ions in the ionic atmosphere when the only forces are interionic. This expression (21) and (16) and (16′) are important in any problem of strong electrolytes. The correctness of this expression has been shown by Fowler † and by Kramers ‡, who started from the phase integral representing the distribution of all particles in the solution according to the Maxwell-Boltzmann statistical interpretation. Kramers was able to calculate this state integral approximately and obtained the same expression for dilute solutions as that of Debye and Hückel.

* P. Debye and E. Hückel, *Physik. Z.* xxiv. pp. 185, 305 (1923).
† R. H. Fowler, Trans. Far. Soc. xxiii. p. 434 (1927).
‡ H. A. Kramers, Proc. Amsterdam, xxx. p. 145 (1927).

Fowler determined the complete conditions necessary for a rigorous solution of the problem from the interpretation of Debye and Hückel. However derived, the equations hold for low concentrations only, for at high concentrations the ions forming the atmosphere are sufficiently near to the central ion to make the series approximation of the exponential incorrect. The potential ψ_i^{I} is large when very close to the central ion, but as it decreases inversely with the distance and the volume increases with the third power of the distance there is a limiting distance from the central ion beyond which (16) is an excellent approximation. This distance can be calculated from potential theory or more readily from the work of Kramers †, and the maximum concentration of electrolyte which does not force the ions within this distance may be determined ‡.

The equation (21) was first developed by Debye and Hückel, who used it in their original discussions of the problem of electrolyte solutions. Later Onsager § and Debye and Falkenhagen || used the equation in calculating conductivity effects and the dispersion of conductivity.

(c) *General Case with External Disturbances.*

We have now determined distribution functions for two cases: random arrangement with no forces and distribution due to electrostatic forces only. It is readily seen from equations (16) and (16′) that the functions f_{ij}^0 are dominant, for we may write accurately

$$f_{ij}^{\mathrm{I}} = f_{ij}^0 + f_{ij}^*, \quad \ldots\ldots \quad (22)$$

where f_{ij}^* is a very small correction factor. This factor is small because it depends upon the potential which, though very large when close to the central ion, decreases rapidly at distances at which other ions will be found. Similarly we can write for the distribution functions f_{ij}, the functions

† H. Falkenhagen, Rev. of Mod. Phys. iii. p. 412 (1931); H. Falkenhagen (monograph 'Electrolyte'): S. Hirzel, Leipzig (1932). The English translation will appear in the series of monographs edited by Prof. R. H. Fowler (Cambridge, England).

‡ Although a theory of more concentrated solutions has been attempted many times, the exact theory has not yet been developed. There are forces between the particles making up the solution which are not only of electrostatic nature but of quantum mechanic nature. A solution of this problem would be particularly important in the field of non-aqueous solutions.

§ L. Onsager, *Physik. Z.* xxvii. p. 388 (1926); *ibid.* xxviii. p. 277 (1927).

|| P. Debye and H. Falkenhagen, *Physik. Z.* xxix. p. 401 (1928).

expressing density when there are external disturbances in addition to interionic forces,

$$f_{ij} = f_{ij}^{\mathrm{I}} + g_{ij}. \quad . \quad . \quad . \quad . \quad . \quad . \quad (23)$$

These functions f_{ij} are those with which we are concerned.

The potential in this general case will be

$$\psi_i = \psi_i^{\mathrm{I}} + \psi_i', \quad . \quad . \quad . \quad . \quad . \quad . \quad (24)$$

where ψ_i' indicates the change in potential of the atmosphere of an i-ion caused by external forces. We have shown above the interrelation of potential and distribution function, so from (13)

$$\nabla_{\mathrm{Q}}^2 \psi_i = -\frac{4\pi}{\mathrm{D}} \frac{1}{n_i} \sum_j f_{ij} e_j, \quad . \quad . \quad . \quad . \quad (25)$$

and from (23), (24), and (25) we obtain

$$\nabla_{\mathrm{Q}}^2 \psi_i' = -\frac{4\pi}{\mathrm{D}} \frac{1}{n_i} \sum_j g_{ij} e_j. \quad . \quad . \quad . \quad . \quad (26)$$

As the distribution functions represent densities, they have to satisfy the general continuity equation of hydrodynamics,

$$\frac{\partial \delta}{\partial t} = -\mathrm{div}\,(\delta \mathbf{v}), \quad . \quad . \quad . \quad . \quad . \quad (27)$$

where δ is density and $\mathbf{v}$ is velocity. Let $\mathbf{v}_i$ and $\mathbf{v}_j$ be the velocities of i- and j-ions in the vicinity of j- and i-ions. Then (27) becomes

$$\frac{\partial f_{ij}}{\partial t} = -[\mathrm{div}_{\mathrm{P}}\,(f_{ji}\mathbf{v}_i) + \mathrm{div}_{\mathrm{Q}}\,(f_{ij}\mathbf{v}_j)]. \quad . \quad . \quad (28)$$

But, as this is a stationary case,

$$\frac{\partial f_{ij}}{\partial t} = 0,$$

and (28) becomes

$$-[\mathrm{div}_{\mathrm{P}}\,(f_{ji}\mathbf{v}_i) + \mathrm{div}_{\mathrm{Q}}\,(f_{ij}\mathbf{v}_j)] = 0. \quad . \quad . \quad (29)$$

The velocities of the ions result from forces which may be separated into their several components. If we take v_0 as the absolute velocity of i-ions at $d\mathrm{S}_{\mathrm{P}}$, their actual velocity will include the term $\mathbf{i}v_0$, where $\mathbf{i}$ is a unit vector parallel to the x-axis (fig. 1). The velocity of the j-ions then contains the fundamental term $\mathbf{i}[v_0 + b(z_{\mathrm{Q}} - z_{\mathrm{P}})]$, where the factor $b(z_{\mathrm{Q}} - z_{\mathrm{P}})$ represents the excess of velocity of j-ions over that of i-ions as a result of position in $d\mathrm{S}_{\mathrm{Q}}$. b is a measure of

velocity gradient which is measured in the direction of the z-axis (fig. 2) ; but there must also be terms dependent on the velocity of the solvent. The velocity of i-ions will be increased by a term $\mathbf{i}(v_s - v_0)$, where the factor $(v_s - v_0)$ indicates the change of velocity of i-ions in $d\mathrm{S_P}$ from the

Fig. 1.

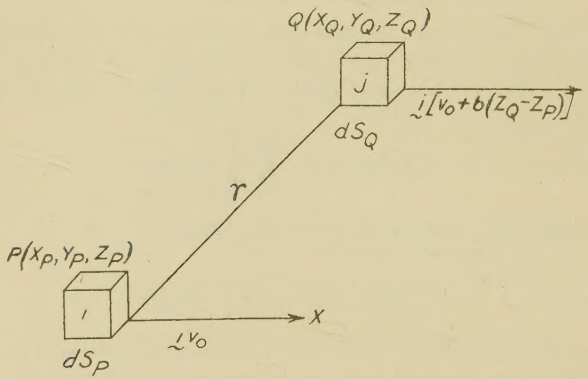

Fig. 2.

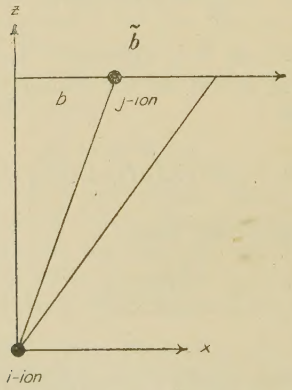

Velocity gradient. $\tilde{b}$, solvent; b, ion.

absolute velocity v_0 to the absolute velocity of the solvent v_s at the same point. Similarly the velocity of j-ions in $d\mathrm{S_Q}$ will have an additional term,

$$\mathbf{i}\{[v_s+\tilde{b}(z_\mathrm{Q}-z_\mathrm{P})]-[v_0+b(z_\mathrm{Q}-z_\mathrm{P})]\}$$
$$=\mathbf{i}[v_s-v_0+(\tilde{b}-b)(z_\mathrm{Q}-z_\mathrm{P})].$$

Here $\tilde{b}$ is a measure of the additional velocity gradient due to motion of the solvent (fig. 2) and b has the same significance as above.

There is a diffusion of ions for which the constant is known. In the case of i-ions this will be $\frac{kT}{\rho_i}$, where k is Boltzmann's constant, T is the absolute temperature, and ρ_i is a known frictional constant. ρ_i is a quantity of which the reciprocal is the mobility of the ion and which is related to the ionic molar conductance $\bar{L}_i$ through the equation

$$\frac{1}{\rho_i} = u_i = \frac{\bar{L}_i}{15{\cdot}34\, z_i^2} \times 10^8 \text{ *}, \quad . \quad . \quad . \quad . \quad (30)$$

* We have

$$e_i E = \rho_i v_i$$

as a balance of electric and frictional forces, where e_i is charge on an i-ion, E is electric field strength, and v_i is velocity, or

$$v_i = \frac{e_i E}{\rho_i}.$$

Then the current density

$$i = \sum_{i=1}^{s} n_i e_i v_i = \sum_{i=1}^{s} n_i \frac{e_i^2 E}{\rho_i}$$

and the specific conductance (in $\text{ohm}^{-1}\,\text{cm.}^{-1}$)

$$\lambda = \frac{\lambda\ (\text{e.s.u.})}{9\times10^{11}} = \sum_{i=1}^{s} \frac{n_i e_i^2}{\rho_i} \frac{1}{9\times10^{11}}.$$

Since

$$n_i = N\gamma \frac{\nu_i}{1000},$$

where $N = 6{\cdot}06\times10^{23}$, γ is molar concentration, ν_i is the dissociation number of an ion i, and z_i is the numerical value of the valence of an i-ion,

$$\lambda = \frac{1}{9\times10^{11}} \frac{N\epsilon^2}{1000} \gamma \sum_{i=1}^{s} \frac{\nu_i z_i^2}{\rho_i}.$$

The molar conductance at infinite dilution

$$\Lambda_\infty = \frac{1000\lambda}{\gamma} = \frac{1}{9\times10^{11}} N\epsilon^2 \sum_{i=1}^{s} \frac{\nu_i z_i^2}{\rho_i} = \sum_{i=1}^{s} \nu_i \bar{L}_i,$$

where the molar ionic conductance at infinite dilution

$$\bar{L}_i = \frac{1}{9\times10^{11}} N \frac{\epsilon^2 z_i^2}{\rho_i},$$

and ϵ is the unit charge ($\epsilon = 4{\cdot}77\times10^{-10}$). Then

$$\frac{1}{\rho_i} = u_i = \frac{\bar{L}_i}{N\epsilon^2 z_i^2} 9\times10^{11} = \frac{\bar{L}_i}{15{\cdot}34\, z_i^2} \times 10^8.$$

where $\bar{L}_i$ is the molar ionic conductance at infinite dilution, $\Lambda_x = \sum_i \nu_i L_i$, z_i is the numerical value of the valence of an i-ion, and u_i is the mobility. The diffusion depends upon the position in such a manner that the modifications of velocity will be, according to Fick's law *,

$$-\frac{kT}{\rho_i f_{ji}} \mathrm{grad}_P f_{ji} \quad \text{and} \quad -\frac{kT}{\rho_j f_{ij}} \mathrm{grad}_Q f_{ij}.$$

There are also the forces $\mathbf{K}_i$ and $\mathbf{K}_j$, defined in (8) and (8′) which affect the velocities by the terms $\frac{\mathbf{K}_j}{\rho_i}$ and $\frac{\mathbf{K}_i}{\rho_j}$.

Then the velocities of the ions are

$$\mathbf{v}_i = \frac{1}{\rho_i}\left[\mathbf{K}_j - \frac{kT}{f_{ji}} \mathrm{grad}_P f_{ji}\right] + \mathbf{i}v_0 + \mathbf{i}(v_s - v_0), \quad . \quad . \quad . \quad . \quad (31)$$

$$\mathbf{v}_j = \frac{1}{\rho_j}\left[\mathbf{K}_i - \frac{kT}{f_{ij}} \mathrm{grad}_Q f_{ij}\right] + \mathbf{i}[v_0 + b(z_Q - z_P)] + \mathbf{i}[v_s - v_0 + (\tilde{b} - b)(z_Q - z_P)]. \quad (31')$$

If, for convenience, we take only the first term of (29) and substitute (31), making use of (8′),

$$\mathrm{div}_P(f_{ji}\mathbf{v}_i) = -\frac{1}{\rho_i} \mathrm{div}_P[e_i f_{ji} \mathrm{grad}_P \psi_j + kT \mathrm{grad}_P f_{ji}] + \mathrm{div}_P[f_{ji}, \mathbf{i}v_0 + \mathbf{i}(v_s - v_0)].$$

But f_{ji} enters here in the product $f_{ji} \mathrm{grad}_P \psi_j$, so the approximations (22) and (23) may be used and all factors but the dominant term $f_{ij}^0 = n_i n_j$ dropped. Thus, from (17′), we obtain

$$\mathrm{div}_P(e_i f_{ji} \mathrm{grad}_P \psi_j) = e_i n_i n_j \mathrm{div}_P \mathrm{grad}_P \psi_j = -\frac{4\pi}{D} \frac{n_i n_j}{n_j} e_i \sum_p f_{pj} e_p.$$

Therefore the equations for f_{ij} are

$$[\mathrm{div}_P(f_{ji}\mathbf{v}_i) + \mathrm{div}_Q(f_{ij}\mathbf{v}_j)] = -\frac{1}{\rho_i}\left[-\frac{4\pi}{D} n_i e^i \sum_p f_{pj} e_p + kT \nabla_P^2 f_{ji}\right] + \mathrm{div}_P[f_{ji}, \mathbf{i}v_0 + \mathbf{i}(v_s - v_0)]$$

* Fick, Pogg. *Ann.* xciv. p. 59 (1855).

$$-\frac{1}{\rho_j}\left[-\frac{4\pi}{\mathrm{D}}n_j e_j \sum_p f_{ip}e_p + kT\nabla_Q^2 f_{ij}\right]$$
$$+\mathrm{div}_Q\left[f_{ij}, \mathbf{i}[v_0 + b(z_Q - z_P)]\right.$$
$$\left.+\mathbf{i}[v_s - v_0 + (\tilde{b}-b)(z_Q - z_P)]\right] = 0. \quad \ldots \quad (32)$$

If we also make the change of variable

$$x = x_Q - x_P : y = y_Q - y_P : z = z_Q - z_P,$$

so that

$$f_{ij}(x_Q - x_P, y_Q - y_P, z_Q - z_P) = \mathrm{F}_{ij}(x, y, z),$$
$$\frac{\partial f_{ij}}{\partial x_Q} = \frac{\partial \mathrm{F}_{ij}}{\partial x}, \ldots \qquad \frac{\partial f_{ij}}{\partial x_P} = -\frac{\partial \mathrm{F}_{ij}}{\partial x}, \ldots$$
$$\frac{\partial^2 f_{ij}}{\partial x_Q^2} = \frac{\partial^2 \mathrm{F}_{ij}}{\partial x^2}, \ldots \qquad \frac{\partial^2 f_{ij}}{\partial x_P^2} = \frac{\partial^2 \mathrm{F}_{ij}}{\partial x^2}, \ldots$$

equation (32) becomes

$$kT\left(\frac{1}{\rho_i}+\frac{1}{\rho_j}\right)\nabla^2 \mathrm{F}_{ij} - \frac{4\pi}{\mathrm{D}}\left[\frac{n_i e_i}{\rho_i}\sum_p \mathrm{F}_{pj}e_p + \frac{n_j e_j}{\rho_j}\sum_p \mathrm{F}_{ip}e_p\right]$$
$$= \tilde{b}z\frac{\partial \mathrm{F}_{ij}}{\partial x}. \quad (33)$$

The approximation (23) is transformed to

$$\mathrm{F}_{ij} = \mathrm{F}_{ij}^{\mathrm{I}} + \mathrm{G}_{ij}, \quad \ldots \quad (34)$$

where G_{ij} is very small compared to $\mathrm{F}_{ij}^{\mathrm{I}}$. As $\mathrm{F}_{ij} \to \mathrm{F}_{ij}^{\mathrm{I}}$ when there are no external forces, the functions F_{ij} are solutions of (33) when $\tilde{b} \to 0$, or

$$\left.\begin{aligned}
\mathrm{F}_{11}^{\mathrm{I}} &= n_1^2\left(1 - \frac{e_1^2}{\mathrm{D}kT}\frac{e^{-\kappa r}}{r}\right),\\
\mathrm{F}_{22}^{\mathrm{I}} &= n_2^2\left(1 - \frac{e_2^2}{\mathrm{D}kT}\frac{e^{-\kappa r}}{r}\right),\\
\mathrm{F}_{12}^{\mathrm{I}} &= \mathrm{F}_{21}^{\mathrm{I}} = n_1 n_2\left(1 - \frac{e_1 e_2}{\mathrm{D}kT}\frac{e^{-\kappa r}}{r}\right).
\end{aligned}\right\} \quad \ldots \quad (35)$$

If (34) is substituted in (33) we obtain

$$kT\left(\frac{1}{\rho_i}+\frac{1}{\rho_j}\right)\nabla^2 \mathrm{G}_{ij} - \frac{4\pi}{\mathrm{D}}\left[\frac{n_i e_i}{\rho_i}\sum_p \mathrm{G}_{pj}e_p + \frac{n_j e_j}{\rho_j}\sum_p \mathrm{G}_{ip}e_p\right]$$
$$= \tilde{b}z\frac{\partial \mathrm{F}_{ij}^{\mathrm{I}}}{\partial x}. \quad (36)$$

Solutions of (36), G_{ij}, will be the variation of the distribution functions caused by external forces. The equations (33) are the fundamental equations of the problem of viscosity, as their solutions, combining the special solutions (35) and the solutions of (36), describe the effect of the ions dispersed throughout the solvent. This set of equations can be solved exactly for the case of two kinds of ions, so henceforth we shall speak of ions (1) and (2).

4. Solution of the Problem.

It is a simplification to introduce spherical polar co-ordinates

$$x = r\sin\theta\cos\phi : y = r\sin\theta\sin\phi : z = r\cos\theta,$$

which permit an immediate separation of variables

$$G_{ij} = R_{ij}Y(\theta, \phi), \quad . \quad . \quad . \quad . \quad . \quad (37)$$

where

$$Y(\theta, \phi) \sim \cos\theta\sin\theta\cos\phi.$$

This represents a known spherical harmonic of the second order, so that

$$Y(\theta, \phi) = 3\sin\theta\cos\theta\cos\phi. \quad . \quad . \quad . \quad (38)$$

On completing the separation of variables r, θ, ϕ, we obtain a set of differential equations for R_{ij}:

$$\left.\begin{aligned}
&\frac{1}{r^2}\frac{d}{dr}\left(r^2\frac{dR_{11}}{dr}\right) - \frac{6R_{11}}{r^2} - \kappa_1^2 R_{11} + \frac{\kappa_2^2}{2}(R_{12}+R_{21}) \\
&\qquad = \frac{\tilde{b}r}{6kTu_1}\frac{dF_{11}^{I}}{dr}, \\
&\frac{1}{r^2}\frac{d}{dr}\left(r^2\frac{dR_{22}}{dr}\right) - \frac{6R_{22}}{r^2} - \kappa_2^2 R_{22} + \frac{\kappa_1^2}{2}(R_{12}+R_{21}) \\
&\qquad = \frac{\tilde{b}r}{6kTu_2}\frac{dF_{11}^{I}}{dr}, \\
&\frac{1}{r^2}\frac{d}{dr}\left(r^2\frac{dR_{12}}{dr}\right) - \frac{6R_{12}}{r^2} - [\kappa_1^2 R_{12} - \kappa_2^2 R_{22}]\frac{u_1}{u_1+u_2} \\
&\qquad - [\kappa_2^2 R_{12} - \kappa_1^2 R_{11}]\frac{u_2}{u_1+u_2} = -\frac{\tilde{b}}{3kT}\frac{r}{u_1+u_2}\frac{dF_{11}^{I}}{dr}, \\
&\frac{1}{r^2}\frac{d}{dr}\left(r^2\frac{dR_{21}}{dr}\right) - \frac{6R_{21}}{r^2} - [\kappa_2^2 R_{21} - \kappa_1^2 R_{11}]\frac{u_2}{u_1+u_2} \\
&\qquad - [\kappa_1^2 R_{21} - \kappa_2^2 R_{22}]\frac{u_1}{u_1+u_2} = -\frac{\tilde{b}}{3kT}\frac{r}{u_1+u_2}\frac{dF_{11}^{I}}{dr},
\end{aligned}\right\} \quad (39)$$

where

$$\frac{1}{\rho_1} = u_1 : \frac{1}{\rho_2} = u_2,$$

and

$$\kappa_1^2 = \frac{4\pi}{DkT} n_1 e_1^2 : \kappa_2^2 = \frac{4\pi}{DkT} n_2 e_2^2,$$

so that

$$\kappa_1^2 + \kappa_2^2 = \kappa^2.$$

This set of non-homogeneous differential equations can be solved by the ordinary methods of differential equation theory (variation of constants) * and the following equations for R_{ij} obtained :

$$\left.\begin{aligned}
R_{11} &= \frac{\kappa_2^2}{\kappa_1^2}\frac{a}{2}R - \frac{a'}{2}R' - \frac{\kappa_2^2 u_1}{\kappa_1^2 u_2}a''R'' \\
&\qquad + \frac{\kappa_2^2}{\kappa_1^2}\frac{b}{2}P - \frac{b'}{2}P' - \frac{\kappa_2^2 u_1}{\kappa_1^2 u_2}b''P'', \\
R_{22} &= \frac{\kappa_1^2}{\kappa_2^2}\frac{a}{2}R - \frac{a'}{2}R' + a''R'' + \frac{\kappa_1^2}{\kappa_2^2}\frac{b}{2}P - \frac{b'}{2}P' + b''P'', \\
R_{12} = R_{21} &= \frac{a}{2}R + \frac{a'}{2}R' - \frac{(\alpha_3^2 - \kappa_2^2)}{\kappa_1^2}a''R'' \\
&\qquad + \frac{b}{2}P + \frac{b'}{2}P' - \frac{(\alpha_3^2 - \kappa_2^2)}{\kappa_1^2}b''P'',
\end{aligned}\right\} \quad (40)$$

where these abbreviations have been made :

$$R = \left[\frac{d^2}{dr^2}\frac{1}{r} - \frac{1}{r}\frac{d}{dr}\frac{1}{r}\right] = \frac{3}{r^3},$$

$$R' = \left[\frac{d^2}{dr^2}\frac{e^{-\kappa r}}{r} - \frac{1}{r}\frac{d}{dr}\frac{e^{-\kappa r}}{r}\right] = \frac{e^{-\kappa r}}{r^3}(\kappa^2 r^2 + 3\kappa r + 3),$$

$$R'' = \left[\frac{d^2}{dr^2}\frac{e^{-\alpha_3 r}}{r} - \frac{1}{r}\frac{d}{dr}\frac{e^{-\alpha_3 r}}{r}\right] = \frac{e^{-\alpha_3 r}}{r^3}(\alpha_3^2 r^2 + 3\alpha_3 r + 3),$$

$$P = \frac{\alpha e^{-\kappa r}}{\kappa^4 r^3}(\kappa^3 r^3 + 3\kappa^2 r^2 + 6\kappa r + 6),$$

$$P' = -\frac{\alpha e^{-\kappa r}}{8\kappa^4 r^3}(24\kappa^4 r^4 - 15\kappa^2 r^2 - 45\kappa r - 45),$$

$$P'' = -\frac{\alpha e^{-\kappa r}}{(\alpha_3^2 - \kappa^2)^2 r^3}\{\kappa(\alpha_3^2 - \kappa^2)r^3 + (\alpha_3^2 - 3\kappa^2)r^2 - 6\kappa r - 6\},$$

* H. Falkenhagen, *Physik. Z.* xxxii. p. 745 (1931).

and

$$\alpha_3^2 = \frac{u_1\kappa_1^2 + u_2\kappa_2^2}{u_1 + u_2} : \alpha = \frac{\tilde{b}}{6kT}\frac{n_1 e_1^2}{Dk\mathrm{T}}.$$

The values a, a', a'', b, b', b'' are constants which may be evaluated from the boundary conditions of equations (39) : that the functions be finite when r is zero and zero when r is infinite. The values are

$$a = -\frac{2\alpha}{\kappa^4}b : a' = -\frac{15}{8}\frac{\alpha}{\kappa^4}b' : a'' = -\frac{2\alpha}{(\alpha_3^2 - \kappa^2)^2}b'';$$

$$b = \frac{2\kappa_1^2\kappa_2^2(u_1 - u_2)^2}{u_1u_2\kappa^2(u_1\kappa_1^2 + u_2\kappa_2^2)} : b' = -\frac{2(u_1\kappa_2^2 + u_2\kappa_1^2)}{u_1u_2\kappa^2};$$

$$b'' = \frac{(u_1 - u_2)\kappa_1^2}{u_1(u_1\kappa_1^2 + u_2\kappa_2^2)}.$$

With these solutions it is now possible to calculate the changes in electric densities Π_1' and Π_2'. Equations (12) and (12′) give the connexion with distribution functions, so we may write

$$\Pi_1' = \frac{1}{n_1}[e_1G_{11} + e_2G_{12}], \quad . \quad . \quad . \quad . \quad (41)$$

$$\Pi_2' = \frac{1}{n_2}[e_1G_{21} + e_2G_{22}], \quad . \quad . \quad . \quad . \quad (41')$$

or

$$\Pi_1' = \frac{1}{n_1}[e_1R_{11} + e_2R_{12}]Y(\theta, \phi) = R_1(r)Y(\theta, \phi), \quad (42)$$

$$\Pi_2' = \frac{1}{n_2}[e_1R_{21} + e_2R_{22}]Y(\theta, \phi) = R_2(r)Y(\theta, \phi). \quad (42')$$

From Poisson's equations (9) and (9′) the potentials will satisfy the differential equations

$$\nabla^2\psi_1' = -\frac{4\pi}{D}\frac{1}{n_1}[e_1G_{11} + e_1G_{12}], \quad . \quad . \quad . \quad (43)$$

$$\nabla^2\psi_2' = -\frac{4\pi}{D}\frac{1}{n_2}[e_1G_{21} + e_2G_{22}]. \quad . \quad . \quad . \quad (43')$$

5. Determination of Viscosity.

The variations of the functions R_1 and R_2 with respect to κr have been calculated for the case of $BaCl_2$, where ion (1) is positive and ion (2) is negative. The curves shown in fig. 3 are for a molar concentration of $\gamma = 0{\cdot}0001$. With

increasing γ the peaks become higher and shift slightly toward the origin. These curves show the probable distribution of ions around any one ion, or the probable variation of electric density with distance from the central ion. The variation of Π_1 due to the angular term is best shown

Fig. 3.

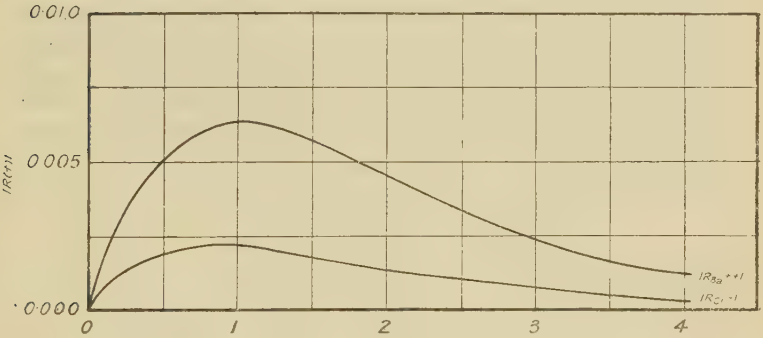

Distribution of additional density $\sim R(r)$ for $BaCl_2$.
[sign $(R_{Ba^{++}}) = -$sign (R_{Cl^-}).]

Fig. 4.

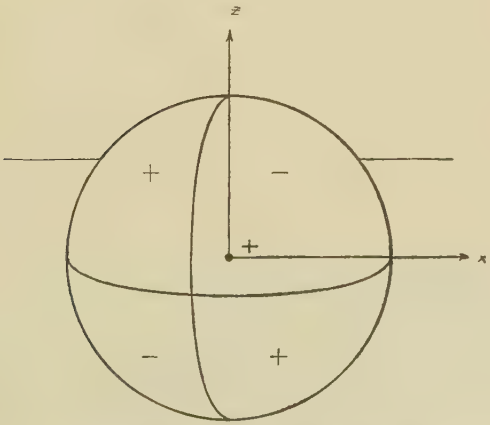

Distribution of additional electric density as a function of θ, ϕ.

schematically on the surface of a sphere, as in fig. 4. The sign predominating in each of the quadrants varies as in the diagram. Negative ions have a precisely similar but complementary distribution of charges.

If the ions are in motion there is an unsymmetrical distribution, the degree of asymmetry depending upon the velocity gradient along a plane perpendicular to the x-axis, which is taken as the direction of motion. This lack of symmetry is shown in a distortion of the original central-symmetric ionic atmosphere from spherical to a form which may be shown to be ellipsoidal (fig. 5). It is easy to see from the diagram that such a displacement of the electric charges occurring progressively along the velocity gradient must result in a force on the central ion parallel to the x-direction. This distortion is equivalent to the sliding of each of the infinitely thin parallel lamellæ comprising the medium upon

Fig. 5.

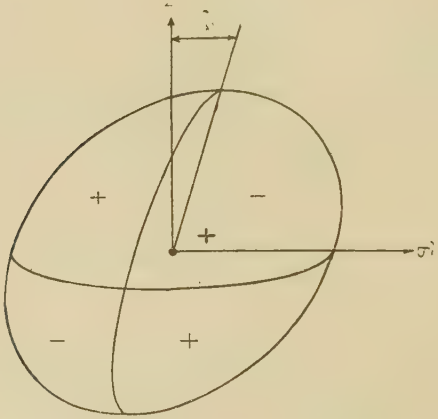

Distortion of original ionic atmosphere.

the next below it to give a displacement which must be proportional to the perpendicular distance of the lamella from the plane of reference. The force producing this displacement or shear is the shearing force, and consequently is proportional to the displacement which is measured by the velocity gradient.

When the ionic atmosphere is distorted the electric charges are displaced from their equilibrium positions and the forces they exert on the central ion are unbalanced. The electric densities defined in equations (42) and (42′), Π_1' and Π_2', describe the asymmetrical distribution of electric charges and are proportional to the velocity gradient. The electric charges in dS of the changed ionic atmosphere exert a force

upon a central ion of type (1) through the distance r which may be expressed

$$F_1 = \frac{e_1 \Pi_1'}{Dr^2}\, dS.$$

If we want to calculate the force exerted upon a central ion and resolved parallel to the x-axis it will be necessary to integrate the force function parallel to x,

$$F_{1_x} = \frac{e_1 \Pi_1' dS}{Dr^2} \sin\theta \cos\phi,$$

over all space above the h-plane (fig. 6), taken perpendicular to the velocity gradient. It is necessary to integrate over the entire plane, though the force $H(h)$ falls practically to

Fig. 6

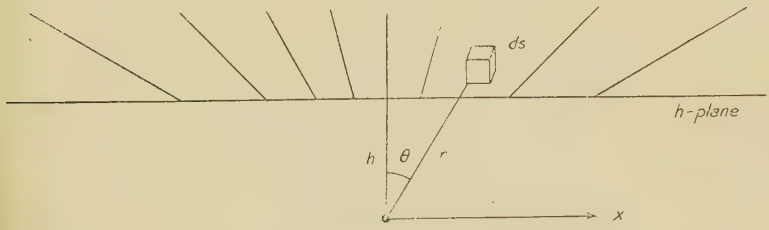

zero at a very short distance from the central ion. The forces for the ions (1) and (2) are

$$H_1(h) = \int_0^{2\pi} d\phi \int_{\cos\theta=\frac{h}{r}}^{\cos\theta=1} d\theta \int_h^{\infty} \frac{e_1 \Pi_1'}{Dr^2}\, r^2 \sin^2\theta \cos\phi\, dr, \quad (44)$$

$$H_2(h) = \int_0^{2\pi} d\phi \int_{\cos\theta=\frac{h}{r}}^{\cos\theta=1} d\theta \int_h^{\infty} \frac{e_2 \Pi_2'}{Dr^2}\, r^2 \sin^2\theta \cos\phi\, dr. \quad (44')$$

But there are n_1 of ions (1) and n_2 of ions (2). Then to obtain the total force exerted by all ions on a square centimetre perpendicular to the velocity gradient we must take the sum of the forces for all ions and integrate the forces over all values of h from zero to infinity (fig. 7), or

$$H = \int_{h=0}^{\infty} n_1 H_1(h)\, dh + \int_{h=0}^{\infty} n_2 H_2(h)\, dh. \quad . \quad . \quad (45)$$

The force H, which depends on the electric densities Π_1' and Π_2', is proportional to the velocity gradient $\tilde{b}$, and from our

definition of viscosity in section 2 the proportionality factor is our desired coefficient of viscosity.

If we make use of equations (42), (42′), and (38), and integrate first with respect to the angle variables θ, ϕ, we obtain

$$H = -\tfrac{3}{4}\pi \frac{1}{D}\int_0^{\infty} dh \int_h^{\infty} [n_1 e_1 R_1(r) + n_2 e_2 R_2(r)] \left[1 - \frac{2h^2}{r^2} + \frac{h^4}{r^4}\right] dr. \quad (46)$$

Since the conditions imposed upon the solutions of the differential equations from which $R_1(r)$ and $R_2(r)$ were obtained are that they be finite at zero and zero at infinity,

Fig. 7.

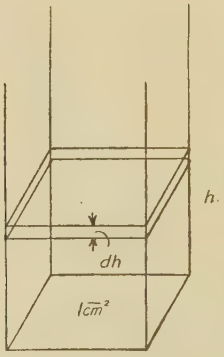

the definite infinite integral may be evaluated. $R_1(r)$ and $R_2(r)$ may be written more simply as

$$R_1(r) = \frac{\alpha}{n_1}\left\{\frac{b'}{8}\beta r e^{-\kappa r} + \frac{b''}{(\alpha_3^2-\kappa^2)^2}\beta'\left[e^{-\alpha_3 r}\left(\frac{2\alpha_3^2}{r} + \frac{6\alpha_3}{r^2} + \frac{6}{r^3}\right) + e^{-\kappa r}\left(\alpha_3^2\left(\kappa + \frac{1}{r}\right) - \kappa^3 - \frac{3\kappa^2}{r} - \frac{6\kappa}{r^2} - \frac{6}{r^3}\right)\right]\right\},$$

$$R_2(r) = \frac{\alpha}{n_2}\left\{-\frac{b'}{8}\beta r e^{-\kappa r} + \frac{b''}{(\alpha_3^2-\kappa^2)^2}\beta''\left[e^{-\alpha_3 r}\left(\frac{2\alpha_3^2}{r} + \frac{6\alpha_3}{r^2} + \frac{6}{r^3}\right) + e^{-\kappa r}\left(\alpha_3^2\left(\kappa + \frac{1}{r}\right) - \kappa^3 - \frac{3\kappa^2}{r} - \frac{6\kappa}{r^2} - \frac{6}{r^3}\right)\right]\right\},$$

where the abbreviations

$$\beta = e_1 - e_2 : \beta' = e_1 \frac{\kappa_2^2 u_1}{\kappa_1^2 u_2} + e_2 \frac{\alpha_3^2 - \kappa_2^2}{\kappa_1^2} :$$

$$\beta'' = e_1 \frac{\alpha_3^2 - \kappa_2^2}{\kappa_1^2} - e_2$$

are made. Then by straightforward integration

$$\begin{aligned} H = -\frac{3}{4}\pi \frac{\alpha}{D} \int_0^\infty \Bigg\{ & \frac{b'\beta^2}{8} \Bigg[\frac{1}{\kappa^2} e^{-\kappa h} + \frac{h}{\kappa} e^{-\kappa h} + \frac{h^2}{2} e^{-\kappa h} - \frac{\kappa h^3}{2} e^{-\kappa h} \\ & - \left(2h^2 - \frac{\kappa^2 h^4}{2}\right) \int_h^\infty \frac{e^{-\kappa r}}{r} dr \Bigg] + \frac{b''(\beta' + \beta'')}{(\alpha_3^2 - \kappa^2)^2} \Bigg[\frac{1}{h^2} e^{-\alpha_3 h} \\ & + \frac{\alpha_3}{h} e^{-\alpha_3 h} - \frac{\alpha_3^2}{4} e^{-\alpha_3 h} + \frac{5}{12} \alpha_3^3 h e^{-\alpha_3 h} + \frac{1}{24} \alpha_3^4 h^2 e^{-\alpha_3 h} \\ & - \frac{1}{24} \alpha_3^5 h^3 e^{-\alpha_3 h} - \left(\alpha_3^2 + \frac{\alpha_3^4 h^2}{2} - \frac{\alpha_3^6 h^4}{24}\right) \int_h^\infty \frac{e^{-\alpha_3 r}}{r} dr \\ & + \frac{\alpha_3}{4} \Bigg(e^{-\kappa h} + 3\kappa h e^{-\kappa h} - \frac{\kappa^2 h^2}{2} e^{-\kappa h} + \frac{\kappa^3 h^3}{2} e^{-\kappa h} \\ & + \left(4 + 4\kappa^2 h^2 - \frac{\kappa^4 h^4}{2}\right) \int_h^\infty \frac{e^{-\kappa r}}{r} dr \Bigg) - \frac{1}{h^2} e^{-\kappa h} - \frac{\kappa}{h} e^{-\kappa h} \\ & + \frac{\kappa^3 h}{3} e^{-\kappa h} + \frac{\kappa^4 h^2}{12} e^{-\kappa h} - \frac{\kappa^5 h^3}{12} e^{-\kappa h} \\ & + \left(\frac{\kappa^6 h^4}{12} - \frac{\kappa^4 h^2}{2}\right) \int_h^\infty \frac{e^{-\kappa r}}{r} dr \Bigg] \Bigg\} dh. \quad . \quad . \quad . \quad . \quad . \quad (47) \end{aligned}$$

The only terms which appear troublesome in further integration are the general definite integrals

$$\int_0^\infty h^n dh \int_h^\infty \frac{e^{-\kappa r}}{r} dr = \int_0^\infty \frac{e^{-\kappa r}}{r} dr \int_0^r h^n dh$$

$$= \frac{1}{n+1} \int_0^\infty r^n e^{-\kappa r} dr = \frac{n!}{n+1} \frac{1}{\kappa^{n+1}}.$$

Making use of this, (47) simplifies to

$$H = -\frac{3}{4}\pi \frac{\alpha}{D} \left\{ \frac{b'}{8} \beta^2 \frac{16}{15} \frac{1}{\kappa^3} + \frac{b''(\beta' + \beta'')}{(\alpha_3^2 - \kappa^2)^2} \frac{16}{15} \frac{1}{\kappa} (\alpha_3 - \kappa)^2 \right\} \quad (48)$$

If we substitute in (48) the values of the various factors and make an extended reduction we obtain

$$H = \frac{\tilde{b}}{30}\frac{\sqrt{\frac{N}{1000}}\sqrt{\nu_1 z_1}\,\epsilon\sqrt{\gamma}}{\sqrt{D\,kT}\sqrt{z_1+z_2}\sqrt{4\pi}}\left\{\frac{1}{4}\frac{u_1z_2+u_2z_1}{u_1u_2} - \frac{z_1z_2(u_1-u_2)^2}{u_1u_2(\sqrt{u_1z_1+u_2z_2}+\sqrt{u_1+u_2}\sqrt{z_1+z_2})^2}\right\}, \quad (49)$$

where ϵ is the unit charge of electricity in e.s.u. ($\epsilon = 4{\cdot}77\times10^{-10}$), N is Avogadro's number ($N = 6{\cdot}06\times10^{23}$), ν_1 is the number of ions of type (1) formed in dissociation, u_1 and u_2 are the mobilities defined in (30), z_1 and z_2 are numerical values of the valences of ions (1) and (2), D is the dielectric constant of the solvent, k is Boltzmann's constant ($k = 1{\cdot}37\times10^{-16}$ ergs/degree), T is the absolute temperature, γ is molar concentration of electrolyte, and $\tilde{b}$ is the measure of velocity gradient discussed above.

Equation (49) may be written shortly as

$$H = \tilde{b}A^*\sqrt{\gamma}. \quad . \quad . \quad . \quad . \quad . \quad . \quad (50)$$

The force H is proportional to the velocity gradient $\tilde{b}$, and consequently the proportionality factor $A^*\sqrt{\gamma}$ is our additive coefficient of viscosity due to ionic forces. Then, if η_γ is the coefficient of viscosity at molar concentration γ and η_0 the coefficient at zero concentration,

$$\eta_\gamma - \eta_0 = A^*\sqrt{\gamma}, \quad . \quad . \quad . \quad . \quad . \quad (51)$$

or

$$\frac{\eta_\gamma}{\eta_0} = 1 + A\sqrt{\gamma}, \quad . \quad . \quad . \quad . \quad (52)$$

where

$$A = \frac{1}{30}\frac{\sqrt{\frac{N}{1000}}\sqrt{\nu_1 z_1}\,\epsilon}{\sqrt{D\,kT}\sqrt{z_1+z_2}\sqrt{4\pi}}\frac{1}{\eta_0}\left\{\frac{1}{4}\frac{u_1z_2+u_2z_1}{u_1u_2} - \frac{z_1z_2(u_1-u_2)^2}{u_1u_2(\sqrt{u_1z_1+u_2z_2}+\sqrt{u_1+u_2}\sqrt{z_1+z_2})^2}\right\}. \quad (53)$$

Thus in (52) we have an expression for the relative viscosity containing a term proportional to the square root of the concentration, as was predicted by Jones and Dole. Finkelstein * has discussed the viscosity of electrolyte solutions from the point of view of Einstein's correction and

* B. N. Finkelstein, *Physik. Z.* xxxi. pp. 130, 165 (1930).

obtained a result proportional to the concentration. This work is not quantitative, because it is impossible to calculate the orientation energy of dipoles in the solution quantitatively, and because, as we have shown, in dilute solutions of strong electrolytes the interionic forces introduce a square root term. In other cases the interionic forces and a depolymerization effect may be very important for this linear term.

This coefficient A is applicable to any electrolyte of any valence type, but may be simplified considerably for special cases. When we have a binary electrolyte for which $e_1 = -e_2$, A reduces to the form

$$A = \frac{1}{30}\frac{\sqrt{\frac{N}{1000}}\epsilon z}{\sqrt{DkT}\sqrt{8\pi}}\frac{1}{\eta_0}\left\{\frac{1}{4}\frac{u_1+u_2}{u_1u_2} - \frac{(u_1-u_2)^2(1-\sqrt{2})^2}{u_1u_2(u_1+u_2)}\right\}, \quad . \quad . \quad . \quad (54)$$

which is identical with the formula obtained by Falkenhagen * in his special consideration of binary electrolytes. If, further, we have the simplification that the mobilities u_1 and u_2 are equal, A becomes

$$A = \frac{1}{60}\frac{\sqrt{\frac{N}{1000}}\epsilon z}{\sqrt{DkT}\sqrt{8\pi}}\frac{1}{\eta_0}\frac{1}{u_1}, \quad . \quad . \quad . \quad (55)$$

the formula obtained by Falkenhagen and Dole † in the original discussion of the problem.

Computation of A from (53) and (54) is readily carried out for cases in which experimental data are available. The mobilities are to be found in several places, notably in Landolt-Börnstein, 'Tabellen'; Ostwald-Drucker, 'Handbuch der allgemeinen Chemie'; and Ulich, "Beweglichkeit der elektrolytischen Ionen," *Fortschritte Chem.* xviii. no. 10. In Table I. are listed the molar ionic conductances $\overline{L_i}$ at infinite dilution of a number of ions in water at various temperatures. The values u_i may be computed from these conductances by use of equation (30).

6. Application of Viscosity Correction.

(a) *Influence of Valence and Mobility.*

In Table II. the computed values of A are listed for a number of more common electrolytes when the solvent is

* H. Falkenhagen, *Physik. Z.* xxxii. p. 745 (1931).

† H. Falkenhagen and M. Dole, *Physik. Z.* xxx. p. 611 (1929).

water. The electrolytes are grouped according to valence type, and, although the mobilities of the electrolytes in any one group may vary greatly, the values of A for a valence type

Table I.

Molar Ionic Conductances $\overline{L_i}$ at infinite dilution of various Ions in Water.

Ion.	0°.	18°.	25°.	100°.
H^+	222·5	315	351·5	636
Cs^+	44	68	78·1	203
Rb^+	—	67·5	—	—
I^-	—	67·4	—	—
Cl^-	41·3	65·5	76·3	208
K^+	40·6	64·4	74·8	115
NO_3^-	40·2	61·83	71	187
IO_3^-	—	34	—	—
Li^+	19·2	33	40	117
NEt_4^+	16	28·1	33	103
Picrate$^-$	15·0	25·3	30·1	94
SO_4^{--}	82	136	—	—
Ba^{++}	67	110	130	400
Mg^{++}	—	92	—	—
La^{+++}	—	150	—	—

Table II.

Computed Values of A with Water as Solvent at 18° C.

Valence type.	Electrolyte.	$A_{Theor.}$	Valence type.	Electrolyte.	$A_{Theor.}$
1–1	HCl	0·0020	1–1	$LiNO_3$	0·0069
1–1	HNO_3	0·0021	1–1	NEt_4Cl	0·0071
1–1	KI	0·0048	1–1	$LiIO_3$	0·0094
1–1	$CsNO_3$	0·0048	1–2	K_2SO_4	0·0128
1–1	$RbNO_3$	0·0049	2–1	$BaCl_2$	0·0145
1–1	KCl	0·0049	2–1	$MgCl_2$	0·0163
1–1	KNO_3	0·0050	2–2	$MgSO_4$	0·0223
1–1	LiCl	0·0067	3–1	$LaCl_3$	0·0318

are of the same order of magnitude. The effect of mobility is shown in Table III., where $u' = u \times 10^{-8}$. From this table it appears that an increase of mobility of either ion will decrease the viscosity coefficient. In the 1–1 group of electrolytes, compounds containing H^+ ion, which has the highest mobility, show the lowest A, while compounds with the NEt_4^+ ion, which has a very low mobility, show a higher value of A.

(b) *Influence of Temperature.*

The coefficient A depends upon the temperature in a very complicated manner through the dielectric constant and viscosity of the solvent and the mobilities of the ion, in addition to varying inversely with the square root of the absolute temperature. In Table IV. computed values of A

TABLE III.

$u' = u \times 10^{-8}$.

Effect of Mobility on A. Temperature = 18° C.

$u'_{Li^+} = 2{\cdot}143$. $u'_{NO_3^-} = 4{\cdot}015$.

$u'_{Cl^-} = 4{\cdot}954$	$A_{LiCl} = 0{\cdot}0067$	$u'_{H^+} = 20{\cdot}45$	$A_{HNO_3} = 0{\cdot}0021$
$u'_{NO_3^-} = 4{\cdot}015$	$A_{LiNO_3} = 0{\cdot}0069$	$u'_{K^+} = 4{\cdot}182$	$A_{KNO_3} = 0{\cdot}0050$
$u'_{IO_3^-} = 2{\cdot}208$	$A_{LiIO_3} = 0{\cdot}0094$	$u'_{Li^+} = 2{\cdot}143$	$A_{LiNO_3} = 0{\cdot}0067$

for a few electrolytes dissolved in water at various temperatures are listed. There is probably some inaccuracy due to experimental difficulties in measuring mobilities, and, most important from a theoretical point of view, because the dielectric constant D is not well known. It is probably impossible to state the change of A with temperature without an error of ± 15 per cent., because $\frac{dD}{dT}$ is not known accurately within ± 25 per cent.*

Regardless of possible experimental errors the relationships found are of great interest. Walden's rule states that $\Lambda_\infty \eta_0 = \text{const.}$, where Λ_∞ is the conductivity of the electrolyte at infinite dilution and η_0 the viscosity of the pure solvent under the same conditions of temperature. But since

$$\Lambda_\infty = \sum_i \nu_i \bar{L}_i,$$

we have, as a corollary to Walden's rule, $\bar{L}_i \eta_0 = \text{const.}$ In

* E. Lange, *Zs. f. Elektrochem.* xxxvi. p. 772 (1930).

TABLE IV.

The Coefficients A for various Electrolytes.

Electrolyte.	0°.	18°.	25°.	100°.
HCl	0·0018	0·0020	0·0021	0·0033
HNO_3	0·0018	0·0021	0·0022	0·0034
$CsNO_3$	0·0044	0·0048	0·0050	0·0065
KCl	0·0045	0·0049	0·0051	0·0062
LiCl	0·0064	0·0067	0·0067	0·0080
$LiNO_3$	0·0065	0·0069	0·0069	0·0084
NEt_4Cl	0·0069	0·0071	0·0074	0·0084
NEt_4–Picrate	0·0119	0·0118	0·0119	0·0128
$BaCl_2$	0·0138	0·0145	0·0147	0·0149
D_{H_2O}	88·2	81·3	78·8	55·3
$\eta_0 \times 10^2$	1·791	1·06	0·895	0·284

TABLE V.

Λ_∞ and $\Lambda_\infty \eta_0$ for various Electrolytes.

Electrolyte.		0°.	18°.	25°.	100°.
HCl	Λ_∞	263·8	380·5	427·8	844
	$\Lambda_\infty \eta_0$	4·72	4·04	3·82	2·34
HNO_3	Λ_∞	262·7	376·83	422·5	823
	$\Lambda_\infty \eta_0$	4·71	3·99	3·78	2·34
$CsNO_3$	Λ_∞	84·2	129·83	149·1	390
	$\Lambda_\infty \eta_0$	1·51	1·37	1·33	1·11
KCl	Λ_∞	81·9	130·1	151·1	406
	$\Lambda_\infty \eta_0$	1·42	1·38	1·35	1·15
LiCl	Λ_∞	60·5	98·5	116·3	325
	$\Lambda_\infty \eta_0$	1·08	1·04	1·04	0·923
$LiNO_3$	Λ_∞	59·4	94·83	111·0	304
	$\Lambda_\infty \eta_0$	1·06	1·01	0·993	0·864
NEt_4Cl	Λ_∞	57·3	93·6	109·3	311
	$\Lambda_\infty \eta_0$	1·03	0·992	0·977	0·884
NEt_4–Picrate	Λ_∞	31·0	53·4	63·1	202
	$\Lambda_\infty \eta_0$	0·555	0·565	0·564	0·574
$BaCl_2$	Λ_∞	149·6	241·0	282·6	816
	$\Lambda_\infty \eta_0$	2·68	2·57	2·53	2·32

Table V. are shown the values of Λ_∞ and $\Lambda_\infty\eta_0$ for the electrolytes listed in Table IV., and in Table VI. are the values of $\overline{L_i\eta_0}$ for the ions involved.

Since the two ions showing the greatest constancy of the product $\overline{L_i\eta_0}$ are NEt_4^+ and $Picrate^-$, the values of A for an electrolyte formed from these ions are included in Table IV. These values of A are practically constant for the temperature range. Electrolytes which contain only one ion with a constant product $\overline{L_i\eta_0}$ show a marked approach to constancy of A, as may be seen in lithium compounds. Variation from a constant value of A appears to be uniformly in a positive direction, resulting in a positive temperature coefficient, but

Table VI.

$\overline{L_i\eta_0}$ for various Ions.

	0°.	18°.	25°.	100°.
H^-	3·99	3·32	3·14	1·81
Cs^+	0·786	0·720	0·699	0·577
Cl^-	0·741	0·691	0·682	0·59
K^+	0·728	0·680	0·669	0·560
NO_3^-	0·718	0·655	0.635	0·532
Li^+	0·344	0·350	0·358	0·330
NEt_4^+	0·287	0·296	0·295	0·293
$Picrate^-$	0·269	0·267	0·274	0·267
Ba^{++}	1·20	1·16	1·16	1·13

there is no apparent reason why this order should hold for all electrolytes.

(c) *Influence of Solvent.*

Data for mobilities in non-aqueous solvents could be obtained in only a few cases. Table VII. lists the values of A for three electrolytes in three different non-aqueous solvents, and compares them with values in water at the same temperature. In addition to the large variation of mobilities discussion is complicated by wide variation of dielectric constant and viscosity of the solvent. The mobilities used in these computations are those recently determined by Hartley and Raikes * and Ulich †.

* H. Hartley and H. R. Raikes, Trans. Far. Soc. xxiii. pp. 393-396 (1927).

† H. Ulich, Trans. Far. Soc. xxiii. p. 388 (1927).

(d) *Comparison of Theory and Experiment.*

It is of interest to note that the value $A = 0{\cdot}0049$ computed for KCl at 18° C. has recently been verified experimentally by Joy and Wolfenden*, who obtained $A = 0{\cdot}0052$. There has been very little other experimental work with which computed values of A can logically be compared. The value for $BaCl_2$ at 25°, $A = 0{\cdot}0201$, given by Jones and Dole† compares in order of magnitude with the computed value, $A = 0{\cdot}0147$. But the experimental value was obtained from a concentration range of 0·005 to 0·9913 molar with a greater portion of values in the upper range. Jones and Dole list their results to 1 : 10000 with the next figure questionable. If we consider their last significant figure to be doubtful,

Table VII.

Computed Values of A in Non-aqueous Solvents at 25° C.

	H_2O.	MeOH.	EtOH.	Acetone.
KCl	0·0051	0·0190	0·0243	0·0239
LiCl	0·0067	0·0221	0·0287	0·0237
$BaCl_2$	0·0147	0·0475	—	0·0649
D	79	30·	24	21
$\eta_0 \times 10^2$	0·894	0·545	1·087	0·3158

the theoretical value of A is within the range of experimental error. Joy and Wolfenden and Jones are continuing the experimental work on viscosities, and it will be interesting to compare the results of this paper with their later experimental work.

One can find a more complete comparison of the theory with the experimental results in the monograph 'Elektrolyte,' by H. Falkenhagen, p. 249 (1932).

7. Summary.

The ionic atmosphere, which has been shown by Debye and Hückel, Onsager, and Falkenhagen to be of great importance in the modern electrostatic theory of electrolytes, has been used to develop a system of probability functions

* W. E. Joy and J. M. Wolfenden, 'Nature,' cxxvi. pp. 994–5 (1930). Proc. Roy. Soc. A. cxxxiv. p. 413 (1931).

† G. Jones and M. Dole, J. A. C. S. li. p. 2950 (1929).

f_{ij} describing the distribution of ions in the atmosphere around a central ion. These functions have been discussed in relation to electrolyte solutions and calculated in this problem of viscosity of dilute solutions of strong electrolytes. It has been shown that the original central-symmetric electric density of the ionic atmosphere is deformed when a gradient of velocity exists in the solution, and the related shearing force has been calculated to give a term, proportional to the square root of the concentration, which is additive to the viscosity :

$$\eta_\gamma = \eta_0(1 + A\sqrt{\gamma}).$$

A formula has been derived for the proportionality factor A as a function of the absolute temperature T, the dielectric constant D, and the viscosity η_0 of the pure solvent, the numerical values of the valences of the ions z_i, the number of each ion formed in dissociation of a molecule of electrolyte ν_i, the mobilities of the ions u_i, and certain general constants. In the most general case of a simple electrolyte the coefficient A has the form

$$A = \frac{1}{30}\frac{\sqrt{\frac{N}{1000}}\sqrt{\nu_1 z_1 \epsilon}}{\sqrt{DkT}\sqrt{z_1+z_2}\sqrt{4\pi}}\frac{1}{\eta_0}\left\{\frac{1}{4}\frac{u_1z_2+u_2z_1}{u_1u_2} - \frac{z_1z_2(u_1-u_2)^2}{u_1u_2\left(\sqrt{u_1z_1+u_2z_2}+\sqrt{u_1+u_2}\sqrt{z_1+z_2}\right)^2}\right\}. \quad (56)$$

Madison, Wis., U.S.A., and
Cologne, Germany.

LXIII. *Central Deflexion of a Square Plate with Clamped Edges and subject to a Uniform Pressure over One Face.* *By* K. R. Gunjikar, *M.A.*, *and* V. D. Majmudar, *M.Sc.**

THE complete analytical solution of the problem of a rectangular plate with clamped edges and bent by pressure applied to one face has not been obtained, but an approximate method of solution has been devised by Ritz [1]. Knott [2] worked out the case of a square plate by Ritz's method, but he gives only the relative displacements of different points of the plate and not the absolute magnitudes. In this paper, the absolute value of the central displacement of a square plate has been worked out by the same method

* Communicated by Dr. T. S. Wheeler, F.R.C.Sc.I., F.I.C.

and the results are compared with those obtained on thin glass plates subjected to small differences of pressure between the two faces.

The equation to be satisfied by the normal displacement w at any point of the plate, when it is subjected to a pressure difference p is [3]

$$D\left(\frac{\partial^4}{\partial x^4}+\frac{2\partial^4}{\partial x^2\partial y^2}+\frac{\partial^4}{\partial y^2}\right)w=-p,$$

or more simply

$$D\nabla^2 w=-p \qquad \left[\nabla \text{ standing for } \frac{\partial^2}{\partial x^2}+\frac{\partial^2}{\partial y^2}\right],$$

where D is the flexural rigidity of the plate and is equal to

$$\frac{1}{12}\frac{Et^3}{1-\sigma^2},$$

E is the Young's Modulus, σ is the Poisson's ratio, and t is the thickness of the plate.

The solution must satisfy the boundary conditions

$$w=0, \quad \frac{dw}{dz}=0$$

at the boundaries $x=0$, $x=a$, $y=0$, $y=a$, the origin of the coordinates being taken at one of the corners, with the z axis perpendicular to the plate. "a" is the length of the edge.

Ritz has given a solution of this equation with these boundary conditions in the form of a series [1]:

$$\frac{w}{l}=0{\cdot}674\xi_1\eta_1+0{\cdot}308(\xi_1\eta_1+\xi_3\eta_3)+0{\cdot}0032\xi_3\eta_3 +0{\cdot}0040(\xi_1\eta_5+\xi_5\eta_1)+0{\cdot}0004(\xi_3\eta_5+\xi_5\eta_3) +0{\cdot}0000\xi_5\eta_5 \text{ to the third approximation,}$$

where [4]

$$\frac{10^4 l}{8a^4}=\frac{p}{D}=\frac{12p(1-\sigma^2)}{Et^3},$$

i. e.

$$l=\frac{96a^4(1-\sigma^2)}{Et^3\times 10^4}p,$$

and

$$\xi_n=\frac{\cos k_n x}{a}-\frac{\cosh k_n x}{a}-\left(\frac{\sin k_n x}{a}-\frac{\sinh k_n x}{a}\right)\frac{\cos k_n-\cosh k_n}{\sin k_n-\sinh k_n}$$

and η_n is a similar function of y, and k_n is the nth root of

$$\cos k_n \cosh k_n=1.$$

Taking $\frac{x}{a}=\frac{y}{a}=\frac{1}{2}$, we get the value of the displacement

at the centre $w = 1{\cdot}5915\, l$, whence substituting for l, we get

$$w = \frac{96 \times 1{\cdot}5915(1-\sigma^2)a^4}{Et^3 \times 10^4}\, p.$$

This formula has been tested by direct experiment.

The method followed in these experiments to determine the depression at the centre of the clamped plate was that of Wagstaff[5], somewhat modified. The glass plate A under experiment was clamped between two thick brass plates B and C, with exactly equal square holes in each, and so arranged that the hole in one was accurately superimposed over the hole in the other. This arrangement which allowed only a small square of the glass plate to be exposed to light, was then fixed to the pressure chamber, as was done by

Fig. 1.

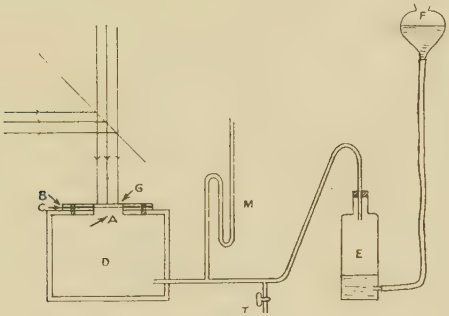

Wagstaff. The pressure chamber D was connected to a stout bottle E, which in its turn was connected to a mercury reservoir F, with india-rubber tubing. The raising or lowering of the vessel F increased or decreased the pressure in D. The manometer M indicated the pressure in D, whilst air could be let in or out by means of the tap T.

Over the glass plate, clamped to the pressure-chamber, was placed another glass plate G, about 1 mm. thick and of exactly the same size as the aperture. By a suitable optical arrangement a beam of parallel monochromatic light was thrown on the plate G. The Newton's fringes formed between the plates A and G were then observed by a microscope from above.

When a pressure p_1 is applied to the plate A, it acquires a curvature. If the pressure be now changed to p_2 the sag of the plate at its centre corresponding to the pressure

TABLE I.

Thickness of the plate = 0·0148 cm.
$E = 5{\cdot}57 \times 10^{11}$ dynes per sq. cm.
$\sigma = 0{\cdot}316$.

Pressures in cms. of Hg.	N. No. of fringes that appear.	$\frac{N}{2} \times 5{\cdot}89 \times 10^{-5}$ cm. Deflexion =	Deflexion calculated from the formula $\times 10^{-5}$ cm.
2·20	20	58·9	85·8
4·45	50	147·2	171·6
6·50	80	235·6	253·6
7·95	100	294·5	310·2
9·55	120	353·4	372·7
10·80	140	412·3	421·5
13·80	180	530·1	538·6
15·55	200	589·0	606·8
19·00	250	736·2	745·0

Fig. 2.

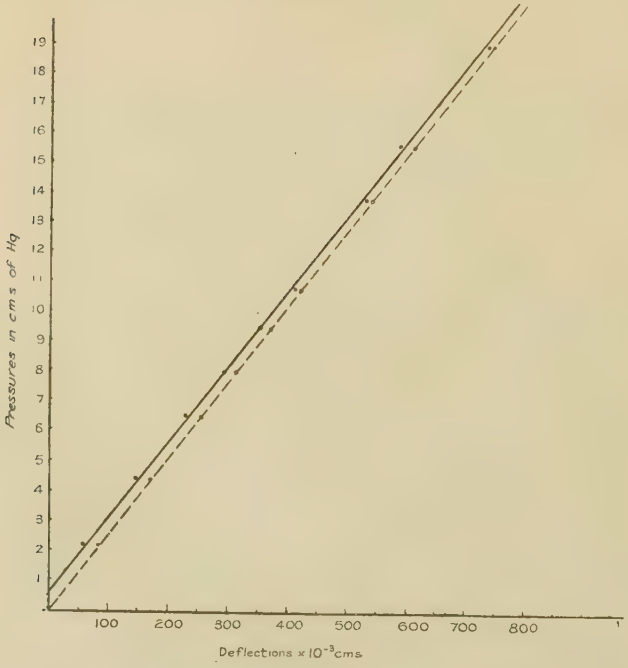

change $p_1 - p_2$ is determined by counting the number of fringes that spread out of the centre as the pressure changes

from p_1 to p_2. If N is the number of fringes that appear then the depression

$$w = \frac{N\lambda}{2}.$$

Table I. shows the observations recorded for one of the plates for one size of the aperture. The values of depressions are plotted against the corresponding pressures. The continuous graph shows the actual depressions under different pressures, whilst the broken one represents the calculated

TABLE II.

Plate I.

t=0·0130 cm. E=5·84×10^{11} dynes per sq. cm. σ=0·316.

Side of the square.	Pressure in cms. of Hg.	Experimental depression.	Calculated depression.
1·40 cm.	11·50	5·89×10^{-3}	6·32×10^{-3}
1·45 „	10·75	6·48 „	6·79 „
1·50 „	10·80	7·36 „	7·81 „

Plate II.

t=0·0148 cm. E=5·57×10^{11} dynes per sq. cm. σ=0·316.

1·40 cm.	19·0	7·36×10^{-3}	7·41×10^{-3}
1·45 „	9·75	4·42 „	4·38 „
1·50 „	11·40	5·89 „	5·86 „
1·60 „	8·75	5.89 „	5·83 „

Plate III.

t=·0137 cm. E=5·99×10^{11} dynes per sq. cm. σ=0·320.

1·40 cm.	13·35	5·89×10^{-3}	6·09×10^{-3}
1·45 „	11·05	6·48 „	5·81 „
1·50 „	9·85	5·89 „	5·92 „
1·60 „	10·00	7·36 „	7·78 „

depressions under these pressures. It will be seen from the graph that the depressions are proportional to the applied pressure.

Table II. gives deflexions of the centre of the plate for three different plates clamped under squares of different sizes. The average deflexions for these plates have been obtained from graphs similar to the one given.

It will be seen that the experimental values of deflexions are in fair agreement with the values calculated from the

equation. The values of σ were determined by Straubel's [6] method, and those of E were determined by Wagstaff's method and also by the method of flexures.

Summary.

1. A mathematical formula for the depression of the centre of a square plate clamped at the boundaries and subjected to a uniform pressure over a face has been worked out.

2. This formula agrees with experiments performed on thin microscopic cover-slips.

References.

(1) Crelle's Journ. Bd. 135, p. 1 (1909).
(2) C. G. Knott, Proc. Roy. Soc. Edinb. xxxii. p. 390 (1912).
(3) A. E. H. Love, 'Theory of Elasticity,' 3rd ed. pp. 298, 310.
(4) A. E. H. Love, 'Theory of Elasticity,' 3nd ed. ch. xii.
(5) J. E. P. Wagstaff, Proc. Camb. Phil. Soc. xxi. p. 14 (1922).
(6) Cl. Schäfer, Mechanik, i. p. 540 (1922).

Physics Department,
Royal Institute of Science,
Bombay.
February 27, 1932.

LXIV. *Theory of Heat Conduction and Convection from Tall Hot Vertical Cylinders and High Walls at Uniform Temperature.* *By* W. S. Kimball *and* W. J. King *.

1. *Introduction.*

THIS paper is a theory of heat transfer from hot high walls and tall cylinders in air, being an extension of the analysis that has been recently † made of heat flow from hot vertical planes less than two feet high. This previous theory interpreted experimental data ‡ giving actual air temperatures and velocities near a small hot plate. The present theory interprets experimental data § on heat transfer from high walls and tall cylinders at a series of temperature excesses by E. Griffiths and A. H. Davis.

* Communicated by the Authors.

† W. S. Kimball and W. J. King, "Theory of Heat Conduction and Convection from a Low Hot Vertical Plate," Phil. Mag. xiii. p. 888 (1932).

‡ E. Schmidt, *Zeits. des Gesamte Kalte-Industrie*, Nov. 1928, p. 213.

§ E. Griffiths and A. H. Davis, Food Inv. Bd., Rept. no. 9 (1922). H.M. Stationery Office.

Previously it was assumed that heat transfer took place by pure conduction through gas in stream-line motion. And it was this assumption that restricted the applicability of the theory to low vertical plates not more than about two feet high. For experiment* shows that above this limiting height turbulence sets in and an entirely different state of affairs obtains.

This theory for low vertical hot plates has already been extended† to include short vertical hot cylinders. The previous assumption of heat transfer by pure conduction through gas in stream-line motion was maintained, thereby restricting the applicability of the theory to short cylinders under a height of about two feet.

Both for the short cylinders and the low hot plate, the theory accounts for the known laws of heat transfer and checks all available data to a satisfactory degree of accuracy.

A special study was made of occurrences inside the isothermal surface at temperature half-way between the hot body and the ambient air :

$$T_m = \frac{T_1 + T_0}{2}.$$

This isothermal included a layer or film of air whose thickness coincided at the top of the plate with the well-known Langmuir film of uniform thickness, and within this film opposite the hot plate the temperature was given empirically by

$$T = T_1 - ax(1 + be^{-\alpha y}),$$

where a, b, and α are constants. And the thickness of this film with isothermal boundary is given by solving the above temperature equation for x, taking

$$T = T_m = \frac{T_1 + T_0}{2}; \qquad x = \frac{T_1 - T_0}{2a(1 + be^{-\alpha y})}.$$

Two new empirical laws were found to apply to the stream-line conditions that prevail opposite vertical hot surfaces of such small heights :

Law I. The locus of the maxima of the convection velocity curves, one for each height y opposite the hot

* E. Griffiths and A. H. Davis, *loc. cit.*

† W. S. Kimball and L. D. Childs, "Theory of Heat Conduction and Convection from Short Hot Vertical Cylinders," Phil. Mag. xiv. p. 337 (1932).

body, is an isothermal surface whose temperature is half-way between that of the hot body and that of the ambient air.

Thus fig. 1 shows how the maxima of the velocity curves all lie on the isothermal film boundary.

Law II. Half the heat is convected up away inside the film, and half outside.

At any height, y (disregarding those near the bottom affected by end conditions), this law may be checked by graphical integration.

Fig. 1.

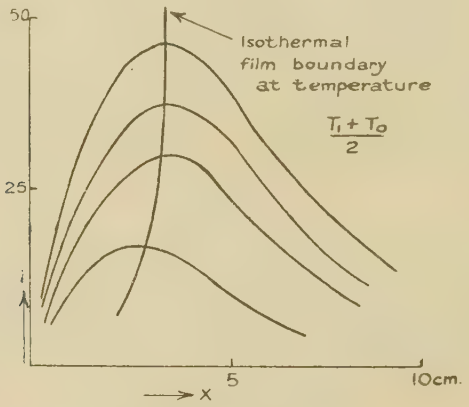

Thus, referring to Schmidt's * graphs, we can tabulate the temperature, velocity, etc., for different squares numbered from the left, out from the hot plate (Table I.).

The sums on the right, when multiplied by $\frac{3}{2}p$, are

$$\Sigma \frac{3}{2} pv \frac{T-T_0}{T} = \Sigma \frac{3}{2} k(T-T_0)nv,$$

using the gas law $p=nkT$. And this is seen to be the upward flux of heat since $\frac{3}{2}k(T-T_0)$ is the heat supplied to a molecule by the hot plate and n is the number per c.c. and v is the vertical velocity (horizontal velocities are neglected).

* E. Schmidt, *loc. cit.*

The equivalence of the two sums, then, shows that equal amounts of heat are disposed of inside and outside the film by vertical convection currents. Likewise, Law II. may be checked at the top of Schmidt's 25 cm. square hot plate, as shown by the table at the end of our previous paper *.

Using these empirical laws, the analysis is based on the simplified equations of hydrodynamics as applied to viscous fluid in stream lines, neglecting inertia effects, second order velocity effects, horizontal velocities, and using the gas law :

$$\eta \frac{d^2v}{dx^2} = mg(n-n_0), \quad . \quad . \quad . \quad . \quad . \quad (1)$$

TABLE I.

For $y=12{\cdot}5$, half-way up the plate.

No. of square.	Abs. temp.	Temp. dif.	Vel.	$\frac{T-T_0}{T}$.	$V\frac{T-T_0}{T}$.	Sum.
1	379	87·5	8	·230	1·845	
2	365	74·5	24	·204	4·90	10·496
First 3(3/4)	350	58·5	30	·167	3·75	
Last 3(1/4)	343	51·5	31	·150	1·16	
4	336	44·5	29·5	·135	3·90	
5	323	31·5	26	·098	2·54	
6	313	21·5	21	·069	1·44	
7	304	12·5	17·5	·041	·72	10·494
8	300	8·5	14	·0273	·396	
9	296	4·5	11	·0152	·167	
10	295	3·5	9	·0118	·107	
11	294	2·5	8	·008	·064	

η = viscosity coefficient,
m = molecular mass,
g = acceleration of gravity,

n, n_0 are the number of molecules per c.c. when temperature is T and T_0;

and the equation of heat flow by pure conduction :

$$q = -K\frac{\partial T}{\partial x}, \quad . \quad . \quad . \quad . \quad . \quad . \quad (2)$$

* Kimball and King, *loc. cit.*

q = heat flux through unit area in unit time, and
K = conductivity coefficient.

All the known heat transfer laws and the known data for vertical plates of small height are checked by the results of the analysis *, which gives for the important constant a,

$$a = \left(\frac{p^2 mg(T_1 - T_0)}{28k\eta T_0 T_1^2 (1 + be^{-aL})^3 KL}\right)^{1/4} (T_1 - T_0) \quad . \quad (3)$$

and hence for the heat transfer coefficient h_c, defined by

$$q = h_c(T_1 - T_0) = -K\frac{\partial T}{\partial x} = Ka(1 + be^{-ay}), \quad . \quad (4)$$

$$h_c = \frac{Ka}{T_1 - T_0}(1 + be^{-ay})$$

$$= K^{3/4}\left(\frac{p^2 mg(T_1 - T_2)}{28k\eta T_0 T_1^2 (1 + be^{-aL})^3 L}\right)^{1/4}(1 + be^{-ay}).$$

Stream-line conditions and conduction across them may thus be considered established for vertical bodies of small height.

It should be noted that Laws I. and II. and the above theory were developed with a check-up on experimental data where the temperature excess † was about 100° C. There is evidence (see Griffiths and Davis's fig. 6) ‡ that they also hold for hot vertical plates with small temperature drop, but this needs further testing.

2. *Law III.*

For tall vertical hot bodies, we begin by laying down a new and third empirical law to build on:

Law III. Above the limiting height Y (beyond which turbulence is presumably established), the rate of heat transfer is constant and equal to the average rate of heat transfer below this limiting height.

The significance of this law becomes clear by examination of fig. 2, which is the graph (Griffiths and Davis's fig. 12) showing variation of heat transfer coefficients with height y

* E. Schmidt, *loc. cit.*
† E. Schmidt, *loc. cit.*
‡ Griffiths and Davis, *loc. cit.*

opposite a heated vertical wall 9 ft. high. If the straight vertical part of the graph is extended by a dotted line it will be seen that the two areas included between the smooth curve and the dotted line are approximately equal. Hence

Fig. 2.

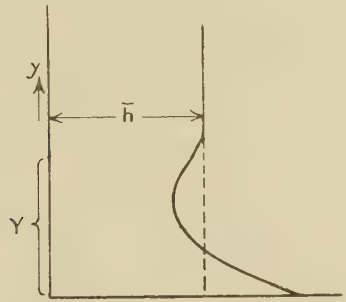

the average value of h below Y equals the constant value that it has above Y, where turbulence sets in:

$$\bar{h} = \frac{1}{Y}\int_0^Y h\,dy = h \text{ (above Y)}. \quad . \quad . \quad . \quad (5)$$

Fig. 3.

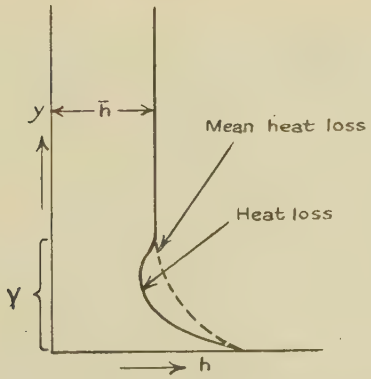

This law is also verified by Griffiths and Davis's data on heat transfer from vertical cylinders, as shown in fig. 3 (fig. 18, Griffiths and Davis's report). The smooth curve gives the heat transfer coefficient at each elevation y from the bottom. The dotted curve gives the *mean* heat transfer

coefficient for a cylinder of total height y. These are seen to coincide above the limiting height $Y = 2$ feet. This, of course, would be impossible unless h in this upper region was equal to $\bar{h}$, the mean value of the heat transfer coefficient for the corresponding height.

A further qualitative corroboration of Law III. is to be found in Koch's recent paper * on heat transfer from different sized cylinders heated at a *uniform rate* over all the surface for a series of tests. He finds that above a limiting height of about 2 ft. = Y, the cylinders have a uniform temperature, as shown graphically in his figs. 32–39, indicating a constant heat transfer in this upper region. Furthermore, he finds that this constant temperature is the mean temperature of the cylindrical surface (see his p. 23), just as, according to Law III., the constant heat transfer coefficient in this region is also the mean value of the heat transfer coefficient over the entire height of the cylinder, as found by Griffiths and Davis. This is merely qualitative corroboration, since it refers to a somewhat different state of affairs.

Since the values of h above the Y shown in the graphs are equal to $\bar{h}$, it is obvious that (5) holds good for any upper limit Y, provided that limit is not below the place indicated in the graph, *i. e.*, Y can be taken anywhere in the region where h equals $\bar{h}$ where the steady uniform turbulent state is established.

3. *Above the Limiting Height*, Y, *the Isothermal Surface of Half Temperature Drop is at Uniform Distance from the Hot Surface and Coincides with the Langmuir Film Boundary.*

An examination of Griffiths and Davis's table 6, giving temperature and velocity distribution opposite a 9-foot wall, shows that the temperature distribution at ·5 cm. from the wall becomes uniformly 36° above heater number 20, which is at almost exactly height $Y = 2$ ft. above the bottom. Furthermore, the slope of the temperature curves is probably constant † near the hot wall, so we may calculate by simple proportion the distance from the wall at which occurs the half temperature drop from hot wall to ambient air. We have

$$59° - 36° = 23° = \text{temperature drop for } \cdot 5 \text{ cm.}$$

* W. Koch, "Bei hefte zum Gesundheits," *Ingenieur*, Sr. i. Heft. 22 (1927).

† Kimball and King, *loc. cit.*

$$\frac{T_1-T_2}{2} = \tfrac{1}{2}(59°-20°) = 19{\cdot}5° = \text{half temperature drop.}$$

$$\frac{x}{{\cdot}5} = \frac{19{\cdot}5°}{23°} \qquad x = {\cdot}42 \text{ cm.}$$

This numerical value ·42 cm. approximates the known thickness of the Langmuir film opposite a hot vertical wall. Hence we see that above the limiting height Y, the film bounded by the isothermal surface of half temperature drop coincides with the Langmuir film.

This conclusion is confirmed unavoidably when we consider

$$T = T_1 - ax(1+be^{-ay}), \quad . \quad . \quad . \quad . \quad . \quad (6)$$

in connexion with Griffiths and Davis's table 6. We have seen* that this temperature expression applies inside the film to the stream-line conditions at the lower part of the plate and that it reduces to

$$T = T_1 - ax \quad . \quad . \quad . \quad . \quad . \quad . \quad (7)$$

at the upper part of this region as the limiting height Y = 2 ft. is approached. Now table 6 (Griffiths and Davis) shows, as nearly as can be judged, that there is no appreciable change in the temperature distribution inside a 5-millimeter layer all the way from two feet up to the top of the 9-foot wall. Therefore the expression (7), demonstrated by the previous theory † to be the temperature distribution approached at the top of the stream-line conditions at the lower part of the plate (about two feet up), is required apparently by the data of table 6 (Griffiths and Davis) to be the empirical temperature expression inside the film from two feet up to the top of the 9-foot wall.

Furthermore, the thickness of the isothermal film given by solving (6) for x, taking

$$T = T_m = \frac{T_1+T_0}{2}$$

$$x = \frac{T_1-T_0}{2a(1+be^{-ay})}, \quad . \quad . \quad . \quad . \quad . \quad (8)$$

was shown ‡ to give the thickness of the Langmuir film in the upper region where the exponential term is negligible:

$$x = d = \frac{T_1-T_0}{2a} \quad . \quad . \quad . \quad . \quad . \quad . \quad (9)$$

* Kimball and King, *loc. cit.*
† Kimball and King, *loc. cit.*, eq. (1).
‡ Kimball and King, *loc. cit.*, eq. (1).

Now Law III. shows that heat transfer coefficients h above two feet are the same as the mean value of these, $\bar{h}$ below this region, which latter determine the above Langmuir film thickness in the lower region. Hence the rate of heat transfer above two feet cannot alter the thickness of the Langmuir film, which is determined by the h's averaged over the entire region, being $\bar{h}=h$ in the upper region. Hence we conclude that both (7) and (9) apply to the upper region where turbulence is established. Comparison of (7) and (9) shows that in this region the constant value of x given by taking

$$T = \frac{T_1+T_0}{2}$$

is the Langmuir film thickness given by (9). Thus the Langmuir film boundary is, in the upper region, at temperature half-way between hot surface and ambient air.

4. *Generalization and Limitations of Law I.*

Combining section 3 with Law I. for hot bodies of small height, we find that the correct generalization is:

> *The isothermal surface at half temperature drop, between vertical hot body and ambient fluid*, is: (*a*), above the limiting height Y = 2 ft., where turbulence is established, *the boundary of a film of constant thickness which coincides with the Langmuir film*; and (*b*), below this limiting height, *the locus of the maxima of the convection velocity curves.*

Examination of table 6 (Griffiths and Davis) shows that for values of y = height *above* the limiting height Y = 2 ft. the maxima of the velocity curves is much farther from the wall than the ·42 cm., where the half temperature drop uniformly occurs. It is only below Y that the maxima of the velocity curves lie on the isothermal surface under consideration, that determines the boundary of the isothermal film.

5. *Limitations of Law II.*

It can readily be shown by graphical integration that Law II. probably is restricted in its application to heights below about two feet.

Thus, referring again to table 6 (Griffiths and Davis), we may tabulate the data for height $4\frac{1}{2}$ ft. (Table II.), corresponding to heater number 13.

When multiplied by $\frac{3}{2}p$ the sums on the right give the heat flux, as shown above (see p. 572). The maximum velocity appears to be at about one centimeter out. Between this and 5 cm. the sum 4·225 indicates much more heat flux than 2·66 within 1 cm., and, furthermore, we have not considered the heat flux outside 5 cm. which is not negligible. Thus Law II. does not apparently apply at this height.

Likewise, the same procedure for $y=9$ ft., which is the top of the wall, indicates that the half-way point for energy flux is between 3 cm. and 4 cm. out from the wall.

According to the data given, this seems clearly to be 2 or 3 cm. beyond the place of maximum velocity (about

TABLE II.

Distance out.	T.	$T-T_0$.	Velocity.	$\frac{T-T_0}{T}$.	$\frac{T-T_0}{T}$ V.	Sum.
1/4	320·5	27·5	35	·0858	1·50	2·66
3/4	307	14	51	·0455	1·16	
2	304	11	50	·0362	1·31	4·225
3	302	9	43·5	·0298	1·295	
4	300·5	7·5	37·5	·0249	·935	
5	299·5	6·5	31·5	·0217	·685	

1 cm. out). Therefore we infer that Law II. applies only below the critical height where turbulence sets in.

6. *The Mechanism of Heat Transfer Above the Limiting Height* Y = 2 *ft.*

By definition, the Langmuir film is one of such thickness d, that if its outer boundary were at the ambient temperature T_0, then the actual heat transferred could be accounted for by pure conduction across an included stationary film of gas. That is to say, speaking mathematically (for a wall of unit area),

$$q = K\frac{T_1-T_0}{d} \quad . \quad . \quad . \quad . \quad . \quad . \quad (10)$$

defines the Langmuir film thickness d, since the other quantities are all measurable. For the actual *half* tempera-

ture drop, with constant temperature gradient within the film, the heat flux that can be accounted for by conduction actually is

$$q_c = \mathrm{K}\frac{\mathrm{T}_1-\mathrm{T}_0}{2d} = \frac{q}{2}. \quad . \quad . \quad . \quad . \quad . \quad (11)$$

Comparison of (10) and (11) shows the remarkable fact that exactly half the heat transferred is to be accounted for by pure conduction along the actual constant temperature gradient within the film. The other half is presumably due to some mechanism of heat transfer involved in turbulence.

Now the empirical expression for temperature at the lower part of the hot wall,

$$\mathrm{T} = \mathrm{T}_1 - ax(1+be^{-ay}), \quad . \quad . \quad . \quad . \quad . \quad (6)$$

becomes, as we saw above in section 3, up above Y where the exponential term is negligible,

$$\mathrm{T} = \mathrm{T}_1 - ax. \quad . \quad . \quad . \quad . \quad . \quad . \quad (7)$$

Hence, the heat transfer by conduction is

$$q_c = -\mathrm{K}\frac{d\mathrm{T}}{dx} = \mathrm{K}a = h_c(\mathrm{T}_1-\mathrm{T}_0) \quad . \quad . \quad . \quad (12)$$

The partial heat transfer coefficient h_c involved in (12) is exactly the expression (4) for pure conduction for values of y larger than Y where the exponential term is negligible. Hence, we conclude that (4) holds everywhere opposite the hot wall so far as heat transfer by pure conduction is concerned. The difference between h and h_c may be shown graphically by reproducing fig. 12 (Griffiths and Davis) (see fig. 4), which gives h as a function of the height y. The dotted curve is added to represent

$$h_c = \frac{\mathrm{K}a}{\mathrm{T}_1-\mathrm{T}_0}(1+be^{-ay}).$$

Notice that h_c above Y is half of h, and the differences are attributed to turbulence.

7. *Proof of the Relation,*

$$\mathrm{H} = \frac{b}{a}(1-e^{-a\mathrm{H}}).$$

Below the turbulent region and where heat is transferred by pure conduction, the h involved in (5) is equal to h_c, as shown in fig. 4. Now we substitute h_c in place of h in

(5) and consider what changes in the limits of integration are required to maintain the relation :

$$\bar{h} = h \text{ (above Y)} = \frac{1}{Y}\int_0^Y h dy = \frac{1}{H}\int_0^H h_c dy. \quad . \quad (13)$$

The object of this procedure is to find what condition is imposed on (4), which is h_c, by Law III. Eq. (5) does not serve this purpose as it stands, since the h involved in (5) is an unknown h, distinct from h_c, and one for which we have no mathematical expression.

A glance at fig. 5 shows that the right-hand integral of (13) will equal $\bar{h}$ as required provided the shaded areas are

Fig. 4.

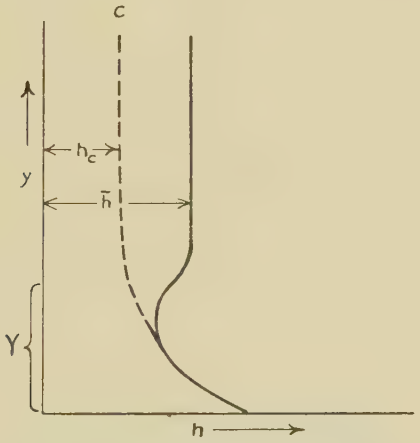

equal, because in this case the areas included on opposite sides of the straight line $h = \bar{h} =$ constant, between this vertical line and $\bar{h}$, will be equal (with the help of Law III.).

This H will be somewhere near the point of inflexion of the h curve, and the shaded areas mark the gradual transsition from the state of pure conduction through stream-line flow below the shaded portion, to the "steady" turbulent state above it. Now evaluate the integral on the right hand of (13), using (4) :

$$\bar{h} = \frac{Ka}{H(T_1 - T_0)}\int_0^H (1 + be^{-ay})dy \quad . \quad . \quad . \quad (14)$$

$$= \frac{Ka}{H(T_1 - T_0)}\left(H + \frac{b}{a}(1 - e^{-aH})\right).$$

From (10), (11), and (12), however, we have

$$\left.\begin{aligned} q &= 2q_c = 2\mathrm{K}a = \bar{h}(\mathrm{T}_1-\mathrm{T}_0) \\ \text{or} \qquad \bar{h} &= \frac{2\mathrm{K}a}{\mathrm{T}_1-\mathrm{T}_0}. \end{aligned}\right\} \quad . \quad . \quad . \quad (15)$$

Comparison of (14) and (15) shows that

$$\mathrm{H} = \frac{b}{a}(1-e^{-a\mathrm{H}}). \quad . \quad . \quad . \quad . \quad . \quad (16)$$

Fig. 5.

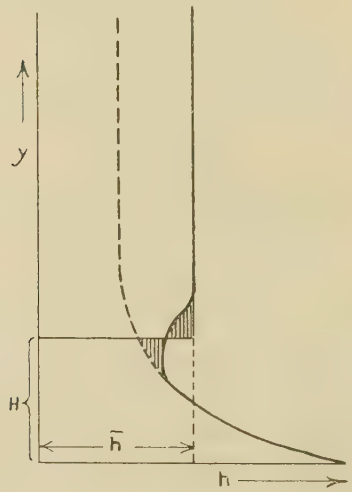

A contrast between (5), which is the middle member of (13), and the right member of (13) is especially to be noted. Eq. (5) holds good for any limit $y=\mathrm{Y}$ above the region where $h=\text{constant}=\bar{h}$. On the other hand, the limit H in the right member of (13) is uniquely determined by the condition that the shaded areas must be equal. This H is a really critical height, whereas Y can be any value of y above the place where turbulence is established and is necessarily greater than H. In fact, H is the lower limit that Y would have if turbulence set in discontinously with a sudden jump.

The relation

$$\mathrm{L} = \frac{b}{a}(1-e^{-a\mathrm{L}}), \quad . \quad . \quad . \quad . \quad . \quad (17)$$

used previously * in case of low walls of height L, with stream-line conditions opposite them, is thus now definitely shown in case of high walls to be exact for the critical height H, that separates the stream-line conditions below from turbulence above.

8. *The Five-fourths Power Law for High Walls.*

If we use the relation (16) which applies to high walls, in place of (17), the corresponding change in "a" given by (3) is found by substituting H in place of L. Thus:

$$a = \left(\frac{p^2 mg(T_1 - T_0)}{28k\eta T_0 T_1^2 (1 + be^{-\alpha H})^3 (HK)}\right)^{1/4} (T_1 - T_0), \quad . \quad (18)$$

and for high walls:

$$\bar{h} = \frac{2Ka}{T_1 - T_0} = 2\left(\frac{p^2 mg(T_1 - T_0)K^3}{28k\eta T_0 T_1^2 H(1 + be^{-\alpha H})^3}\right)^{1.4}, \quad . \quad (19)$$

and for the total heat flow per unit width and height L:

$$Q = \bar{h}(T_1 - T_0)L = 2L\left(\frac{p^2 mg(T_1 - T_0)K^3}{28k\eta T_0 T_1^2 H(1 + be^{-\alpha H})^3}\right)^{1/4} (T_1 - T_0),$$

. . . (20)

according to the five-fourths power law.

9. *Vertical Cylinders.*

Apparently no measurements of temperature drop and convection velocity around vertical hot cylinders have been made, since no such data appears in the literature.

Until such measurements are made, the question of whether Laws I., II. apply to vertical cylinders cannot be positively settled in all detail. Nevertheless, we note that large cylindrical surfaces approximate a plane surface. Hence, we conclude that these laws in their present form certainly do apply to large cylinders, unless the foregoing data and analysis for plane surfaces is wrong. Law III., however, is better established for vertical cylinders than for vertical planes. Griffiths and Davis's tables 8 A and 8 B, together with the graphs of their figs. 15 and 18, show that this law holds good over a large range of temperature excess (10° to 100°) as well as for various heights of cylinder up to 9 ft.,

* Kimball and King, *loc. cit.*, eq. (14); Kimball and Childs, *loc. cit.*, seq. (22), (23).

and seem to justify its being called a "law". All these data refer, however, to cylinders of 17·43 cm. diameter.

Since the five-fourths power law holds equally well for vertical cylinders and planes, and there is much data on heat transfer coefficients of the same kind for planes and cylinders, it seems likely that Laws I. and II. hold as well as Law III. for vertical cylinders—at least to a certain degree of approximation.

Hence, we have employed the theory developed by Kimball and Childs* for cylinders shorter than the critical height H. Combining this with Law III., which certainly applies at least to cylinders of diameter 17·43 cm., we may calculate the heat dissipated by cylinders and develop formulas analagous to (19) and (20) for tall cylinders, which can be checked by available data.

Thus the heat transfer by pure conduction is given for a cylinder of radius r_0 by (Kimball and Childs, eq. (38)):

$$h_c = \frac{\mathrm{K}a(1+be^{-ay})}{r_0(\mathrm{T}_1-\mathrm{T}_0)} \quad . \quad . \quad . \quad . \quad . \quad . \quad (21)$$

Above the critical height H, the exponential term vanishes, and the resulting simplified form of (21) has to be doubled in accord with (11) and (15), since the actual heat transfer is twice that due to pure conduction:

$$\bar{h} = \frac{2\mathrm{K}a}{r_0(\mathrm{T}_1-\mathrm{T}_0)} = \left(\frac{\mathrm{K}^3p^2mg(\mathrm{T}_1-\mathrm{T}_0)\mathrm{M}}{k\eta\mathrm{T}_0\mathrm{T}_1^2\mathrm{H}(1+be^{-a\mathrm{H}})^3}\right)^{1/4}; \quad (22)$$

here †

$$a = r_0(\mathrm{T}_1-\mathrm{T}_0)^{5/4}\left(\frac{p^2mg\mathrm{M}}{16k\eta\mathrm{T}_0\mathrm{T}_1^2\mathrm{KH}(1+be^{-a\mathrm{H}})^3}\right)^{1/4}, \quad (23)$$

and M is a zero dimensional series of terms that depends on the temperatures T_1 and T_0, and $x_\mathrm{L} = \log\frac{r_\mathrm{L}}{r_0}$, the logarithm of the ratio of the Langmuir film radius r_L to the radius r_0 of the cylinder.

The total heat given off by a cylinder of radius r_0 and height L is then

$$\begin{aligned} \mathrm{Q} &= 2\pi r_0\mathrm{L}\bar{h}(\mathrm{T}_1-\mathrm{T}_0) \\ &= 2\pi r_0\mathrm{L}\left[\frac{\mathrm{K}^3p^2mg\mathrm{M}}{k\eta\mathrm{T}_0\mathrm{T}_1^2\mathrm{H}(1+be^{-a\mathrm{H}})^3}\right]^{1/4}(\mathrm{T}_1-\mathrm{T}_0)^{5/4}. \quad (24) \end{aligned}$$

* Kimball and Childs, *loc. cit.*

† Kimball and Childs, *loc. cit.*, eq. (27).

10. *Characteristics of the Critical Height* H.

(*a*) Below H, the isothermal of half temperature drop is the locus of the maxima of the convection velocity curves—(Law I.)

Above H, the isothermal of half temperature drop is the boundary of the Langmuir film, and is of uniform distance from the hot body, and the maxima of the velocity curves are outside of it.

(*b*) Below H, half the heat is convected up away inside the film boundary (of half temperature drop, and maximum velocity locus), and half outside of it—(Law II.).

Above H, the half-way point for energy convection is outside of the locus of maximum velocity, as well as outside the isothermal of half temperature drop.

(*c*) Below H, stream line conditions prevail and the heat transfer takes place all by pure conduction, and decreases exponentially with increase of height up to the critical H :

$$h_c = \frac{\mathrm{K}a}{\mathrm{T}_1 - \mathrm{T}_0}(1 + be^{-ay}).$$

Above H, the heat transfer takes place horizontally and seemingly half by conduction and half by some mechanism presumably due to turbulence. And the rate of the combined process is exactly equal (per unit area) to the *average* rate per unit area below H—(Law III.).

(*d*), (*a*) and (*c*) together lead to the mathematical relation

$$\mathrm{H} = \frac{b}{a}(1 - e^{-a\mathrm{H}}).$$

(*e*) No explanation is offered as to why turbulence sets in at height H, which seems to be about 40 centimetres.

(*f*) The critical height H seems to be about the same for all vertical cylinders and for vertical plates, and all usual temperature excesses.

(*g*) The critical height H is near the point of inflexion of the h graph, at such a position that the two indicated shaded areas on opposite sides of the h curve are equal (see fig. 5). This is obviously (see sec. 7) required to make

$$\frac{1}{\mathrm{H}}\int_0^{\mathrm{H}} h_c\,dy = \bar{h},$$

according to Law III. The gradual change of h from h_c to $\bar{h}$ around the shaded areas shows the gradual transition from the state of pure stream line flow to the turbulent state above H.

11. *Experimental Check.*

The relation between the constant a and $x_L = \log \frac{r_L}{r_0}$ is given (eq. (34), Kimball and Childs) by

$$a = \frac{T_1 - T_0'}{2 \log \frac{r_L}{r_0}} = \frac{T_1 - T_0}{2x_L}. \quad . \quad . \quad . \quad . \quad (25)$$

Substituting in (22) gives

$$\bar{h} = \frac{K}{r_0 x_L} = \frac{K}{r_0 \log \frac{r_L}{r_0}}. \quad . \quad . \quad . \quad . \quad . \quad (26)$$

Comparison of the right member of (22) with (26) gives $r_0 x_L$ in terms of the physical constants plus H, the empirical critical height separating stream-line conditions from turbulence. By first calculating this $r_0 x_L$, we may then calculate h for a series of r's and temperature excesses, and plot the relation between them. We take:

$H = 40$ cm.,

$1 + be^{-\alpha H} =$ unity, approximately,

$T_0 = 293°$,

$m = 28(1{\cdot}66)10^{-24} =$ mass of an air molecule,

$p = 1{\cdot}013 \times 10^6 =$ pressure in dynes/cm.^{2},

$K = 1{\cdot}37 \times 10^{-16} =$ Boltzmann's constant;

and, by a somewhat lengthy computation, using (26), obtain theoretical values of $\bar{h}$ in terms of r_0 and $T_1 - T_0$, which we have plotted in fig. 6. The procedure follows.

The values of M are tabulated in Table III., using (26) in Kimball and Child's paper, and taking $L = H = 40$ cm. for various values of temperature excess $T_1 - T_0$ and $x_L = \log \frac{r_L}{r_0}$, taking $T_0 = 293°$.

The tabulated values of the G's (Kimball and Childs, table i.) and M's enable us to calculate $r_0 x_L$ according to (41) Kimball and Childs as the fourth root of the ratio G/M. For each $T_1 - T_0$, with the help of (26) we can now get a series of values for r_0, the radius of the cylinder, and the corresponding heat transfer coefficient h, and graph the relation between them. Thus, for $T_1 - T_0 = 40°$, we have as Table IV.

TABLE IV.

$T_1 - T_0 = 40°$. K = 2510 in c.g.s. units.

$x_L = \log \frac{r_L}{r_0}$.	$r_0 x_L = \left(\frac{G}{M}\right)^{1/4}$.	$r_0 = \frac{r_0 x_L}{x_L}$, in cm.	$h_e = \frac{K}{r_0 x_L}$, c.g.s. units.	$h = \frac{h_e}{4 \times 10^7}$, cal./cm.²/sec.	$q = h(T_1 - T_0) = 40\,h$ cal./cm.²/sec.	$h_K = 36000\,h$ k.c./m.²/h.	
·6	·369	·615	6800	$·17 \times 10^{-3}$	$·68 \times 10^{-2}$	6·01	
·5	·397	·794	6320	·158 „	·632 „	5·68	
·4	·422	1·06	5950	·149 „	·595 „	5·35	
·3	·453	1·51	5540	·139 „	·554 „	4·98	Koch
·25	·470	1·88	5340	·134 „	·534 „	4·60	(3·17)
·2	·489	2·45	5130	·128 „	·513 „	4·36	(3·13)
·17	·497	2·92	5050	·126 „	·505 „	4·33	
·14	·506	3·62	4960	·124 „	·496 „	4·30	
·1	·518	5·18	4840	·121 „	·484 „	4·28	
·09	·521	5·8	4815	·120 „	·4815 „		
·08	·524	6·55	4790	·1198 „	·479 „		
·07	·5275	7·54	4760	·119 „	·476 „		
·06	·530	8·83	4730	·1183 „	·473 „		
·05	·532	10·64	4720	·118 „	·472 „		
·04	·534	13·3	4700	·1175 „	·470 „		
·03	·537	17·9	4675	·117 „	·467 „		
·02	·540	26·97	4650	·116 „	465 „		

The fourth column gives the heat transfer coefficient in ergs per square centimeter per degree per second. The fifth column gives it in calories, and the seventh in kilogram calories per square metre per degree per hour. The latter compare favourably with data on various sized cylinders observed by Koch and given in parenthesis.

Likewise we have tabulated the relations between r_0 and h for the other twelve temperature differences and plotted

Fig. 6.

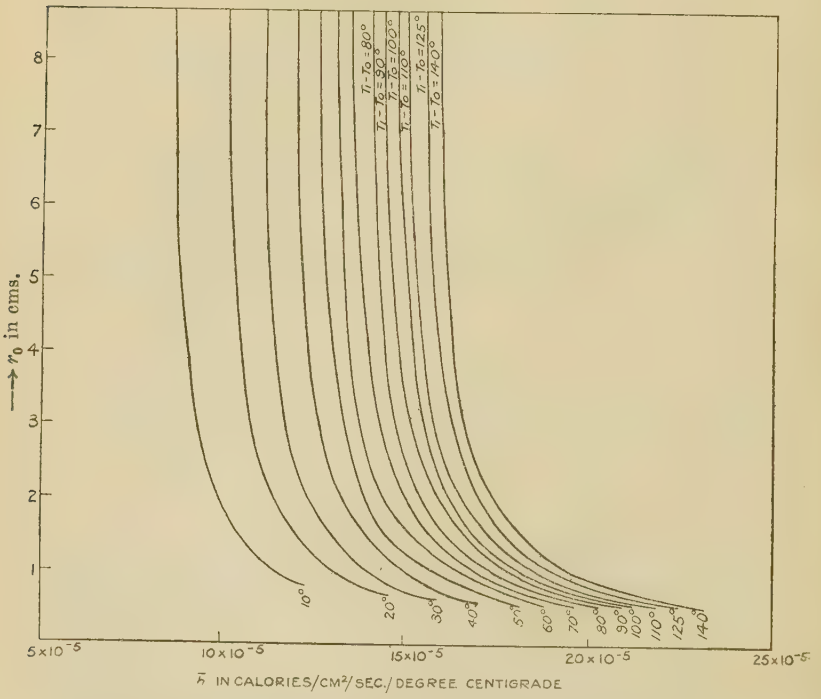

each in the accompanying graph (fig. 6). The heat transfer coefficients, in cals/cm.^{2}/deg./sec. are plotted as abscissas against the radius r_0 of the cylinder as ordinate, and the parameters are the temperature differences.

Since the horizontal line that bounds the figure at the top cuts those graphs (fig. 6) at height $r_0=8{\cdot}7$, the points of intersection of this line with the curves, give the heat transfer coefficients for cylinders of radius 8·7 or diameter 17·4. These when multiplied by the temperature differences give $q=h(T_1-T_0)$ the heat in calories transferred per cm.^{2}

per sec. These are tabulated below (Table V.) and compared with the data given by Griffiths and Davis, table 8 A. It is to be remembered that these data refer to the mean heat transfer coefficients above the limiting height $Y = 2$ ft.

It will be noted that the theoretical heat transfer is from five to seven per cent. too small for the larger temperature differences. Neglect of inertia effects within the film is sufficient to account for this as it was for the too large value of V_m in case of the hot plate. Each of these discrepancies can be accounted for by the constant "a's" being a few per cent. too small due to neglect of inertia effects. If this is

TABLE V.

$T_1 - T_0 =$	10°.	20°.	30°.	40°.	50°.
$q = \frac{h(T_1-T_0)}{\text{calc.}}$	$\cdot085\times10^{-2}$	$\cdot20\times10^{-3}$	$\cdot33\times10^{-2}$	$\cdot475\times10^{-2}$	$\cdot63\times10^{-}$
q observed by G. & D.	$\cdot085\times10^{-2}$	$\cdot21\times10^{-2}$	$\cdot34\times10^{-2}$	$\cdot495\times10^{-2}$	$\cdot65\times10^{-2}$

$T_1 - T_0 =$	60°.	70°.	80°.	90°.	100°.
$q = \frac{h(T_1-T_0)}{\text{calc.}}$	$\cdot78\times10^{-2}$	$\cdot945\times10^{-2}$	$1\cdot12\times10^{-2}$	$1\cdot29\times10^{-2}$	$1\cdot47\times10^{-2}$
q observed by G. & D.	$\cdot85\times10^{-2}$	$1\cdot00\times10^{-2}$	$1\cdot20\times10^{-2}$	---	$1\cdot55\times10^{-2}$

the correct explanation, then we conclude that inertia effects are of less importance where the temperature excess is smaller, since here the experimental check is fairly close.

Recent data of Koch * is in qualitative agreement with the graphs which show a marked increase in heat transfer coefficients when the radius of the vertical cylinders is smaller than about three centimetres. Table VI. shows how the theoretical values of h compare with those of Koch for four different temperature excesses, and for cylinders of four different radii.

The theoretical values of h are taken off the accompanying graph and then multiplied by 36000, so as to appear in

* W. Koch, *loc. cit.*, table 28.

Table VI. as k.c./m.²/h. for comparison with Koch's data. It will be noted that the experimental data show a marked increase in heat transfer coefficients for cylinders of small radius in much the same proportion as required by theory. Discrepancies in magnitude can be attributed to inertia effects or to the fact that Koch's data refer to a different situation from that considered here, in that his cylinders are heated at a *uniform rate* all over, instead of maintained at a uniform temperature.

TABLE VI.

$\bar{h}$ in kilogram calories per square metre per hour.

$T-T_0$.	r_0 in cm.	·7.	1·55.	3·4.	5·025.
140°	h_{ex}	9·4	7·66	6·02	7·15
	h_{th}	7·75	6·53	5·925	5·8
125°	h_{ex}	8·78	—	—	7·03
	h_{th}	7·46	—	5·8	5·66
90°	h_{ex}	8·40	—	3·85	
	h_{th}	6·94	—	5·4	
40°	h_{ex}	—	—	3·17	3·14
	h_{th}	—	—	4·30	4·27

12. *Conclusions.*

The theory accounts for :

(*a*) The five-fourths power law for variation of heat transfer with temperature excess for high walls and tall cylinders.

(*b*) Heat transfer coefficients are proportional to the square root of the pressure and to the fourth root of the temperature excess, and increase notably when the cylinder diameter becomes smaller than 6 cm.

(*c*) The thickness of the film varies inversely as fourth root of the temperature excess, and checks the numerical experimental value.

(*d*) Data of Griffiths and Davis on heat transfer from cylinders of radius 8·7 cm. are checked for a series of temperature excesses, due allowance being made for neglected inertia effects.

(*e*) Data by Koch on heat transfer from cylinders of different radii at a series of temperature excesses show an increase in heat transfer for smaller cylinders in just the proportions that this theory requires.

(*f*) Laws I. and II. have been checked by direct measurements only for (*a*) hot vertical planes, and (*b*) where the temperature excess was in the neighbourhood of 100° C. Until further direct tests of velocity and temperature fields are made, these laws are to be considered tentative experimental laws. On the other hand, they together lead directly to the five-fourths power law of heat transfer and other well-established conclusions covering a wide range of temperature excess and of cylinder radii. Hence these laws probably hold over the same wide range.

(*g*) Law III. is better established than Laws I. and II., it being shown by Griffiths and Davis's data to hold over a considerable range of temperature excess and height of cylinders, as well as planes. It needs testing for a series of cylinders with different radii.

(*h*) Heat transfer from tall cylinders and planes is given by theoretical formulas in terms of the known physical constants and dimensions of the case considered. Only one unknown empirical constant enters raised to the one-fourth power. This is the critical height H=about 40 cm., that separates the stream-line conditions below from the turbulent state above it. This height H seems to be about the same for planes and for all sized cylinders, and all usual temperature excesses in the case of free convection in air under consideration. Since it enters the formulæ raised to the one-fourth power, an estimated error of 8 per cent. in its magnitude will effect the results about 2 per cent.

Michigan State College, East Lansing, Michigan.
General Electric Company, Schenectady, N.Y.

LXV. *On Atoms of Action, Electricity, and Light.* *By* Sir Ambrose Fleming, *F.R.S.**

THE number of optical phenomena which seem to demand some form of corpuscular or photon theory of light are small compared with the number of those which are well explicable in terms of the classical uniform wave theory of light.

* Communicated by the Author.

When we recall to mind the very complicated and beautiful effects due to the passage of polarized light through crystals, some of which, such as conical refraction, were predicted in advance, and notice that all of these have been explained in terms of the normal wave theory as well as those of diffraction and interference generally, we see that this theory is not lightly to be discarded.

On the other hand, the phenomena which seem to require the photon or corpuscular theory are, first, the photoelectric effects, second, the ionization of gases, third, the distribution of energy in the black body spectrum, and, lastly, probably such effects as the Compton.

All the theories of light which assume propagation of vibrations along lines of force as discrete entities in various forms labour under the same difficulty as a corpuscular or photon theory, in that they can give no satisfactory explanation of the fundamental fact of interference presented at every step in optical phenomena.

On the other hand, it seems clear that some kind of atomicity is associated with radiation. In all parts of nature we see this atomicity evident, by which we mean that the entities considered are not indefinitely divisible in quantity, but that there is an ultimate minimum amount which loses its identity when divided beyond a certain point. We have that atomicity in matter complex and simple; also in electricity, with its ultimate atoms, protons, and electrons.

Again, the success of Planck's formula for the energy density of black body radiation at various frequencies shows that the dynamical quantity called Action, or the time-integral of energy, has a curious atomic structure, and that the atom of Action is Planck's constant denoted by h. With great diffidence I suggest, then, that this h should be called 1 Planck, just as the unit of electric quantity is called 1 electron.

The peculiarity of both these quantities, action and electric charge, is that they are invariant, or the numerical value of them is the same to all observers no matter how the observers are moving with respect to them. This is not the case for mass, energy, or momentum. The other notable invariant is the velocity of light.

Hence we have three fundamental quantities which are all invariant, viz., the velocity of light (c), the electron or unit of electric charge (e), and the Planck or unit of action (h).

In all those phenomena in which radiation enters or leaves a material atom in exchange for an electron which also at the same time leaves or enters the atom the exchange is conducted on the principle that the product of the radiant

energy so entering or leaving the atom multiplied by the periodic time of its vibration must be equal to the unit of action or to h or else an integer multiple of it.

The apparent atomicity of light may be therefore only a consequence of the atomicity of action and also of electricity.

It is impossible to understand how energy could travel through space in discrete separate bundles or parcels yet unassociated with atomic matter of some kind, yet nevertheless its entrance into or exit from matter may be accomplished in gushes or quanta which have definite amount, corresponding to the fact that the electric charge entering or leaving can only do so in integer multiples of the atom of electric quantity or the electron.

Moreover, radiation has intrinsically a certain kind of atomicity, in that it repeats its cycle of operations in a definite time, viz., the periodic time of the oscillation.

We have no exact knowledge as yet of the mechanism by which radiation causes an emission of an electron from an atom.

It is not a process of resonance, but takes place instantly by a sort of exlosion under certain conditions.

It may perhaps be accomplished as follows:—On the solar system theory of the structure of material atoms the orbital electrons are held on their orbits by the electric attraction between them and the nucleus.

If a wave of radiation passes through the atom it may happen that the electric force of that wave in some position or at some time neutralizes or reduces the electric force holding an electron in its orbit, and it is then flung out to a larger orbit or released entirely from the atom. To do this a certain energy must be given to the electron.

The case is similar to that of a bullet or projectile shot straight up from the earth. If the initial velocity given to the bullet is less than a certain amount it will fall back on the earth. If that velocity (v) is such that $v^2 = 2g\mathrm{R}$, where R is the radius of the earth and g the acceleration of gravity at the surface, then the bullet will just escape from the earth. That velocity v corresponds to an initial kinetic energy

$$\tfrac{1}{2}mv^2 = mg\mathrm{R} = \mathrm{WR},$$

where W is the weight of the bullet at the earth's surface. If more energy than this is imparted it is utilized in increasing the velocity of the bullet.

It may be the same with the emission of an electron from an atom of a metal. A certain energy is necessary to release

the electron, and any excess is used to give it velocity. It is usual to represent this work as the product of a certain voltage called the ionizing voltage V_0, and the electron charge in electromagnetic units, q, which is

$$1{\cdot}6 \times 10^{-20} \text{ E.M.U.}$$

For most of the ordinary metals this voltage is not far from 3·5 volts, though for the very electropositive metals it may be below 2. Thus for sodium it is 1·7 and for platinum 3·9. The product of V_0 and q is then the ionizing energy in ergs, and varies from

$$2{\cdot}72 \times 10^{-12} \text{ erg to } 6{\cdot}24 \times 10^{-12} \text{ erg.}$$

The necessary condition, however, is that the action during one period of the radiation T or product of $V_0 q$ and T must be 1 unit or 1 Planck ($=h=6{\cdot}55 \times 10^{-27}$ erg seconds).

Hence the frequency ν must have a value $V_0 q/h$ at least, and be not less than 4×10^{14} for the alkali metals and about 10^{15} for the noble metals.

This makes the wave-length for the former about 7500 Å.U., which lies within the visible spectrum, whilst for the noble metals about 3000 Å.U. in the ultra-violet part.

There is, however, one great difficulty which is the chief reason for advocating a corpuscular or photon theory of light which assumes the energy to be concentrated in certain specks or parts of the wave-front and not smoothly distributed. It is as follows :—

It is well known that a photoelectric emission of electrons can occur with an impact of radiation, the surface density of which is so low that the amount captured on the surface of a single atom is far below the known ionizing energy. Thus a surface of potassium or sodium on which light from a single candle falls at a distance of 9 or 10 feet will certainly emit photoelectrons *in vacuo*, yet this radiation is only equivalent to imparting to the surface about 1 erg per cm. sq. per sec. The apparent diameter of a metal atom may be taken as about 2×10^{-8} cm. and its area as about 4×10^{-16} cm.^{2}

Hence if the only energy which can enter the atom is that which is drawn from an area of the wave-front equal to the atomic apparent area it would require an exposure of about a quarter of an hour to such feeble light before the potassium surface could emit electrons. As a matter of fact they are emitted at once. Hence arose the conception of a concentration of light energy in certain spots or specks on the wave-front. This difficulty is mentioned in Norman Campbell's

'Modern Electrical Theory,' 2nd ed. p. 249, as justification for such modified theory.

But there are certain phenomena in connexion with wireless telegraphy which are not as well known to physicists as they should be which show that a material atom may perhaps draw energy from an area of a wave-front of radiation which is hundreds or thousands of times greater than the apparent atomic area. They are as follows :—

As far back as 1906 M. Camille Tissot, then a lieutenant in the French navy, described some quantitative experiments in radio telegraphy of the following kind *.

He constructed a transmitter in which he could measure the energy given out as radiation and by which he could

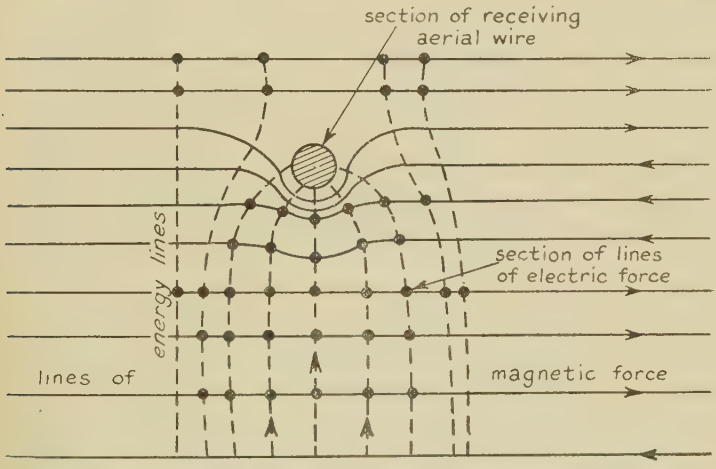

Diagram representing the nature of the electromagnetic field near a receiving aerial in wireless telegraphy.

The dotted lines represent the direction in which the energy is advancing on the aerial.

determine the radiation density at any distance near the earth's surface. He set up a single-wire receiving aerial at a known distance, and measured the radiant energy captured by this wire. If the apparent area of the aerial was A and the energy density of the wave at that point was E and its velocity *c*, it might have been thought that the aerial would only capture energy per second equal to A*Ec*. Tissot found, however, that it captured several hundred times as much.

* 'Étude de la Résonance des Systèmes d'antennes dans la télegraphie sans fils' (Gauthier-Villars, Paris, 1906), see p. 191.

He says that an aerial wire 3 or 4 mm. wide drew energy from the wave-front spread over an area of 1 or 1·5 metres in width.

Tissot gave no explanation of this fact, but it seems to the writer to be explicable as follows:—Let the small circle in the figure represent the horizontal section of the vertical aerial wire, and let the firm black lines denote the direction of the lines of magnetic force in the advancing electric wave and the small dots the section of the lines of electric force. Then, according to Poynting's Theorem, the lines along which the energy travels are perpendicular to both the lines of magnetic and electric force and are denoted by the dotted lines.

Now, when the lines of magnetic force of the wave come up against the copper aerial wire and cut through it they induce in the aerial wire electric currents which create circular lines of magnetic force round the wire, and these, combining with the magnetic force of the wave, distort the field, as shown in the figure.

It will be seen that the result of the bending of the lines of magnetic force round the aerial is to converge on it the lines of energy, so that the aerial sucks out of the wave-front energy spread over a much wider area, it may be 300 or 400 times wider than the apparent area of the receiving wire.

The suggestion may then be made that the same kind of operation takes place when an electromagnetic wave of radiation passes over an atom of matter. The atom so to speak creates a dimple in the wave-front, and so causes it to absorb energy from an area in the wave-front which may be many thousands of times greater than its own apparent area. Moreover, just as the wireless aerial must have its direction parallel to, or nearly parallel to, the direction of the magnetic vector of the incident wave in order that in may absorb energy, so in the case of the material atom there may be some axis or direction in it which must be in a certain position as regards the light vectors of the incident wave if it is to absorb radiation at all.

When it does absorb, the Action law must hold good, viz., that the energy absorbed E, multiplied by the time period T of the wave, must be equal to the Planck unit, or to h, which fixes the limit of the effective wave frequency ν, since it must not be less than E/h.

Hence these two assumptions meet the difficulty that when radiation passes through a gas or falls on a photoelectric surface it is not every atom which is ionized.

The fact that only a certain number of atoms emit electrons

may not be due to the concentration of radiation energy in small spaces on the wave-front, but to the fact that the atom is ionized only when it holds a certain position with regard to the passing wave.

The quantum absorption is due to the fact that Action is a more fundamental quantity than energy alone, and is atomic in nature.

Action is measured by the product of energy and time. We do not know why there should be a limit to the divisibility of action and a sort of atom of action denoted by h when dealing with atomic phenomena ; but then we do not know either why there should be a limit to the divisibility of electricity and an atom of it called the electron.

The importance of action as a physical quantity may arise from the fact that in the production of physical effects it is not merely energy that counts, but a certain time for its availability or use, and hence their product is fundamental ; but why there should be a lower limit to this product we cannot say.

Nevertheless this atomicity furnishes an explanation of the main fact of photoelectric emission and gas ionization, provided we also admit that for reasons above suggested the atom can absorb energy from an area vastly greater than its own apparent area.

The same principles can be used to explain the emission of radiation from an atom which has already been ionized and therefore can take up an electron.

In an incandescent black body there are free electrons moving at various speeds which may be considered to plunge into atoms down to various energy levels, and hence to lose some of their energy.

Some of these electrons enter perhaps only the outer layers of atoms, others plunge more deeply into atoms. In all cases the electrons lose energy. The sudden entrance of the electron into the family circle of the atom causes a violent disturbance of the electric field in it, and the result is to create an electromagnetic impulse which spreads out in space and conveys away the difference of the energies of the electron before and after entrance.

The probability of a feeble or "soft" impact is greater than that of a "hard" or direct or deep impact, because the latter must involve something like a "head on" collision of an electron with an atom, these impacts producing "pulses" of electric force which can, in virtue of Fourier's Integral Theorem, be expanded into continuous spectra of electric vibrations. Those that arise from "soft" collisions would

be equivalent to low temperature spectra, and those from "hard" collisions would be high temperature spectra.

In each of these spectra the energy of various wave-lengths would be distributed in accordance with Wien's Law and be a maximum for some wave-length λ_m, such that $\lambda_m K$ would be a constant $=0{\cdot}294$, where K is absolute temperature. Wien's Law has been demonstrated by thermodynamic reasoning and also from "dimensions" without calling for any assumption of light quanta or photons (see 'The Quantum Theory,' Fritz Reiche, p. 128). Hence we might say that the result of such complex collisions of electrons and atoms would be to yield a radiation equivalent to a vast number of superimposed spectra, very many with small maximum energy near or beyond the red end, a few with large maximum energy near the violet end, and others in between, the resulting integral spectrum having therefore maximum energy corresponding to some definite wave-length.

If we knew the form of graph of each pulse of electric force and the form of the function in Wien's formula which connects radiation energy for each wave-length with the wave-length, it would be possible to determine the energy distribution according to wave-length in the final or resultant spectrum for the incandescent black body.

In default of this knowledge Planck was obliged to proceed by a more tentative or artificial method. He assumed that the radiation took place from ideal Hertzian oscillators which could contain or radiate energy only in an integer number of "quanta" proportional in energy to their frequency, and that the probability of their containing small quanta was greater than their probability of containing large quanta.

Then, assuming that the relation of frequency ν and quantum energy E was $E=h\nu$, where h is some constant, which proved to be of the dimension of action, he was able to arrive at his well-known formula for the energy of radiation at various wave-lengths of a black body. Experiment has shown that it agrees extremely well with the facts over a wide range of temperature; nevertheless it does not give any absolute proof of the existence of these energy quanta in space during the transmission of light.

The ordinary classical theory of radiation cannot, however, account for the existence of a maximum energy radiation at some wave-length intermediate between very long and very short waves which does occur.

It is clear, however, that the basic fact is not the division of radiant energy into "quanta," but the unexpected appearance of an atomic quality in that dynamical quantity we

call Action. This seems to imply that there is an ultimate limit to the divisibility of each of the two factors, energy and time, the product of which gives action, and this may be the consequence of a more fundamental atomicity, viz., that neither time nor space is infinitely divisible.

LXVI. *On Magnetic Effects in Iron Crystals. By* A. G. Hill, *B.Sc., Research Student, Physics Department, University College, Dundee*.*

THE form of the curve of magnetization for iron crystals still remains somewhat unsettled, some workers holding that, though continuous, it may consist of knees linked by straight lines.

That the curve should allow such irregularities is not attributed to any Barkhausen effect but to some quasi-regular rearrangement of the elementary magnets within the crystal itself ; and it was partly to study this phenomenon that the present work was done.

Foster and Bozorth ('Nature,' Sept. 1930) have questioned the existence of such straight-line portions and attribute them purely to end-effects in the specimen itself, and they show that when corrections for such effects are applied the curve of magnetization becomes continuous and entirely non-linear. But the derivation of this corrected curve seems unfortunate in that the correction curve is itself non-linear, and hence its application to a partly linear curve would not at first sight be expected to produce a wholly linear curve.

Gerlach in 1926 (*Z. für Phys.* p. 836), working with a crystalline rod, found no evidence of sharp knees whatever, and further found that considerable hysteresis existed, whereas Dussler and Gerlach (*Z. für Phys.* p. 279, 1927) claimed that knees existed for magnetization along the tetragonal and digonal axes, and that there was little hysteresis. The knees in this case, however, could not be considered to be very distinct. Dussler again attacked the problem in 1928, and found, after applying a non-linear correction curve to his experimental partly linear curve, that the knees still existed, and concluded that the curve of magnetization for iron crystals at room and liquid air temperatures along the tetragonal and digonal axes is partly linear.

* Communicated by Prof. W. Peddie, D.Sc., F.R.S.E.

The divergence of opinion is perhaps only increased by the work of G. G. Sizoo (*Z. für Phys.* p. 649, 1929) on single iron crystals, whereby he found such a number of knees and the curve to be of such a shape that it reasonably could have been regarded as either partly linear or wholly non-linear. His later work indicated little hysteresis and coercivity, and again showed the existence of linearities already referred to, the latter, however, becoming somewhat indistinct when end corrections are applied.

Reference may also be made to the work of K. Honda and S. Kaya (Sc. Rep. Tohoku Univ. xv. p. 721, 1926) and to that of W. L. Webster (Proc. Phys. Soc. p. 235, August 1930), etc.

It would appear therefore that end-effects necessitate corrections of such relative magnitude that the form of the final curve must always be in doubt, and it seemed desirable to devise some method independent of such corrections and the present work was undertaken with this idea.

An iron crystal composed of parallel groups of octahedral form, obtained from Messrs. Vickers of Manchester, provided two cylinders of lengths 1·525 and 1·436 cm. and diameter 1·242 and 1·015 cm. respectively, the axes of the cylinders being parallel to the main axis of the parent. The cores of these cylinders were removed, leaving cylindrical shells of thickness 0·85 and 0·55 cm. which could be magnetized circularly by a current passing along the axis and through the cylinder. There were thus no ends on the specimen in the direction of magnetization so produced. The induction was measured by a secondary coil wound to surround the crystal completely, the section of the coil being perpendicular to the lines of the flux. A special highly sensitive form of Ayrton Mather galvanometer was used at first, but later a sensitive Broca galvanometer was employed. The latter, when used at night, gave the sensitivity necessary for the measurement of the induction and was eventually used throughout. In conjunction with the Broca galvanometer, in order to magnify the readings, it was possible to use at room temperatures as many as 700 turns of very fine wire on the secondary coil, but for the high temperature series of experiments it was necessary to use stouter wire, the whole series eventually being done with a winding of 84 turns of copper wire no. 36 S.W.G. In this way the specimen, in the form of a hollow cylinder with axis in the direction of a cube axis, was magnetized circularly in a face plane. Included in the primary circuit were two graded resistances each of 26 ohms and capable of carrying 25

amps. These resistances were regulated to produce any desired change in the magnetizing current, the subsequent ballistic deflexions giving a measure of the change in magnetization so produced. The maximum value of the applied field was limited by the design of the apparatus to 25 gauss—all previous investigators having reached their conclusions with the use of fields of 7 gauss. Slight modifications in the apparatus will enable fields of 100 gauss to be obtained in further research. To minimize external magnetic effects and temperature variations the crystal, with its perforated ebonite plugs, was surrounded concentrically by a long cylindrical iron shield, the whole being immersed in a Dewar flask for low temperature work and in Extra-Hecla mineral oil for higher temperatures. The oil bath was heated by a gas flame and the temperature was maintained constant by a thermostat.

The object of this work being primarily to investigate the shape of the magnetization curve the experiments were carried out to show the effects of (*a*) low fields of one or two gauss, (*b*) fields approaching 25 gauss, (*c*) temperature, and (*d*) to investigate the magnitude of the hysteresis.

It must be noted that this method of estimating the magnetic flux round the whole shell may mask any straight part in the magnetization curve, since the result so obtained must represent the sum of magnetizations for all directions in a face plane of the crystal. Hence, should there be several directions of magnetization giving straight-line effects, it follows that the curve obtained by summing these will contain the sum of all such straight lines superposed one on the other. So, should there be in any crystal only a few particular directions giving partly linear magnetization curves, the curve obtained by summing these magnetizations will be partly linear also, but should there be many such directions then the resultant curve, as was found in this work, will be practically non-linear. This point was tested by winding four geometrically equal sections in series, and in the tests carried out the results obtained were so similar to those obtained with the complete winding that the latter more accurate arrangement was finally used throughout.

Observational Results.

(*a*) Results of investigations with the small crystal in low fields at room temperature are shown in fig. 1.

Graphs A and B indicate that the magnetization is linear for increasing fields up to 1·0 gauss and that the curve

retraces itself accurately as the field is withdrawn. The return curve B is plotted above A for clearness. Graph C again shows the linear variation in this case for fields up to 2·0 gauss. Deviation from rectilinearity occurs just above this value. Graph D shows the return path after magnetizing the crystal suddenly, and is also linear for fields of 2·0 gauss downwards.

Later experiments show that this initial linearity exists at all the temperatures of observation.

Fig. 1.

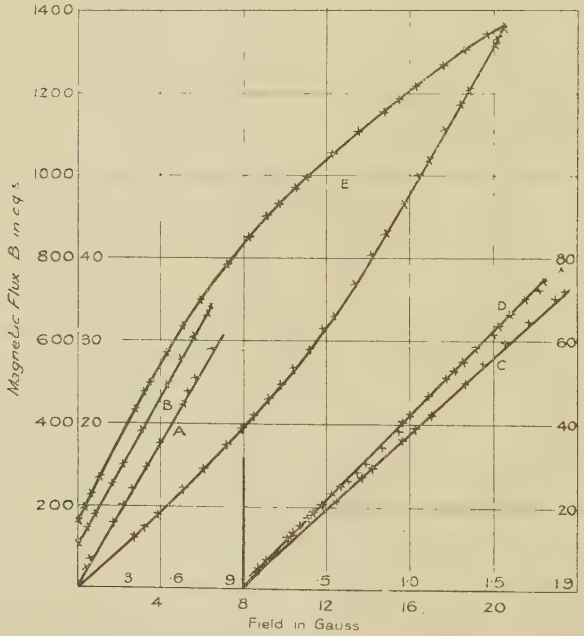

(*b*) Investigations with the large crystal at room temperatures, using fields in each case of initial value 1·4 gauss and final values 9·0, 9·9, 11·8 gauss respectively, the latter values being chosen to correspond to observations by previous investigators.

The curves obtained were not linear in any portion whatsoever, and were exactly similar in shape to curve F (fig. 2).

(*c*) Investigations with the large crystal at temperatures 13·5, 50·15, 110·5 degrees Centigrade, and fields rising from ·16 to 11·5, 11·3, and 8·8 gauss respectively, led to curves exactly similar to curve F in fig. 2, and contained no linear portions.

The Ayrton Mather galvanometer used in the above experiments being then replaced by a Broca galvanometer, the work had to be carried out during the night, as the magnetic effect of the earth-return current due to the tramways made the use of this galvanometer impossible during the daytime.

(*d*) Investigations with the large crystal at temperatures −190, −79, 0, 102·6, and 162·0 degrees Centigrade, with special reference to magnetic lag.

These investigations consisted in taking one set of readings, using fields which had an approximate maximum value of 12·0 gauss, at one particular temperature, then immediately

Fig. 2.

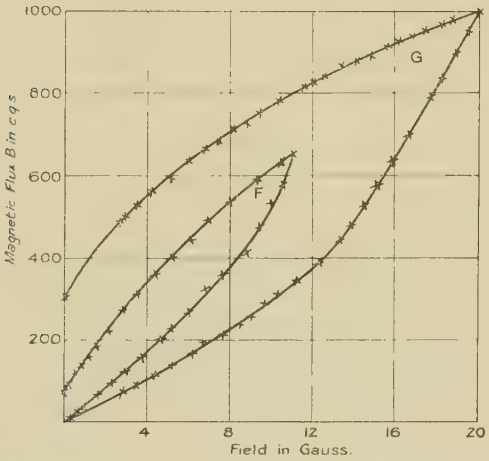

taking another set at the same temperature, using fields of maximum value 20 gauss. Fig. 1, graph E, and fig. 2, graphs F and G, illustrate the results obtained, the details of which are given in the following table :—

Fig.	Graph.	Temp. °C.	Make field gauss.	Maximum field gauss.	Residual magnetization C. G. S.
1	E.	162	2·77	20·6	151
2	F.	0	0·17	11·0	63·5
2	G.	−190	2·80	19·8	290

It will be seen from graphs F and G that the magnetization after reaching the maximum decreases with decrease of the field more rapidly at high than at low temperatures, so that at lower temperatures the curve is broader and the residual magnetization greater. There was no evidence of any linear portions in these curves.

With the exception of one high-field curve at 0° C., which was exceptionally broad, all the curves obtained in the above investigations were similar to those shown in the selected figures, and they indicated that a lowering of temperature produces greater magnetic lag. Further work at still higher temperatures was found to be impossible owing to the creation of a very irregular electromotive force in the secondary circuit, apparently thermal in origin, but as yet unlocated and ungovernable.

(*e*) Investigations with four geometrically equal sectional windings at room temperature gave results exactly similar to the above.

Conclusions.

From this work it appears that the following conclusions can be deduced :—

(1) There is a sharply defined initial linearity of the magnetization curve at all temperatures for fields less than 2·0 gauss, and there is no magnetic lag therein.

(2) For temperatures between −190 and 162° C. and for fields up to 20·0 gauss the shape of the curve is consistently non-linear apart from the very flat initial stage.

(3) The lower the temperature the greater is the magnetic lag.

Future work will consist of a continuation of these investigations at fields producing practical saturation, and at higher temperatures when the extraneous electromotive force in the secondary coil has been eliminated.

I am much indebted to Prof. Peddie for his supervision and advice and to Dr. J. Forrest for discussion and guidance in the work:

Thanks are also due to Mr. J. Stark and my friends Messrs. A. McGregor, B.Sc., and R. B. Robertson, whose help at night was of great value and much appreciated.

LXVII. *Numerical Values of Atomic Constants and X-Ray Terms.* *By* Prof. H. R. Robinson, *F.R.S., East London College, University of London* *.

IN a series of papers † on the "magnetic spectroscopy" of secondary cathode rays, numerical values have been given for a number of X-ray terms. The principle of these experiments is as follows:—The irradiation of an element by monochromatic X-rays leads to the emission of a number of groups of homogeneous secondary cathode rays, each group corresponding to the excitation of a definite X-ray level. If, for example, the atom is left in the K-ionized state, the energy, W, of the photoelectron is given by $W = h(\nu_0 - \nu_K)$, where ν_0 is the frequency of the primary X-radiation, and ν_K the critical K-absorption frequency of the element under examination, both in sec.$^{-1}$. The surface work function may here be ignored in comparison with the other quantities involved. If, then, the absolute value of ν_0 is known, and W is measured accurately, the critical X-ray excitation energies, or the X-ray terms, may be calculated directly by inserting these quantities in the Einstein photoelectric equation.

In the experiments now under discussion, W is calculated from measurements of the effect of a uniform magnetic field upon the path of the photoelectron. In the majority of cases where this method has been applied to the evaluation of X-ray terms, it has been possible to compare the results with the corresponding terms obtained by Siegbahn and others with the X-ray (crystral) spectrometer. The agreement is, on the whole, very fair, but there is evidence of systematic differences between the sets of term values obtained in the two ways. For brevity the two sets may be called the "photoelectric" and the "crystal" values respectively.

The photoelectric results are, on the whole, low compared with the crystal values. This has already been pointed out in a number of the papers referred to above, and more recent (as yet unpublished) work suggests that the discrepancies may have been slightly under- rather than over-estimated. It seems probable that they are at least in part due to inaccuracies in the values of the atomic constants which were adopted in the course of the calculation of the

* Communicated by the Author.

† Robinson, Proc. Roy. Soc. A, civ. p. 455 (1923); Phil. Mag. l. p. 241 (1925); Robinson and Cassie, Proc. Roy. Soc. A, cxiii. p. 282 (1926); Robinson and Young, Proc. Roy. Soc. A, cxxviii. p. 92 (1930).

results. As there is still considerable doubt as to the accuracy of our knowledge of these constants, it seems well worth while to examine a little more closely the evidence which may be derived from the experiments on the magnetic spectra.

There is, first of all, a possible source of error in the value assumed for ν_0 in the photoelectric equation. This point will be more fully discussed at a later stage. It is obvious that the tabulated "crystal" frequencies of both X-ray lines and terms will be affected in the same proportion by any error in the conventional effective lattice constants adopted by X-ray spectroscopists. The "photoelectric" term values will be affected in the same sense, though not in the same proportion: hence our method of comparison does not constitute a sensitive test for small errors arising from this cause.

The position is now becoming clearer, though it is still far from satisfactory, with respect to the other constants which have to be assumed in working out the magnetic spectra. In these experiments the quantities directly measured are the strength, H, of the magnetic field, and the radius of curvature, r, of the trajectory of a photoelectron moving in a plane perpendicular to H. The kinetic energy, W, of the electron is calculated as follows from the value of the product rH:—

$$mv/e = r\mathrm{H} \text{ (cm. gauss)},$$

where v is the speed of the electron in cm. per sec. and e/m its specific charge in e.m.u. per gm.

Then $\beta = v/c$ is given by the equation

$$\beta^2 = \frac{\left(\frac{mv}{e}\right)^2 \times \left(\frac{e}{m_0}\right)^2}{c^2 + \left(\frac{mv}{e}\right)^2 \cdot \left(\frac{e}{m_0}\right)^2},$$

and, finally,

$$\mathrm{W} = m_0c^2\{(1-\beta^2)^{-\frac{1}{2}} - 1\} = m_0c^2\left\{\sqrt{1+\left(\frac{er\mathrm{H}}{m_0c}\right)^2} - 1\right\}.$$

This gives W in ergs; for comparison with the tabulated X-ray data, this must be transformed into the equivalent quantum frequency, W/h.

It will be seen that in the course of the calculations we have to assume values for e*, e/m_0, and h. The effect of

* e does not occur explicitly in the equation for W, but m, has to be calculated from $\frac{e}{m_0}$ and e.

errors in the constants and measurements is most readily seen, for moderately small electron speeds (say of order $c/20$), from the non-relativistic approximation

$$W \doteq \tfrac{1}{2}(rH)^2 \times e/m_0 \times e.$$

that is, e/m and e/h appear linearly in the equivalent frequency, while percentage errors in the measurement of rH are approximately doubled. The probable error in c, the velocity of light, is of too small an order to be taken into account in the discussion of the present experiments.

For convenience in calculating the large numbers of energies measured, I prepared in 1922 a short table giving W/h in terms of rH, and this table has been used in all the subsequent work. It is only within the last few months that it has seemed worth while to re-compute the table, using revised values of the constants. Originally I took e as $4{\cdot}774 \times 10^{-10}$ e.s.u. (Millikan's "oil-drop" value) and $h = 6{\cdot}545 \times 10^{-27}$ erg sec. (Flamm's* semi-spectroscopic value). My results are practically unaltered if I take the more recent values for these constants; Millikan's work is scarcely likely to be improved upon, and it seems highly probable that e lies between the value just quoted and the revised value † of $4{\cdot}770 \times 10^{-10}$. Similarly, Flamm's h lies extraordinarily near the mean of the best modern determinations. For present purposes it is perhaps most rational to rely mainly on the photoelectric determinations, as these experiments give e/h directly. The results of the photoelectric measurements of Lukirsky and Prilezaev ‡, as slightly modified by Birge §, give for this ratio the value $7{\cdot}289 \times 10^{16}$ e.s.u. erg^{-1} sec.$^{-1}$ ($4{\cdot}770 \times 10^{-10} \div 6{\cdot}543 \times 10^{-27}$), as compared with the value $7{\cdot}294 \times 10^{16}$ used in the construction of my tables. The more recent value of h obtained in similar experiments by Olpin || differs from that of Lukirsky and Prilezaev by less than one part in 3000. My values of W/h can then barely be altered by as much as 0·1 per cent. by substituting the most appropriate modern values of e/h for the one adopted ten years ago.

The position is very different with respect to the value of e/m_0. Until quite recently there has been a very marked divergence between the accepted "deflexion" and "spectroscopic" values of this constant. The value which I used

* Flamm, *Phys. Zeits.* xviii. p. 515 (1917).

† Birge, Rev. of Mod. Phys. i. p. 1 (1929); Millikan, 'Science,' lxix. p. 481 (1929), and Phys. Rev. xxxv. p. 1231 (1930).

‡ Lukirsky and Prilezaev, *Zeits. f. Phys.* xlix. p. 236 (1928).

§ *Loc. cit.*

|| Olpin, Phys. Rev. xxxvi. p. 251 (1930).

($1{\cdot}7686 \times 10^7$ e.m.u./gm.) was taken from Flamm (*loc. cit.*), and was based on a re-computation of the data in Paschen's * classical paper on "Bohrs Heliumlinien"—*i. e.*, it was a "spectroscopic" value. Oddly enough, this value agrees extraordinarily well with that obtained in 1927 † in a very careful "deflexion" experiment ($1{\cdot}7689 \times 10^7$), and is very close to the value adopted in the International Critical Tables (published in 1926). It was largely for the former reason that I retained Flamm's value in the later calculations; in experiments in which the kinetic energy of an electron is deduced from the measurement of the deflexion in a magnetic field, it seems most direct and most rational to use the value of e/m_0 obtained in accurate deflexion experiments.

As recently as 1929, Birge, in his well-known summary, quoted two distinct values of e/m_0, viz. $(1{\cdot}769 \pm {\cdot}002) \times 10^7$ deflexion and $(1{\cdot}761 \pm {\cdot}001) \times 10^7$ spectroscopic, the difference being so large compared with the estimated individual errors that it has given rise to a great deal of speculation as to whether the two types of measurement do, in fact, relate to the same quantity, or to two fundamentally different quantities. The latter view has been somewhat discouraged from the theoretical side, and recent experimental work has very appreciably reduced the discrepancy.

One of the latest spectroscopic determinations ‡ (very careful measurements by Campbell and Houston of Zeeman separations for lines for which the g-factors are accurately known) gives a yet lower value, $e/m_0 = (1{\cdot}7579 \pm 0{\cdot}0025) \times 10^7$ e.m.u./gm. When this is considered in the light of Birge's discussion of the earlier work—and particularly in that of the close agreement of the values obtained by different spectroscopic methods—there remains practically no chance of raising the spectroscopic values to "meet" the deflexion results. On the other hand, the most recent "deflexion" experiments have yielded results which not only are lower than the previously accepted value, but which are even in agreement, within the estimated errors of measurement, with the latest and lowest spectroscopic values. The new "deflexion" values are:—Perry and Chaffee § $(1{\cdot}761 \pm 0{\cdot}001) \times 10^7$; Kirchner ‖ $(1{\cdot}7598 \pm 0{\cdot}0025)$

* Paschen, *Ann. d. Phys.* (4) l. p. 901 (1916).

† Wolf, *Ann. d. Phys.* lxxxiii. p. 849 (1927). Wolf's actual value is $1{\cdot}7679 \times 10^7$; the figure quoted above is this result as corrected by Birge for the electrical standards.

‡ Campbell and Houston, Phys. Rev. xxxix. p. 601 (1932).

§ Perry and Chaffee. Phys. Rev. xxxvi. p. 904 (1930).

‖ Kirchner, *Ann. d. Phys.* viii. p. 975 (1931) and xii. p. 503 (1932).

$\times 10^7$, later revised to $(1{\cdot}7585 \pm 0{\cdot}0012) \times 10^7$. There is thus, at the moment, excellent agreement between the results of the two methods, although the position cannot be regarded as satisfactory until the earlier discrepancies have been explained.

I have, however, re-computed a number of the published magnetic spectra, and also a few more recent, as yet unpublished, values, on the basis of the lower e/m_0. For these calculations I have taken $e = 4{\cdot}770 \times 10^{-10}$ e.s.u., $h = 6{\cdot}543 \times 10^{-27}$ erg sec., $c = 2{\cdot}998 \times 10^{10}$ cm./sec., $e/m_0 = 1{\cdot}760 \times 10^7$ e.m.u./gm. The reasons for adopting these values have been outlined above, and the point has been emphasized that it is a value of the ratio e/h which is adopted, rather than values of e and h separately. It has been seen that there is a great deal of experimental evidence in favour of these values, but it must be pointed out that they lead to a value of

$$h/m_0c = \frac{h}{ec} \times \frac{e}{m_0} = 2{\cdot}414 \times 10^{-10}\,\text{cm.} = 0{\cdot}02414\,\text{A.}$$

A recent re-determination of the Compton shift by Gingrich *, using the double crystal spectrometer, leads to $h/m_0c = (0{\cdot}02424 \pm 0{\cdot}00004)$ A, in very fair agreement with Sharp's † earlier determination $(0{\cdot}02432 \pm 0\ 00009)$ A. If the ruled grating, instead of the calcite crystal, be taken as standard for the measurement of X-ray wave-lengths, the true value of the Compton shift comes still higher, and it scarcely seems possible to reconcile the observed shift with otherwise acceptable values of e and h and with a low value of e/m_0.

The situation, therefore, remains full of interest, and it seems likely that new experimental work will be forthcoming almost immediately, or alternatively, that some at least of the discrepancies (and of the concordances) may be explained away by a refinement of the theoretical treatment of collision processes.

So far as the evidence of the magnetic spectra is applicable, I can say quite definitely that the use of the lower value of e/m_0, unaccompanied by any other serious change in the constants, leads to a much closer agreement between the "photoelectric" and the "crystal" values. That is, the *systematic* differences between the two sets are thereby diminished ; there are still a few outstanding individual cases where the discrepancy between the two values cannot be

[* Gingrich, Phys. Rev. xxxvi. pp. 364, 1050 (1930).
† Sharp, Phys. Rev. xxvi. p. 691 (1925).

satisfactorily disposed of by manipulating the constants, and where it is much too large to be ascribed to errors in the magnetic measurements. These cases, which have a different kind of interest, will shortly be re-investigated with increased accuracy.

This represents all which can at the moment be usefully said about the general nature of the photoelectric results. The effect of the other doubtful factor (the uncertainty as to the absolute values of the standard X-ray wave-lengths) needs further investigation. So far, I have retained the Siegbahn values for the primary frequencies, and used the corresponding level values for comparison ; that is to say, the values used are based on the assumption that the absolute length of the X-unit is exactly 10^{-11} cm. It is evident, from the work of Siegbahn and others, that the *relative* values of the wave-lengths in many emission-spectra are now known with amazing accuracy. Further, independent determinations of crystal grating spaces are very satisfactorily concordant. Most wave-length tables have been based on the calcite spacing adopted as standard by Siegbahn* (3·02945 A at 18° C.), which is a conventional value chosen to agree with Moseley's figure for rock-salt. The most recent determination of the calcite spacing is that of Bearden † (3·02810 A at 18° C.). Using this value, Bearden ‡ finds for the wave-length of $CuK\alpha_1$, in measurements with the double crystal spectrometer, 1536·717 X.U., which may be compared with the result of Siegbahn §, 1537·396, and that of Wennerlöf ‖, 1537·395.

These differences are negligible compared with the probable errors in the results of the magnetic spectra. The only point, then, which needs to be considered here, is that of the possible error in the absolute value of the X-unit. The latest work with ruled gratings indicates that the X-unit may be as large as $1{\cdot}0025 \times 10^{-11}$ cm., and therefore that the tabulated X-ray frequencies may all be about $\frac{1}{4}$ per cent. too large. The cause of this discrepancy is not yet understood. Bearden ¶, as the result of his recent deduction of wave-lengths from measurements of X-ray dispersion in quartz, has concluded that the ruled grating, and not the crystal spectrometer, wave-lengths are the more seriously in

* Siegbahn, *Ark. f. Mat., Ast. o. Fys.* 21 A, no. 21 (1929).
† Bearden, Phys. Rev. xxxviii. p. 2089 (1931).
‡ Bearden, Phys. Rev. xl. p. 133 (1932).
§ Siegbahn, *loc. cit.*
‖ Wennerlöf, *Ark. f. Mat., Ast. o. Fys.* 22 A, no. 8 (1930).
¶ Bearden, Phys. Rev. xxxix. p. 1 (1932).

error, and has suggested that the explanation is to be sought in some imperfection in the theory of the action of ruled gratings. It is not certain how far this view can be sustained, but at all events it is not unreasonable, in the light of the existing evidence, to set $\frac{1}{4}$ per cent. as an upper limit to the probable error in the standard X-ray spectral tables.

In view of the nature of the calculations and of the uncertainties in the other constants, it would not be easy to detect with certainty the effect of an error of this magnitude, without a fairly full range of magnetic spectra, taken with a suitable variety of primary radiations under otherwise identical conditions. Unfortunately these are not yet available. The published results range from copper K to silver K primary radiations, but owing to a number of circumstances each set was obtained either with different field coils, or with coils of which the setting had been disturbed between the different series of measurements. There is, in fact, some internal evidence of the effects of slight differences in the setting of the field and compensating coils. It follows that the different sets of results are not well suited for detailed inter-comparison, but I hope that more accurate results for a few selected elements will shortly be available. New work* has been begun at East London College, in collaboration with Dr. J. P. Andrews and Dr. E. J. Irons; the magnetic fields are being very carefully calibrated, and special attention has been given to securing mechanical rigidity in the essential parts of the apparatus. It is hoped that the new work, by yielding more reliable absolute values of the secondary cathode ray energies over a sufficiently wide range, may contribute to the settlement of some of the outstanding difficulties which have been outlined above. Unfortunately, magnetic spectrometry alone does not provide a direct method of measuring any one atomic constant, but the inferences which may be made from its results should be of value at a time when there is a peculiarly persistent difficulty in reconciling the data obtained in independent, and apparently equally reliable, methods of determining relations between the constants.

I may perhaps add that the results of a short series of experiments (not yet completed for publication) made in collaboration with Professor R. T. Dunbar, using yet softer primary radiations, are quite definitely in favour of the lower value of e/m_0 (that is, assuming that no serious

* The greater part of the cost of apparatus for this work has been defrayed from funds allotted by the Government Grant Committee of the Royal Society, for which I desire to make acknowledgment here.

adjustment is required to the values of the other constants). These later experiments were conducted under better working conditions than those prevailing for some of the earlier work ; one troublesome correction for non-uniformity of field was entirely eliminated, and other corrections were carefully revised and re-calculated by Prof. Dunbar. The results of this work, while they are in general agreement with the earlier work, indicate that the differences between the crystal and photoelectric values may have been slightly underestimated.

[*Note inserted in proof, September* 10*th*, 1932.—Since the above was written, there has been much further discussion of the values of the atomic constants and recomputation of existing experimental data, including a new paper by Birge. Further, Meibom and Rupp have published the results of a new determination of e/h, based upon the measurement of the de Broglie wave-lengths of electrons moving with known speeds. Their value of e/h is $7{\cdot}247 \times 10^{16}$ e.s.u. erg ^{1} sec.$^{-1}$ (assuming Kirchner's e/m_0)—which differs very seriously from that adopted above.—H. R. R.]

LXVIII. *A Geometrical Method of determining the Crystal Axes of Single Crystal Wires.* *By* Bruce Chalmers, *Ph.D.**

1. *Introduction.*

FOR the purpose of analyzing the mechanical properties of single crystal wires it is necessary to know the relation of the crystal axes to the axis of the wire. The structure of cadmium, to take an example, is hexagonal, and in this case the elements required are the angle between the hexagonal axis and the axis of the wire, and the angle between one of the digonal axes and the axis of the wire, or alternatively between the digonal axis and the plane containing the axis of the wire and the hexagonal axis. The determination of these axes by the X-ray method is a somewhat lengthy process, and it is often very convenient to have a direct geometrical method. That described in the following pages involves the stretching of the wire. In many types of experiments, and, in particular, in those for which it was devised, the stretching of the wire is an essen-

* Communicated by Professor E. N. da C. Andrade.

tial part of the investigation; there are, in any case, probably few investigations in which there is any reason why the wire should not be so treated after the other measurements have been made.

The extension of single crystal wires of soft metals leads to glide, accompanied by elliptical surface-markings, as first shown by E. N. da C. Andrade *. In the case of the metal cadmium, for which the method has been used, the glide takes place on a set of parallel planes normal to the axis of the crystal, the surface-markings being due to the fact that the main displacement occurs on certain members of the set of parallel planes, separated by distances of the order of 0·1 mm.; it is not known what local irregularities cause this preferential effect in certain ones among planes which are all crystallographically equivalent. These planes contain the digonal axes. Measurements made on one of these elliptical markings, representing the intersection of the glide plane with the surface of the wire, and the displacement of this plane relative to a fixed parallel plane, allow the directions of the required axes to be calculated. It is generally accepted that in such cases as cadmium the deformation takes place entirely by glide, and that there is no distortion of the lattice, and this assumption lies at the basis of the following calculations.

2. *Geometrical Considerations.*

Let DEF be the intersection of a glide plane with the surface of the wire, cylindrical before glide. Fig. 1 (*a*) represents an oblique view of the wire, fig. 1 (*b*) the same part of the wire turned so that DEF is in the plane of the paper. DEF being considered fixed, LMN represents a parallel elliptical section before glide, RST the same elliptical section after glide, LMN and RST being, of course, in the same plane.

Let z be the distance between the planes DEF and LMN; ϕ be the angle between the axis of the wire before glide and the projection of this axis on the glide plane; ϕ' be the angle between the axis of the stretched (flattened) wire after glide and its projection on the glide plane; α be the angle between the direction of glide BC and the projection on the glide plane of the wire axis before glide, *i. e.*, the major axis AD of the ellipse; β be the angle between the projection of the axis of the stretched wire and AD. Then, if a and b are the major and minor axes respectively of the

* Phil. Mag. xxvii. p. 986 (1914).

ellipse DEF, and AB and AC in fig. 1 (*b*) are now considered as lengths measured in the plane of DEF, namely, as the projections on that plane of the lengths in question,

$$\sin\phi = b/a, \quad . \quad . \quad . \quad . \quad . \quad . \quad . \quad . \quad (1)$$

$$\tan\phi' = z/\mathrm{AC}, \quad . \quad . \quad . \quad . \quad . \quad . \quad . \quad . \quad (2)$$

$$\frac{\tan\phi'}{\tan\phi} = \frac{z}{\mathrm{AB}} \Big/ \frac{z}{\mathrm{AC}} = \frac{\mathrm{AC}}{\mathrm{AB}}. \quad . \quad . \quad . \quad . \quad (3)$$

If z, b, a, and AC are known, then ϕ and ϕ' are given by (1) and (2), and AB can be found from (3). Hence the point B, which bears no simple geometrical relation to the observable sections DEF and RST of the stretched wire, can be found. If, in addition, the angle DAC is measured, then

Fig. 1.

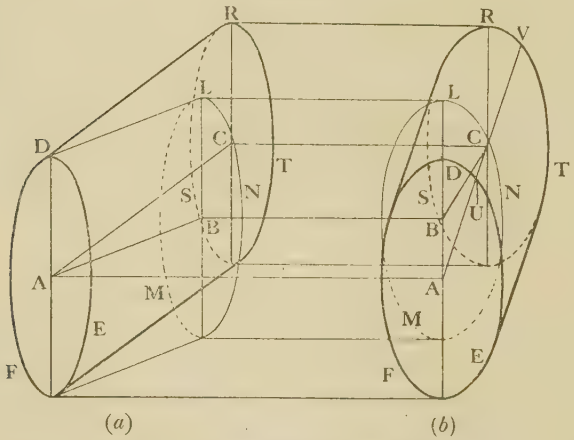

the triangle BAC is completely known, and the angle DBC = α can be found.

3. *Method of Measurement.*

The microscope used for the measurements was fitted with a wide-aperture objective having a small depth of focus (8 mm., N.A. 0·65) and with an eyepiece carrying a graticule divided into 0·1 mm. squares, each tenth division being strong, as with ordinary squared paper. The specimen of stretched wire was mounted on a slide which allowed the axis to be placed at any required angle to the axis of the microscope. The specimen was adjusted under almost horizontal illumination from a pointolite lamp, until the whole semi-ellipse visible was sharply in focus, which ensured that the glide plane was being viewed perpendicularly, as

represented in fig. 1 (*b*). The eyepiece was then rotated to make one of the coordinate directions parallel to the position of AC on the plane DEF, which could be checked by racking the microscope up and down, so as to focus on different planes of the wire, and using either edge of the wire, which runs parallel to AC, for the adjustment. Co-ordinates of about thirty chosen points of the ellipse were read off on the eyepiece scale. These points were plotted on a large scale on graph paper, the centre of the ellipse determined as the intersection of the loci of centres of parallel chords, and the axes a and b fixed. The angle β between the major axis and the projection of the wire axis can be measured directly from the plotted diagram, since one of the coordinate directions has been made parallel to the projection of the wire axis.

The angle ϕ' was found by measuring the vertical distance z through which the microscope had to be moved in order to focus on the two different glide ellipses represented in fig. 1 (*b*) by DEF and RST. The horizontal distance AC between the centres of these ellipses was found by measuring distances along or parallel to the wire axis between corresponding points on the two ellipses, such as UV. A calibration of eyepiece and focussing scales enables $\tan\phi'$ to be found from equation (2). This completes the measurement of the necessary elements.

4. *Results.*

The accuracy obtainable with this method of determining the angles, as applied to single crystal wires of cadmium of approximate diameter 0·5 mm., appears to lie within about 1°, which is quite sufficient for most considerations of mechanical properties. The angles on the plotted ellipse are measured with a protractor, and while they can be easily read to the nearest degree the uncertainty of determination does not make it profitable to subdivide the degree. The following table shows the results of measurements at three different parts of one particular single crystal wire of cadmium :—

	a. (Arbitrary units.)	b.	ϕ.	ϕ'.	β.	α.
1.....	151	106	44·6°	11°	8°	9°
2.....	152	104	43·3	11	8	10
3.....	152	104	43·3	10	8	10
	Mean		43·7	10·7	8	9·7

The method is clearly applicable to the determination of the angles made by the glide plane and glide direction in any single crystal wires in which glide takes place on a unique set of planes.

Physics Laboratory,
University College, London.

LXIX. *On the Spontaneous Generation of Oscillation in Low Pressure Discharges.* *By* Prof. S. K. Mitra, *D.Sc.*, *Khaira Professor of Physics, Calcutta University, and* Premtosh Syam, *M.Sc.**

[Plate X.]

1. *Introduction.*

THE phenomenon of direct current discharge in low pressure has long been known to be a source of electrical oscillations under suitable conditions. These oscillations may be broadly divided into two types. The first type is generally known as ionic oscillation, and its frequency is found to be independent of the electrical constants of the external circuit, depending generally upon the condition of ionization of the gas in the interior of the tube †. The second type is, however, considered to arise out of periodic discharges through the tube, and its frequency is dependent on the electrical constants of the external circuit‡.

This latter type of oscillations, which we are going to consider in the present paper, seems to have been discovered by Gassiot in 1863. The phenomenon has been investigated by many workers since Gassiot's discovery, the latest investigation being by E. W. B. Gill in 1929‡. These oscillations are generated by connecting a condenser across the terminals of the discharge-tube and inserting an external high resistance in series with E.M.P. source, which furnishes the necessary voltage for the maintenance of the discharge (fig. 1). The

* Communicated by the Authors.

† Appleton and West, Phil. Mag. xlv. p 879 (1923); Clay, Phil. Mag. l. p. 985 (1925); Penning, 'Nature,' cxviii. p. 301 (1926); Langmuir and Tonks, Phys. Rev. xxxiii. p. 195 (1929); Pardue and Webb, Phys. Rev. xxxii. p. 946 (1928); J. J. Thomson, Phil. Mag. xi. p. 697 (1931).

‡ Gassiot, Proc. Roy. Soc. (1863); Hittorf, *Ann. d. Phys.* vii. p. 566 (1879); Schallreuter, *Sammlung Vieweg*, Heft lxvi. (1923); Geffcken, *Phys. Zeit.* nr. 5, p. 241 (1925); Clay, Phil. Mag. l. p. 985 (1925); Gill, Phil. Mag. viii. p. 955 (1929).

observations of all the previous workers, including those of Gill, are confined in determining the relations between the frequency and the electrical constants of the circuit and the characteristics of the tube. None of the workers have studied the exact conditions under which the discharge changes over from oscillatory to continuous, or *vice versa*. Neither has any one attempted to take records of the instantaneous currents flowing in the various branches of the circuit, a knowledge of which is very necessary for properly understanding the phenomenon. In the present investigation we have studied these two questions, and, as a preliminary, we have also made observations on the relations

Fig. 1.

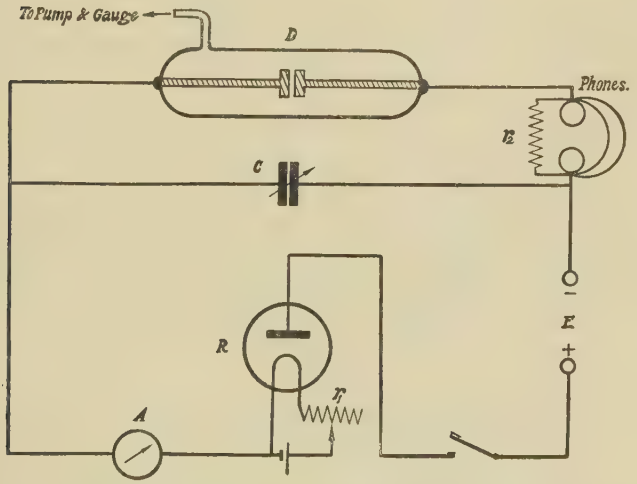

between the frequency, and the current, capacity, and pressure within the discharge-tube in the audible range of frequency, the investigation by all previous workers being confined in the supersonic region of frequency. The results obtained by us on this latter point generally confirm the observations of Gill. The records of the current flowing in the various branches during the intermittent discharge, obtained by means of a cathode-ray oscillograph, confirm the assumption made by all previous workers that the discharge of the condenser through the tube is almost instantaneous. Regarding the conditions at which the discharge changes over from oscillatory to continuous, a simple formula is deduced, involving the H.T. voltage, the extinction potential of the tube, and the

values of the external high resistance and the internal resistance of the discharge-tube.

The investigations were originally undertaken by Mr. N. B. Mukherjee, M.Sc., at the suggestion of the senior author of this note. He had begun making some preliminary observations but could not complete the investigation as he was called away for other work. The investigation was continued and brought to a conclusion by us.

2. *Experiments and Results.*

The experiments and results to be described have been divided into three parts. In the first part we investigate the relations between the frequency of the oscillations and (*a*) the current through the discharge-tube, (*b*) the capacity of the associated condenser, (*c*) the pressure within the tube, and (*d*) the separation of the electrodes in the audible range of frequency.

In the second part we discuss the theory of the phenomenon and investigate the condition under which the discharge passes over from oscillatory to continuous.

In the third part we observe the wave-forms of the current in the different branches of the circuit by means of a cathode-ray oscillograph, in order to have accurate information regarding the nature of the intermittent discharge. We also investigate the duration of the discharge by taking photographs with the help of a falling-plate camera.

Part I.

The experimental arrangement for the first part is shown in fig. 1. The discharge tube D is one of a common type, with aluminium disk electrodes of diameter about 8 mm., the distance between which can be varied at will. The diode R, with the filament rheostat r_1, is used as an adjustable high resistance in series with the discharge-tube, in order to control the current. The use of a diode for this purpose seems to have been first made by Geffcken*. The high tension E is taken from 350 small accumulators, and the current in the tube being very small, a micro-ammeter A is used to measure the same. C is a calibrated variable air condenser in parallel with the discharge electrodes. For the purpose of detection of the oscillations a pair of head-phones is used in series with the discharge-tube, as shown in fig. 1. It is shunted with a resistance r_2 in order to bring down the intensity of the note in the phones, which is very loud. The

* *Loc. cit.*

frequency of the note emitted was determined with the help of a sonometer. The sound was rich in harmonics, but the fundamental was strong enough to enable the tuning to be correctly carried out.

A range of frequency between 100 and 1000 p.p.s. was selected for our purpose. The frequency having been found to diminish with the reduction of current and the increase of the distance between the two electrodes, the current had to be kept at a low value (20 to 60 micro-amperes), and the electrodes were placed at a comparatively large distance (7·5 to 9 millimetres) from one another in our experiments.

The frequency of the oscillations having been found to depend upon (i.) the current i through the discharge-tube, (ii.) the distance d between the electrodes, (iii.) the pressure p of air within the tube, and (iv.) the capacity c of the associated condenser, one of these factors was varied, keeping the others constant, and the corresponding frequency was determined. The results of the observations are given below.

(i.) *Frequency-current.*—On keeping the capacity, pressure, and the distance between the electrodes constant, and varying the current through the tube by changing the filament resistance of the diode, it was observed that the ratio of this current i and corresponding frequency n was always a fairly constant quantity for any set of observations, *i. e.*, the frequency was directly proportional to the current. Thus we have

$$\frac{n}{i} = \text{A (constant)},$$

or

$$n = \text{A}i \quad . \quad . \quad . \quad . \quad . \quad . \quad . \quad . \quad . \quad . \quad (1)$$

(ii.) *Frequency - distance.*—On varying the distance between the electrodes, while keeping the other factors constant, it was observed that the frequency diminished as the distance increased, but no simple relation holding between the two was found.

(iii.) *Frequency-pressure.*—The frequency of the oscillations was found to increase progressively with the reduction of pressure within the tube, while the other factors were kept constant. In this case too no simple relation between the two could be observed.

(iv.) *Frequency-capacity.*—The frequency was found to decrease as the capacity C of the associated condenser was increased, keeping the other factors constant. On expressing

this frequency in the corresponding wave-length ($\lambda = \frac{c}{n}$, where c = velocity of light) it was observed that the relation between the wave-length and the capacity could be expressed accurately by a straight line (fig. 2). This straight line was always found to meet the capacity-axis on the negative side of the origin, when drawn for different values of the discharge current, so that the intercept C′ was always negative, as shown in fig. 2. The equation of such a line may be put down as

$$\lambda = b(C + C'), \quad . \quad . \quad . \quad . \quad . \quad . \quad (2)$$

whence the frequency

$$n = \frac{B}{C + C'}, \quad . \quad . \quad . \quad . \quad . \quad . \quad (3)$$

where b and B are constants.

Fig. 2.

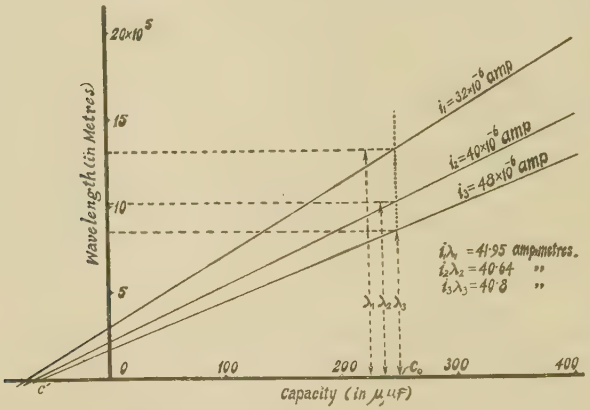

(v.) On drawing several straight lines represented by equation (2) for different values of the discharge current, keeping the pressure within the tube and the separation of the electrodes constant, it was found that the slope of the lines decreased rapidly as the current increased, but all these lines very nearly met at the same point on the capacity-axis, giving the same value for the intercept C′. Any small deviation that was noticeable indicated that C′ diminished regularly with the increase of current. Taking therefore C′ roughly as a constant, we may combine the equations (1) and (3), and put it as

$$n = \frac{Ki}{C + C'}, \quad . \quad . \quad . \quad . \quad . \quad . \quad (4)$$

where K is a constant depending on the pressure and the separation of the electrodes.

All these observations in the region of audible frequency (excepting (v.), to which we shall refer later), as well as the equations given above, are in general accordance with those of Gill and others. Some of these observations are also in accordance with those made with neon lamp at low frequency *, and indicate that the same laws generally hold throughout all ranges of frequency in various gases.

Regarding the observations (v.), we remark that they do not tally with those of Gill, who finds that the intercept C′ increases with the increase of current. We find, on the contrary, that C′ remains nearly constant, and the small change it undergoes is in a sense opposite to that mentioned by Gill. The observations from which Gill has drawn the conclusion regarding the increase of C′ with current i seems to have been somehow vitiated; this will be apparent from the following considerations and from the example given below, taken from Gill's paper.

Referring back to fig. 2, the straight lines are obtained by plotting wave-length against capacity for different values of the discharge current, the pressure and separation of the electrodes remaining constant throughout. Again, from equation (1) the variation of n with i may be expressed as $\lambda i = \text{constant}$, where λ is the corresponding wave-length, provided the capacity, pressure, and electrode separation remain unaltered. In the observations of fig. 2 we have the pressure and electrode separation the same throughout, so that if we now select any definite value of capacity, say C_0 in the figure, then, according to equation (1), we must have

$$\lambda_1 i_1 = \lambda_2 i_2 = \lambda_3 i_3,$$

where λ_1, λ_2, and λ_3 are the wave-lengths for currents i_1, i_2, and i_3 respectively, when the value of the associated capacity is C_0. Thus the straight lines shown in fig. 2 must conform to the above rule. But in the example given by Gill † to prove that C′ increased with the current we do not find a conformity with the above rule. Taking the product for both the examples given by Gill at a value of capacity $c = 15$ cm., we find

$$i_1\lambda_1 = (\cdot 21 \times 10^{-3}) \times (8200) = 1\cdot 72 \text{ amp.} \times \text{metres.}$$

$$i_2\lambda_2 = (1\cdot 35 \times 10^{-3}) \times (2500) = 3\cdot 38 \text{ amp.} \times \text{metres.}$$

* Robinson, Exp. Wireless, i. p. 12 (1923–24); Taylor and Clarkson, Exp. Wireless, ii. p. 97 (1924–25) and Journ. Sci. Inst. i. p. 173 (1924).

† Gill, *loc. cit.* p. 957.

This proves that Gill's observations must be in error, and hence his conclusion regarding the increase of C′ with current does not hold.

In fig. 3 of his paper Clay * shows the intercept C′ to be positive ; this is also a mistake and is due to an error in marking the time-axis. When this is corrected Clay's observations agree with ours.

Fig. 3.

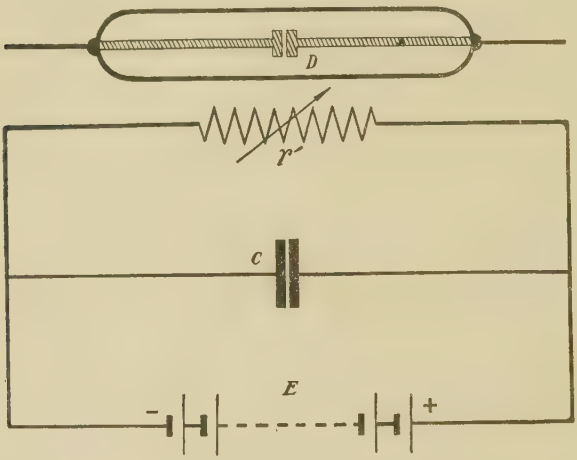

Part II.

As mentioned in the introduction many investigators have attempted to determine the relation between the frequency of the oscillation generated and the electrical constants of the circuit and of the discharge-tube. Of these relations two important ones may be mentioned. The first one, due to Righi †, who seems to be the originator of the theory of the maintenance of oscillation by repeated charge and discharge of the condenser, is

$$T = CR \log_e \frac{E - V_b}{E - V_c},$$

where T is the time-period of the oscillations, C the capacity of the external condenser, R the external high resistance, E the voltage of the H.T. battery, and V_b and V_c the extinction and the sparking voltages respectively of the discharge-tube. This formula is deduced on the assumption that the time of

* Clay, *loc. cit.* p. 988, fig. 3.

† Righi, *Rend. d. Accad. d. Scienze di Bologna*, p. 108 (1902).

discharge is negligibly small. The wave-forms observed by us and to be described later justify this assumption. The other formula due to Gill has already been referred to. Though both these formulæ have been experimentally verified, the former by Schallreuter * and the latter by Gill himself and by us in the audible range, yet there still seems to remain some uncertainty as to the actual mechanism of the charge and discharge.

In what follows we propose to explain the production of oscillations from a standpoint which, though not essentially different from that taken up by previous observers, is purported to bring into prominence the important rôle played by the external resistance R. That an external condenser is essential for the maintenance of the oscillatory discharge has been noticed by all observers †; but that the external high resistance is equally important and plays an essential part in the maintenance of the oscillatory discharge seems to have escaped the observation of most of the workers. It has been found by us that there is a critical value of the external resistance below which no oscillations are possible.

We will first show that it is impossible to obtain the oscillatory discharge if the external resistance R is totally absent. We will next deduce the value of the critical resistance R_c which is just necessary for the production and maintenance of the oscillation.

In fig. 3 let E be the high tension voltage battery, C a condenser, and let D represent the discharge-tube. We will idealize the behaviour of the discharge-tube by assuming it to be a variable resistance r', such that ordinarily r' is equal to infinity; but when a voltage equal to or greater than V_c acts across it the value of r' drops down from infinity to a small value of the order of a few thousand ohms. It maintains this value as long as the voltage across does not fall below V_b. If the voltage drops below V_b then r' reverts to its original value infinity. Now suppose that E is greater than V_c; then, on switching the battery, the first effect will be the charging up of the condenser C, and assuming that the resistance in the circuit CE is negligible the charging up will be almost instantaneous. Simultaneously the voltage

* *Loc. cit.*

† It is found that the actual value of the condenser necessary for the production of oscillation is not critical. It is possible to maintain the oscillatory discharge without any external condenser at all. In this case the capacity due to the electrodes and associated circuits is found to be sufficient. It must be remembered that some form of capacity, however small, is always necessary where the electrical energy supplied by the battery is temporarily stored before it passes on to the discharge-tube.

E will begin to act across the terminals of r', and since E is greater than V_c the resistance of r' will drop down from infinity to a value of a few thousand ohms, say r. The battery E will thereon maintain the discharge current through r steadily, since there is no agency to bring down the voltage across the tube below V_b. The condenser C, of course, once it has been charged to the potential of E will not draw any current from the H.T. battery.

Let us next consider the effect of inserting an external resistance R (fig. 4). In this case the first effect of switching the battery on will be, as in the previous case, to charge up the condenser. Owing to the presence of R, however, the

Fig. 4.

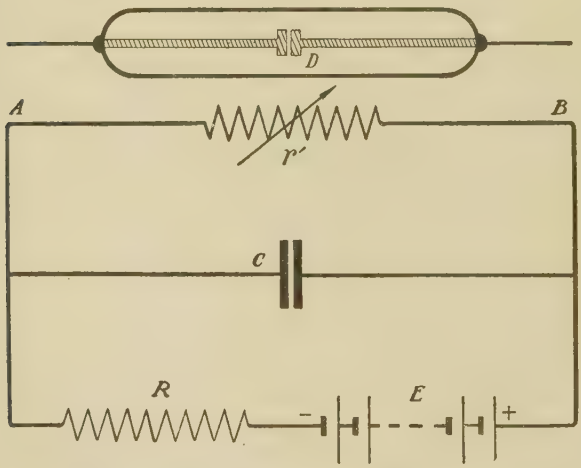

condenser voltage will rise slowly, in accordance with the formula, $V = E(1 - e^{-\frac{t}{CR}})$. When the condenser voltage attains the value V_c the resistance of r' drops down from infinity to a small finite value r, and the charge on the condenser starts leaking away through it. Now, if the leakage be faster than the rate at which the condenser receives charge from E through R the net effect will be to lower speedily the voltage across AB. When the voltage falls below V_b, r' resumes its value infinity, and the leakage of the condenser now stops; but since the condenser continues to receive charge from E its voltage again rises to the value V_c, and the whole phenomenon is repeated. It is therefore obvious from these considerations, as well as from what has been said in the previous paragraph, that the

interruption of the discharge—that is to say, the alternation of the value of r' from infinity to r, and *vice versa*—will only occur if there is a high resistance R of suitable value in the external circuit. The minimum value of this resistance necessary to just maintain the discharge can be calculated by equating the rate of charging with that of discharging of the condenser. As the resistance falls just below the critical value, the rate at which the condenser will deliver current to the discharge-tube must equal the rate at which it will receive charge from the battery E.

An expression for the above condition can be readily deduced as follows :—Let V_c be the voltage across the condenser when the discharge starts. If the resistance of the discharge-tube be r, then

$$Q = V_c C e^{-\frac{t}{Cr}},$$

where Q is the quantity of electricity stored in the condenser C at time t after the discharge has started. The current flowing through the discharge-tube from the condenser at the instant t is obviously equal to

$$\frac{dQ}{dt} = -\frac{V_c}{r} e^{-\frac{t}{Cr}}.$$

Now the discharge will continue till the voltage across the condenser has fallen from V_c to V_b. The time t_b required for this voltage drop may be calculated from

$$V_b = V_c e^{-\frac{t_b}{Cr}}.$$

Whence

$$t_b = Cr \log_e \frac{V_c}{V_b}.$$

Therefore the current $\frac{dQ}{dt}$ in the condenser branch immediately before the discharge ceases is given by

$$\frac{dQ}{dt} = -\frac{V_c}{r} e^{-\frac{t_b}{Cr}} = -\frac{V_c}{r} e^{-\log_e \frac{V_c}{V_b}} \quad . \quad . \quad . \quad . \quad (1)$$

Now the condenser will always be receiving charge due to the battery E, and at the instant t_b, when the voltage across the tube is V_b, the rate is evidently given by

$$\frac{E - V_b}{R} \quad . \quad . \quad . \quad . \quad . \quad . \quad . \quad . \quad (2)$$

Now if the discharge is to be continuous then the value of the potential across the discharge-tube must not be allowed to fall below V_b, the extinction potential. Therefore the rate at which the condenser will be losing charge when its potential is just above V_b—that is, at the time t_b (equation 1)—must equal the rate at which it will be receiving charge from E (equation (2)) at that instant. The value of R which is necessary to supply this requisite current from E may be called the *critical resistance* R_c, and is easily found by equating (1) and (2). Thus

$$\frac{E-V_b}{R_c}=\frac{V_c}{r}e^{-\log_e\frac{V_c}{V_b}},$$

hence

$$\frac{R_c}{r}=\frac{E-V_b}{V_b} \quad . \quad . \quad . \quad . \quad . \quad . \quad . \quad (3)$$

This expression shows that the value of the critical resistance R_c depends on E, V_b, and r only, and that it is independent of the external capacity used. In deriving this expression we have assumed that the resistance r of the discharge-tube is constant—*i. e.*, it is independent of the current flowing through the tube. It is, however, well known that the current-voltage relation of a discharge-tube does not follow Ohm's Law, and that the resistance is a complicated function of the current flowing through it. In general an increase of the current is accompanied by a decrease of the resistance. On account of this the critical resistance R_c cannot be expected to be constant in actual practice, but to vary with the value of the capacity used. With a large capacity the discharge current i at any instant t is necessarily higher than the discharge current at the corresponding time with a smaller capacity. As a consequence the discharge-tube has on the average a lower resistance when a larger capacity is shunted across it. The value of R_c may therefore be expected to decrease with the increase of capacity C. In the experiments conducted by us and to be described presently $\frac{R_c}{r}$ was found to be fairly constant and equal to $\frac{E-V_b}{V_b}$ when the capacity was varied over a wide range of values. R_c was, however, found to decrease by about 50 per cent. when the capacity C was increased fifty times.

Relation (3) can also be derived in a very simple way if we remember that when no current is flowing in the condenser branch the voltage developed across it must simply be

$$V=E-Ri=ri,$$

where i is the current flowing through the discharge-tube. In order that the discharge may not be interrupted this voltage must never fall below V_b. The critical resistance is therefore obviously given by the formula

$$V_b = E - R_c i = r i \; ;$$

hence

$$\frac{R_c}{r} = \frac{E - V_b}{V_b}.$$

The results tabulated below were obtained in the following way :—With a given value of the capacity C and battery E the external resistance R was continually diminished till the discharge suddenly became steady. This was indicated by the sound in the head-phones, which stopped at that moment, and by the simultaneous change of form of the glow. The current flowing through the discharge-tube just before the stopping of the oscillation was measured by means of a milli-ammeter. We thus obtained the value of $R_c i$, which also permitted the calculation of $r = \frac{E - R_c i}{i}$, and hence $\frac{R_c}{r} = \frac{R_c i}{E - R_c i}$. The value of V_b was determined independently, when no condenser was present. Knowing V_b, we could also calculate $\frac{R_c}{r}$ from the formula $\frac{E - V_b}{V_b}$. This calculated value of $\frac{R_c}{r}$ was compared with the observed value of $\frac{R_c}{r}$ obtained by noting the discharge current for different values of C and E. The results have been tabulated below. It will be seen that the observed and calculated values of $\frac{R_c}{r}$ agree within the limits of experimental error, and also that it is independent of the value of the capacity C.

E (volts).	Calculated. $\frac{R_c}{r} = \frac{E - V_b}{V_b}$.	Observed $\frac{R_c}{r} = \frac{R_c i}{E - R_c i}$, for different values of the external condenser C.		
		For C = 0.	For C = ·0002 μF.	For C = ·01 μF.
235	·77	·70	·79	·68
225	·69	·65	·73	·59
215	·61	·58	·59	·53
195	·45	—	·44	·39
185	·38	·32	·35	·32
165	·24	·24	·18	·17

Part III.

In order to have accurate information regarding the nature of these oscillations it was decided to observe the wave-forms of the current in the different branches of the circuit For this purpose a cathode-ray oscillograph manufactured by the Standard Telephones and Cables Company was used. The cathode-ray beam, which forms a spot of light on the fluorescent screen has to travel through the space between two pairs of parallel plates, as shown in the inset diagram (fig. 5). (In the diagram the beam travels at right angles

Fig. 5.

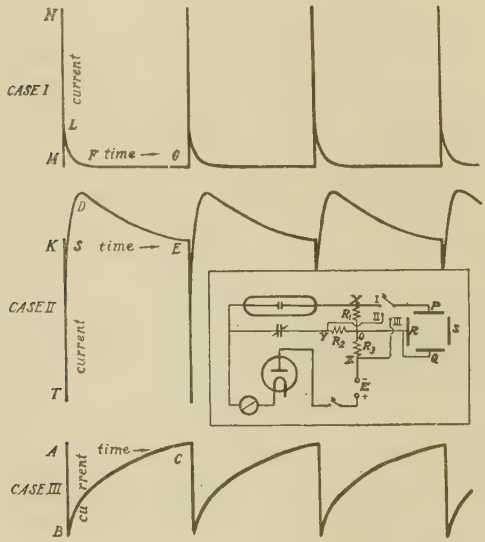

to the plane of the paper.) The two pairs of plates are not of course in the same plane, but the one pair, say PQ, is above the other. The electric field due to one pair of plates is at right angles to that due to the other pair. The pair RS, having horizontal field, is connected to an oscillatory circuit, which deflects the spot of light horizontally. This is the time-base. The oscillator is so arranged as to make the time-base linear *. The spot of light moves from left to right with uniform velocity; it stops suddenly and then returns almost instantaneously to the left.

* Appleton, Watson Watt, and Herd, Proc. Roy. Soc. A, cxi. p. 618.

In order to obtain a picture of the variation of current with time three resistances, R_1, R_2, R_3, all of equal value (30,000 ohms), were interposed in the circuit, as shown in the diagram (fig. 5, inset). The common junction O of these three was connected to one of the plates Q of the oscillograph, while the other plate P was connected successively to the points X, Y, and Z. It will be noticed that the oscillations going on in the circuit are not disturbed in any way when the connexions are changed. The wave-forms could not be photographed owing to insufficiency of light, but they were closely observed and are reproduced by drawing in fig. 5. As the general forms of the waves were found to remain the same on changing the values of the condenser, current, etc., the drawings are hoped to give sufficient idea regarding the surging of the current in the respective branches.

The wave-forms obtained depict the potentials developed across each resistance at every instant; but since the potential developed at any instant is the product of the resistance and the current at that instant, and the resistance remains constant, the wave-forms really give us the current variations at each instant in the different branches of the circuit. We shall now consider each of the cases separately.

Case I. (P connected to X).—These wave-forms delineate the nature of the current through the discharge-tube. As the discharge passes a large current suddenly flows through R_1 in the direction from X to O. Consequently the potential of the point X becomes very much higher than that of O, and, X being connected to P and O to Q, the beam of electron is suddenly deflected upwards, as indicated by the portion MN of the wave-form (fig. 5, case I.). But since the discharge starts and ends almost instantaneously the beam rapidly returns to its normal position, as indicated by NL. The wave-forms therefore stand as direct evidence to the instantaneous character of the discharge. The flattening out of the discharge curve near the foot LF is due to the fact that the internal resistance of the tube increases as the current through it decreases to a small value before the discharge is actually extinguished. The portion FG indicates that no current is flowing through the tube, as the discharge has already been extinguished. During this period the condenser is again charged up to the sparking potential V_c of the tube.

Case II. (P connected to Y).—In this case we obtain the nature of the current in the condenser circuit both when it

is charging up and also when it is discharging itself through the tube. When the discharge passes a large current flows through R_2 in the direction from O to Y. Thus, Q being raised to a higher potential than P, the beam is suddenly deflected downwards, as indicated by KT (fig. 5, Case II.). When the discharge is over the beam returns to its normal position, indicated by TS, which shows that the discharge is almost instantaneous. Since now the condenser begins to be charged up by the H.T. battery, a current flows through R_2 in a direction opposite to the former, and the beam is deflected upwards to D. As the condenser potential rises the current gradually diminishes, as shown by the portion of the curve DE.

Case III. (P connected to Z).—These wave-forms give us the nature of the current passing through the diode. The current is a maximum immediately after the discharge has ceased, and the condenser has started receiving fresh charge from the H.T. battery. Since the current flows in the direction O to Z, the spot is deflected downwards, and the current at this stage is indicated by AB (fig. 5, Case III.). As the condenser voltage rises with charging, the current gradually decreases and we obtain the curve BC in accordance with the well-known law of condenser charging.

Gill has assumed the current through the diode to be of constant magnitude i, and has used it as one of the variables in his formula connecting the wave-length λ of the oscillation with the electrical constants of the circuit and the discharge-tube. The oscillographic records obtained by us and as described in Case III. above show that the current is far from constant and that it undergoes a periodic fluctuation (as shown in fig. 5, Case III.).

The oscillographic records obtained and described above show vividly the nature of the pulsating current flowing in the various branches of the circuit when the discharge-tube is in operation. They show that the theory of the maintenance of the oscillations by repeated charging and discharging of the condenser, as originally proposed by Righi, is substantially correct.

In order to compare the period during which the discharge-tube is lighted with that during which it is extinguished falling-plate photographs of the discharge were taken, and a typical one is reproduced in Pl. X. The photograph shows (1) that the duration of flash is very small compared

with the period during which the tube is extinguished, and (2) that the extinction is complete.

The photograph, as well as the oscillographic records, justify the assumptions usually made regarding the instantaneous character and the total extinction of the discharge.

3. *Conclusion.*

The nature of the oscillations generated in low-pressure discharge in the air when a condenser is connected across the discharge-tube and a high resistance is inserted in series with the H.T. source has been investigated in the audible range of frequency between 100 and 1000 p.p.s. Observations have been made on the relations between the frequency of the generated oscillations and (*a*) the current through the discharge-tube, (*b*) the capacity of the associated condenser, (*c*) the pressure within the discharge-tube, and (*d*) the separation of the electrodes. These observations generally confirm those made by Gill in the supersonic range of frequency.

The important part played by the external resistance in the maintenance of the interruptions has been discussed. It has been shown that there is a critical value of this resistance below which no oscillations will occur. The value of the critical resistance R_c has been deduced in terms of the extinction potential V_b, the internal resistance r of the discharge-tube, and the battery voltage E. Experiments confirm this relation.

The wave-forms of the pulsating current flowing in the different branches of the circuit have been obtained with a cathode-ray oscillograph. These confirm in a general way the charge and discharge theory originated by Righi.

Falling-plate photographs of the discharge have been taken. They show that the duration of the discharge is very small compared with the period during which the tube is extinguished, and thus justify the assumption usually made that the discharge is almost instantaneous.

Wireless Laboratory,
University College of Science,
92 Upper Circular Road, Calcutta, India.
February 26, 1932.

LXX. *The Mehler-Dirichlet Integral and some other Legendre Function Formulæ. By* T. M. MacRobert, *Professor of Mathematics, University of Glasgow* *.

§ 1. *Introductory.*

THIS paper contains, in the first place, a new proof of the Mehler-Dirichlet formula for the Associated Legendre Functions of the First Kind. The formula is then employed to establish some expansions for Legendre Functions of non-integral degree in terms of Legendre Functions of integral degree. These expansions were originally given by Dr. Dougall †, who proved them by contour integration. The formulæ as given here differ in some respects from Dougall's, and the proofs do not involve the complex variable. With the aid of these formulæ it is quite easy to deduce the addition theorem for the Legendre Functions of the First Kind from the corresponding theorem for the Legendre Coefficients. An elementary proof of the latter theorem, depending on the induction method, is given in § 6. In the following section an alternative proof of the Mehler-Dirichlet formula is given. The method employed in this proof is also, in §§ 8 and 10, applied to derive the recurrence formulæ for the Associated Legendre Functions from the corresponding formulæ for the Legendre Functions. In § 9 some formulæ analogous to the Mehler-Dirichlet formula are established. These formulæ were given by Hobson in his paper ‡ "On a Type of Spherical Harmonics of Unrestricted Degree, Order, and Argument." Instead, however, of making references to that paper, it has seemed more convenient in the present discussion to give them to Professor Hobson's recently published treatise on "Spherical and Ellipsoidal Harmonics." Some notes on the history of the Mehler-Dirichlet formula will be found on p. 27 of that work. A principal object of the present paper is to give comparatively elementary proofs of formulæ of which the proofs hitherto published depended on contour integration.

§2. *Observations on some Formulæ employed in the Discussion.*

The proof of the Mehler-Dirichlet formula is based on the expansion

* Communicated by the Author.

† Proc. Edin. Math. Soc. xviii. p. 78 (1900); xlii. p. 93 (1923).

‡ Phil. Trans. clxxxvii. A, pp. 443–531 (1896).

$$\cos nx = \cos x \, \mathrm{F}\left(\frac{1+n}{2}, \frac{1-n}{2}; \frac{1}{2}; \sin^2 x\right), \quad -\pi < x < \pi. \quad . \quad . \quad . \quad (1)$$

This formula is most easily established by a consideration of the integrals of the differential equation,

$$\frac{d^2y}{dx^2} + n^2 y = 0.$$

The transformation $u = \sin^2 x$ leads to the equation

$$u(1-u)\frac{d^2y}{du^2} + (\tfrac{1}{2}-u)\frac{dy}{du} + \tfrac{1}{4}n^2 y = 0,$$

of which two independent solutions are:

$$\mathrm{F}\left(\frac{n}{2}, -\frac{n}{2}; \frac{1}{2}; \sin^2 x\right), \qquad \sin x \, \mathrm{F}\left(\frac{1+n}{2}, \frac{1-n}{2}; \frac{3}{2}; \sin^2 x\right).$$

As $\cos nx$ and $\sin nx$ are solutions of the original equation, it follows that

$$\sin nx = n \sin x \, \mathrm{F}\left(\frac{1+n}{2}, \frac{1-n}{2}; \frac{3}{2}; \sin^2 x\right),$$

$$\cos nx = \mathrm{F}\left(\frac{n}{2}, -\frac{n}{2}; \frac{1}{2}; \sin^2 x\right).$$

On differentiating these equations, or applying the transformation

$$\mathrm{F}(\alpha, \beta; \gamma; z) = (1-z)^{\gamma-\alpha-\beta} \, \mathrm{F}(\gamma-\alpha, \gamma-\beta; \gamma; z), \quad (2)$$

to the hypergeometric functions, the two formulæ (1) and

$$\sin nx = n \sin x \cos x \, \mathrm{F}\left(1+\frac{n}{2}, 1-\frac{n}{2}; \frac{3}{2}; \sin^2 x\right)$$

are obtained. The method has been here given in detail, as further applications of it will be made in § 9.

The expansion

$$\cos(n+\tfrac{1}{2})\phi = \frac{\sin n\pi}{\pi} \sum_{p=0}^{\infty} (-1)^p \left(\frac{1}{n-p} - \frac{1}{n+p+1}\right) \cos(p+\tfrac{1}{2})\phi, \quad (3)$$

where $-\pi < \phi < \pi$ may be established by evaluating the contour integral

$$\frac{1}{2\pi i} \int \frac{\pi \cos(z+\frac{1}{2})\phi}{(z-n)\sin \pi z} \, dz,$$

taken round a large circle with the origin as centre. It can, however, be derived independently of contour integration in more than one way. For example, on multiplying the Fourier expansions

$$\cos n\phi = \frac{\sin n\pi}{\pi}\left\{\frac{1}{n} + \sum_{p=1}^{\infty}(-1)^p \frac{2n\cos p\phi}{n^2-p^2}\right\}, \qquad -\pi \leq \phi \leq \pi,$$

$$\sin n\phi = \frac{\sin n\pi}{\pi}\left\{\sum_{p=1}^{\infty}(-1)^p \frac{2p\sin p\phi}{n^2-p^2}\right\}, \qquad -\pi < \phi < \pi,$$

by $\cos\frac{1}{2}\phi$, $\sin\frac{1}{2}\phi$ respectively, and subtracting, it is found that

$$\begin{aligned}\cos(n+\tfrac{1}{2})\phi &= \frac{\sin n\pi}{\pi}\left\{\frac{\cos\frac{1}{2}\phi}{n} + \sum_{p=1}^{\infty}(-1)^p \frac{n\cos(p+\tfrac{1}{2})\phi + n\cos(p-\tfrac{1}{2})\phi}{n^2-p^2}\right.\\ &\qquad\left. + \sum_{p=1}^{\infty}(-1)^p \frac{p\cos(p+\tfrac{1}{2})\phi - p\cos(p-\tfrac{1}{2})\phi}{n^2-p^2}\right\}\\ &= \frac{\sin n\pi}{\pi}\left\{\frac{\cos\frac{1}{2}\phi}{n} + \sum_{p=1}^{\infty}(-1)^p \frac{\cos(p+\tfrac{1}{2})\phi}{n-p}\right.\\ &\qquad\left. + \sum_{q=0}^{\infty}(-1)^{q+1}\frac{\cos(q+\tfrac{1}{2})\phi}{n+q+1}\right\},\end{aligned}$$

where $q=p-1$. From this (3) follows.

Again

$$\begin{aligned}\cos(n+\tfrac{1}{2})\phi\cos(n+\tfrac{1}{2})\psi &= \tfrac{1}{2}\cos\{(n+\tfrac{1}{2})(\phi+\psi)\}\\ &\qquad + \tfrac{1}{2}\cos\{(n+\tfrac{1}{2})(\phi-\psi)\}\\ &= \frac{\sin n\pi}{\pi}\sum_{p=0}^{\infty}(-1)^p\left(\frac{1}{n-p} - \frac{1}{n+p+1}\right)\\ &\qquad \times\left[\begin{array}{l}\tfrac{1}{2}\cos\{(p+\tfrac{1}{2})(\phi+\psi)\}\\ +\tfrac{1}{2}\cos\{(p+\tfrac{1}{2})(\phi-\psi)\}\end{array}\right],\end{aligned}$$

by (3). Hence

$$\cos(n+\tfrac{1}{2})\phi\cos(n+\tfrac{1}{2})\psi = \frac{\sin n\pi}{\pi}\sum_{p=0}^{\infty}(-1)^p \left(\frac{1}{n-p} - \frac{1}{n+p+1}\right)\cos(p+\tfrac{1}{2})\phi\cos(p+\tfrac{1}{2})\psi, \quad (4)$$

where $-\pi < \phi \pm \psi < \pi$.

Similar formulæ for the products of three or more cosines may be established in the same manner.

Ferrers' Associated Legendre Function.—This function will be denoted by $T_n^m(x)$, and defined by the equation

$$T_n^m(x) = e^{\frac{1}{2}m\pi i} P_n^m(x), \quad . \quad . \quad . \quad . \quad . \quad (5)$$

where *

$$P_n^m(z) = \frac{1}{\Gamma(1-m)} \left(\frac{z+1}{z-1}\right)^{\frac{1}{2}m} F\left(-n, n+1 ; 1-m ; \frac{1-z}{2}\right). \quad . \quad . \quad . \quad (6)$$

The latter function is real when z is real and >1; in (5) $P_n^m(x)$ is the value of $P_n^m(z)$ when z is real and lies between -1 and $+1$, on the upper side of the cross-cut along the x-axis. Thus

$$T_n^{-m}(x) = \frac{1}{\Gamma(1+m)} \left(\frac{1-x}{1+x}\right)^{\frac{1}{2}m} F\left(-n, n+1 ; m+1 ; \frac{1-x}{2}\right). \quad . \quad . \quad . \quad (7)$$

The definition in (5) is Hobson's †; it differs from that usually given—for instance, in Ferrers' 'Spherical Harmonics,' p. 75, Whittaker and Watson's 'Analysis' (second edition), p. 317, and the author's 'Spherical Harmonics,' p. 125—by the presence in (5) of the factor $e^{\frac{1}{2}m\pi i}$ in place of $e^{-\frac{1}{2}m\pi i}$. The advantage of Hobson's definition is that $T_n^m(x)$ remains real, for $-1<x<1$, when m is real and not an integer. Hobson and "Whittaker and Watson" use the notation P_n^m in place of T_n^m, but the advantage would seem to be with the latter notation, as it avoids confusion with the function $P_n^m(z)$ defined in (6).

When m is a positive integer,

$$T_n^{-m}(x) = (1-x^2)^{-\frac{1}{2}m} \int_x^1 \int_x^1 \cdots \int_x^1 P_n(x)(dx)^m, \quad . \quad (8)$$

$$T_n^m(x) = (-1)^m (1-x^2)^{\frac{1}{2}m} \frac{d^m}{dx^m} P_n(x), \quad . \quad . \quad (9)$$

and

$$T_n^{-m}(x) = (-1)^m \frac{\Gamma(n-m+1)}{\Gamma(n+m+1)} T_n^m(x). \quad . \quad . \quad (10)$$

Formulæ (8) and (9) differ by a factor $(-1)^m$ from the corresponding formulæ for the Tesseral Harmonics as defined by Ferrers.

* Hobson, p. 188. [The references to "Hobson" are to Prof. Hobson's book 'Spherical and Ellipsoidal Harmonics.']

† Hobson, pp. 90, 94, 99, 227.

§ 3. *Proof of the Mehler-Dirichlet Formula.*

In the integral

$$I \equiv \int_0^\theta \cos(n+\tfrac{1}{2})\phi(\cos\phi-\cos\theta)^{m-\frac{1}{2}}d\phi, \quad 0<\theta<\pi, \quad m>-\tfrac{1}{2},$$

expand $\cos(n+\frac{1}{2})\phi$ by means of (1) with $(2n+1)$ in place of n and $\frac{1}{2}\phi$ in place of x: thus

$$I=2^{m-\frac{1}{2}}\int_0^\theta \cos\tfrac{1}{2}\phi \mathrm{F}(n+1,\ -n\ ;\ \tfrac{1}{2}\ ;\ \sin^2\tfrac{1}{2}\phi) \times(\sin^2\tfrac{1}{2}\theta-\sin^2\tfrac{1}{2}\phi)^{m-\frac{1}{2}}d\phi.$$

Here put $\sin\frac{1}{2}\phi=x^{\frac{1}{2}}\sin\frac{1}{2}\theta$; then

$$I=2^{m-\frac{1}{2}}(\sin\tfrac{1}{2}\theta)^{2m}\int_0^1 \mathrm{F}(n+1,\ -n\ ;\ \tfrac{1}{2}\ ;\ x\sin^2\tfrac{1}{2}\theta) \times(1-x)^{m-\frac{1}{2}}x^{-\frac{1}{2}}dx.$$

Now integrate term by term, and get

$$I=2^{m-\frac{1}{2}}(\sin\tfrac{1}{2}\theta)^{2m}\mathrm{B}(m+\tfrac{1}{2},\ \tfrac{1}{2})\mathrm{F}(n+1,\ -n\ ;\ m+1\ ;\ \sin^2\tfrac{1}{2}\theta),$$

from which, with (7), is obtained the Mehler-Dirichlet Formula,*

$$(\sin\theta)^m \mathrm{T}_n^{-m}(\cos\theta) = \frac{2}{\Gamma(m+\frac{1}{2})\sqrt{(2\pi)}}\int_0^\theta \cos(n+\tfrac{1}{2})\phi(\cos\phi-\cos\theta)^{m-\frac{1}{2}}d\phi, \quad . \ . \ . \quad (11)$$

where $0<\theta<\pi$, $m>-\frac{1}{2}$. If $m>0$ the formula holds also for $\theta=0$.

Note.—If $m=\frac{1}{2}$ it follows from (11) that

$$(\sin\theta)^{\frac{1}{2}}\mathrm{T}_n^{-\frac{1}{2}}(\cos\theta)=\frac{4\sin(n+\frac{1}{2})\theta}{(2n+1)\sqrt{(2\pi)}}, \qquad 0\leq\theta<\pi.$$

Similar results can be obtained when $m=\frac{3}{2}, \frac{5}{2}, \ldots$. These can also be derived from the asymptotic expansion for T_n^{-m} when n is large.

§ 4. *Dougall's Expressions for Legendre Functions in Terms of Leyendre Coefficients.*

By substituting from (3) for $\cos(n+\frac{1}{2})\phi$ in (11), integrating term by term, and cancelling the factor $(\sin\theta)^m$, it is found that

* Hobson, p. 267.

$$\mathrm{T}_n^{-m}(\cos\theta) = \frac{\sin n\pi}{\pi} \sum_{p=0}^{\infty} (-1)^p \left(\frac{1}{n-p} - \frac{1}{n+p+1} \right) \mathrm{T}_p^{-m}(\cos\theta), \quad \ldots \quad (12)$$

where $-\pi < \theta < \pi$, $m \geqq 0$.

In particular, if $m = 0$,

$$\mathrm{P}_n(\cos\theta) = \frac{\sin n\pi}{\pi} \sum_{p=0}^{\infty} (-1)^p \left(\frac{1}{n-p} - \frac{1}{n+p+1} \right) \mathrm{P}_p(\cos\theta). \quad \ldots \quad (13)$$

Again, from (11),

$$\mathrm{T}_n^{-l}(\cos\theta)\, \mathrm{T}_n^{-m}(\cos\theta') = \frac{2(\sin\theta)^{-l}}{\Gamma(l+\frac{1}{2})\sqrt{(2\pi)}} \int_0^{\theta} \cos(n+\tfrac{1}{2})\phi\, (\cos\phi - \cos\theta)^{l-\frac{1}{2}} d\phi \times \frac{2(\sin\theta')^{-m}}{\Gamma(m+\frac{1}{2})\sqrt{(2\pi)}} \int_0^{\theta'} \cos(n+\tfrac{1}{2})\psi\, (\cos\psi - \cos\theta')^{m-\frac{1}{2}} d\psi.$$

Here substitute for $\cos(n+\frac{1}{2})\phi \cos(n+\frac{1}{2})\psi$ from (4), and integrate term by term; thus

$$\mathrm{T}_n^{-l}(\cos\theta)\, \mathrm{T}_n^{-m}(\cos\theta') = \frac{\sin n\pi}{\pi} \sum_{p=0}^{\infty} (-1)^p \left(\frac{1}{n-p} - \frac{1}{n+p+1} \right) \mathrm{T}_p^{-l}(\cos\theta)\, \mathrm{T}_p^{-m}(\cos\theta'), \quad \ldots \quad (14)$$

where

$$-\pi < \theta + \theta' < \pi, \quad -\pi < \theta - \theta' < \pi, \quad l \geqq 0, \quad m \geqq 0.$$

Similar expressions for the products of three or more such functions can be obtained in the same manner.

Next, in (14) let l be zero and m a positive integer, and replace $\cos\theta$ and $\cos\theta'$ by x and x' respectively. Then, on differentiating m times with regard to x and multiplying by $(-1)^m(1-x^2)^{\frac{1}{2}m}$, it results from (9) that

$$\mathrm{T}_n^{m}(x)\, \mathrm{T}_n^{-m}(x') = \frac{\sin n\pi}{\pi} \sum_{p=m}^{\infty} (-1)^p \left(\frac{1}{n-p} - \frac{1}{n+p+1} \right) \mathrm{T}_p^{m}(x)\, \mathrm{T}_p^{-m}(x'), \quad \ldots \quad (15)$$

where

$$0 < \theta < \pi, \quad 0 < \theta' < \pi, \quad \theta + \theta' < \pi \ (x = \cos\theta, \ x' = \cos\theta'),$$

and m is zero or a positive integer.

The proof of (15) is incomplete without some discussion of the convergence of the series. This involves no difficulty

if the asymptotic expansion of T_p^m for p large is made use of. A proof depending on more elementary considerations will be here given ; it follows on lines suggested by some work of H. Burkhardt's *.

From Laplace's Integral,

$$P_p(x) = \frac{1}{\pi}\int_0^\pi \{x + i\sqrt{(1-x^2)}\cos\phi\}^p\, d\phi,$$

it follows that, for $-1 < x < 1$,

$$\begin{aligned} |P_p(x)| &\leqq \frac{1}{\pi}\int_0^\pi \{x^2 + (1-x^2)|\cos\phi|\}^{\frac{1}{2}p}\, d\phi \\ &= \frac{2}{\pi}\int_0^{\frac{\pi}{2}} \{x^2 + (1-x^2)\cos\phi\}^{\frac{1}{2}p}\, d\phi \\ &= \frac{2}{\pi}\int_0^{\frac{\pi}{2}} \{1 - 2(1-x^2)\sin^2\tfrac{1}{2}\phi\}^{\frac{1}{2}p}\, d\phi. \end{aligned}$$

Here put

$$\sin\tfrac{1}{2}\phi = \frac{u}{\sqrt{p}};$$

so that, for $0 \leqq \phi \leqq \frac{1}{2}\pi$, $u^2 \leqq \frac{1}{2}p$: then

$$|P_p(\cos\theta)| \leqq \frac{2}{\pi}\int_0^{\sqrt{\left(\frac{p}{2}\right)}} \left(1 - \frac{2u^2\sin^2\theta}{p}\right)^{\frac{1}{2}p} \frac{2du}{\sqrt{p}\cdot\sqrt{\left(1-\frac{u^2}{p}\right)}}.$$

Now, if

$$0 \leqq \frac{\alpha}{p} \leqq 1,$$

$$1 - \frac{\alpha}{p} \leqq e^{-\frac{\alpha}{p}}.$$

Therefore

$$\left(1 - \frac{\alpha}{p}\right)^{\frac{1}{2}p} \leqq e^{-\frac{1}{2}\alpha}.$$

Hence, in the integral,

$$\left(1 - \frac{2u^2\sin^2\theta}{p}\right)^{\frac{1}{2}p} \leqq e^{-u^2\sin^2\theta};$$

and also

$$1 - \frac{u^2}{p} \geqq \tfrac{1}{2}.$$

* *Sitzungsber. Akad. München*, 1909, 10th Abhand.

Thus

$$|\mathrm{P}_p(\cos\theta)| \leqq \frac{4\sqrt{2}}{\pi\sqrt{p}}\int_0^{\sqrt{\left(\frac{p}{2}\right)}} e^{-u^2\sin^2\theta}\,du$$

$$< \frac{4\sqrt{2}}{\pi\sqrt{p}}\int_0^{\infty} e^{-u^2\sin^2\theta}\,du$$

$$= \frac{4}{\sqrt{(2p\pi)}.|\sin\theta|},^{*} \quad . \quad . \quad . \quad (16)$$

where $0<\theta<\pi$.

Thus, if

$$0<\epsilon\leqq\theta\leqq\pi-\epsilon,$$

$$\sqrt{p}.|\mathrm{P}_p(\cos\theta| < k_0,$$

where k_0 is a constant independent of p (but not of ϵ).

Again, from the formula

$$(1-x^2)\mathrm{P}_p'(x) = p\mathrm{P}_{p-1}(x)-px\mathrm{P}_p(x),$$

it follows that, for the same range,

$$\sqrt{p}.|\mathrm{T}_p^{1}(\cos\theta)| < k_1 p, \quad . \quad . \quad . \quad . \quad (17)$$

where k_1 is a constant independent of p.

On differentiating the differential equation

$$(1-x^2)\mathrm{P}_p''(x)-2x\mathrm{P}_p'(x)+p(p+1)\mathrm{P}_p(x) = 0$$

$(m-1)$ times and multiplying by $(-1)^{m-1}(1-x^2)^{\frac{1}{2}m}$, it is found that

$$\sqrt{(1-x^2)}\mathrm{T}_p^{m+1}(x)+2mx\mathrm{T}_p^{m}(x)+$$
$$(p-m+1)(p+m)\sqrt{(1-x^2)}\mathrm{T}_p^{m-1}(x) = 0. \quad (18)$$

From (18), with (16) and (17), it results that, for

$$0<\epsilon\leqq\theta\leqq\pi-\epsilon,$$

$$\sqrt{p}.|\mathrm{T}_p^{m}(\cos\theta)| < k_m p^m, \quad . \quad . \quad . \quad . \quad (19)$$

where k_m is a constant independent of p (but not of ϵ). By applying the transformation (10) to (19) it can be seen that a similar inequality holds when m is a negative integer.

From (19) it follows that (15) is absolutely and uniformly convergent for the ranges $0<\epsilon\leqq\theta\leqq\pi-\epsilon$, $0<\epsilon'\leqq\theta'\leqq\pi-\epsilon'$, where ϵ and ϵ' can be taken arbitrarily small. Thus (15) holds for $0<\theta<\pi$, $0<\theta'<\pi$, $\theta+\theta'<\pi$.

* For further references to inequalities of this type see Hobson, p. 311; Proc. Edin. Math. Soc. xli. p. 93 (1922); xlii. p. 92 (1923).

§ 5. *The Recurrence Formulæ.*

Formula (13) can be employed to deduce the recurrence formulæ for the Legendre functions from the corresponding formulæ for the Legendre coefficients. Thus

$$(n+1)\mathrm{P}_{n+1}(x)-(2n+1)x\mathrm{P}_n(x)+n\mathrm{P}_{n-1}(x)$$

$$=\frac{\sin n\pi}{\pi}\sum_{p=0}^{\infty}(-1)^p$$

$$\left\{-\frac{n+1}{n+1-p}-\frac{2n+1}{n-p}x-\frac{n}{n-1-p}\right.$$

$$\left.+\frac{n+1}{n+1+p+1}+\frac{2n+1}{n+p+1}x+\frac{n}{n-1+p+1}\right\}\mathrm{P}_p(x)$$

$$=\frac{\sin n\pi}{\pi}\sum_{p=0}^{\infty}(-1)^p$$

$$\left\{-\frac{p}{n-p+1}-\frac{2p+1}{n-p}x-\frac{p+1}{n-p-1}\right.$$

$$\left.-\frac{p+1}{n+p+2}-\frac{2p+1}{n+p+1}x-\frac{p}{n+p}\right\}\mathrm{P}_p(x)$$

$$=\frac{\sin n\pi}{\pi}\sum_{p=0}^{\infty}(-1)$$

$$\left[\frac{1}{n-p}\{(p+1)\mathrm{P}_{p+1}(x)-(2p+1)x\mathrm{P}_p(x)+p\mathrm{P}_{p-1}(x)\}\right.$$

$$\left.+\frac{1}{n+p+1}\{p\mathrm{P}_{p-1}(x)-(2p+1)x\mathrm{P}_p(x)+(p+1)\mathrm{P}_{p+1}(x)\}\right];$$

and therefore

$$(n+1)\mathrm{P}_{n+1}(x)-(2n+1)x\mathrm{P}_n(x)+n\mathrm{P}_{n-1}(x)=0. \quad (20)$$

Again,

$$\mathrm{P}'_{n+1}(x)-\mathrm{P}'_{n-1}(x)-(2n+1)\mathrm{P}_n(x)$$

$$=\frac{\sin n\pi}{\pi}\sum_{p=0}^{\infty}(-1)^p$$

$$\left\{-\frac{1}{n+1-p}\mathrm{P}_p'(x)+\frac{1}{n-1-p}\mathrm{P}_p'(x)-\frac{2n+1}{n-p}\mathrm{P}_p(x)\right.$$

$$\left.+\frac{1}{n+1+p+1}\mathrm{P}_p'(x)-\frac{1}{n-1+p+1}\mathrm{P}_p'(x)+\frac{2n+1}{n+p+1}\mathrm{P}_p(x)\right\}$$

$$= \frac{\sin n\pi}{\pi} \sum_{p=0}^{\infty} (-1)$$

$$\left\{ -\frac{1}{n-p+1} P_p'(x) + \frac{1}{n-p-1} P_p'(x) - \frac{2p+1}{n-p} P_p(x) \right.$$

$$\left. + \frac{1}{n+p+2} P_p'(x) - \frac{1}{n+p} P_p'(x) - \frac{2p+1}{n+p+1} P_p(x) \right\}$$

$$= \frac{\sin n\pi}{\pi} \sum_{p=0}^{\infty} (-1)^p$$

$$\left[\frac{1}{n-p} \{ P'_{p+1}(x) - P'_{p-1}(x) - (2p+1) P_p(x) \} \right.$$

$$\left. + \frac{1}{n+p+1} \{ -P'_{p-1}(x) + P'_{p+1}(x) - (2p+1) P_p(x) \} \right],$$

and consequently

$$P'_{n+1}(x) - P'_{n-1}(x) = (2n+1) P_n(x). \quad . \quad . \quad (21)$$

The other recurrence formulæ can be obtained in the same manner or deduced from (20) and (21).

Recurrence Formulæ for the Tesseral Harmonics.

If the equation (21) is differentiated $(m-1)$ times and the resulting equation multiplied by $(-1)^{m-1}(1-x^2)^{\frac{1}{2}m}$, it is found that

$$T^m_{n-1}(x) - T^m_{n+1}(x) = (2n+1)\sqrt{(1-x^2)} T^{m-1}_n(x). \quad (22)$$

Again, if (21) be integrated $(m+1)$ times from x to 1 and the result multipled by $(1-x^2)^{-\frac{1}{2}m}$, the equation

$$T^{-m}_{n-1}(x) - T^{-m}_{n+1}(x) = (2n+1)\sqrt{(1-x^2)} T^{-m-1}_n(x)$$

is obtained. Thus (22) holds for all integral values of m, positive or negative.

If now (20) be differentiated m times and the result multiplied by $(-1)^m(1-x^2)^{\frac{1}{2}m}$, it is found that

$$(n+1)T^m_{n+1}(x) - (2n+1)xT^m_n(x) + nT^m_{n-1}(x)$$
$$+ (2n+1)m\sqrt{(1-x^2)} T^{m-1}_n(x) = 0.$$

Hence, from (22),

$$(n-m+1)T^m_{n+1}(x) - (2n+1)xT^m_n(x) + (n+m)T^m_{n-1}(x) = 0.$$
$$. \quad . \quad . \quad (23)$$

On applying the transformation (10) to this equation, and simplifying, it becomes

$$(n+m+1)\mathrm{T}_{n+1}^{-m}(x)-(2n+1)x\mathrm{T}_n^{-m}(x)$$
$$+(n-m)\mathrm{T}_{n-1}^{-m}(x)=0.$$

Thus (23) holds for negative as well as positive integral values of m.

From the differential equation it can be deduced, just as was formula (18), that

$$\sqrt{(1-x^2)}\mathrm{T}_n^{m+1}(x)+2mx\mathrm{T}_n^{m}(x)$$
$$+(n-m+1)(n+m)\sqrt{(1-x^2)}\mathrm{T}_n^{m-1}(x)=0, \quad (24)$$

and, by applying (10), it can be shown that this formula holds when m is a negative integer.

Again, on adding together (22) multiplied by $(n-m+1)\times(n+m)$, (23) multiplied by $2m$, and (24) multiplied by $(2n+1)$, the formula

$$(n-m)(n-m+1)\mathrm{T}_{n+1}^{m}(x)-(n+m)(n+m+1)\mathrm{T}_{n-1}^{m}(x)$$
$$=(2n+1)\sqrt{(1-x^2)}\mathrm{T}_n^{m+1}(x) \quad (25)$$

is obtained. It may also be deduced from (22) by applying the transformation (10).

Next, between (22) and (23) eliminate $\mathrm{T}_{n+1}^{m}(x)$ and $\mathrm{T}_{n-1}^{m}(x)$ in turn and so derive the formulæ

$$\mathrm{T}_{n-1}^{m}(x)-x\mathrm{T}_n^{m}(x)=(n-m+1)\sqrt{(1-x^2)}\mathrm{T}_n^{m-1}(x), \quad (26)$$

$$x\mathrm{T}_n^{m}(x)-\mathrm{T}_{n+1}^{m}(x)=(n+m)\sqrt{(1-x^2)}\mathrm{T}_n^{m-1}(x). \quad . \quad (27)$$

Similarly, by eliminating $\mathrm{T}_{n+1}^{m}(x)$ and $\mathrm{T}_{n-1}^{m}(x)$ in turn from (23) and (25), or by applying the transformation (10) to (26) and (27), it can be shown that

$$(n-m)x\mathrm{T}_n^{m}(x)-(n+m)\mathrm{T}_{n-1}^{m}(x)=\sqrt{(1-x^2)}\mathrm{T}_n^{m+1}(x)$$
$$. \quad . \quad . \quad (28)$$

and

$$(n-m+1)\mathrm{T}_{n+1}^{m}(x)-(n+m-1)x\mathrm{T}_n^{m}(x)=\sqrt{(1-x^2)}\mathrm{T}_n^{m+1}(x),$$
$$. \quad . \quad . \quad (29)$$

All these recurrence formulæ have thus been established for all integral values of m, positive or negative.

§ 6. *The Addition Theorem for the Legendre Functions of the First Kind.*

It has been shown * that the formula

$$P_n(z) = P_n(x)P_n(x') + 2\sum_{m=1}^{\infty} \cos m\phi\, T_n^m(x)T_n^{-m}(x'), \quad (30)$$

where

$$z = xx' - \sqrt{(1-x^2)}\sqrt{(1-x'^2)}\cos\phi$$

and n is not an integer, can be deduced from the corresponding formula

$$P_p(z) = P_p(x)P_p(x') + 2\sum_{m=1}^{p} \cos m\phi\, T_p^m(x)T_p^{-m}(x') \quad (31)$$

for the Legendre Polynomials by means of (13) and (15).

For, from (13),

$$P_n(z) = \frac{\sin n\pi}{\pi}\sum_{p=0}^{\infty}(-1)^p\left(\frac{1}{n-p} - \frac{1}{n+p+1}\right)P_p(z);$$

and, on substituting from (31) for $P_p(z)$ and changing the order of summation, it is found that

$$P_n(z) = \frac{\sin n\pi}{\pi}\sum_{p=0}^{\infty}(-1)^p\left(\frac{1}{n-p} - \frac{1}{n+p+1}\right)P_p(x)P_p(x')$$
$$+ \frac{2\sin n\pi}{\pi}\sum_{m=1}^{\infty}\cos m\phi \sum_{p=m}^{\infty}(-1)^p\left(\frac{1}{n-p} - \frac{1}{n+p+1}\right)$$
$$. T_p^m(x)T_p^{-m}(x').$$

Hence, on applying (15), formula (30) is obtained.

The formula (31) can be established by induction. Let it be assumed to hold for the values 0, 1, 2, 3, ..., p of p; then, from (20),

$$(p+1)P_{p+1}(z)$$
$$= (2p+1)zP_p(z) - pP_{p-1}(z)$$
$$= (2p+1)\{xx' - \sqrt{(1-x^2)}\sqrt{(1-x'^2)}\cos\phi\}$$
$$\times\left\{P_p(x)P_p(x') + 2\sum_{m=1}^{p} T_p^m(x)T_p^{-m}(x')\cos m\phi\right\}$$
$$-p\left\{P_{p-1}(x)P_{p-1}(x') + 2\sum_{m=1}^{p-1} T_{p-1}^m(x)T_{p-1}^{-m}(x')\cos m\phi\right\}.$$

* Proc. Edin. Math. Soc. xlii. p. 94 (1923).

The coefficient of $\cos m\phi$ in this expression is

$$(2p+1)xx'2\mathrm{T}_p^{\,m}(x)\mathrm{T}_p^{\,-m}(x')-(2p+1)\sqrt{(1-x^2)}\sqrt{(1-x'^2)}$$
$$\times\{\mathrm{T}_p^{\,m-1}(x)\mathrm{T}_p^{\,-m+1}(x')+\mathrm{T}_p^{\,m+1}(x)\mathrm{T}_p^{\,-m-1}(x')\}$$
$$-2p\mathrm{T}^m_{p-1}(x)\mathrm{T}^{-m}_{p-1}(x').$$

On applying (23), (22), and (25) this is seen to be equal to

$$\frac{2}{2p+1}\{(p-m+1)\mathrm{T}^m_{p+1}(x)+(p+m)\mathrm{T}^m_{p-1}(x)\}$$
$$\times\{(p+m+1)\mathrm{T}^{-m}_{p+1}(x')+(p-m)\mathrm{T}^{-m}_{p-1}(x')\}$$
$$+\frac{1}{2p+1}\{\mathrm{T}^m_{p+1}(x)-\mathrm{T}^m_{p-1}(x)\}\{(p+m)(p+m+1)\mathrm{T}^{-m}_{p+1}(x')$$
$$-(p-m)(p-m+1)\mathrm{T}^{-m}_{p-1}(x')\}$$
$$+\frac{1}{2p+1}\{(p-m)(p-m+1)\mathrm{T}^m_{p+1}(x)$$
$$-(p+m)(p+m+1)\mathrm{T}^m_{p-1}(x)\}\{\mathrm{T}^{-m}_{p+1}(x')-\mathrm{T}^{-m}_{p-1}(x')\}$$
$$-2p\mathrm{T}^m_{p-1}(x)\mathrm{T}^{-m}_{p-1}(x')$$
$$=\frac{1}{2p+1}\mathrm{T}^m_{p+1}(x)\mathrm{T}^{-m}_{p+1}(x')\{2(p-m+1)(p+m+1)$$
$$+(p+m)(p+m+1)+(p-m)(p-m+1)\}$$
$$=(p+1)2\mathrm{T}^m_{p+1}(x)\mathrm{T}^{-m}_{p+1}(x').$$

The term independent of ϕ is

$$(2p+1)xx'\mathrm{P}_p(x)\mathrm{P}_p(x')-(2p+1)$$
$$\times\sqrt{(1-x^2)}\sqrt{(1-x'^2)}\mathrm{T}_p^{\,1}(x)\mathrm{T}_p^{\,-1}(x')-p\mathrm{P}_{p-1}(x)\mathrm{P}_{p-1}(x')$$
$$=\frac{1}{2p+1}\{(p+1)\mathrm{P}_{p+1}(x)+p\mathrm{P}_{p-1}(x)\}$$
$$\times\{(p+1)\mathrm{P}_{p+1}(x')+p\mathrm{P}_{p-1}(x')\}$$
$$+\frac{1}{2p+1}\{p(p+1)\mathrm{P}_{p+1}(x)-p(p+1)\mathrm{P}_{p-1}(x)\}$$
$$\times\{\mathrm{P}_{p+1}(x')-\mathrm{P}_{p-1}(x')\}-p\mathrm{P}_{p-1}(x)\mathrm{P}_{p-1}(x')$$
$$=(p+1)\mathrm{P}_{p+1}(x)\mathrm{P}_{p+1}(x').$$

Thus the expansion (31) holds for $\mathrm{P}_{p+1}(z)$. But it holds for $\mathrm{P}_0(z)$ and $\mathrm{P}_1(z)$, since

$$\mathrm{P}_1(z)=xx'-\sqrt{(1-x^2)}\sqrt{(1-x'^2)}\cos\phi$$
$$=\mathrm{P}_1(x)\mathrm{P}_1(x')+2\cos\phi\mathrm{T}_1^{\,1}(x)\mathrm{T}_1^{\,-1}(x').$$

Hence it holds for all positive integral values of p.

§ 7. *Alternative Proof of the Mehler–Dirichlet Formula.*

Up to this point the use of contour integrals has been avoided. The formula (13) can be easily established by that method, and it can then be employed, along with (3), to deduce the Mehler–Dirichlet formula for $P_n(\cos\theta)$ from the same formula for $P_p(\cos\theta)$, where p is a positive integer. The latter expression can be derived in more than one way from the expansion

$$(1-2hx+h^2)^{-\frac{1}{2}} = \sum_{p=0}^{\infty} h^p P_p(x).$$

The procedure is as follows. In (13) replace $P_p(\cos\theta)$ by the Mehler–Dirichlet integral; then

$$P_n(\cos\theta) = \frac{\sin n\pi}{\pi} \sum_{p=0}^{\infty} (-1)^p \left(\frac{1}{n-p} - \frac{1}{n+p+1}\right) \times \frac{2}{\pi}\int_0^{\theta} \frac{\cos\left(p+\frac{1}{2}\right)\phi\, d\phi}{\sqrt{(2\cos\phi - 2\cos\theta)}},$$

where $0<\theta<\pi$. Next, change the order of addition and integration, and apply (3); thus

$$P_n(\cos\theta) = \frac{2}{\pi}\int_0^{\theta} \frac{\cos\left(n+\frac{1}{2}\right)\phi\, d\phi}{\sqrt{(2\cos\phi - 2\cos\theta)}}, \qquad 0<\theta<\pi. \quad (32)$$

When m is a positive integer, (32) can be derived from (11) by differentiating m times with regard to $\cos\theta$, and multiplying by $(-1)^m$. Conversely (11) may be deduced from (32) by integrating m times with regard to $\cos\theta$ between the limits $\cos\theta$ and 1. [As (32) does not hold when $\cos\theta = 1$, the first integration should be from $\cos\theta$ to $1-\epsilon$; then ϵ can be allowed to tend to zero.]

For non-integral values of m the same result can be obtained by the following method, which can be regarded as a generalization of the above operation of integrating m times from $\cos\theta$ to 1.

If $n>-1$, $m>0$,

$$\int_x^a (a-\xi)^n(\xi-x)^{m-1}\, d\xi = (a-x)^{n+m}\int_0^1 \eta^n(1-\eta)^{m-1}\, d\eta,$$

where

$$\xi = a-(a-x)\eta;$$

hence

$$\frac{1}{\Gamma(m)}\int_x^a (a-\xi)^n(\xi-x)^{m-1}\, d\xi = \frac{\Gamma(n+1)}{\Gamma(n+m+1)}(a-x)^{n+m}. \quad (33)$$

By this operation the expression on the right is derived from $(a-\xi)^n$. If m were a positive integer the same result would be obtained by integrating $(a-x)^n$ m times between the limits x and a.

Now let the above operation be applied to $P_n(\xi)$; thus

$$\frac{1}{\Gamma(m)}\int_x^1 P_n(\xi)(\xi-x)^{m-1}\,d\xi$$
$$= \frac{1}{\Gamma(m)}\int_x^1 F\left(-n,\ n+1\ ;\ 1\ ;\ \frac{1-\xi}{2}\right)(\xi-x)^{m-1}d\xi,$$

and, on integrating term by term, this is found to be equal to

$$(1-x)^m \frac{1}{\Gamma(m+1)} F\left(-n,\ n+1\ ;\ m+1\ ;\ \frac{1-x}{2}\right).$$

Hence, from (7),

$$(1-x^2)^{\frac{1}{2}m}\,T_n{}^{-m}(x) = \frac{1}{\Gamma(m)}\int_x^1 P_n(\xi)\,(\xi-x)^{m-1}\,d\xi, \quad (34)$$

where $m>0$, $-1<x\leqq 1$.

Again, from (32),

$$P_n(\xi) = \frac{\sqrt{2}}{\pi}\int_0^{\cos^{-1}\xi} \cos\,(n+\tfrac{1}{2})\phi\ (\cos\phi-\xi)^{-\frac{1}{2}}d\phi, \text{ where}$$

$-1<\xi<1$. Hence, by (34),

$$(1-x^2)^{\frac{1}{2}m}\,T_n{}^{-m}(x)$$
$$= \frac{\sqrt{2}}{\pi\Gamma(m)}\int_x^1 (\xi-x)^{m-1}d\xi \int_0^{\cos^{-1}\xi} \cos(n+\tfrac{1}{2})\phi\,(\cos\phi-\xi)^{-\frac{1}{2}}d\phi,$$

where $m>0$, $-1<x<1$. The area of integration is the area in the figure, bounded by the lines $\phi=0$, $\xi=x$, and the curve $\xi=\cos\phi$. On changing the order of integration the expression on the right becomes

$$\frac{\sqrt{2}}{\pi}\int_0^{\cos^{-1}x} \cos(n+\tfrac{1}{2})\phi\,d\phi \frac{1}{\Gamma(m)}\int_x^{\cos\phi} (\cos\phi-\xi)^{-\frac{1}{2}}(\xi-x)^{m-1}\,d\xi$$
$$= \frac{\sqrt{2}}{\pi}\int_0^{\cos^{-1}x} \cos\,(n+\tfrac{1}{2})\phi \frac{\Gamma(\frac{1}{2})}{\Gamma(m+\frac{1}{2})}(\cos\phi-x)^{m-\frac{1}{2}}\,d\phi$$

by (33). Hence, if $x=\cos\theta$,

$$(\sin\theta)^m\,T_n{}^{-m}(\cos\theta)$$
$$= \frac{2}{\Gamma(m+\frac{1}{2})\sqrt{(2\pi)}}\int_0^{\theta} \cos\,(n+\tfrac{1}{2})\phi\,(\cos\phi-\cos\theta)^{m-\frac{1}{2}}\,d\phi,$$

where $0\leqq\theta<\pi$, $m>0$. This is formula (11).

§ 8. *Further Generalisations of the Recurrence Formulæ.*

The operation employed in the previous section can be used to prove the recurrence formulæ of § 5 for non-integral values of m.

From (21) and (34)

$$\frac{1}{\Gamma(m+1)}\int_x^1 \mathrm{P}_{n+1}'(\xi)(\xi-x)^m\,d\xi - \frac{1}{\Gamma(m+1)}\int_x^1 \mathrm{P}_{n-1}'(\xi)(\xi-x)^m\,d\xi = (2n+1)(1-x^2)^{\frac{m+1}{2}}\mathrm{T}_n^{-m-1}(x).$$

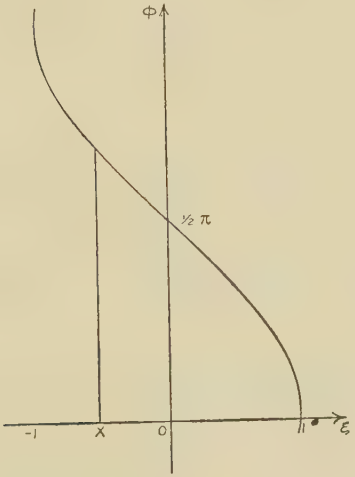

The expression on the left, on integration by parts, becomes, if $m>0$,

$$-\frac{1}{\Gamma(m)}\int_x^1 \mathrm{P}_{n+1}(\xi)(\xi-x)^{m-1}d\xi + \frac{1}{\Gamma(m)}\int_x^1 \mathrm{P}_{n-1}(\xi)(\xi-x)^{m-1}d\xi,$$

and this, on application of (34) and division by $(1-x^2)^{\frac{1}{2}m}$, gives

$$\mathrm{T}_{n-1}^{-m}(x)-\mathrm{T}_{n+1}^{-m}(x) = (2n+1)\sqrt{(1-x^2)}\mathrm{T}_n^{-m-1}(x), \quad (35)$$

where $m\geqq 0$. This is (22) with $-m$ in place of m.

Again, from (20) and (34),

$$(1-x^2)^{\frac{1}{2}m}\{(n+1)\mathrm{T}_{n+1}^{-m}(x)+n\mathrm{T}_{n-1}^{-m}(x)\}$$

$$=(2n+1)\frac{1}{\Gamma(m)}\int_x^1 \xi \mathrm{P}_n(\xi)(\xi-x)^{m-1}\,d\xi$$

$$=(2n+1)\frac{1}{\Gamma(m)}\int_x^1 \mathrm{P}_n(\xi)\{(\xi-x)^m+x(\xi-x)^{m-1}\}\,d\xi$$

$$=(2n+1)m(1-x^2)^{\frac{m+1}{2}}\mathrm{T}_n^{-m-1}(x)+(2n+1)x(1-x^2)^{\frac{1}{2}m}\mathrm{T}_n^{-m}(x).$$

Thus

$$(n+1)\mathrm{T}_{n+1}^{-m}(x)+n\mathrm{T}_{n-1}^{-m}(x)$$
$$=(2n+1)m\sqrt{(1-x^2)}\mathrm{T}_n^{-m-1}(x)+(2n+1)x\mathrm{T}_n^{-m}(x).$$

Hence, from (35),

$$(n+m+1)\mathrm{T}_{n+1}^{-m}(x)-(2n+1)x\mathrm{T}_n^{-m}(x)$$
$$+(n-m)\mathrm{T}_{n-1}^{-m}(x)=0, \quad (36)$$

where $m\geqq 0$. This again is (23) with $-m$ for m.

If (34) is applied to the differential equation

$$\frac{d}{d\xi}\{(1-\xi^2)\mathrm{P}_n'(\xi)\}=-n(n+1)\mathrm{P}_n(\xi),$$

it gives

$$\frac{1}{\Gamma(m+1)}\int_x^1 \frac{d}{d\xi}\{(1-\xi^2)\mathrm{P}_n'(\xi)\}(\xi-x)^m\,d\xi$$
$$=-n(n+1)(1-x^2)^{\frac{m+1}{2}}\mathrm{T}_n^{-m-1}(x).$$

On integration by parts the expression on the left becomes, if $m>0$,

$$-\frac{1}{\Gamma(m)}\int_x^1 (1-\xi^2)\mathrm{P}_n'(\xi)(\xi-x)^{m-1}\,d\xi$$

$$=-\frac{1}{\Gamma(m)}\int_x^1 \mathrm{P}_n'(\xi)\{(1-x^2)-2x(\xi-x)-(\xi-x)^2\}(\xi-x)^{m-1}\,d\xi,$$

and, on again being integrated by parts, this takes the form, for $m>1$,

$$\frac{1}{\Gamma(m)}\int_x^1 P_n(\xi)\{(1-x^2)(m-1)$$
$$-2xm(\xi-x)-(m+1)(\xi-x)^2\}(\xi-x)^{m-2}\,d\xi$$
$$=(1-x^2)^{\frac{m+1}{2}}T_n{}^{-m+1}(x)-2mx(1-x^2)^{\frac{1}{2}m}T_n{}^{-m}(x)$$
$$-m(m+1)(1-x^2)^{\frac{m+1}{2}}T_n{}^{-m-1}(x).$$

Hence, on division by $(1-x^2)^{\frac{1}{2}m}$,

$$\sqrt{(1-x^2)}T_n{}^{-m+1}(x)-2mxT_n{}^{-m}(x)$$
$$+(n-m)(n+m+1)\sqrt{(1-x^2)}T_n{}^{-m-1}(x)=0, \quad (37)$$

where $m\geqq 1$. This is (24) with $-m$ in place of m.

As in § 5 the formulæ (25) to (29), with $-m$ in place of m, can be deduced from (35), (36), and (37).

On applying the theory of analytical continuation it can be shown that these formulæ hold for all values of m. Thus formulæ (22) to (29) are true for all values of m*.

§ 9. *Further Mehler–Dirichlet Integrals.*

Hobson (page 270) has given the formula

$$(\sinh\psi)^m P_n{}^{-m}(\cosh\psi)=\frac{2}{\Gamma(m+\frac{1}{2})\sqrt{(2\pi)}}$$
$$\times\int_0^\psi \cosh(n+\tfrac{1}{2})u\,(\cosh\psi-\cosh u)^{m-\frac{1}{2}}\,du, \quad (38)$$

where $m>-\frac{1}{2}$, $\psi>0$. It can be established by a method similar to that employed in § 3 for (11).

The formula

$$\cosh nx=\cosh x\,F\left(\frac{1+n}{2},\ \frac{1-n}{2};\ \tfrac{1}{2};\ -\sinh^2 x\right), \quad (39)$$

where $|\sinh x|<1$, can be deduced from (1), or derived, in the same manner as (1), from a differential equation.

On being transformed by the substitution $u=\sinh^2 x$, the equation

$$\frac{d^2y}{dx^2}-n^2y=0$$

becomes

$$u(1+u)\frac{d^2y}{du^2}+(\tfrac{1}{2}+u)\frac{dy}{du}-\tfrac{1}{4}n^2y=0. \quad . \quad . \quad (40)$$

* Formulæ (23), (24), (28), (29) are given by Hobson, pp. 289, 290.

The solutions in ascending powers of u are

$$\mathrm{F}\Big(-\frac{n}{2},\ \frac{n}{2};\ \tfrac{1}{2};\ -u\Big), \qquad u^{\frac{1}{2}}\mathrm{F}\Big(\frac{1-n}{2},\ \frac{1+n}{2};\ {}^{3};\ -u\Big).$$

Hence

$$\cosh nx = \mathrm{F}\Big(-\frac{n}{2},\ \frac{n}{2};\ \tfrac{1}{2};\ -\sinh^2 x\Big)$$

and

$$\sinh nx = n\sinh x\,\mathrm{F}\Big(\frac{1-n}{2},\ \frac{1+n}{2};\ \tfrac{3}{2};\ -\sinh^2 x\Big).$$

Formula (39) can be derived by applying the transformation (2) to the first of these equations, or by differentiating the second.

Now substitute for $\cosh(n+\frac{1}{2})u$ in (38) from (39), with $\frac{1}{2}u$ in place of x and $(2n+1)$ in place of n; then, if $\sinh\frac{1}{2}\psi<1$,

$$\mathrm{I} \equiv \int_0^{\psi} \cosh(n+\tfrac{1}{2})u\,(\cosh\psi-\cosh u)^{m-\frac{1}{2}}\,du$$
$$= 2^{m-\frac{1}{2}}\int_0^{\psi} \cosh\tfrac{1}{2}u\,\mathrm{F}(n+1,\ -n\ ;\ \tfrac{1}{2}\ ;\ -\sinh^2\tfrac{1}{2}u)$$
$$\times(\sinh^2\tfrac{1}{2}\psi-\sinh^2\tfrac{1}{2}u)^{m-\frac{1}{2}}\,du.$$

Here put $\sinh\frac{1}{2}u = x^{\frac{1}{2}}\sinh\frac{1}{2}\psi$; then, as in § 3,

$$\mathrm{I} = 2^{m-\frac{1}{2}}(\sinh\tfrac{1}{2}\psi)^{2m}\mathrm{B}(m+\tfrac{1}{2},\ \tfrac{1}{2})$$
$$\times\mathrm{F}(n+1,\ -n\ ;\ m+1\ ;\ -\sinh^2\tfrac{1}{2}\psi),$$

whence, on comparing this result with (7), formula (38) is obtained. The restriction $\sinh\frac{1}{2}\psi<1$ may now be removed.

Note.—When $m=\frac{1}{2}$ (38) reduces to

$$(\sinh\psi)^{\frac{1}{2}}\mathrm{P}_n^{-\frac{1}{2}}(\cosh\psi) = \frac{4\sinh(n+\frac{1}{2})\psi}{(2n+1)\sqrt{(2\pi)}}, \qquad \psi\geqq 0.$$

Formulæ for $\mathrm{Q}_n{}^{-m}(\cosh\psi)$.

The function $\mathrm{Q}_n{}^m(z)$ will here be defined by the equation

$$\mathrm{Q}_n{}^m(z) = \frac{\Gamma(n+m+1)\Gamma(\frac{1}{2})}{2^{n+1}\Gamma(n+\frac{3}{2})}\,\frac{(z^2-1)^{\frac{1}{2}m}}{z^{n+m+1}}$$
$$\times\mathrm{F}\Big(\frac{n+m+2}{2},\ \frac{n+m+1}{2}\ ;\ n+\tfrac{3}{2}\ ;\ \frac{1}{z^2}\Big). \quad (41)$$

A factor $e^{m\pi i}$, present in Hobson's definition *, is omitted in

* Hobson, p. 195.

order that, z being real and >1, $Q_n^m(z)$ may be real when m is real and fractional. As a consequence of the alteration in the definition the following relations hold:

$$Q_n^{-m}(z) = \frac{\Gamma(n-m+1)}{\Gamma(n+m+1)} Q_n^m(z); \quad . \quad . \quad (42)$$

and, when m is a positive integer,

$$Q_n^m(z) = (-1)^m(z^2-1)^{\frac{1}{2}m} \frac{d^m}{dz^m} Q_n(z), \quad . \quad . \quad . \quad (43)$$

$$Q_n^{-m}(z) = (z^2-1)^{-\frac{1}{2}m} \int_z^\infty \int_z^\infty \dots \int_z^\infty Q_n(z)(dz)^m. \quad (44)$$

Hobson (page 276) has given the formula

$$(\sinh\psi)^m Q_n^{-m}(\cosh\psi) = \frac{\sqrt{(2\pi)}}{2\Gamma(m+\frac{1}{2})} \int_\psi^\infty e^{-(n+\frac{1}{2})u}(\cosh u - \cosh\psi)^{m-\frac{1}{2}} du, \quad (45)$$

where $m > -\frac{1}{2}$, $n-m+1>0$, $\psi>0$. It can be established as follows.

Transform the equation

$$\frac{d^2y}{dx^2} - n^2y = 0$$

by the substitution $u = \cosh^2 x$. It becomes

$$u(u-1)\frac{d^2y}{du^2} + (u-\tfrac{1}{2})\frac{dy}{du} - \tfrac{1}{4}n^2y = 0,$$

and the solutions in descending powers of u are

$$u^{\frac{1}{2}n}\mathrm{F}\left(-\frac{n}{2}, \frac{1-n}{2}; 1-n; \frac{1}{u}\right), \quad u^{-\frac{1}{2}n}\mathrm{F}\left(\frac{n}{2}, \frac{1+n}{2}; 1+n; \frac{1}{u}\right).$$

It follows that, if n is positive and $x>0$,

$$e^{-nx} = (2\cosh x)^{-n}\mathrm{F}\left(\frac{n}{2}, \frac{1+n}{2}; 1+n; \frac{1}{\cosh^2 x}\right),$$

whence, on differentiating, or applying (2),

$$e^{-nx} = (2\cosh x)^{-n}\tanh x\,\mathrm{F}\left(1+\frac{n}{2}, \frac{1+n}{2}; 1+n; \frac{1}{\cosh^2 x}\right). \quad . \quad . \quad . \quad (46)$$

Note.—Since both sides of these equations are meromorphic in n, they hold also when n is negative.

On substituting from (46) in the integral on the right of (45), it is found that

$$I \equiv \int_{\psi}^{\infty} e^{-(n+\frac{1}{2})u}(\cosh u - \cosh\psi)^{m-\frac{1}{2}}\,du$$

$$= \int_{\psi}^{\infty} (2\cosh u)^{-n-\frac{1}{2}} \times \tanh u\, F\left(\frac{2n+5}{4}, \frac{2n+3}{4}; \frac{2n+3}{2}; \frac{1}{\cosh^2 u}\right) \times (\cosh u - \cosh\psi)^{m-\frac{1}{2}}\,du.$$

Here let $\cosh u = \cosh\psi/y$; then

$$I = 2^{-n-\frac{1}{2}}(\cosh\psi)^{m-n-1} \times \int_0^1 y^{n-m} F\left(\frac{2n+5}{4}, \frac{2n+3}{4}; \frac{2n+3}{2}; \frac{y^2}{\cosh^2\psi}\right)(1-y)^{m-\frac{1}{2}}\,dy$$

$$= 2^{-n-\frac{1}{2}}(\cosh\psi)^{m-n-1} \frac{\Gamma\left(\frac{2n+3}{2}\right)}{\Gamma\left(\frac{2n+5}{4}\right)\Gamma\left(\frac{2n+3}{4}\right)} \times \sum_{r=0}^{\infty} \frac{\Gamma\left(\frac{2n+5}{4}+r\right)\Gamma\left(\frac{2n+3}{4}+r\right)}{\Gamma\left(\frac{2n+3}{2}+r\right)\Gamma(r+1)} \times \frac{\Gamma(n-m+2r+1)\Gamma(m+\frac{1}{2})}{\Gamma(n+2r+\frac{3}{2})} \frac{1}{(\cosh\psi)^{2r}}.$$

Now from the formula

$$\Gamma(2z)\,\Gamma(\tfrac{1}{2}) = \Gamma(z)\,\Gamma(z+\tfrac{1}{2})2^{2z-1}, \quad . \quad . \quad (47)$$

it follows that

$$\frac{\Gamma(n-m+2r+1)}{\Gamma(n+2r+\frac{3}{2})} = \frac{\Gamma\left(\frac{n-m+1}{2}+r\right)\Gamma\left(\frac{n-m+2}{2}+r\right)}{\Gamma\left(\frac{2n+3}{4}+r\right)\Gamma\left(\frac{2n+5}{4}+r\right)} 2^{-m-\frac{1}{2}}$$

and

$$\frac{\Gamma\left(\frac{2n+3}{2}\right)}{\Gamma\left(\frac{2n+5}{4}\right)\Gamma\left(\frac{2n+3}{4}\right)} = \frac{2^{n+\frac{1}{2}}}{\sqrt{\pi}}.$$

Hence

$$I = \frac{2^{-m-\frac{1}{2}}}{\sqrt{\pi}}(\cosh\psi)^{m-n-1}\frac{\Gamma\left(\frac{n-m+1}{2}\right)\Gamma\left(\frac{n-m+2}{2}\right)\Gamma(m+\frac{1}{2})}{\Gamma\left(\frac{2n+3}{2}\right)}$$

$$\times F\left(\frac{n-m+1}{2},\ \frac{n-m+2}{2};\ \frac{2n+3}{2};\ \frac{1}{\cosh^2\psi}\right)$$

$$= 2^{-n-\frac{1}{2}}(\cosh\psi)^{m-n-1}\frac{\Gamma(n-m+1)\,\Gamma(m+\frac{1}{2})}{\Gamma(n+\frac{3}{2})}$$

$$\times F\left(\frac{n-m+1}{2},\ \frac{n-m+2}{2};\ \frac{2n+3}{2};\ \frac{1}{\cosh^2\psi}\right),$$

by (47). Hence, on comparing this with (41), (45) is obtained.

Note.—If $m=\frac{1}{2}$, (45) reduces to

$$(\sinh\psi)^{\frac{1}{2}}Q_n^{-\frac{1}{2}}(\cosh\psi) = \frac{\sqrt{(2\pi)}}{2n+1}e^{-(n+\frac{1}{2})\psi},\quad \psi>0,\quad n+\tfrac{1}{2}>0.$$

Other formulæ can be obtained in the same manner. For example, if equation (40) is solved in descending powers of u, the solutions obtained are

$$u^{\frac{1}{2}n}F\left(-\frac{n}{2},\ \frac{1-n}{2};\ 1-n;\ -\frac{1}{u}\right),$$

$$u^{-\frac{1}{2}n}F\left(\frac{n}{2},\ \frac{1+n}{2};\ 1+n;\ -\frac{1}{u}\right),$$

whence, if n and x are positive, and $\sinh x>1$,

$$e^{-nx} = (2\sinh x)^{-n}F\left(\frac{n}{2},\ \frac{1+n}{2};\ 1+n;\ -\frac{1}{\sinh^2 x}\right).$$

Thus

$$e^{-nx} = (2\sinh x)^{-n}\coth x\,F\left(\frac{n}{2}+1,\ \frac{n+1}{2};\ n+1;\ -\frac{1}{\sinh^2 x}\right).$$

. . . (48)

On substituting in the integral I above it is found that, for $\sinh\frac{1}{2}\psi>1$,

$$I = \int_\psi^\infty (2\sinh\tfrac{1}{2}u)^{-2n-1}\coth\tfrac{1}{2}u$$

$$\times F\left(n+\tfrac{3}{2},\ n+1;\ 2n+2;\ -\frac{1}{\sinh^2\frac{1}{2}u}\right)$$

$$\times 2^{m-\frac{1}{2}}(\sinh^2\tfrac{1}{2}u-\sinh^2\tfrac{1}{2}\psi)^{m-\frac{1}{2}}\,du.$$

Here put $\sinh\frac{1}{2}u = \sinh\frac{1}{2}\psi/\sqrt{y}$, then

$$\begin{aligned}
\mathrm{I} &= 2^{m-2n-\frac{3}{2}}(\sinh\tfrac{1}{2}\psi)^{2m-2n-2} \\
&\quad\times\int_0^1 y^{n-m}\mathrm{F}\Big(n+\tfrac{3}{2}, n+1;\ 2n+2;\ -\frac{y}{\sinh^2\frac{1}{2}\psi}\Big)(1-y)^{m-\frac{1}{2}}dy \\
&= 2^{m-2n-\frac{3}{2}}(\sinh\tfrac{1}{2}\psi)^{2m-2n-2}\,\mathrm{B}(n-m+1,\ m+\tfrac{1}{2}) \\
&\quad\times\mathrm{F}\Big(n-m+1,\ n+1\ ;\ 2n+2\ ;\ -\frac{1}{\sinh^2\frac{1}{2}\psi}\Big).
\end{aligned}$$

Hence, from (45), if $\sinh\frac{1}{2}\psi>1$,

$$\begin{aligned}
\mathrm{Q}_n^{-m}(\cosh\psi) &= (\tanh\tfrac{1}{2}\psi)^m(2\sinh\tfrac{1}{2}\psi)^{-2n-2}\frac{\Gamma(\frac{1}{2})\Gamma(n-m+1)}{\Gamma(n+\frac{3}{2})} \\
&\quad\times\mathrm{F}\Big(n-m+1,\ n+1\ ;\ 2n+2\ ;\ -\frac{1}{\sinh^2\frac{1}{2}\psi}\Big), \qquad (49)
\end{aligned}$$

a formula first given by Barnes *.

§ 10. *Recurrence Formulæ for* $\mathrm{Q}_n^{-m}(z)$.

The formulæ (20) and (21) hold for $\mathrm{Q}_n(z)$. That this is so may be verified directly from (41), or deduced by applying to (20) and (21) the relation

$$2\sin n\pi\mathrm{Q}_n(x) = \pi\{e^{-n\pi i}\mathrm{P}_n(x)-\mathrm{P}_n(-x)\}.$$

The formulæ for Q_n^{-m} may be derived by a process similar to that employed in § 8.

From the equation

$$\int_x^\infty \xi^{-p}(\xi-x)^{m-1}\,d\xi = x^{-p+m}\int_0^1 \eta^{p-m-1}(1-\eta)^{m-1}\,d\eta,$$

where $m>0$, $p-m>0$, $\xi=x/\eta$, it follows that

$$\frac{1}{\Gamma(m)}\int_x^\infty \xi^{-p}(\xi-x)^{m-1}\,d\xi = \frac{\Gamma(p-m)}{\Gamma(p)}\,x^{-p+m}. \qquad (50)$$

When m is a positive integer the same result is obtained by integrating x^{-p} m times from x to $+\infty$.

When $m=0$ (41) may be written in the form

$$\mathrm{Q}_n(\xi) = \tfrac{1}{2}\sum_{r=0}^{\infty}\frac{\Gamma\Big(\frac{n+2}{2}+r\Big)\Gamma\Big(\frac{n+1}{2}+r\Big)}{\Gamma(n+\frac{3}{2}+r)\,\Gamma(r+1)}\,\frac{1}{\xi^{n+2r+1}},$$

* Quart. Journ. of Maths. xxxix. p. 107 (1908); Hobson, p. 202.

since, by (47),

$$\Gamma(n+1)\,\Gamma(\tfrac{1}{2}) = \Gamma\Big(\frac{n+1}{2}\Big)\,\Gamma\Big(\frac{n+2}{2}\Big)\,2^n.$$

Thus, by (50), if $x>1$, $m>0$, $n-m+1>0$,

$$\mathrm{I} \equiv \frac{1}{\Gamma(m)}\int_x^\infty Q_n(\xi)(\xi-x)^{m-1}\,d\xi$$

$$= \tfrac{1}{2}\sum_{r=0}^{\infty} \frac{\Gamma\Big(\frac{n+2}{2}+r\Big)\Gamma\Big(\frac{n+1}{2}+r\Big)\Gamma(n+2r+1-m)}{\Gamma(n+\frac{3}{2}+r)\Gamma(r+1)\Gamma(n+2r+1)}\,x^{m-n-2r-1}.$$

But, by (47),

$$\frac{\Gamma(n+2r+1-m)}{\Gamma(n+2r+1)} = \frac{\Gamma\Big(\frac{n-m+1}{2}+r\Big)\,\Gamma\Big(\frac{n-m+2}{2}+r\Big)}{\Gamma\Big(\frac{n+1}{2}+r\Big)\,\Gamma\Big(\frac{n+2}{2}+r\Big)}\,2^{-m}.$$

Therefore

$$\mathrm{I} = \frac{1}{2^{m+1}}\,\frac{1}{x^{n-m+1}}\,\frac{\Gamma\Big(\frac{n-m+1}{2}\Big)\Gamma\Big(\frac{n-m+2}{2}\Big)}{\Gamma(n+\frac{3}{2})} \times \mathrm{F}\Big(\frac{n-m+1}{2},\ \frac{n-m+2}{2};\ n+\tfrac{3}{2};\ \frac{1}{x^2}\Big)$$

$$= \frac{\Gamma(n-m+1)\Gamma(\frac{1}{2})2^{m-n}}{2^{m+1}x^{n-m+1}\Gamma(n+\frac{3}{2})} \times \mathrm{F}\Big(\frac{n-m+1}{2},\ \frac{n-m+2}{2};\ n+\tfrac{3}{2};\ \frac{1}{x^2}\Big)$$

by (47). Thus, from (41),

$$\frac{1}{\Gamma(m)}\int_x^\infty Q_n(\xi)(\xi-x)^{m-1}\,d\xi = (x^2-1)^{\frac{1}{2}m}Q_n^{-m}(x), \quad (51)$$

where $x>1$, $m>0$, $n-m+1>0$.

By applying (51) the recurrence formulæ can then be found. They are *

$$Q_{n-1}^{-m}(x) - Q_{n+1}^{-m}(x) = (2n+1)\sqrt{(x^2-1)}\,Q_n^{-m-1}(x), \quad (52)$$

$$(n+m+1)\,Q_{n+1}^{-m}(x) - (2n+1)xQ_n^{-m}(x) + (n-m)\,Q_{n-1}^{-m}(x) = 0, \quad (53)$$

. . .

* Formulæ (53), (54), (58), (59) are given by Hobson, pp. 289, 290.

$$\sqrt{(x^2-1)}\,Q_n^{-m+1}(x) + 2mxQ_n^{-m}(x) - (n-m)(n+m+1)\sqrt{(x^2-1)}\,Q_n^{-m-1}(x) = 0, \quad (54)$$

$$(n-m)(n-m+1)Q_{n-1}^{-m}(x) - (n+m+1)(n+m)Q_{n+1}^{-m}(x) = (2n+1)\sqrt{(x^2-1)}\,Q_n^{-m+1}(x), \quad (55)$$

$$Q_{n-1}^{-m}(x) - xQ_n^{-m}(x) = (n+m+1)\sqrt{(x^2-1)}\,Q_n^{-m-1}(x), \quad (56)$$

$$xQ_n^{-m}(x) - Q_{n+1}^{-m}(x) = (n-m)\sqrt{(x^2-1)}\,Q_n^{-m-1}(x), \quad . \quad (57)$$

$$(n-m)Q_{n-1}^{-m}(x) - (n+m)xQ_n^{-m}(x) = \sqrt{(x^2-1)}\,Q_n^{-m+1}(x), \quad . \quad . \quad . \quad (58)$$

$$(n-m+1)xQ_n^{-m}(x) - (n+m+1)Q_{n+1}^{-m}(x) = \sqrt{(x^2-1)}\,Q_n^{-m+1}(x). \quad (59)$$

The restrictions on m can now, with the aid of (42), be removed.

LXXI. *Incidence of Lattice Distortion and Orientation in Cold-rolled Metals.* *By* W. A. Wood, *M.Sc. (Physics Department, National Physical Laboratory, Teddington, Middlesex)* *.

Summary.

The rate of production of lattice-distortion and preferred orientation during the cold-rolling of certain metals and alloys has been determined by X-ray methods. It was found: (1) That the degree of distortion plotted against the percentage reduction of thickness gives a definite type of curve, which is marked by an initial rapid rise of distortion to a constant value which further reduction maintains; this steady value is characteristic of the metal. (2) The preferred orientation does not occur gradually from commencement of working; it appears after about 35 to 50 per cent. reduction, according to the metal, and then grows rapidly. (3) Lattice-distortion, when it occurs, reaches its maximum value before preferred orientation appears; it is shown that the latter cannot play a primary part in the changes of properties produced by cold-working.

Introduction.

THE present paper records quantitative measurements of the rate at which lattice-distortion and orientation are produced in certain metals as strips of the material are

* Communicated by Dr. G. W. C. Kaye, O.B.E.

reduced in thickness by successive stages of cold-rolling. The method of X-ray diffraction is utilized.

In similar work on hard-drawn wires [1] it was found that the growth of lattice-distortion as the diameter of the wire was reduced by drawing exhibited two characteristics; first, a remarkably rapid appearance and growth in the early stages of drawing; and second, a steady maximum value which was maintained throughout further drawing. The first aim of the work was to find if these peculiarities marked the production of lattice-distortion also in the cold-rolling process. A similar result would confirm the suggestion previously advanced by the author, that associated with any given metal is a measurable maximum of lattice-distortion, a quantity of physical significance in its bearing on the stability of the lattice and the degree by which physical properties can be carried by cold-work.

It has been shown also that variations in degree of lattice-distortion may modify the electrical[1], magnetic, and hardness[2] properties of a metal. But orientation is another structural change produced by cold-work. A further aim of the work was therefore to attempt an estimate of the relative importance of the two factors in causing the changes in physical properties.

In view of the different meanings attached by metallurgists to distortion and orientation [3], the sense in which they are used here is emphasized. The working of a metal or alloy will in general alter the size and shape of the constituent grains. The external deformation of the grain may result in a small permanent disturbance of the crystal or inter-atomic structure. In that event lattice-distortion is understood to occur. It is recognized by its effect on the breadth of the lines in a spectrum of the metal formed by diffraction of *monochromatic* X-rays [4]. It is distinguished by the same criterion from grain deformation not accompanied by lattice-distortion. The latter type of disturbance leaves the line-breadths unaffected.

By preferred orientation is implied a state of the material in which a majority of the grains are set with the same crystallographic axis in the same direction.

Estimation of Lattice-distortion.

The breadth of a line in the X-ray diffraction spectrum will have a minimum value, B_0, when the specimen is annealed and thereby freed from distortion. If the specimen is then cold-worked, the breadth will in general increase to a value B depending on the degree of distortion produced.

The values of B_0 and B can be estimated from photometer measurements. The quantity $B-B_0$ then obtainable will be some measure of the lattice-distortion. This is the process followed in the present work.

It is assumed that the grains of the material exceed in size the limit, about 10^{-4} cm., below which imperfect resolution occurs. It can be shown that this is normally the case [6]. Also that each specimen is photographed under suitable standard experimental conditions. The geometry of these conditions is not affected by the changes in dimensions of specimens due to rolling, provided that the penetration of the material by the X-ray beam is less than the total thickness. This condition is satisfied by choice of a working wave-length which is quickly absorbed.

The physical interpretation of $B-B_0$ will involve a closer knowledge of the way in which the lattice distorts. This is not yet known. It is, however, convenient to adopt in the meantime some arbitrary interpretation which will permit results on various materials by different observers to be placed in a proper perspective. The value $B-B_0$ is here expressed in terms of the equivalent change in lattice parameter which produces the same displacement of a spectrum line as would correspond to the measured changes in breadth. Thus, taking the case of a narrow parallel pencil of incident X-rays of wave-length λ we can assume the change in breadth to correspond to a variation $\delta\theta$ in the angle θ at which the rays are reflected to form the line considered. These quantities are related by the Bragg formula $2d \sin\theta = \lambda$, where d is the spacing of the reflecting planes. Therefore $\delta\theta$ can be expressed in terms of a change in spacing, since, by differentiation,

$$\frac{\delta d}{d} = -\cot\theta \, d\theta. \quad . \quad . \quad . \quad . \quad . \quad . \quad (1)$$

If the line is photographed in a circular camera by radius R, then

$$2\delta\theta = B - B_0/R. \quad . \quad . \quad . \quad . \quad . \quad . \quad (2)$$

From (1) and (2) we have the quantity $B-B_0$ given in terms of an equivalent change of spacing or lattice-parameter.

Estimation of Orientation.

A quantitative estimate of the preferred orientation present in a specimen was made as follows :—Two suitable lines in the X-ray photograph were chosen, and the intensities I and I_0 of these lines were measured at the points where they

cross the equatorial line of the photograph. The ratio of I to I_0 will be a constant in the case of specimens in which the grains are oriented at random, since there will be the same number of grains in a position to contribute a reflexion to I as to I_0. The value of the ratio will be fixed fundamentally by the atomic structure. With the onset of preferred orientation, however, the random distribution no longer holds, and both I and I_0 will vary at different rates according to the proportion of preferred orientation present. The ratio of I to I_0 therefore can be taken to represent the degree of preferred orientation. Choice of suitable lines was guided by the following considerations:—The lines were such that as orientation appeared the intensity at I increased whilst that at I_0 decreased. The points were "orientation maxima" and "minima" respectively. The ratio was therefore especially sensitive to changes in orientation. Further, the lines occurred at small values of the glancing angle θ where there is least resolution in the spectrum. Consequently the broadening effect of lattice-distortion is there minimized. It was found in practice that the distribution of intensity across the width of the lines as shown on the photometer records was the same for the different rollings of the same material, experimental conditions being constant. The maximum height of the intensity peaks was therefore taken as a measure of the whole intensity for purposes of obtaining the ratio of I to I_0.

Consequently, after a specimen had been photographed set at a large angle to the beam, a second setting was used and lines occurring at lesser values of θ obtained in focus. The first photograph formed a basis for the lattice-distortion measurements, and the second for the orientation measurements. The specimen was then rolled and the process repeated, geometrical conditions being the same, until the rate of production of distortion and orientation, starting with normal annealed material, was secured throughout a long range of reduction.

Details of Experiment.

Detailed examination was made of copper and of the alloy, consisting of 70 per cent. nickel, 25 per cent. iron, and 5 per cent. copper, termed mumetal. The results were confirmed on nickel, constantan, and the transformer steels iron-aluminium (Al, 4 per cent.), and iron-silicon (Si, 4 per cent.). Aluminium[4], lead, and bismuth were found to exhibit no measurable distortion, and platinum very little. In general

an alloy was found to be much more susceptible to lattice-distortion than any pure metal.

The radiation used was the Kα wave-length of copper, except for the iron-alloys when the iron Kα was substituted. The incident rays were collimated by a tubular slit 4 cm. long and 1 mm. in bore, and entered a cylindrical camera, radius 5·5 cm., in a direction perpendicular to the camera-axis. The beam encountered the surface of the specimen, set parallel to the axis, as it passed over the centre of the camera. A special type of specimen-holder was designed to ensure that the surface of each specimen came into the same position and faced the incident beam at the same angle. In the case of copper, the specimens were set at an angle of 70°

Fig. 1.

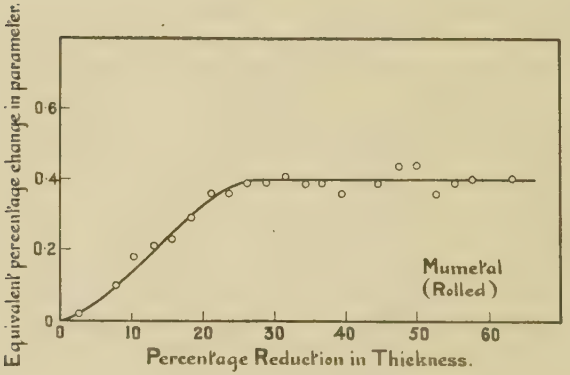

to the beam in the first instance, and then at 25°. The former setting gave a photograph of the (420) line on the film, which was at the circumference of the camera. This line was suited to the measurement of distortion. The second setting gave the (111) and (200) lines which were used in the orientation measurements. The corresponding settings for the face-centred cubic mumetal were 75° and 30° ; the lattice-distortion was estimated on the (311) line, iron Kα radiation being used, and the orientation on the (111) and (200) lines.

Exposures were reduced to a minimum consistent with easy visibility to avoid any spreading of the lines due to halation, which produces appreciable errors in long-exposed films. Preliminary experiments were made to determine the limits of safe exposure. The after-processing of the film

was conducted under conditions of constant time and temperature to eliminate artificial variations in contrast.

The breadths and the relative intensities of the lines were measured with the aid of a Moll microphotometer, the density-deflexion calibration curve of which was known. In determining the line-breadths, allowance has to be made for the doublet nature of the lines which arises from the α_1 and α_2 constituent wave-lengths of the radiation. This was done by a method previously described [1], in which a measurement is taken of the distance, along the base formed by the background of general radiation, between the position of maximum intensity of the line and the position of minimum intensity on the side of the peak away from the α_2 satellite. When a similar value has been obtained for the annealed parent specimen of a series of rollings, the difference between the two gave the value of the maximum degree of distortion produced at that stage of the rolling process. This difference was finally divided by the magnification introduced by the microphotometer, which was seven times, and the value $B-B_0$ thereby secured.

The amount of distortion in copper and the alloys was sufficient to cause the α_1 α_2 doublet, sharply separated by about 1 mm. in the normal specimens, to appear as a single diffuse band. The measurements in these cases are therefore obtainable with an accuracy corresponding to an equivalent lattice change of about $\pm 0{\cdot}02$ per cent.

Results.

(i.) *Incidence of Lattice-distortion.*—The measurements made on a typical specimen of copper are given in Table I. In the first column is the number of times the specimen was rolled, in the second is the thickness at each rolling, in the third is the measured breadth of the line on the microphotometer record, and in the last column is the final change in breadth $B-B_0$, calculated in the manner described above.

It is seen from the table that lattice-distortion increases as the amount of cold-work put into the material with successive rollings becomes larger, and that this increase occurs in a definite manner. The changes are brought out more clearly in fig. 2, where the variation on line-breadth, expressed in this case in terms of an equivalent lattice change by means of the formulæ given earlier, is plotted against the percentage reduction in thickness from the initial value of 1·61 mm. It is of interest to note that as soon as the metal undergoes any working whatsoever, lattice-distortion sets in and increases very rapidly. But after a certain degree of

reduction, here about 30 per cent., the initial rise dies away and the curve assumes a steady value. Results on the metals and alloys enumerated above are the same as for copper. Different metals and alloys differ only in respect of the degree of distortion at which the curve steadies up, and at

TABLE I.

(Copper reduced from 1·61 mm.).

Times rolled.	Thickness.	Line breadth.	$B-B_0$.
1	1·53 mm.	0·45 cm.	0·007 cm.
2	1·45	0·60	0·029
3	1·38	0·70	0·043
4	1·30	0·95	0·079
6	1·19	1·20	0·114
7	1·16	1·15	0·107
8	1·13	1·20	0·114
9	1·09	1·14	0·106
11	0·98	1·21	0·116
13	0·86	1·25	0·121
14	0·82	1·20	0·114
15	0·78	1·24	0·120
16	0·72	1·21	0·116
17	0·68	1·20	0·114
18	0·63	1·30	0·129
19	0·57	1·21	0·116
20	0·53	1·20	0·114

Fig. 2.

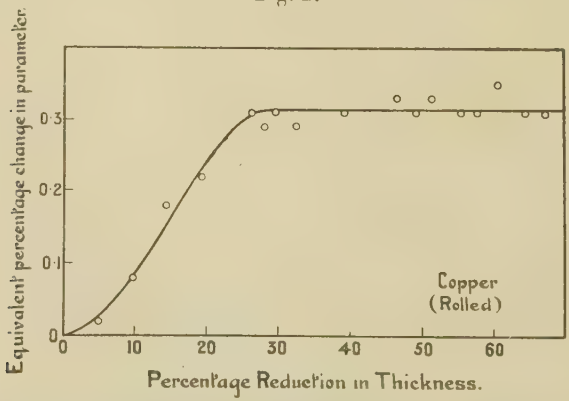

the rate at which the maximum value is reached. The observations on mumetal are tabulated in Table II., and the degree of distortion plotted against the percentage reduction of thickness is shown in fig. 1. It is seen that the graph conforms to what appears to be the universal type of curve for lattice-distortion/work, thus corroborating the original thesis.

A tentative explanation of the curve is as follows :—The sloping part corresponds to the crystal grains taking up the strains in the lattice, brought about by the rolling stresses. The straight part of the curve then represents a state where the lattice of the grains is distorted to the limit. Further stress would result in disruption. This breaking down is presumably accompanied by re-crystallization. The evidence for the latter process is partly in the nature of the curve. For if the grain size diminished indefinitely, the breadth of

TABLE II.

(Mumetal reduced from 0·38 mm.).

Times rolled.	Thickness.	Line breadth.	$B-B_0$.
1	0·37 mm.	0·45 cm.	0·007 cm.
2	0·35	0·60	0·029
3	0·34	0·75	0·050
4	0·33	0·80	0·057
5	0·32	0·85	0·064
6	0·31	0·95	0·079
7	0·30	1·10	0·100
8	0·29	1·10	0·100
9	0·28	1·15	0·107
10	0·27	1·15	0·107
11	0·26	1·20	0·114
12	0·25	1·15	0·107
13	0·24	1·15	0·107
14	0·23	1·10	0·100
15	0 21	1·15	0·107
16	0·20	1·25	0·121
17	0·19	1·25	0·121
18	0·18	1·11	0·101
19	0·17	1·15	0·107
20	0·16	1·17	0·110
21	0·14	1·18	0·111

the lines would increase indefinitely, since the second cause of line-broadening would be introduced as the grains became less than about 10^{-4} cm. in size, namely [5], the imperfect resolution due to the reduction in the number of reflecting planes in the crystallites. This would be contrary to the evidence of the horizontal level of the curve. Further proof appeared directly in the case of lead and bismuth, where continued rolling often introduced and increased the spotted nature of the diffraction lines associated with reflexions from single large crystals. Metals like aluminium or zinc, which do not exhibit line-broadening on working, are, on this view, built up on lattices which are easily broken down.

It is suggestive that alloys usually show lattice-distortion more than pure metals. The distortion might be expected to be produced by the introduction of heterogeneity from point to point in the alloy. This type of distortion would be facilitated in the case of pure metals if the element consisted of atoms of two or more different sizes, being itself virtually an alloy.

(ii.) *Incidence of Orientation.*—The quantitative measurements on the production of preferred orientation led to the following observations :—

No measurable indication of preferred orientation appeared until the later stages of reduction, and in the cases where lattice-distortion was present, not until the lattice-distortion

Fig. 3.

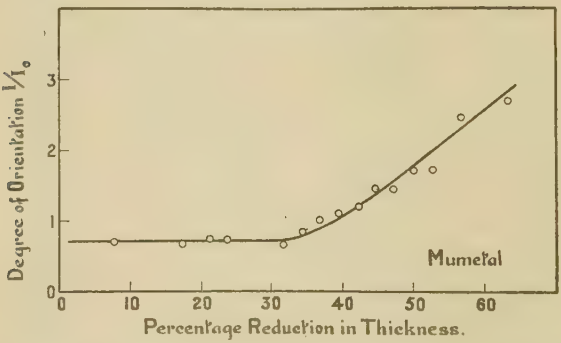

had reached its steady maximum value. Thus the observations on the typical case of mumetal are given in fig. 3. The change in orientation, measured by the ratio I/I_0 as specified earlier, is plotted against the percentage reduction in thickness of the material. It is seen that I/I_0 is constant up to about 35 per cent. reduction. In that region, therefore, there is no departure from a random orientation. On further reduction the ratio increases rapidly, preferred orientation being definitely produced. A comparison of figs. 3 and 1 shows that the appearance of preferred orientation is subsequent to the attainment of maximum lattice-distortion. It is surprising that the preferred orientation does not grow regularly from the beginning. The first appearance in the case of copper was at about 40 per cent. reduction, nickel at 45 per cent. aluminium at 45 per cent., and the transformer steels at 35 per cent.

This observation is of interest in connexion with the question of the relative importance of lattice-distortion and orientation in the modification of physical properties produced by cold-working. Up to about 40 per cent. reduction, of the two factors only lattice-distortion is varying, and it is in this region that normally such properties as hardness, temperature-coefficient of resistance, and (in the transformer steels) magnetic coercive force are known to be changing rapidly. Therefore, lattice-distortion will call for the main consideration, not orientation.

In conclusion the author expresses his thanks to Mr. J. A. G. Smith for extensive help in securing the photographs and preparing specimens, and to Dr. G. W. C. Kaye for his interest in the researches of which this is part.

Summary.

The rate of production of lattice-distortion and preferred orientation during the cold-rolling of certain metals and alloys has been determined by X-ray methods. It was found: (1) that the degree of distortion plotted against the percentage reduction of thickness gives a definite type of curve, which is marked by an initial rapid rise of distortion to a constant value, which further reduction maintains; this steady value is characteristic of the metal; (2) the preferred orientation does not occur gradually from commencement of working—it appears after about 35 to 50 per cent. reduction, according to the metal, and then grows rapidly; (3) Lattice-distortion, when it occurs, reaches its maximum value before preferred orientation appears: it is shown that the latter cannot play a primary part in the changes of properties produced by cold-working.

References.

(1) W. A. Wood, Proc. Phys. Soc. xliv. p. 97 (1932).
(2) W. A. Wood, Phil. Mag. (7) xiii. p. 355 (1932).
(3) Discussion, Inst. of Met. xliv. p. 241 (1930).
(4) *Cf.* Dehlinger, *Z. für Krist*, lxv. p. 615 (1927).
(5) V. Laue, *Zeit. für Krist.* lxiv. p. 115 (1926).
(6) W. A. Wood, 'Nature' (in press).

LXXII. *The B.A. Standards of Resistance*, 1865–1932. *By* Sir R. T. Glazebrook, *K.C.B., F.R.S., and* L. Hartshorn*. (*From the National Physical Laboratory.*)

THE original Electrical Standards Committee of the British Association was appointed at the Manchester meeting in 1861. In their first Report (Cambridge 1862) they point out that they had first to determine "what would be the most convenient unit of resistance, and second, what would be the best form and material for the standard representing that unit."

The C.G.S. system of measurement was the outcome of their deliberations on the first question, and they determined to adopt as a practical standard of resistance the ohm, equal to 10^9 C.G.S. units of resistance. Experiments were made at King's College by Maxwell and Fleeming Jenkin to obtain the ohm in a material form, and reports giving the result of these were issued in 1863 and 1864. Experiments were carried out by Matthiessen and Hockin to determine the best form and material for a series of standard coils. The reports which followed give an account of the process of these experiments, and in Appendix A to the 1865 Report we have their final conclusions and a description of the form of standard coil they recommended. As a material for the wire of which the coil was constructed an alloy containing 66 per cent. silver and 33 per cent. platinum was chosen for reasons given in the Report. It was agreed that copies of the Standard should be made and preserved at Kew Observatory, and the Report for 1867 contains a table of the values of the standards in question. A copy of this is given in Table I. The Committee was dissolved in 1870.

Soon after Maxwell's appointment as Cavendish Professor at Cambridge the coils with the bridge used for their comparison were brought to the Cavendish Laboratory and were use by Chrystal and Saunder in their work on Ohm's law in 1876.

Lord Rayleigh became Cavendish Professor in 1879 and was immediately interested in electrical measurements. Various investigations, particularly those of

* Communicated by the Authors.

Rowland at Baltimore and some deductions from Joule's work, had thrown doubts on the accuracy of the absolute

TABLE I.

Comparison of B.A. Units to be deposited at Kew Observatory *. By C. Hockin.

The following Table shows the value of the different copies of the B.A. units that have been made for preservation at Kew :—

Material of coil.	No. of coil.	Date of observation.	Temperatures at which coil has a resistance $=10^7$ m/s.	Observer.
			°	
Platinum-iridium alloy.	2	January 4, 1865	15·5 C.	C.H.
		June 6, 1865	16·0	A.M.
		February 10, 1867	16·0	C.H.
Platinum-iridium alloy.	3	January 4, 1865	15·3	C.H.
		June 6, 1865	15·8	A.M.
		February 10, 1867	15·8	C.H.
Gold-silver alloy	10	January 5, 1865	15·6	A.M.
		February 10, 1867	15·6	C.H.
Gold-silver alloy	58	April 10, 1865	15·3	A.M.
		June 6, 1865	15·3	A.M.
		February 10, 1867	15·3	C.H.
Platinum	35	January 7, 1865	15·7	C.H.
		August 18, 1866	15·7	A.M.
		February 10, 1867	15·7	C.H.
Platinum	36	January 7, 1865	15·5	C.H.
		August 18, 1866	15·5	A.M.
		February 10, 1867	15·7	C.H.
Platinum-silver alloy .	43	February 15, 1865	15·2	C.H.
		March 9, 1865	15·2	A.M.
		February 10, 1867	15·2	C.H.
Mercury	I.	February 2, 1865	16·0	A.M.
		July 18, 1866	16·0	A.M.
		February 11, 1867	16·7	C.H.
Mercury	II.	February 3, 1865	14·8	A.M.
		August 18, 1866	14·8	A.M.
		February 11, 1867	14·8	C.H.
Mercury	III.	February 11, 1867	17·9	C.H.

* Further references to these coils are made in the Reports for 1883 and 1908.

measurements of the B.A. Committee. These doubts were confirmed by measurements made at Cambridge by himself and Schuster, and from 1881 onwards there was great activity at the Cavendish Laboratory and

elsewhere in connexion with the question of electric units.

During 1879–1881 a very careful comparison of the coils was made by Dr. Fleming. It was clear that their relative values had changed appreciably since 1867, and he adopted as a definition of the B.A. Unit the mean value of the resistance of all the coils at the temperatures at which they were originally said to be correct. For his comparisons he employed Carey Foster's method and devised a special form of bridge, which after his time was employed for the purpose for many years.

The Electrical Standards Committee was reappointed at the Swansea meeting in 1880, and in the following year 1881 at York, one of the present authors (R. T. G.) became connected with the work; he was formally appointed Secretary at the Southport meeting in 1883, and from that date up to the year 1919 the coils were in his charge. They are still at the National Physical Laboratory. The Committee was dissolved in 1912, when its reports were collected in a volume published by the Association under the Editorship of Mr. F. E. Smith (now Sir Frank Smith, Secretary, Royal Society). Up to that date comparisons of the coils among themselves were continually in progress. Between 1881 and 1884 their values were determined in "ohms" and also in terms of the length of a column of mercury by Lord Rayleigh and Mr. Glazebrook. In 1888 a further very detailed examination of their values was made by Mr. Glazebrook and Mr. Fitzpatrick. In 1908 Mr. F. E. Smith reported very fully on their values and on the changes which had occurrred, while the concluding portion of this paper consists of an account of a comparison made during the current year by Dr. Hartshorn at the National Physical Laboratory and a discussion of the results up to date.

The records show that most of the coils have changed appreciably during their long life, but that the two platinum coils marked * 35 and 36 in the original table have remained unchanged.

The relative changes are known during the period in question, and the following Table II., based on Sir Frank Smith's report of 1908, is of importance as

* About 1880 the coils were remarked, and these coils have since been known as D and E.

showing that during the period 1880 to 1888 the value of the B.A. unit expressed in terms of mercury remained unaltered. The diagram and tables given later in the Report enable the changes which have taken place to be followed in detail.

TABLE II.

Resistance of Mercury Column 100 cm. long and 1 square mm. section at 0° C. in B.A. Units.	
Value found in 1881 by Lord Rayleigh, corrected for temperature of cups	=0·953 88 B.A.U.
Value found in 1888 by R.T.G.	=0·953 52 B.A.U.

Resistance of 1 B.A. Unit in terms of length of Mercury Column.	
Value found in 1881 by Lord Rayleigh	=104·842 cm.
Value found in 1888 by R.T.G.	=104·875 cm.

The next table (Table III.) gives the values of two of the platinum silver coils examined by Lord Rayleigh in 1881 and Sir Frank Smith in 1908. It shows that, allowing for the recorded alterations in these coils during that period, the value assumed for the B.A. unit was satisfactorily known.

TABLE III.

Resistance of Coils F and Flat in terms of Mercury. (Length of Column of 1 sq. mm. section at 0° C.)	
Values found by Lord Rayleigh in the year 1881 :—	
F at 16·0° C.	=104·805 cm.
Flat at 16·0° C.	=104·871 cm.
Values found by Mr. Smith in 1908 for the resistance of the coils in 1881, assuming them to have altered between 1881 and 1908 by the amounts shown in the B.A. Reports :—	
F at 16·0° C.	=104·808 cm.
Flat at 16·0° C.	=104·874 cm.

The point of most importance which emerged from Sir Frank's measurements of 1908 was the permanence of the two platinum coils. A reference to Table I.

shows an apparent change of 0·2° in the standard temperature of N. 36 (E) between 1865 and 1867. It would appear from Table IV. that this apparent change was not a real one but arose from some error in the 1867 experiments. At any rate Table IV., which is brought up to date by the inclusion of Dr. Hartshorn's observations of 1932, gives the values observed for the difference E–D between these coils and shows that with this one exception this difference has lain between ·00059 B.A.U. and ·00063 B.A.U. during the whole 67 years of their

TABLE IV.

Differences between the Values for the Platinum Coils D and E at 16·0° C.

Year.	Difference E–D. Parts in 100,000.
1865	59
1866	59
1867	−1
1876	63
1879–81	50
1888	60
1908	60
1932	59 using 0·1 amp.
	60 using 0·12 „
	65 using 0·2 „

Note.—A change in temperature of 0·1° C. causes a change in resistance of the coils of 31 parts in 100,000.

life. This will appear all the more remarkable when it is remembered that an error of 0·1° in the temperature means a change of resistance of 0·00031 B.A.U., while a variation in the measuring current of from 0·1 to 0·2 amperes produces an alteration of 0·0006 B.A.U., a larger amount than the whole change observed.

The inference is clear that during this period these two coils have retained their values unaltered, and this is confirmed by the following statement of values taken from a later table in this Report.

Value * of Coils D and E in B.A. Units in 1888, 1908, and 1932 obtained from a Comparison with Mercury Tubes, assuming the resistance of 1 metre of Mercury to be 0·95352 B.A.U.

Coil.	1888. R.T.G.	1908. F.E.S.	1932. L.H.
D	1·00013	1·00012	1·00011
E	1·00073	1·00072	1·00071

* See Table VII.

We come now to the detailed account of the recent work at the National Physical Laboratory by one of us (L. H.).

The old standard resistance coils of the British Association, made in 1865 by Matthiessen and Hockin, have been re-measured during 1932, and a comparison of the results with the old values is of considerable interest.

Several features in the construction of the coils make it impossible to obtain the same precision in these measurements as is obtained with modern coils. The coils are embedded in solid paraffin wax, so that the attainment of thermal equilibrium with the bath containing them is not easy. It is, therefore, difficult to obtain the temperature of the coil itself, and as in some cases the temperature coefficient of the material is very large, the accuracy is almost entirely limited by the thermal conditions. Also the coils have no potential terminals. However, preliminary measurements having shown that certain of the coils had probably remained nearly constant over a period of more than sixty years, it was considered desirable to aim at an accuracy of 1 part in 100,000 in the present determinations. This requires an accuracy in temperature measurement for certain of the coils of $\pm 0{\cdot}003^\circ$ C., and although it is hardly likely that this could be realized, the general consistency of a large number of observations has shown that the temperature was usually correct to $\pm 0{\cdot}01^\circ$ C. The coils were immersed in a bath of water, which was surrounded on all sides by cork lagging, and kept throughout the measurements in a constant-temperature vault. The measurements were made by means of a Smith

bridge, assembled with standard manganin coils in an oil-bath, kept by means of a thermostat at 20° C. in an adjoining room. The terminal rods of the B.A. coils dipped into mercury cups, and from these cups double leads passed to the bridge in the adjoining room. The resistance of these leads is eliminated from the results by taking two readings in the manner described by Smith. Thus the observer did not have to approach the coils during the resistance measurements. The thermometer dipping into the water-bath was read from a distance by means of a telescope; readings were taken at intervals during each day, as well as before and after the resistance measurements, and it was always ascertained that the temperature had remained constant to 0·01° C. for several hours before each measurement. The mercury thermometer used was graduated in hundredths of a degree, and was calibrated on the hydrogen scale.

A factor of some importance is the heating effect of the measuring current. This has, of course, long been known, but as the magnitude of the effect is surprisingly large for some of the coils, and as no record of it appears to exist, it was measured in each case. The procedure was as follows. The galvanometer circuit was kept permanently closed, and when balancing the bridge the current was reversed, but was allowed to flow for as short a time as possible. Readings were obtained, first with as small a current as would give the required sensitivity, then with rather larger currents. The relation between bridge reading and the square of the current strength was always approximately linear, and thus the resistance corresponding to "zero current," and to any other value of current, were readily obtained. The actual value of current used in the older comparisons is not known, but the usual practice was to connect two quart size Leclanché cells in series with the bridge, which had an overall resistance of a little more than 1 ohm, when 1 ohm coils were being compared. A trial experiment has shown that the total current obtained in this way is about 0·5 ampere, which means that the current in each coil was about 250 milliamp. This probably represents the maximum current used in the older comparisons. Its heating effect has been found to cause an error of as much as 5 parts in 10,000 for

certain of the coils, but there is no doubt that in the more recent comparisons, particularly those of 1908, there is no question of an uncertainty of this magnitude. An examination of the results suggests that a current of the order of 120 milliamp. was used on this occasion, and for purposes of comparison this will be assumed

TABLE V.

Results obtained in 1932 *for the British Association Standard Resistance Coils of* 1865.

Values at 16·00° C. in terms of the B.A. Unit determined by the relation 1 International ohm = 1·01367 B.A. Units *.

Coil.	Material.	Value for zero current. 1932.	Value for 0·120 amp. 1932.	Value. 1908.	Heating correction for 250 milliamp.	Temp. coeff.
A..	Pt. Ir.	1·000 55	1·000 67	1·000 50	49×10^{-5}	148×10^{-5}
B..	Pt. Ir.	1·000 32	1·000 42	1·000 26	44×10^{-5}	148×10^{-5}
C..	Au. Ag.	1·001 15	1·001 16	1·001 01	4×10^{-5}	70×10^{-5}
D..	Pt.	1·000 12	1·000 19	1·000 20	28×10^{-5}	308×10^{-5}
E..	Pt.	1·000 69	1·000 79	1·000 80	40×10^{-5}	306×10^{-5}
F..	Pt. Ag.	1·001 02	1·001 05	1·000 88	11×10^{-5}	27×10^{-5}
G..	Pt. Ag.	1·001 01	1·001 04	1·001 03	13×10^{-5}	28×10^{-5}
Flat.	Pt. Ag.	1·000 48	1·000 50	1·000 53	9×10^{-5}	27×10^{-5}

* In 1892 in accordance with the experiments made at the Cavendish Laboratory, the value of the ohm (10^9 c.g.s. units) was taken as 1·01358 B.A.U. and became the unit in general use. In 1903 it was shown by Mr. Smith that this unit was equal to 106·291/106·300 International ohms. Thus the International ohm = 1·01367 B.A.U.

to represent the standard condition. The results of the 1932 measurements given in Table V. show the values for "zero current," 120 milliamp., and the maximum correction, *i. e.*, the difference between the values for "zero current" and 250 milliamp. The values obtained in 1908 are given alongside of those for 1932 with 120 milliamp. for the purpose of comparison.

A glance at Table V. is sufficient to show that there have been no large changes in the values of the coils in

the last twenty-four years. In all cases the change is less than 2 parts in 10,000, which must be considered very satisfactory behaviour, the more remarkable since, so far as is known, the coils are connected to the terminal rods by means of soft soldered joints. In spite of this fact, and also of the presence of the paraffin wax in which the coil is embedded, the coils are probably as satisfactory as standards of resistance as when they were first constructed 67 years ago. The paraffin wax has become discoloured, having become yellow with age, and in some cases having acquired a greenish tinge from its chemical action on the copper terminal rods, and on this account the insulation was suspected as early as 1886. However, at that time the leakage resistance between coil and case was measured and found to be of the order of 8000 to 10,000 megohms. The insulation was again tested in 1890 and found to be several thousand megohms. Measurements made in 1932 gave the following values :—

Insulation Resistance 1932.

Coil.	Insulation resistance. Megohms.
A	9 000
B	40 000
C	1 000
D	1 400
E	1 000
F	300
G	4
Flat	200

The value is definitely low in some cases, but not low enough to affect the resistance measurements by an appreciable amount.

In the following paragraphs the significance of the results is considered from several points of view of practical importance.

(i.) *The Platinum Coils* D *and* E.

From an examination of the available data in 1908 Mr. F. E. Smith concluded that the platinum coils had probably remained constant since 1867, but that all the other coils had changed. The question of constancy is of such importance that a special study has been made of these two coils. About forty observations were made on each coil in the temperature range 15° to 17° C. over a period of four weeks. The results expressed in terms of the B.A. Unit of Table V. could be represented as follows :—

Coil D .... $R = 1{\cdot}000\,12 + 0{\cdot}003\,08\,(t - 16{\cdot}00°\text{ C.})$.

Coil E .... $R = 1{\cdot}000\,69 + 0{\cdot}003\,06\,(t - 16{\cdot}00°\text{ C.})$.

The mean deviation of all the observed points from the values calculated from these equations was 2·5 parts in 100,000, which corresponds to a temperature difference of 0·008° C. Greater accuracy could not be expected from coils of this construction, and it may be concluded that the coils are at present in a stable condition represented by these equations. The values given in 1908 for the resistance of the coils D and E at 16·0° C. are 8 and 11 parts respectively higher than those given above. However, the above values are corrected to correspond to "zero current," and no such correction was made in the previous measurements. The magnitude of the correction is shown in Table V., and it will obviously account for a discrepancy of this order. It was found that when the current through the coil was 0·12 ampere, the 1908 values were reproduced to 1 part in 100,000. It is interesting to note that, owing to the difference in the heating corrections for the two coils, the value for the difference between them varies with the current. The values for this difference, obtained on various occasions, have been given in Table IV., from which we conclude that this difference has remained constant since 1865, and that the measuring current used was of the order 0·12 ampere. (The low value of 1867 has long been considered as due to an observational error.)

The values obtained for the temperature coefficients are of interest. The following table shows the values obtained on various occasions.

Temperature Coefficients of the Platinum Coils.
B.A. Units per 1° C.

Coil.	1880.	1888.	1908.	1932.
	$\times 10^{-5}$.	$\times 10^{-5}$.	$\times 10^{-5}$.	$\times 10^{-5}$.
D	308	308	312	308
E	304	302	314	306

It is evident that the temperature coefficient of the wire is still very near to its original value, although it is far removed from the value for pure platinum (about 400×10^{-5}).

(ii.) *The Variations in the Alloy Coils.*

Having satisfied ourselves that the platinum coils had remained unchanged, the changes in the other coils were examined. It was not considered necessary to take so many observations on these coils as on the platinum ones, but in each case a few observations were made at a temperature slightly above 16° C. and a few at a temperature slightly below 16° C. The value at 16·00° C. was deduced from the two sets. In every case the difference between the two sets of values was consistent with the 1912 value of the temperature coefficient, which is reproduced in Table V., together with the resistance values at 16·00° C. and the heating correction.

In the older B.A. Reports the values assigned to these coils were usually obtained on the assumption that the mean value of the coils at the temperatures at which they were originally stated to be correct had not altered; in other words, the results were expressed in terms of the Mean B.A. Unit at the time. Mr. F. E. Smith showed in 1908 that it would almost certainly be more correct to assume that the platinum coils alone had remained unaltered, and our results support this conclusion. Acting on this assumption, and taking the known values for the differences between the coils at various dates as given in his records, Mr. Smith was able to give a table of the values of the coils in terms of the original B.A. Unit (1867). Our results enable us to bring this table up to

date (Table VI.). This table is of great interest as showing the most probable variations in the values of the coils throughout their whole existence. The values are plotted in fig. 1. It is apparent from this diagram that the values for 1876 are all comparatively high. At this time the temperature was only observed to 0·1° C., and an error of this amount for the platinum coils would lower all the values to those shown by the dotted lines, which values are regarded as rather more probable than those tabulated.

Fig. 1.

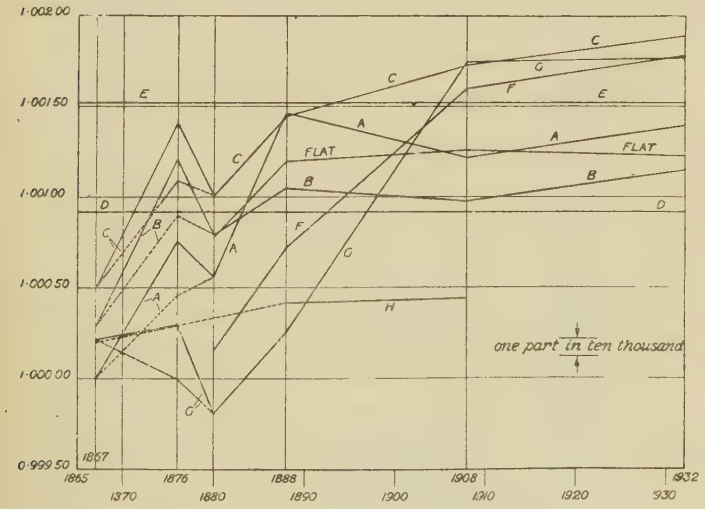

The B.A. Standard Resistance Coils.
Values in terms of the Original B.A. Unit (1167) :—A.B. Platinum-Iridium. C. Gold-Silver. D.E. Platinum. F.G.H. & FLAT. Platinum-Silver.

The curves show clearly the remarkable constancy of the coils in the last twenty-four years, even in the case of coils F and G, which had changed very considerably before that time. This constancy is probably the result of the storage of the coils at constant temperature throughout the whole period. On one or two occasions between 1879 and 1888 the coils had been tested in melting ice, and it was considered that this was probably the cause of some of the observed changes. Throughout the whole

Table VI.

Resistances at 16·0° C. in terms of the original B.A.U. (1867)
(values obtained through the two Platinum Coils D and E shown to have remained unaltered.)

Coil.	Material.	1867.	1876.	1879–81.	1888.	1908.	1932.	Maximum difference.
A....	Pt. Ir.	1·000 00	1·000 77	1·000 56	1·001 47	1·001 22	1·001 40	147×10^{-5}
B....	Pt. Ir.	1·000 29	1·001 21	1·000 80	1·001 04	1·000 98	1·001 15	92×10^{-5}
C....	Au. Ag.	1·000 50	1·001 41	1·001 01	1·001 46	1·001 73	1·001 89	139×10^{-5}
D....	Pt.	1·000 92	1·000 92	1·000 92	1·000 92	1·000 92	1·000 92	0×10^{-5}
E....	Pt.	1·001 52	1·001 52	1·001 52	1·001 52	1·001 52	1·001 52	0×10^{-5}
F....	Pt. Ag.	—	—	1·000 16	1·000 72	1·001 60	1·001 78	162×10^{-5}
G....	Pt. Ag.	1·000 22	1·000 30	0·999 82	1·000 25	1·001 75	1·001 77	195×10^{-5}
H....	Pt. Ag.	1·000 20	—	—	1·000 42	1·000 44	—	24×10^{-5}
Flat..	Pt. Ag.	—	—	1·000 79	1·001 20	1·001 25	1·001 23	44×10^{-5}

of the recent observations the temperature has not differed from 16·0° by more than 1° C.

Two other interesting tables of values recording the history of these coils were given by Mr. F. E. Smith in 1908, and these have also been brought up to date. Table VII. records the values of the coils in terms of the B.A. Unit in general use during the period 1891–1903, and Table VIII. gives the values obtained on a number of occasions in centimetres of mercury.

TABLE VII.

Values of Coils at 16·0° C. in B.A. Units in 1888, 1908, and 1932, obtained from Comparison with Mercury Tubes, assuming the resistance of 1 metre of Mercury to be 0·953 52 B.A.U.

Coil.	1888*.	1908.	1932†.
A	1·000 68	1·000 42	1·000 59
B	1·000 25	1·000 18	1·000 34
C	1·000 67	1·000 93	1·001 08
D	1·000 13	1·000 12	1·000 11
E	1·000 73	1·000 72	1·000 71
F	0·999 70	1·000 80	1·000 97
G	0·999 36	1·000 95	1·000 96
H	0·999 63	0·999 64	—
Flat	1·000 23	1·000 45	1·000 42

* Values subject to a probable error of 4 parts in 100,000, due to the fact that the terminals of the mercury tubes were not exactly at 0° C. No correction has been made for this since the probable errror of the observations were of this order.

† Values for a current of 0·12 ampere (see Table V.).

(iii.) *The Value of the B.A. Unit.*

When changes in the relative values of the coils were first noted the B.A. Unit was taken, as already stated, to be the mean value of the six coils A, B, C, D, E, and G, at the temperatures at which they were originally stated to be equal. This has been referred to as the Mean B.A. Unit for the year in question. The data now available show that the changes in the unit so defined have been approximately as given in Table VIII.

Table VIII.

Values at 16·0° C. of the B.A. Coils in cm. of Mercury in 1881, 1888, 1903 and 1932, obtained from Comparisons with Mercury Standards.

Coil.	1881. Value deduced from Lord Rayleigh's determination of the specific resistance of mercury. F and Flat were used; for relative values of coils see Table VI.	1888. Values at time of Dr. Glazebrook's determination. F, G, and Flat were used; for relative values of coils see Table VI.	1908. Values determined directly through N.P.L. mercury standards of resistance, constructed in 1903.	1932*. Values determined directly through N.P.L. mercury standards, constructed in 1912, recalibrated in 1924.	Maximum difference.
	cm.	cm.	cm.	cm.	cm.
A	104·847	104·946	104·918	104·936	0·099
B	104·872	104·901	104·893	104·910	0·038
C	104·894	104·945	104·972	104·988	0·094
D	104·885	104·888	104·887	104·886	0·003
E	104·948	104·951	104·950	104·949	0·003
F	104·805	104·843	104·959	104·977	0·172
G	104·769	104·807	104·974	104·975	0·206
H	—	104·836	104·837	—	0·001
Flat	104·871	104·898	104·922	104·919	0·051

* Values for a current of 0·12 ampere in the coil.

The value generally used for the ratio of the International ohm to the B.A. Unit is

1 International ohm = 1·013 58 B.A. Unit (1892),

this being the value accepted in 1892. However, as the coils were changing in a manner not accurately known, it is evident that the unit in practical use at the Laboratory, normally the mean of all records, was a variable quantity. For example, in 1903 Mr. F. E. Smith made an estimation of the ratio, taking the platinum silver coils as standards of reference (these are the ones which can be measured most accurately), assuming they were accurate in 1888 and estimating from the records of the changes which had occurred since that time. The value obtained was

1 International ohm = 1·013 67 B.A. Unit (1903),

and this value has been used at the Laboratory for some years. It is to be noted that in the light of our present knowledge, neither of the above values represents the original B.A. Unit. It follows from Table III. that this unit is determined as nearly as can be ascertained by the relation

1 International ohm = 1·014 39 B.A. Unit (1867).

Relative Values of the Mean B.A. Unit.

Year.	Value.
1867	1·000 00
1876	1·000 43
1879–81.....	1·000 18
1888	1·000 53
1908	1·000 76
1932	1·000 85

Of course since 1903 mercury tubes have formed the fundamental standards, and the more recent values have not influenced any actual measurements.

LXXIII. *The Temperature Variation of the Frequency of Piezoelectric Oscillations of Quartz.* *By* R. E. Gibbs, *D.Sc., F.Inst.P., and* V. N. Thatte, *M.Sc.* (*Allahabad*) *.

I. Introduction.

OUR knowledge of the piezoelectric properties of quartz, discovered in 1880 by Curie, and of the converse effect, predicted by Lippmann in 1881, has long remained stationary. Only in recent years has interest in these properties been renewed, owing largely to the possibility of their being put to practical use, *e. g.*, in radio-telegraphic technique, depth sounding, and so on. The application of an alternating electric field to a quartz crystal produces in it a mechanical vibration of the frequency of the applied field. Such vibrations are, however, only of minute amplitude, unless their frequency coincides with that of one of the natural vibrations of the particular crystal, in which case resonant vibrations of large amplitude can be produced. Cady and others have shown how these resonant vibrations may be maintained by regenerative valve circuits.

There are many possible modes of vibration of a crystal, for each of which, of course, the free frequency is determined by the elastic constants and geometrical shape of the specimen. Most of the earlier workers employed longitudinal vibrations along the electric axis, but the existence of many other modes has now been amply demonstrated by Giebe and Scheibe[1] and others.

Among the numerous applications of crystal oscillators and resonators is their employment for frequency stabilization and precision measurements. These have reached such a high degree of accuracy that it is essential to know to what extent the results are dependent upon temperature.

Some measurements of the order of magnitude of the temperature coefficient of frequency of a resonating crystal were made by Dye[2], who showed that over a range of about 30° it amounted to about −40 cycles per million per °C. rise. Strout[3], extending the range of observation down to −200° C., found a linear relationship between the temperature coefficient of frequency and the temperature.

It would appear, however, that greater theoretical interest attaches to an extension of the measurements to higher temperatures, firstly, because the variations of the elastic

* Communicated by Prof. E. N. da C. Andrade, D.Sc, Ph.D.

properties are better known in this range, secondly, because they vary more rapidly and, thirdly, owing to the existence of a transition point for the material at about 573° C. Further it is known that, from symmetry conditions alone, the piezoelectric constant δ_{11} must be zero above the transition point. The present work deals therefore with the variation of frequency of piezoelectric oscillations when the temperature is varied from room values up to as near the critical point as was possible with the apparatus in use.

II. Apparatus.

The quartz crystal was supplied by Messrs. Hilger cut to a disk shape 19·0 mm. diam., 1·94 mm. thickness, with the electric axis perpendicular to the plane of the disk; its normal wave-length was 202 metres. It was mounted directly between two comparatively massive monel metal electrodes, the lower of which rested on an alundum tube so as to be near the middle of a small electric furnace. A very small rim was made on the lower electrode to give the crystal a constant seating upon it. Contact was maintained by the weight of the parts.

As the absolute frequency change is very small for a moderate temperature change, a direct determination of wave-length would be of insufficient accuracy, so that some sort of heterodyne method was essential. The following procedure was that actually adopted. Four circuits were employed, a crystal oscillator, a heterodyne oscillator, a low-frequency oscillator, and a detector and amplifier. The low-frequency oscillator was first adjustod to the known frequency N of a tuning-fork and subsequently used as the fixed standard. The frequency m of the heterodyne oscillator was adjusted at a temperature θ_1 to a value lower by a frequency N than that of the crystal oscillator (frequency n_1). A rise of temperature to θ_2 lowered the crystal frequency n_1 to n_2, and the heterodyne frequency $(n_1 - m)$ decreased, passed through zero, and subsequently increased again to $(m - n_2) = (n_1 - m) = \mathrm{N}$. Thus the temperature interval was determined for which the frequency changed by 2N, giving at a mean temperature $\frac{\theta_1 + \theta_2}{2}$ a temperature coefficient $\frac{2\mathrm{N}}{\theta_2 - \theta_1}$.

Both the audio-frequency notes, viz., the heterodyne and the standard, were impressed on the same telephones in the detector-amplifier, and adjustments made until there was not any "beating." Care was taken to obtain good electrical screening and mechanical rigidity, so that the frequencies

remained constant over a period much longer than that necessary to take a set of readings. Observations were made both with rising and falling temperatures, the rates of which were, by careful manipulation of the furnace current, maintained sufficiently slow to ensure complete uniformity. As higher temperatures were reached it became necessary to employ larger values for N and at the same time slightly to modify the crystal oscillatory circuit. Up to 250° C. or 300° C. the crystal was connected between the plate and grid of the triode, but above that temperature it was interposed, together with a small reaction coil, between the grid and filament, enabling a larger high-tension voltage to be applied to the valve without fear of damage to the crystal. In view of the criticisms of Schulwas-Sorokina [5], Andreeff [14], and others there is to-day some doubt if the diminution of the piezoelectric constant in the neighbourhood of 350° C. recorded by Dawson [4] actually exists ; but be this as it may, it was found that a little extra reaction was helpful. The usual tests were made to ensure that the crystal always maintained complete control.

The temperatures were measured by a calibrated nickel-nichrome couple, the usual potentiometer method being employed, whilst due precautions were taken to ensure that the two block electrodes did not differ in temperature at any part of the range by more than 0·3° C.

III. Results.

It is clear from the experimental results recorded in Tables I., II., and III. that the rate at which the frequency changes with the temperature increases rapidly as the temperature rises. We may look for a simple relation between either $\frac{dn}{d\theta}$ and θ or between $\frac{1}{n}\frac{dn}{d\theta}$ and θ, but as n changes by only a few per cent. over the whole range, the experimental figures do not give a very definite decision, although they incline to support the view that $\frac{1}{n}\frac{dn}{d\theta}$ gives the simpler relation. A decision upon this question could be made more easily had it been possible to extend the observations to higher temperatures, *e. g.*, by employing greater power. To calculate a value of n a hyperbolic relation between $\frac{dn}{d\theta}$ and θ was used ; for this purpose it makes little difference whether $\frac{dn}{d\theta}$ or $\frac{1}{n}\frac{dn}{d\theta}$ is used. As,

TABLE I.

Low frequency N = 256.

$\theta = \frac{\theta_1+\theta_2}{2}$.	$\theta_2-\theta_1$.	$\frac{-2N}{\theta_2-\theta_1} = -\frac{dn}{d\theta}$.	$n \cdot 10^{-3}$.	Experimental. $-\frac{1}{n}\frac{dn}{d\theta} \cdot 10^8$.	Calculated. $-\frac{1}{n}\frac{dn}{d\theta} \cdot 10^8$.
44·85	12·9	39·70	1485	2672	2642
64·25	12·3	41·63	1483	2808	2789
80·95	11·7	43·75	1481	2952	2926
94·65	11·3	45·30	1480	3058	3044
113·60	10·8	47·40	1480	3204	3222
130·20	10·2	50·20	1480	3392	3387
144·00	9·8	52·30	1480	3533	3535
167·07	9·15	56·00	1479	3780	3805
186·30	8·6	59·60	1478	4030	4055
202·15	8·1	63·25	1477	4283	4281
226·55	7·5	68·35	1475	4630	4672
250·60	6·8	75·38	1473	5105	5108
275·65	6·2	82·60	1471	5610	5640
294·05	5·7	89·80	1470	6105	6091
316·80	5·2	98·40	1468	6707	6742
331·05	4·9	104·4	1466	7125	7210
349·00	4·4	116·3	1464	7950	7889
365·65	4·1	124·9	1462	8543	8619

TABLE II.

Low frequency N = 512.

$\theta = \frac{\theta_1+\theta_2}{2}$.	$\theta_2-\theta_1$.	$\frac{-2N}{\theta_1-\theta_2} = -\frac{dn}{d\theta}$.	$n \cdot 10^{-3}$.	Experimental. $-\frac{1}{n}\frac{dn}{d\theta} \cdot 10^7$.	Calculated. $-\frac{1}{n}\frac{dn}{d\theta} \cdot 10^7$.
383·95	7·3	140·4	1460	961·8	956·9
401·55	6·5	157·7	1457	1082	1068
417·85	5·9	173·7	1455	1193	1193
429·60	5·4	189·9	1453	1306	1301
454·70	4·4	232·8	1447	1608	1602
468·05	3·9	262·6	1444	1819	1822
486·70	3·2	320·0	1439	2224	2242
494·50	2·9	353·1	1436	2459	2477
501·50	2·6	394·0	1433	2748	2731
518·70	2·0	512·0	1426	3595	3635
521·05	1·9	540·0	1424	3784	3800

TABLE III.

Low frequency N = 874.

$\theta=\frac{\theta_1+\theta_2}{2}$.	$\theta_2-\theta_1$.	$\frac{-2N}{\theta_2-\theta_1}=-\frac{dn}{d\theta}$.	$n.10^{-3}$.	Experimental. $-\frac{1}{n}\frac{dn}{d\theta}.10^7$.	Calculated. $-\frac{1}{n}\frac{dn}{d\theta}.10^7$.
443·05	8·3	210·9	1450	1455	1448
481·95	5·7	307·0	1440	2132	2118
507·08	4·05	431·5	1431	3018	2972
527·00	2·8	624·5	1421	4395	4312
536·15	2·3	760·5	1415	5379	5414
548·57	1·55	1128	1403	8050	8128

after n had thus been obtained, $\frac{1}{n}\frac{dn}{d\theta}$ appeared to correspond more closely to a hyperbolic relationship than $\frac{dn}{d\theta}$, and as theoretical considerations also seem to favour $\frac{1}{n}\frac{dn}{d\theta}$, the relation can be written in the form

$$\left(\frac{1}{n}\frac{dn}{d\theta}-k\right)(h-\theta)=-\mathrm{P}, \quad . \quad . \quad . \quad . \quad \text{(I.)}$$

where k, h, and P are arithmetically positive constants.

The best estimated values from the results are

$$k=11{\cdot}2.10^{-6}, \quad h=573, \quad \mathrm{P}=2040.10^{-5}.$$

The equation represents a rectangular hyperbola asymptotic to the axes $\frac{1}{n}\frac{dn}{d\theta}=k$ and $\theta=k$, and upon integration becomes

$$\left.\begin{aligned} &\log_e n=k\theta+\mathrm{P}\log(h-\theta)+\mathrm{R} \\ \text{or} \quad &\frac{n}{n_0}=e^{k\theta}\left(\frac{h-\theta}{h}\right)^{\mathrm{P}}. \end{aligned}\right\} \quad . \quad . \quad . \quad \text{(II.)}$$

The accuracy with which this equation represents the results is shown in fig. 1 (A) and Tables I., II., III., in which the maximum percentage difference between the experimental results and those calculated from equation (I.) is 1·3 and the average difference 0·6 per cent.; the full line represents equation (I.), whilst the points are experimental observations.

Equation (I.), thus verified, indicates that when $\frac{1}{n}\frac{dn}{d\theta}$ tends towards negative infinity θ tends to h. The constant h represents then a critical temperature at which either n is zero or $\frac{dn}{d\theta} = -\infty$, or both. It is interesting to see how this value $h = 573°$ C. compares with the various determinations

Fig. 1.

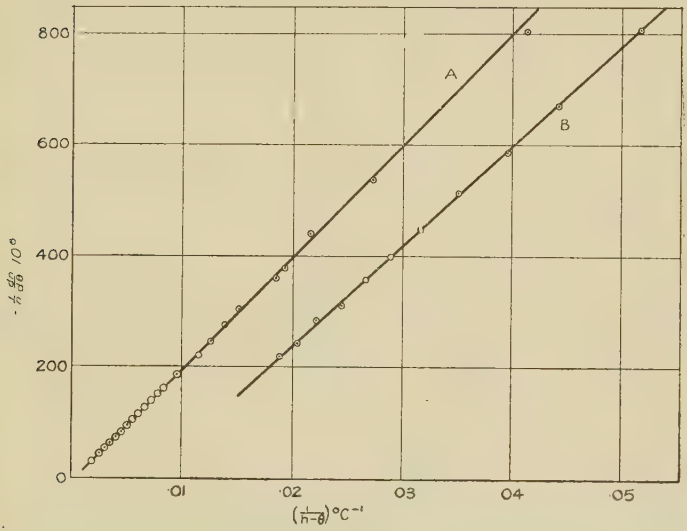

Curve A: both scales as marked.
Curve B: both scales to be read as one-tenth of marked values.

of the transition temperature of quartz obtained by different methods:

TABLE IV.

Observers.	Method.	Value.
Le Chatelier and Mullard ...	Thermal expansion ..... Birefringence, Rotatory power.	570° C.
Fenner	Latent heat ..... Rate of change of temp. (powder).	575° C.
Bates and Phelps	Do. (plates)	573° C.
Wright and Larson	Birefringence (plates)	575° C.
Perrier and Mandrot	Young's modulus	576° C.
Perrier and Roux	Specific heat	575° C.
Shimizu	Electrical conductivity	573° C.

IV. Experiments upon Shear Vibrations.

Before proceeding to any theoretical considerations some similar observations for shear vibrations will be recorded; for this mode of vibration the crystal employed was in the form of a rectangular slab, $0{\cdot}3 \times 1{\cdot}0 \times 1{\cdot}5$ cm. along the Y, X (electric) and Z (optic) axes respectively, *i. e.*, the largest face contains the electric axis instead of its being perpendicular thereto as before. The general mechanical effects arising from an impressed polarization b along the Y-axis are given by Voigt's [6] theory, and allowing for the special symmetry of quartz and for the experimental equality of certain piezoelectric moduli it can finally be stated that

$$b = \delta_{14} Z_x + 2\delta_{11} X_y,$$

where Z_x represents a shearing force in the xz-plane and similarly X_y a shearing force in the xy-plane, whilst δ_{14} and δ_{11} are the usual piezoelectric moduli.

The conditions in this experiment corresponded to those described by Cady [7], in which shears about the z-axis were effective in producing resonant vibrations, the frequency of which, corresponding to a wave-length of about 450 metres, agreed very exactly with the formula given by Lack [8] for this mode of vibration. Shear vibrations have formed the subject of experiments also by Harrison [9], Doerffler [10], and Osterberg [11].

The experimental arrangement and procedure were as previously described, and observations were made up to about 380° C., beyond which (or at most 400° C.) it was not possible to maintain oscillations even with the help of reaction, although the crystal still functioned well at lower temperatures even after high values well above the critical point had been attained.

The results which are given in fig. 1 (B) and Table V. do not cover so wide a range, and are therefore not so useful in determining the type of formula; but the same hyperbolic function with change of constants to allow for a new crystal and conditions proves to be applicable to this case. It will be seen that the values of $\frac{1}{n}\frac{dn}{d\theta}$ are smaller for this shear mode of vibration than in the case of longitudinal vibrations, and the new values of h, k, and P are

$$k = 1{\cdot}28.10^{-5}, \quad h = 573, \quad \mathrm{P} = 1818{\cdot}2.10^{-5}.$$

In both cases the δ_{11} piezoelectric coefficient is effective,

but only in the first case is Young's modulus of elasticity applicable.

TABLE V.

θ.	$-\frac{dn}{d\theta}$.	$n \cdot 10^{-2}$.	Experimental. $-\frac{1}{n}\frac{dn}{d\theta} \cdot 10^{-8}$.	Calculated. $-\frac{1}{n}\frac{dn}{d\theta} \cdot 10^{-8}$.
46·0	14·4	6596	2183	2169
85·2	16·1	6590	2443	2447
122·4	18·6	6583	2826	2754
163·3	20·5	6576	3118	3157
197·3	23·5	6568	3579	3560
226·3	26·0	6561	3963	3964
257·6	29·3	6552	4473	4484
287·5	33·5	6543	5119	5088
319·4	38·4	6532	5879	5889
346·0	43·7	6511	6711	6729
379·0	52·6	6500	8093	8091

V. DISCUSSION.

Probably the main point of interest of these experiments lies in the way in which the formula which represents these results indicates a critical temperature which both the tensile and shear results place at 573° C.

As an expression of his experiments at very low temperatures Strout[3] obtained a linear relation between $\frac{dn}{n\,d\theta}$ and θ, in contrast with the results here recorded. It must be remembered, however, that at low temperatures the hyperbolic relation approximates to a straight line, so that very accurate measurements of the low temperature would be necessary to distinguish between the two laws. If this is taken into account Strout's results cannot be said to be inconsistent with the formula to which we have been led.

It has already been mentioned that, at and above the critical point, symmetry conditions require the piezoelectric constant δ_{11} to be zero, and therefore oscillations are no longer possible, *i. e.*, n must be zero, and the law suggested here agrees in making n zero at 573° C.

To discuss theoretically the variation of n below the critical point it is necessary to employ experimental data for the change of density and elasticity with change of temperature; fortunately both are known and an approximate calculation can be made.

For the longitudinal waves the velocity of propagation in the crystal will be given by

$$n\lambda = \sqrt{\frac{\mathrm{E}}{\rho}},$$

and, as shown experimentally by Hund [12], for disk oscillators the wave-length λ is equal to twice the thickness of the disk; but whereas the density ρ is approximately constant, the elasticity shows a marked variation, and hence approximately

$$n^2 \propto \mathrm{E}, \quad . \quad . \quad . \quad . \quad . \quad . \quad \text{(III.)}$$

though actually

$$\frac{1}{n}\frac{dn}{d\theta} = \frac{1}{2\mathrm{E}}\frac{d\mathrm{E}}{d\theta} + \frac{1}{2z}\frac{dz}{d\theta}, \quad . \quad . \quad . \quad . \quad \text{(IV.)}$$

i. e., the temperature coefficient of frequency is equal to half the sum of the temperature coefficients of Young's modulus along the electric axis and of expansion in the optic axial direction. To employ equation (III.) the present results must be integrated, but before equation (IV.) can be used Perrier and Mandrot's [13] elasticity curve must be differentiated graphically, and of the two the former process is less open to error. Perrier's results, however, refer to the isothermal elasticity, whilst at radio frequencies the adiabatic value only is applicable.

Approximate values for the adiabatic elasticity may be obtained by assuming the applicability of the familiar thermodynamical relation for γ, viz.,

$$\gamma = \frac{\mathrm{E}_\theta{}^i}{\mathrm{E}_\theta{}^a} = \left(1 - \frac{\beta^2 \mathrm{E}_\theta{}^i \theta}{\rho \mathrm{C}_p}\right)^{-1},$$

where $\mathrm{E}_\theta{}^i$ = isothermal elasticity at temp. θ,

$\mathrm{E}_\theta{}^a$ = adiabatic elasticity at temp. θ,

β = temp. coeff. of expansion at constant load,

θ = temperature,

ρ = density at temp. θ,

C_p = specific heat at temp. θ at constant load.

The ordinary specific heat at constant pressure can be

substituted for C_p, and negligible error is introduced in using the ordinary expansion coefficient for β. Using interpolated values, the following table of comparisons was deduced :—

TABLE VI.

θ° C.	n_θ. 10^{-3}.	β . 10^{-5}.	$E_\theta{}^i$ kg./mm.^{2}.	C_p . 10^{-7} erg/gm.	ρ gm./c.c.
15	1485	1·234	8010	·722	2·650
300	1469	2·06	7850	1·063	2·616
400	1457	2·62	7700	1·129	2·601
500	1433	4·00	7250	1·217	2·581
550	1403	6·70	6250	1·320	2·564

θ° C.	γ.	$\frac{E_\theta{}^i}{E_{15}{}^i}$.	$\frac{E_\theta{}^a}{E_{15}{}^a}$.	$\frac{n_\theta{}^2}{n_{15}{}^2}$.
15	1·002	1·000	1·000	1·000
300	1·007	·982	·987	·978
400	1·012	.962	·972	·964
500	1·030	·906	·933	·930
550	1·073	·780	·838	·893

β, from Kozu and Saiti.

$E_\theta{}^i$, from Perrier and Mandrot.

ρ, from Sosman.

C_v, from Int. Crit. Tables.

From the last two columns and from fig. 3 it will be seen hat there is fair agreement, probably as good as could be expected on the simple assumptions made, between the results of our experiments and the values calculated from the adiabatic elasticity. The values calculated from the isothermal elasticity show a wider departure from our figures, and in this way confirm Perrier and Mandrot's observation of a large difference between the two elasticities. Fig. 2 shows the rapid increase of γ with temperature.

About the time this work was completed Andreeff, Fréedericksz, and Kazarnowsky [14] determined the temperature variation of the piezoelectric constant δ_{11} up to 500° C., for which purpose they employed an oscillatory method and determined the wave-length at several temperatures. As

accurate values of $\frac{dn}{n\,d\theta}$ cannot be calculated from these, a comparison cannot be made except by using the integrated equation. It can be shown that their results lead to values for P and k of the same order as those given above for the

Fig. 2.

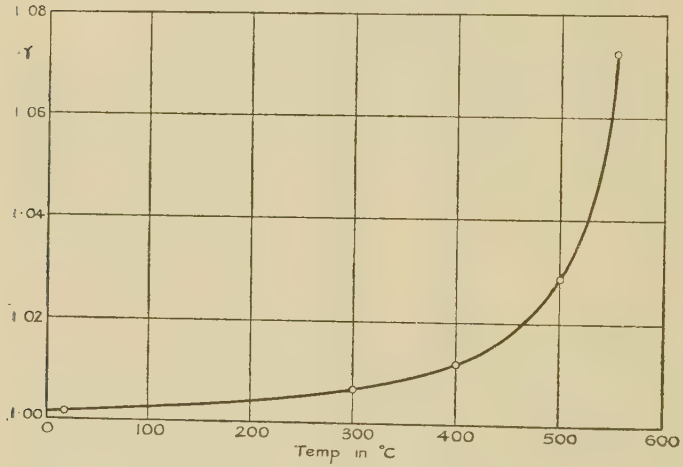

Fig. 3.

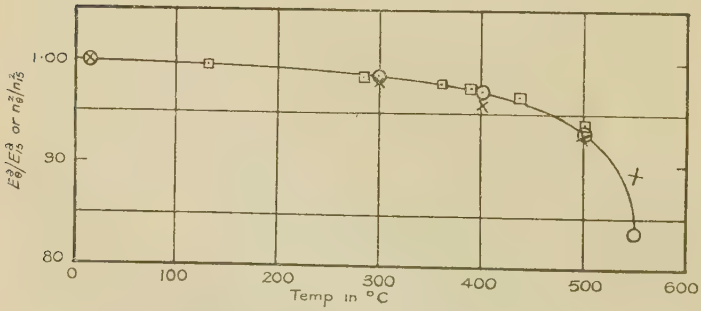

⊙ indicates $E_\theta^{\,a}/E_{15}^{\,a}$; × indicates $n_\theta^{\,2}/n_{15}^{\,2}$;
⊡ indicates calculations from measurements by Andreeff.

corresponding tensile case. As a result possibly of the fact that they were able to measure n_θ directly and were not, as here, dependent upon integrated values, the values of $\left(\frac{n_\theta}{n_{15}}\right)^2$, calculated from their observations, exhibit a closer

agreement with $\frac{E_\theta{}^a}{E_{15}{}^a}$; these values are included in fig. 3.

Owing to the lack of data upon the temperature variation of the pertinent elastic constants corresponding comparisons cannot be made in the case of the shear modes of vibration. However, it is possible to infer from the present results the general temperature variation of the shear modulus, which, assuming a simple connexion between n^2 and the modulus, should be characterized by a large and fairly sharp fall as temperatures lower than but approaching the transition value are reached. Such marked variations at or near the critical temperature are exhibited by most of the physical properties of quartz.

VI. Summary.

The temperature coefficients of the frequency of piezoelectric vibrations of quartz have been measured over a range of several hundred degrees for two types of vibrations, viz.,

(*a*) longitudinal vibrations along the X-axis for an "X-cut,"

(*b*) shear vibrations about the Z-axis for a "Y-cut."

In both cases a simple hyperbolic relation has been found to connect the temperature coefficient with the temperature. The constant temperature axis to which the curve is asymptotic appears to be either the α–β transition temperature, or a value differing only slightly from it.

A comparison, based on very simple assumptions, is made between the temperature variations of elasticity and of the square of the frequency of vibration of the crystal.

VII. Acknowledgment.

In conclusion, it affords us great pleasure to be able to record our thanks to Professor E. N. da C. Andrade for his advice and encouragement during the research.

References.

(1) Giebe and Scheibe, *Zeit. für Phys.* xlvi. p. 607 (1928).
(2) Dye, Proc. Phys. Soc. xxxviii. p. 399 (1926).
(3) Strout, Phys. Rev. xxxii. p. 829 (1928).
(4) Dawson, Phys. Rev. xxix. p. 532 (1927).
(5) Schulwas-Sorokina, Phys. Rev. xxxiv. p. 1448 (1929).

(6) Voigt, 'Die fundamentalen physikalischen Eigenschaften der Krystalle.'
(7) Cady, Phys. Rev. xxix. p. 617 (1927).
(8) Lack, Bell System Tel. Journ. viii. p. 515 (1928).
(9) Harrison, Proc. I. R. E. xv. p. 1040 (1927).
(10) Doerffler, *Zeit. für Phys.* lxiii. p. 30 (1930).
(11) Osterberg, Journ. Opt. Soc. Am. xxii. p. 19 (1932).
(12) Hund, Proc. I. R. E. xiv. p. 447 (1926).
(13) Perrier and Mandrot, *Arch. des Sc. Phys. et Nat.* iv. p. 367 (1922).
(14) Andreeff, Fréedericksz, and Kazarnowsky, *Zeit. für Phys.* liv. p. 477 (1929).

Carey Foster Research Laboratories,
University College, London.

LXXIV. *On the Volume of the Meniscus at the Surface of a Liquid.* *By* Alfred W. Porter, *D.Sc., F.R.S., F.Inst.P., Emeritus Professor in the University of London**.

A KNOWLEDGE of the volume of a meniscus is necessary in various operations of measurement (eudiometers, measuring glasses, etc.). The symbol, V, will be taken to mean the volume enclosed by a tangent plane

Fig. 1.

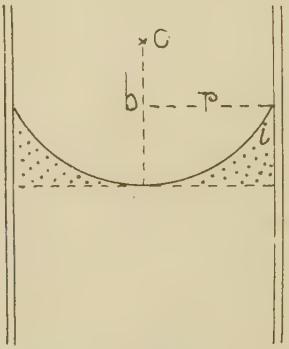

through the mid-point, the liquid surface itself, and the wall of the vessel in the case of a vertical cylinder. Its cross-section is shown dotted in fig. 1 for the case of a surface which is concave upwards.

This volume can be calculated readily by means of the tables of Bashforth and Adams ('Capillary Action,' out of print; referred to as B. and A. Tables), but the range of these is comparatively small, and further information is desirable.

* Communicated by the Author.

PART I.—*Cylindrical Tubes.*

The geometric data of the surface are the rectangular coordinates, x and y, of a point upon it, and the inclination, ϕ; the physical data are expressed by the quantity $\beta^2 \equiv \frac{\sigma}{(g\rho)}$. The dimensions of β are those of a length simply. For tabulating purposes, B and A take the data as $\frac{x}{b}$, $\frac{y}{b}$, ϕ, and $\left(\frac{b}{\beta}\right)^2$, where b is the radius of curvature at the mid-point. These selected data are all pure numbers. When $\phi = 90° - i$, where i is the angle of contact, the corresponding values are $\frac{r}{b}$, $\frac{h}{b}$, and $\frac{\pi}{2} - i$. These values can be read direct from the tables for many values of ϕ.

Now dynamically

$$V g\rho = \sigma 2\pi r \cos i - \frac{2\sigma}{b}\pi r^2,$$

so that

$$\frac{V}{\pi\beta^3} = 2\frac{r}{\beta}\left[\cos i - \frac{r}{\beta}.\frac{\beta}{b}\right],$$

whence the value of V can be calculated. The range of the tables extends, however, only to $\frac{r}{\beta} \doteq 3{\cdot}16$. For water $\beta \doteq 0{\cdot}3$, so that r is then of the order of 1 cm., which is less than is sometimes required in practice.

In order to extend the range recourse may be made to Rayleigh's papers "On the Theory of the Capillary Tube" (Proc. Roy. Soc. A, xcii. pp. 184–195 (1915); reprinted with appendix in 'Collected Papers,' vi. p. 350). In the appendix, which applies only to wide tubes $\left[\frac{r}{\beta}\right.$ ranging from 6 to 10$\left.\right]$, Rayleigh calculates the values of $\frac{h_0}{\beta}$, where h_0 is the elevation at the mid-point for the particular cases in which the angle of contact is zero. Since, from dynamics,

$$2\pi\sigma r = (V + \pi r^2 h_0) g\rho,$$

it follows that

$$\frac{V}{\pi\beta^3} = \frac{r}{\beta}\left\{2 - \frac{r h_0}{\beta^2}\right\},$$

whence I have calculated the following table :—

$\frac{r}{\beta}$.	$\frac{h_0}{\beta}$.	$\frac{V}{\pi\beta^3}$.
5	0·0359	9·077
...	.....	.....
6	0·0149	11·4635
7	·0059	13·7109
8	·0023	15·8528
9	·00089	17·928
10	·00034	19·966

I have added the value for $\frac{r}{\beta}=5$, though this approaches the limit at which the formula can be used with safety.

It must be added that for large values of $\frac{r}{\beta}$, $\frac{V}{\pi\beta^3}$ tends asymptotically to the value $2\frac{r}{\beta}$, so that it ultimately becomes infinite with r.

A curve including these values is drawn as the top curve in fig. 2, together with its asymptote. The same curve shows the numbers from Bashforth and Adams; the two sets are fairly safely joined together to form a continuous curve.

Thus for $i=0$ and cylindrical tubes the problem may be regarded as solved for all values of $\frac{r}{\beta}$.

It may be added that for values of $\frac{r}{\beta}<0{\cdot}8$, the following formula may be used, based on Rayleigh's expansion (*loc. cit.*) for small abscissæ :

$$\frac{V}{\pi\beta^3}=\frac{r^3}{\beta^3}\left[\tfrac{1}{3}-0{\cdot}0644\frac{r^2}{\beta^2}+\frac{0{\cdot}0220r^4}{\beta^4}\right].$$

When the angle of contact is not zero, we have at present (*a*) values calculated from B. and A. Tables, and (*b*) the equation to the asymptote : for in the limit

$$\frac{V}{\pi\beta^3}\longrightarrow 2\frac{r}{\beta}\cos i.$$

Using these data the curves for $i=30°$, 45°, and 60° have been constructed. The lower part of each is accurately determined ; the middle and top parts are drawn tentatively with the asymptotes as a guide [the asymptote is shown

only in the case of $i=0$]. These values are probably as accurate as will be needed in practice.

Fig. 2.

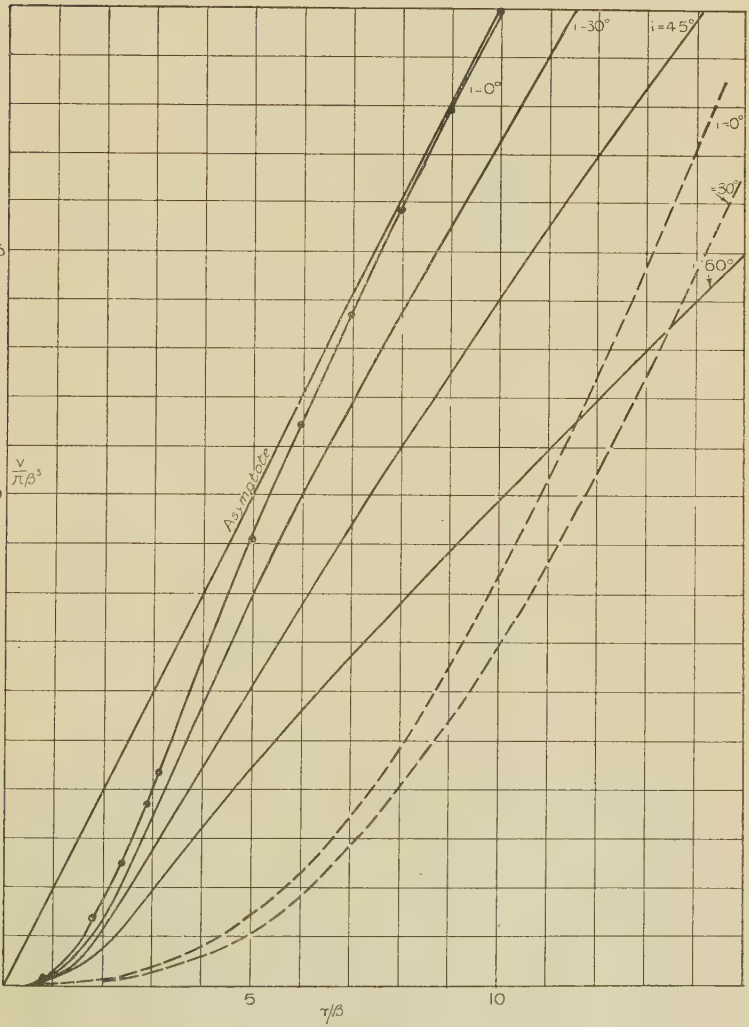

The curves for $i=0°$ and 30° are also represented as broken lines on five times the scale of the main diagram. For these lines the numbered squares are unit squares.

The following are the calculated data for the several cases (based on the B. and A. Tables) which have been used in constructing the diagram :—

Contact angle 0°.		Contact angle 30°.	
$\frac{r}{\beta}$.	$\frac{V}{\pi\beta^3}$.	$\frac{r}{\beta}$.	$\frac{V}{\pi\beta^3}$.
·8853	·2053	·7916	·1178
1·8687	1·4092	1·3507	·5148
2·1688	1·9857	1·7456	·9921
2·4074	2·4966	2·0428	1·4516
2·9192	3·6847	2·280	1·8692
3·1646	4·3264	3·037	3·4154

Contact angle 45°.		Contact angle 60°.	
$\frac{r}{\beta}$.	$\frac{V}{\pi\beta^3}$.	$\frac{r}{\beta}$.	$\frac{V}{\pi\beta^3}$.
·6658	·0550	·4850	·0146
1·178	·2782	·9013	·0889
1·557	·5860	1·2374	·2166
1·848	·8891	1·5094	·3703
2·088	1·2102	1·7342	·5312
2·446	1·7495	1·9243	·6894
2·592	1·9858	2·0991	·8400
2·838	2·4029	2·2326	·9866
		2·476	1·250

Part II.—*Conical Tubes.*

In these cases the shape of the meniscus is the same as for a cylinder whose radius is r and contact angle is $i+\alpha$ (fig. 3) where r is the radius of the line of contact of the liquid with the vessel and α is the semi-angle of the cone. The volume of revolution swept out by GDE in revolving round the axis is equal to the volume calculated by the methods of Part I. for an angle equal to $(i+\alpha)$. From this volume we require to subtract the volume swept out by the triangle FDE in rotating round the axis. If h is the height DE, this volume is

$$v=\tfrac{1}{2}h.h\tan\alpha.2\pi\{r-\tfrac{2}{3}.\tfrac{1}{2}h\tan\alpha\}$$
$$=\pi h^2\tan\alpha\{r-\tfrac{1}{3}h\tan\alpha\}.$$

This volume can therefore be calculated if h is measured experimentally as well as r.

The value of $\frac{h}{\beta}$ can, however, be obtained from B. and A. Tables for various values of $\frac{r}{\beta}$.

Fig. 3.

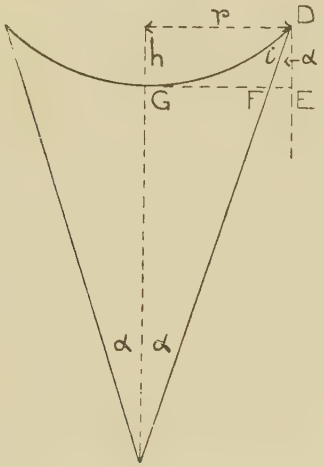

The following summary is given of values so calculated:—

$\iota+\alpha=15°$.			$\iota+\alpha=30°$.		
$\frac{r}{\beta}$.	$\frac{h}{\beta}$.	$\frac{v}{\pi\beta^3}$.	$\frac{r}{\beta}$.	$\frac{h}{\beta}$.	$\frac{v}{\pi\beta^3}$.
·8630	·6006	·0782	·7916	·4292	·0753
1·4414	·8784	·2818	1·3507	·6617	·3095
1·8408	1·0130	·4807	1·7449	·7841	·5649
2·1405	1·0895	·6500	2·0428	·8563	·7946
2·3790	1·1380	·7904	2·2804	·9031	·9919
2·5763	1·1713	·9088	2·4775	·9356	1·1609
2·7445	1·1952	1·0098	2·6455	·9593	1·3074
2·8908	1·2133	1·0977	2·7918	·9773	1·4357
3·1361	1·2383	1·2434	3·0372	1·0025	1·6504

$i+\alpha=45°$.

$\frac{r}{\beta}$	$\frac{h}{\beta}$	$\frac{v}{\pi\beta^3}$	$\frac{r}{\beta}$	$\frac{h}{\beta}$	$\frac{v}{\pi\beta^3}$
·6658	·2660	·0483	2·2790	·6801	·9492
1·1780	·4388	·1986	2·4464	·7030	1·0932
1·5566	·5414	·4034	2·5923	·7206	1·2214
1·8484	·6059	·6044	2·8376	·7456	1·4949
2·0833	·6492	·7868			

The value of $\frac{v}{\pi\beta^3}$ is in each case zero when $\frac{r}{\beta}$ is zero. It is also zero when $i+\alpha$ is zero.

These values can be interpolated in various ways to suit technical needs. In glassware certain angles, α, may be standardized and therefore merit detailed calculation. For many common liquids the angle of contact may be taken as zero*. A few minutes change or even a degree makes very little difference indeed.

The final value of the liquid lying above the height of the mid-point is $V-v$.

87 Parliament Hill Mansions, N.W. 5.

LXXV. *Hot Wire and Spark Shadowgraphs of the Airflow† through an Air-screw.* *By* H. C. H. Townend, *B.Sc.*‡

[Plates XI.–XVII.]

Summary.

A method of delineating the flow-pattern round bodies mounted in an air-stream is described and applied to the case of the flow around an air-screw.

By mounting a grid of fine heated wires near the blades the character of the flow-pattern can be observed if the shadows of the hot air bands cast by an arc lamp are viewed through a stroboscope synchronized with the air-screw blades.

As a further development, the hot wire has been replaced by a periodic electric spark which gives a shadow

* A list is given in Internat. Crit. Tables, iv. p. 434.

† Permission to communicate this paper has kindly been granted by the Aeronautical Research Committee.

‡ Communicated by E. F. Relf, A.R.C.Sc.

consisting of a stream of dots instead of a continuous band. The dots occur at regular intervals of time, so that changes in the relative position of the dots can be determined. It is thus possible to make a fairly complete map of the velocities and directions of small masses of air as they pass through the screw.

Results.

The frequency of the sparks has been taken as high as 1300 per second, and could probably be increased considerably if necessary. Their shadows have been observed with ease up to a wind speed of 30 ft./sec. and photographed with an exposure of about 1/6000th of a second.

By interrupting the illuminating beam of light with a stroboscope driven by the screw, and by changing the phase relations between them, the motions of individual small masses of air could be observed at any point in the field.

Arrangements were made to change the phase relation between the screw and the spark generator while the stroboscope remained synchronized with the latter; the general motion of the dots downstream was thereby arrested, while the deviations produced by the screw were revealed.

Introduction.

IN the study of the motion of gases, or of disturbances occurring in them, one of the methods which have been used to make the motion visible is based upon local variations of refractive index which exist or can be produced in the fluid itself. The photography of sound-waves in air is a well-known example, in which changes of refractive index result from the changes in density which form the waves. The photos are usually obtained either by the Schlieren method of Töpler * or the simpler direct shadow method of Dvorak *.

In an earlier paper † a modification of the latter

* Töpler, A., *Ann. der Phys. u. Chem.* cxxxi, pp. 33–35 (1867); Dvorak, *Ann. der Phys.* ix. p. 502 (1880).

† "On Rendering Airflow Visible by means of Hot Wires," Townend, Aeronautical Research Committee, Reports and Memoranda, No. 1349.

method has been described whereby the stream-lines, appropriate to the steady motion of air past a body mounted in an air-stream, could be rendered visible. The method consists in placing a grid of fine wires electrically heated in front of the body, and casting shadows of the bands of hot air produced by them on to a screen or a photographic plate. Fig. 1 (Pl. XI.) is a shadowgraph reproduced from that paper. It shows the air flow past a model of a slotted wing mounted in a wind tunnel. The frame of the grid can be seen on the right of the picture, the hot wires being perpendicular to the plane of the paper. Owing to the length of the wing span (4 ft.) the shadow of the wing itself is blurred, but its true section, in the plane of the hot wires, has been drawn in in the correct position.

Work of a similar kind has also been done in Japan *, but in this case a broad stream of hot air was produced large enough to envelop the body completely. Photographs were then taken by both of the above methods of the motions of this volume of heated air in passing round the body. The results were applied mainly to the eddying flow associated with bluff bodies.

In the present paper experiments are described in which the hot wire method has been applied to the periodic flow through an air-screw. As a further development, the hot wire has been replaced by a periodic electric spark, the shadow of which consists of a series of dots which enables the velocity and direction of the flow to be mapped out. By interrupting the illuminating beam with a stroboscope the shadows are brought to rest and records can be made from which measurements can be obtained. In unsteady or periodic motions the shadow-bands are the "Filament Lines" referred to in Bairstow's "Aerodynamics."

Apparatus.

For the preliminary air-screw experiments with hot wires an existing air-screw-body combination was available. This comprised a 4-bladed air-screw of $19\frac{1}{4}$ in. diameter and pitch diameter ratio 0·7 mounted as a tractor in the nose of a stream-line body 30 in. long, having a

* 'Kinematographic Study of Aeronautics,' Terazawa, Yamazaki, and Akishino. Report of Aeronautical Research Institute, Tokyo, i. No. 8 (September 1924).

maximum diameter of 12·4 in. The tests were made in a wind tunnel having a cross section 7 ft.×7 ft. A grid of seven wires was supported on a retort stand resting on the floor of the tunnel so that it could be located at any convenient position with reference to the air-screw. The wires of the grid were 1 in. long, 0·002 in. in diameter, and $\frac{1}{2}$ in. apart, and were heated by a 14-volt battery; they took about 1 ampere per wire at a wind speed of 30 ft. per sec.

Shadows of the hot-air bands were cast by an arc lamp shining through a hole in one wall of the tunnel on to a piece of gaslight printing paper ("Slogas") fixed on the opposite wall.

Owing to the periodic nature of the flow past the air-screw, the shadows could not be directly observed behind the screw, except as faint broad bands, but when the rays from the arc lamp were interrupted by a stroboscope synchronized with the air-screw, they were resolved into the patterns shown in fig. 2 (Pl. XII.).

In order to vary the angular position of the shadow of the screw, arrangements were made by which the phase of the stroboscope relative to the screw could be changed while the screw was running. By this means the apparent motion could be slowed down for observation.

Tests with a Periodic Electric Spark substituted for the Hot Wire.

In fig. 2 (Pl. XII.) it will be seen that breaks occur in the filament lines. The significance of these breaks will be discussed later, but it may be noticed here that the ends of the lines serve to identify certain particles of air individually, namely, those bounding the vortex sheets springing from the blades.

In order to identify other particles it was desirable, if possible, to produce a dotted line instead of the continuous line produced by the hot wire, and it was thought that this might be achieved if an electric spark were used in place of the hot wire. This would be equivalent to placing a visible particle at any desired position in the field at any desired instant. The shadow of this particle could then be used to determine the motion of the particle both when the motion was periodic,

as in the case of the air-screw, or when it was steady. By using a stream of sparks, produced for example by an alternator or a magneto, the dots in the shadowgraph would provide a time scale from which the velocity at a point could be determined.

In these experiments an alternator of $\frac{1}{2}$ horse-power was used, giving about 150 volts at 2000 revs. per minute. The output from the alternator was passed through an adjustable resistance of about 100 ohms to a transformer which stepped up the voltage 100 times. There were 40 poles on the rotating field magnet of the alternator, so that a frequency of about 650 cycles per second was obtainable. As a rule only one spark per cycle occurred, probably owing to some lack of symmetry in the circuit.

Shadowgraphs were obtained by casting a shadow of the spark-stream on a screen in the same manner as in the case of a hot wire. To bring the shadow to rest the arc lamp was made to shine through a stroboscope disk which was mounted directly on the shaft, of the alternator. The disk had 20 slits, that is, the same number as the number of sparks produced in one revolution of the alternator.

The preliminary tests were made in a small wind tunnel having a 3-in. square section in which the flow was very steady, and photos of the spark shadows were therefore easily obtained, which extended for a considerable distance down-stream. Figs. 3 and 4 (Pl. XIII.) are shadowgraphs of streams of sparks in the empty tunnel taken directly on gaslight printing paper.

The Electrodes.

Numerous tests were made on the best form and disposition of electrodes constituting the spark gap. At first two bare copper wires were used placed on a common axis parallel to the beam of light and normal to the wind. It was found that with the wind on the spark was drawn into a broad flame having different characteristics according to the air speed. At a low speed, the electrodes were joined by a blue streak which was not blown down-stream. Just behind this was a thick mauve-coloured flame bounded down-wind by another fainter blue streak. There was a succession of these blue streaks and mauve flames alternately up to three or four in number, followed by mauve flames

only up to ten or more. The appearance of the spark can be seen from the photograph in fig. 3 (*a*) (Pl. XIII.). As the speed was raised the rearmost flame would disappear and the audible note of the spark would rise in pitch. Then the next flame would disappear, and so on, until only one streak and one flame were left. The notes emitted by the sparks were in a kind of inverted harmonic series; the pitch of the notes corresponding to two flames was one octave lower than that corresponding to one flame, and so on downwards by harmonic intervals. The shadow band became progressively less complicated as the flames became fewer until, when only one was left, a series of spots resulted as shown in fig. 3 (Pl. XIII.). This case was the most satisfactory from the present point of view.

A similar result to the above was obtained by putting more resistance in the primary circuit instead of increasing the wind speed.

With a spark having several flames it was found that an appreciable length of the electrodes was occupied by the flames. Better results were obtained when the electrodes were made from steel wire 0·024 in. in diameter, the ends of which were held for a second or two in the flame of a carbon arc lamp until a small bead of oxidized metal was formed at the extremity roughly 1/16 in. in diameter. With these electrodes the sparks were very regular and consistent, and seldom showed any tendency to occur erratically, sometimes in the positive and sometimes in the negative half-cycle. The shape of the shadow of the spark was also more satisfactory. This mode of construction has the advantage that since oxidation is complete to begin with no trouble arises from deterioration of the surfaces. Electrodes made from the bare untreated wire were found unsatisfactory.

Fig. 3 (Pl. XIII.) shows some shadowgraphs taken on "Slogas" paper with a spark frequency of about 650 per second. As mentioned above, a spark usually occurred only once per cycle as in (*b*) and (*c*), although sparks could often be caused to occur once per half-cycle as in (*d*), where the spark frequency was about 1300 per second.

Fig. 4 (Pl. XIII.) shows a shadowgraph taken with a bank of four spark-gaps in parallel. It was found rather difficult to make all four gaps give satisfactory sparks

simultaneously, and it will be seen that one of them is out of phase with the other three, indicating one discharge per half-cycle.

Application of Spark Shadowgraphs to an Air-screw.

In order to test out the spark method on an air-screw conveniently a small 4-bladed air-screw of 10 in. diameter was mounted in a wind-stream from a fan of 2 ft. 3 in. diameter. The slip-stream from the fan was contracted to 14 in. diameter, forming a small open-jet wind tunnel. With an air-stream produced in this manner the flow in the jet was very unsteady, and this led to difficulty in obtaining satisfactory photographs. Some idea of the degree of turbulence in this air-stream can be formed from fig. 5 (*a*) (Pl. XIV.) which is a snapshot of the spark-band with the air-screw removed. A hot wire was also mounted in the air-stream to provide a comparison between the shadows given by the spark and the hot wire.

A sketch of the apparatus used for the spark shadowgraphs of the flow through an air-screw is shown in fig. 5 (*b*) (Pl. XIV.). The tunnel is omitted from this sketch, but an arrow is shown which indicates the axis and direction of the jet. The spark-gap was situated in a vertical axial plane, just in front of the air-screw disk and close to the tip circle. The angle θ gives the relation between the spark-gap and the blades in the shadowgraphs shown in figs 6, 7, and 8 (Pls. XV.–XVII.).

In order to secure synchronism between the air-screw and the sparks the screw was driven directly from the alternator shaft through a universal coupling. Since there were 4 blades on the screw and 20 sparks were produced per revolution of the alternator, 5 sparks occurred per blade. The width of the slit in the stroboscope disk was $1\frac{1}{2}°$.

The arc lamp was placed about 8 ft. from the screen and, owing to the narrowness of the slits, an exposure of about 7 seconds was necessary to obtain a print on gaslight paper with four slits on the stroboscope, corresponding to a total absolute exposure of about 1/10 second. On account of the unsteadiness of the stream such a long exposure made it impossible to record more than the first half-dozen dots, although those which were recorded were more accurate as mean values. To obtain

shorter exposures than were possible with gaslight paper, process plates were used. At first these were given an exposure consisting of several successive flashes through the stroboscope. Fig. 6 (Pl. XV.) was taken in this way. In this figure the spark frequency was 500 per second, the wind speed was 13·5 ft./sec., and the air-screw speed was 25 revs. per second. It was found, however, that if extra care was taken to darken the room adequately, and also to shield the plate from the direct rays of the spark itself, a single flash was sufficient to secure a record. In fig. 8 (Pl. XVII.) the photographic plates were screened from the direct rays of the spark by fixing a small disk about $\frac{1}{4}$ in. diameter to the electrode on the side of the spark-gap nearest the plate. The black circle, which can be seen at the end of the electrodes, is the shadow cast by this disk. For this figure a hot wire was mounted in front of the screw in addition to the spark-gap for comparison. Figs. 7 and 8 (Pls. XVI. & XVII.) were taken with a single flash from the stroboscope, the exposure being 1/6000 sec.

Differential Stroboscope.

In order to obtain an exposure consisting of a single flash of the stroboscope, and at the same time to ensure that it should occur at a predetermined phase of the air-screw, a pair of stroboscope disks was used arranged as in text-fig. 9 (p. 708).

In this figure S is the stroboscope spindle, rotating at air-screw speed, carrying two gear-wheels, A and B, of the same diameter (2 in.). Of these A is attached rigidly to the spindle and has 100 teeth, while B rotates on the boss O of A and has 101 teeth. A and B are pressed into frictional contact with each other by the flat spring F.

The wheel B carries one stroboscope disk D, while the second disk E is attached rigidly to the spindle S. A third gear-wheel G, having say 50 teeth, is mounted on a sliding spindle H. It is in permanent mesh with A, and can be made to engage with B simultaneously. When G is in mesh with both A and B, the disk D moves at a speed which is (100/101)ths that of A. As each disk has only one slit, therefore, light is only permitted to pass through the disks once every 101 revolutions

of the spindle, *i. e.*, of the air-screw. One of the slits was $1\frac{1}{2}$ in. in width; the other was somewhat larger.

The process of taking a shadowgraph is then as follows:—

Before starting the screw, the wheel G is withdrawn from mesh with B and the desired phase is adjusted by sliding B over A against the spring F.

Fig. 9.

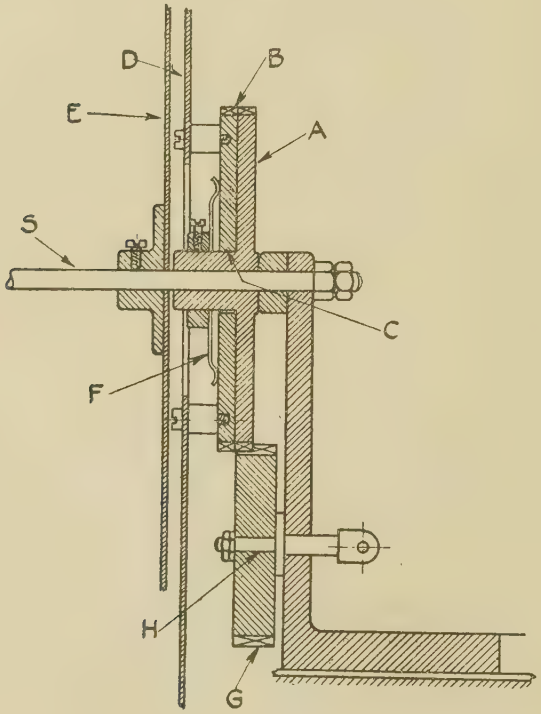

Differential Stroboscope.

Having started the screw and attained steady running conditions, which can be watched on the screen since a shadow is cast every revolution, the wheel G is moved into gear with B.

In this condition one flash occurs every few seconds, and the intervening periods of darkness allow plenty of time in which to operate the shutter of the plate carrier.

All the photos shown were taken with an ordinary arc lamp (5 amp.) without any lenses. Since the stroboscope disk was 3 or 4 in. away from the arc the whole of the plate was not exposed simultaneously, the top being slightly later in time than the bottom. For more accurate timing it would be preferable to place a lens in front of the arc lamp forming an image of the arc, and to place the stroboscope disk in the plane of this image. The exposure would then be virtually instantaneous over the whole plate.

Discussion of Results.

(a) *Results with hot wires.*—The filament lines of fig. 2 (Pl. XII.) show the appearance of the field around and behind the screw. These lines do not represent stream-lines since the flow is periodic, nor do they represent paths of particles, since if the snapshot were taken a moment later the whole filament line would be displaced down-wind with only a slight change in shape, and hence most of the particles are moving at an angle to the direction of the line. This effect is at once rendered obvious by slightly changing the phase between the blades and the hot wires. In consequence the lines cannot in general be extended, as they can in the case of steady motions, by merely placing another grid of hot wires further down-stream.

It will be seen in fig. 2 (*a*) (Pl. XII.) that the lines are broken just behind the screw. This break is caused by the passage of the air-screw blade in front of the grid. The distribution of thrust around the blade gives rise to radial velocities which, over the outer parts of the blades, are outwards behind the blade and inwards in front of it. Any particle, therefore, which crosses the air-screw disk just in front of a blade receives a small outward radial velocity, whilst a particle which, following it an instant later, passes just behind the blade receives an inward velocity, and hence these two particles diverge as they move down-stream, thereby producing a break in the filament line. Since there is a vortex sheet trailing behind the blade, across which this discontinuity of radial velocity exists, a break begins to develop wherever this sheet crosses a hot wire; hence breaks always occur whether the grid is situated in front of

or behind the screw. The breaks therefore mark out the position of the vortex sheet left behind by the blade. If the phase is changed so as to move the sheet down-stream, the radial displacements at the breaks increase; at the same time the breaks near the centre of the blade move down-stream faster than those near the tip on account of their greater axial velocity. This latter effect can be seen very clearly in fig. 2 (*b*) (Pl. XII.) on passing from the centre of the blade to the tip, by noticing how the two ends of the break lie with respect to one another. The boundary of the slip-stream is represented by the line of centres of the eddies coming from the tip.

(b) *Results with sparks.*—During the spark tests arrangements were made for varying the phase relations between the sparks, the air-screw, and the stroboscope. The effects of changing the various phase relations are considered below. The attitude of the air-screw is given on the figures themselves.

An interesting feature of all the figures is the way in which the dots passing close to the tips of the blades are drawn out into elongated shadows, indicating a high velocity at the edge of the vortex sheet trailing from the blade. The high velocity in this region is clearly shown, experimentally, by slowly moving the spark-gap radially inwards across the tip circle while the screw is running, when the motions near the tips are seen to be more rapid than elsewhere. In fig. 7 (*b*) (Pl. XVI.) this acceleration is shown clearly by the three elongated dots, which mark the position of the tip vortex. These dots are spaced more widely than those just behind the spark-gap, which have not encountered the vortex sheet. The lowest of the three dots, which is in the slip-stream, has overtaken the dot which was in front of it; the former has been accelerated and the latter retarded by the edge of the sheet.

If, by changing the phase, the tip vortex is followed as it goes down-stream, it is found to grow in size, and more dots become involved in it as its influence spreads into the surrounding fluid. The beginning of this process can be seen at the right-hand side of fig. 7 (*a*) (Pl. XVI.).

By suitably adjusting the position of the spark-gap it is possible to make one of the dots pass so close to the

screw that it becomes completely lost in the centre of the tip vortex, and is in consequence missing in the shadowgraph. Fig. 6 (*b*) (Pl. XV.) shows this effect.

Effects of changing the Phase Relations.

In the case of the spark experiments an additional variable was present, namely, the phase of the sparks relative to the air-screw and stroboscope. Hence there were three ways of varying the several phase relations. These are considered below :—

(1) *Sparks and stroboscope synchronized* : *air-screw rotating slightly too fast.*—In this case the screw appeared to rotate slowly in its true direction, whilst the dots some distance in front of the screw were brought to rest, since they were synchronized mechanically with the alternator. The dots near and behind the screw, however, appeared to oscillate about mean positions at blade frequency. Thus, considering the region near the tip of the screw, the dot nearest the blade on the inflow side of the disk appeared to move slightly backwards, *i. e.*, up-stream, as the blade approached it, since its axial velocity was reduced by the upwash in front of the blade section, whilst the corresponding dot on the outflow side of the screw was accelerated.

As the tip of the blade cut across and then receded from the spark-stream the motion at the edge of the vortex sheet shed by the blade could be seen. A dot on the down-stream side of the sheet could be observed to move outwards as the sheet approached it, pass rapidly over the tip of the screw in an up-stream direction, and then inwards on the inflow side of the sheet, giving a clear picture of the tip eddy, as shown, for example, in fig. 6 (*a*) and 7 (*b*) (Pls. XV. & XVI.).

The motions of the dots further down-stream were too indistinct to be observed accurately with the small scale screw and turbulent air-stream used. This will be studied in greater detail later, when further work is to be undertaken under more favourable wind tunnel conditions.

(2) *Screw and stroboscope synchronized* : *alternator rotating too fast.*—In this case the dots move down-stream, whilst the screw and shadow pattern as a whole are

stationary. The dots, therefore, merely trace out the hot-wire filament lines of fig. 2 (Pl. XII.) as the phase of the sparks changes.

(3) *Screw and sparks synchronized : stroboscope rotating too slowly.*—This case and case (1) would be identical if hot wires were used instead of sparks, and would be the same as the original experiments fig. 2 (Pl. XII.). But whereas in case (1) the sparks are brought to apparent rest whilst the screw rotates slowly, here they are given the same slow motion as the screw. If things are so adjusted that a dot occurs at the point where the hot-wire filament line stops short, due to a break, then the motion of this dot will obviously be identical with that of the end of that filament line, and will, therefore, trace out the path of that particle. Similarly the intermediate dots will trace other particle-paths. This case then is the one which indicates how a particle moves as it goes down-stream, and also shows plainly the increasing slip-stream velocity on going inwards from the tip, whilst case (1) gives a rather better idea of the *fluctuations* experienced by a particle situated in a given point as the vortex sheets pass it. In particular the " spilling " of the air over the tip of the blade is shown very clearly.

LXXVI. *The Cold Electric Arc in Vacuum. By* F. H. Newman, *D.Sc., A.R.C.S., Professor of Physics, University College, Exeter*.*

[Plate XVIII.]

1. *Introduction.*

IN general an electric arc can be drawn, even in a very high vacuum, by separating two metal electrodes carrying current of the order of a few amperes. The arc is drawn initially in the vapour given off by the vaporization of the metal at the point of last contact, and may be maintained by the vapour which, after contact and separation, continues to be given off from the contact surface.

A new type of electric arc in high vacuum has been described by the author† in which with cold electrodes an

* Communicated by the Author.

† Phil. Mag. xi. p. 796 (1926).

arc can be started and maintained in various gases, provided that an initial temporary electrical discharge is passed between one of the "arc" electrodes and a third electrode, placed within the discharge-tube. Iron electrodes were used in the original experiments, and the spectra of the resulting radiations were entirely composed of lines corresponding to the residual gases. They showed no trace of the iron electrode lines, provided that the current was not allowed to pass for such a period that the electrodes became incandescent. The arc exhibited the usual current-voltage characteristics, and in some respects it was unilateral in that the polarity of the arc had to be related to the polarity of the auxiliary electrical discharge, the arc passing more readily if the electric fields were in the same direction.

The formation of such an arc in the residual gases of the tube and passing currents of high value—as large as 12 amperes—when the gas-pressure is in the neighbourhood of 10^{-2} mm. of mercury is interesting and surprising. With the requisite potential difference applied between the "arc" electrodes a momentary electrical discharge is sufficient to start the arc which is then maintained ; the electrodes are not initially heated. It is evident that the residual gases in the tube must be ionized, the requisite energy coming from the ions which have acquired high velocities under the electric force from the transient electrical discharge, the initiation of the latter being due to stray electrons and ions, particularly the latter. Before these can ionize the gas, a time must elapse which is large in comparison with the time interval between one collision of the ion with a gas molecule and the next one, since before the ion can ionize it must obtain from the electric field energy greater than that corresponding to the ionization potential of the gas, and this energy must be conveyed to an electron within a molecule in order that the electron can be liberated from the latter. Thus there is produced a fairly copious supply of electrons which, under the further influence of the field due to the applied potential difference, form more ions by collisions, provided that the mean free path of the electrons is so large that they attain energy equivalent to the ionization potential of the gas through which the arc passes. It seems, therefore, that the function of the electrical discharge is to generate those electrons which are ordinarily supplied by the incandescent electrode of the ordinary arc, or by the incandescent filament of a low-voltage arc.

Further experiments indicate that the passage of electrons through gases gives rise to X-rays which may be of far higher

frequency than any of the characteristic radiation of the gas. At the lower gas pressures the electrons, owing to their greater mean free path, have large amounts of energy, and they produce radiations of a greater frequency-range than those with smaller amounts, although the energy density is not so great. At each collision the fast electrons may not produce much more radiation than the slow-moving ones, but they are able to make many collisions with atoms and molecules before their energy is so much reduced that they are unable to generate X-rays. Thus the total amount of radiant energy produced by a fast electron will be much greater than that formed by a slow-moving one, with resultant increased ionizing effects. Thus we should expect a greater concentration of the electrons at the lower pressures, and this explains why the arc can be started more easily and more consistently as the pressure is reduced.

Further investigations have now been made on the spectra of the radiation from the arc discharge with different types of electrodes, viz., mercury, sodium, and potassium. The actual apparatus used was similar to that described in the previous paper, a potential difference being applied between two "arc" electrodes and a momentary electrical discharge sent between one of these electrodes and a third one (iron) in the tube. In all cases the pressure of the residual gas within the tube was below 10^{-1} mm. of mercury, and no external heat was applied, so that the vapour-pressure of the "arc" electrode was initially that corresponding to room-temperature, viz., 15° C.

2. *Experimental.*

Mercury.—In the first place one of the "arc" electrodes was a pool of mercury and the other iron, situated about 1·5 cm. above the mercury surface. The arc started and was maintained if the momentary electrical discharge was sent through the tube, provided that the applied potential difference was not less than 31 volts. When running at this voltage the potential difference between the terminals was 12 volts with 8·0 amperes. With 118 volts applied between the "arc" terminals the arc was struck at a gas-pressure of 1 mm. of mercury, but as the pressure decreased the arc could be started with a smaller applied potential difference. The vapour-pressure of the mercury at room-temperature is so low that the number of mercury vapour molecules present initially must be insufficient to carry the large currents indicated. The latter, at any rate initially, must be due to

the ionized residual gas, although as the arc is continued the mercury vapour-pressure increases and the radiation emitted is that characteristic of mercury. The following gives the arc current and the corresponding potential difference between the electrodes after the arc had been started—the applied potential difference being 112 volts:

Potential difference (volts)	42	30	28	23	22
Current (amperes)	2·4	6·1	7·0	11·8	12·2

The arc started more easily if the mercury electrode was made the negative one, but the polarity of the arc electrodes with respect to that of the electrical discharge had little effect.

In other experiments two pools of mercury—6 cm. apart—were used as the arc electrodes, and the arc could be struck and maintained when the momentary electrical discharge was sent through the tube. In this case the arc would just start with an applied potential difference of 70 volts, and one curious feature was that after the arc had been passing for some time the potential difference across the electrodes remained at 22 volts, although by altering the external resistance the current could be varied from 3 to 8 amperes. Sliding the wire rheostat contact and so rapidly varying the current within these limits appeared to have no effect—at any rate within one volt—on the potential difference between the mercury electrodes. This is an unexpected result, as the rapidity with which the current was varied insured that the temperature of the tube remained practically constant. Thus the effect was not due to change of the mercury vapour-pressure.

Spectrograms were taken of the radiation from the positive column of the arc by means of a constant deviation spectrometer, care being taken that the radiation from the immediate neighbourhood of the cathode or anode was *not* incident on the slit of the spectrometer. Two sets of spectrograms were photographed. In the first set the arc was momentarily started and stopped, and thus the temperature of the mercury was not allowed to increase to any extent. The arc was not passing for more than a fraction of a second, and time was allowed between these temporary discharges for the temperature to fall to that of the room. In the second set of spectrograms the exposure was made after the arc had been passing for some time. In this way it was expected that the first set would show the spectrum lines of the residual gas, and in the second set the predominant lines were expected to be those

of mercury. These expectations were realized as shown in spectrograms I. and II. (Pl. XVIII.). In I. the lines of the residual gases, nitrogen, hydrogen, carbon monoxide, etc., are present, as well as mercury lines; whereas in II. most of the former have disappeared owing to the increased mercury vapour-pressure.

Sodium.—With the sodium arc one of the electrodes was of iron and the other solid sodium in contact with an iron lead-in electrode—the distance between the two electrodes being 1·5 cm. The arc could be struck and maintained in the usual manner by passing the momentary electrical discharge, but in general the residual gas-pressure must be lower than in the case of mercury, and the arc operated most easily with the sodium forming the negative electrode. For an applied potential difference of 113 volts the following potentials across the "arc" electrodes were observed:

Potential difference (volts).....	16	13	11	10·5
Current (amperes)	3·2	4·0	5·0	6·8

After the arc had been passing for some considerable time, it was possible quickly to vary the current by altering the external resistance and obtain a steady and constant potential difference across the electrodes, *e. g.*, the potential difference remained at 10 volts while the current was varied rapidly between 3·4 and 8·0 amperes. The rapidity with which the current was changed insured that the heating effect varied little and the sodium vapour-pressure could not have altered to any appreciable extent. The colour of the emitted radiation varied, sometimes it was the characteristic D-line radiation and at other times green—a feature which has been noted previously when experimenting with sodium arc lamps. This green colour is due to the increased brightness of the subordinate series lines relative to the D-lines. The arc could not be started if the applied potential difference fell below 60 volts, although this value obviously depends upon the distance between the electrodes.

In a similar manner the arc could be struck and maintained between two sodium electrodes, solid sodium in contact with iron lead-in electrodes. The spectrograms of the radiation from the arc in this case showed that the residual gases, as well as the sodium vapour, were effective in maintaining the arc. This is particularly so when the arc is first started (spectrogram III., Pl. XVIII.) the H_α-line being prominent together with lines of the other gases remaining in the tube. After the arc has been maintained for some time the sodium

lines become more prominent and the lines of the residual gases get fainter (spectrogram IV., Pl. XVIII.) but do not entirely disappear. The temperature of the tube was not high and, except in the immediate neighbourhood of the cathode, the pressure of the sodium vapour could not have been much greater than that corresponding to room-temperature. Thus the sodium lines are not so predominant as would be expected, but by the application of heat to the tube the relative intensity of the D-line radiation was greatly enhanced.

Potassium.—Similar arcs could be produced by using either one iron electrode and one potassium metal electrode, or two electrodes both of potassium metal in contact with iron lead-in electrodes, but it was difficult to strike the arc if the applied potential difference was below 80 volts. With 110 volts applied, however, the arc could be started and maintained, provided that the residual gas-pressure was less than 10^{-1} mm. of mercury. The radiation had the characteristic violet colour of potassium for the most part, but sometimes the colour changed to green, yellow, or blue. The potassium evaporated fairly quickly from the cathode and deposited upon the surrounding colder parts of the tube, but the arc was found to provide an intense source of potassium light. Spectrograms indicate that the residual gases are even more effective in maintaining the arc than in the other cases, in spite of the fact that the vapour-pressure of potassium is greater than that of sodium at any given temperature. It has always been found difficult to obtain a bright source of potassium light, and the present method is by far the most successful one. In spectrogram VI. (Pl. XVIII.) the hydrogen lines are particularly prominent, even after the arc has been passing for some time and the vapour-pressure of the potassium is high. All the alkali metals contain much gas—particularly hydrogen,—and as the metal evaporates with the passage of the arc these gases are liberated.

Visual observation reveals a high luminosity on the surface of the cathode in all these arcs, giving the impression that the metal surface is at a high temperature, and observations of the spectrum in the visible region from the metallic cathode show a continuous spectrum upon which high intensity emission lines are superimposed. Stark * found that if the cathode spot in a mercury arc faced directly into the spectroscope a continuous spectrum was photographed, and a line spectrum when the slit was faced just outside the cathode spot.

* *Phys. Zeits.* v. p. 550 (1904).

Tanberg and Berkey *, investigating the temperature of the copper cathode in a vacuum arc, noted that the anode glow exists primarily in the residual gases of the arcing chamber and that the cathode vapour does not directly sustain the arc in the region next to the anode. The Brown-Boveri Company † has measured the temperature of the cathode spot in a mercury arc rectifier as being $2087 \pm 25°$ C. by an optical pyrometer, whereas Jones, Langmuir, and Mackay ‡ place the temperature of the cathode spot at 500° C. in a mercury arc.

The cold arc, however, when first started is not sustained by the metallic vapour arising from the cathode, but by the residual gases. The cathode is at room-temperature, and there is no cathode vapour beyond that existing at the appropriate temperature. The momentary electrical discharge produces ions, and after this discharge has ceased the ions must acquire their high velocity within the cathode region, although the density of the gas molecules within the tube, in order to account for the high values of the current, would appear to be greater than that existing under the conditions of the experiments. Any complete theory of the arc must take into account the phenomenon of this cold arc.

LXXVII. *A Spectroscopic Investigation of some Metal Electrodes in Vacuum Arcs.* *By* F. H. Newman, *D.Sc., A.R.C.S., Professor of Physics, University College, Exeter* §.

[Plate XIX.]

1. *Introduction.*

THE potential fall along an arc, measured from the anode to the cathode, is usually composed of three parts, namely: (1) the anode fall at the surface of the positive electrode, (2) the fall in potential along the arc proper or, as it is sometimes named, the positive column, and (3) the cathode fall very close to the negative electrode surface. Thus the potential at any point at a given

* Phys. Rev. xxxviii. p. 296 (1931).
† Brown Boveri Mitteilungen, 16, p. 61 (1929).
‡ Phys. Rev. xxx. p. 201 (1927).
§ Communicated by the Author.

distance from the cathode is composed of that part of the positive column fall between the point in question and the cathode.

Now an arc is differentiated from a glow discharge primarily by the current density at the cathode and the magnitude of the cathode fall. Whereas in a glow discharge the current density at the cathode is normally a small fraction of an ampere per square centimetre, and the cathode fall is usually greater than 100 volts, in an arc the current density at that portion of the cathode which is carrying the current is of the order of hundreds or thousands of amperes per square centimetre. Moreover, the cathode fall is generally of the order of 10 volts. From these facts it is concluded that in the case of a glow discharge most of the current at the cathode is carried by positive ions and only a small percentage by free electrons leaving the cathode; but, on the other hand, in the arc the current is carried primarily by free electrons leaving the cathode and a smaller amount by the positive ions striking the cathode.

Recently the mechanism of the arc has attracted a great deal of attention. This is due to the fact that the theory of thermionic emission from the cathode hot spot is not adequate to explain certain types of arcs, viz., those known as "cold arcs." Langmuir * has suggested that in these the positive space charge, causing the cathode fall, may exert a strong enough electric field at the surface of the cathode to cause a large "field current" from the cathode, even though the latter may be too cool to emit thermions. Many other investigators † have developed this idea, and from energy consideration have shown that in the mercury arc, for example, the electrons emanating from the cathode are due primarily to a high electric field and not to thermal emission. Millikan and Eyring ‡ found that these "field currents," studied in the pulling of electrons out of cold metals, consist of electrons which escape only from isolated points on the surface where the work function has been enormously reduced by

* Gen. Elec. Rev. xxvi. p. 735 (1923).

† Compton, Journ. A. I. E. E. xlvi. p. 1192 (1927); Mackeown, Phys. Rev. xxxiv. p. 611 (1929); Lamar and Compton, Phys. Rev. xxxvii. p. 1069 (1931).

‡ Phys. Rev. xxvii. p. 51 (1926).

microscopic geometrical roughness or chemical impurities or both. Evidence deduced by Stern, Gossling, and Fowler * from cold cathode currents drawn from small wires also seems to show that the current densities are extremely high, though the emitting areas are very small.

The cathode fall of potential in various arcs has been measured by different investigators. Thus Killian † found that the drop in potential from the cathode of a mercury arc to a point distant 0·2 cm. from its surface was 10·1 volts, and increased regularly to 11·6 volts as the distance was increased to 3·0 cm. The value of about 10 volts, as extrapolated to the cathode surface, has been taken as significant of the ionizing potential of mercury within the limits of the uncertainty, set by the small unknown contact potential difference between the cathode and the probe which measures the potential. In these experiments the distances were measured from the cathode surface, but they do not represent true distances from the cathode spot, since it wandered rapidly and erratically all over the cathode surface. Lamar and Compton ‡, making corrections for contact potential difference, find the cathode drop to be 9·9 volts.

Nottingham § has also obtained interesting results. With the cadmium arc in argon at atmospheric pressure the cathode fall was equal to, or very slightly greater than, the ionization potential of cadmium, which is 8·9 volts. The anode fall was of the order of one volt. Measurements of the thallium arc in argon showed that the cathode fall was approximately equal to the ionization potential of thallium, viz., 6·08 volts. With carbon there was a cathode fall of about 5·0 volts which agrees with the experimental value 4·4 volts of the ionization potential of the cyanogen molecule. Thus we may say, in general that the cathode fall is equal to, or slightly greater than, the ionization potential of the gas actively involved. On the other hand, Nottingham found that the potential drop in the immediate neighbourhood of a copper arc was very close to 20·5 volts. This

* Proc. Roy. Soc. cxxiv. p. 699 (1929).
† Phys. Rev. xxxi. p. 1122 (1928).
‡ *Loc. cit.*
§ Journ. Franklin Inst. ccvi. p. 43 (1928) ; ccvii. p. 299 (1929).

observation was corroborated spectroscopically by the fact that the entire spark spectrum of copper could be observed at the surface of the cathode in the normal copper arc, if the image of the arc was carefully focussed on the slit of a spectroscope. Hagenbach * also observed this spectrum. In this case, therefore, we have a cathode fall exactly equal to the second ionization potential of the copper atom of 20·5 volts †, *i. e.*, the potential required to remove an electron from a singly-charged copper ion. In the case of the " hissing arc " the cathode fall was 14·0 volts, and if this is to correspond to the ionization of the active vapour, it must be associated with that of copper oxide, CuO_2, for it is much too high to correspond to the first ionization potential of copper, which is 7·7 volts. The anode fall was between 7 and 8 volts.

The temperature of the cathode spot of the mercury arc has been variously estimated from 600° K. to 2000° K. From Stark's ‡ observation of a continuous spectrum at the cathode, early investigators assumed the cathode temperature to be about 2000° K. As pointed out by Compton §, the continuous spectrum may arise from other sources. A spectroscopic investigation of various parts of an arc is likely to provide, however, interesting information regarding the processes that occur therein.

2. *Experimental.*

Before proceeding further it will be useful to give a nomenclature of the vacuum arc which will be followed throughout the paper. The cathode spot is a brilliant localized small area on the surface of the cathode metal and, unfortunately, moves erratically over the cathode surface. This movement interferes with the study of the conditions near the cathode (*e. g.*, potential distribution, electron density, and velocity). Adjacent to the cathode is the cathode glow, followed by a dark space and then the anode glow. When the arc is short the cathode and anode glows adjoin, the dark space disappearing.

* *Phys. Zeits.* xii. p. 1015 (1911).
† See Shenstone, Phys. Rev. xxix. p. 380 (1927).
‡ *Phys. Zeits.* v. pp. 51, 750 (1904).
§ Trans. A. I. E. E. xlvi. p. 868 (1927).

The author * has previously described a method of starting and maintaining a " cold arc " with different electrodes, and the same method was employed in the present work. The metallic electrodes used were mercury, potassium, and sodium. In order to photograph the spectra of the radiation at different parts of the arc, the light from the latter was passed through a lens and two right-angle prisms, and adjusted to form an image of the arc on the slit of a constant deviation spectrometer. The axis of the image was turned into the horizontal position by prisms, so that the light which passed through the slit of the spectrometer all came from the small cylinder in the arc column, bounded by two planes passed perpendicularly to the width of the slit of the spectrometer. In this manner it was possible to photograph the spectra of the cathode hot spot, the cathode glow, and the anode glow.

Iron anodes were used in all experiments, and the gas in the discharge-vessel was maintained below a pressure of 0·1 mm. of mercury by means of a Cenco Hyvac pump working continuously. Exact measurements of the gas pressure were not easily obtained, but in general it was approximately 10^{-2} mm. of mercury, gas (chiefly hydrogen) being continuously evolved from the different electrodes. For this reason no special gases were introduced into the arc tube, so that those present were the usual ones to be found in any electrical discharge-tube which has been exhausted to a low pressure, viz., hydrogen, nitrogen, carbon monoxide, and carbon dioxide.

Before any spectrogram was photographed the cathode metal was allowed to assume room temperature and then a momentary electrical discharge was passed, a potential difference of 100 volts (D.C.) being applied between the arc electrodes. The arc started immediately, and in photographing the radiations an exposure of three seconds was given in all cases after the arc had started. Thus we may assume that the temperature and pressure conditions within the arc vessel were similar for the various exposures. A resistance in the arc circuit maintained the arc current at any desired value.

* Phil Mag. xi. p. 796 (1926).

3. *Experimental Results.*

With the three cathode metals investigated—mercury, sodium, and potassium, the characteristic bright cathode spot was observed in each case, and, as the spectrograms show, it is from this spot that most of the characteristic luminosity comes. With sodium the spot did not move so erratically as in the case of mercury. Another interesting feature noted was that, in addition to the arc lines of the cathode metal, hydrogen lines were particularly prominent in the cathode glow. In the anode glow the hydrogen lines were much less prominent, while in the radiation from the cathode spot the only lines visible were the arc lines of the cathode metal. This is to be expected, since the temperature of the spot, although lower than that previously assumed, is sufficiently great to give a comparatively high vapour pressure of the more volatile metals in its immediate vicinity. These facts apply to all three metals investigated, but particularly to sodium and potassium. The spectrograms of the sodium arc are shown in Pl. XIX., an examination of which indicates the relative brightness of H_α and H_β compared with the subordinate series lines of sodium in the cathode glow, whereas in the anode glow the reverse is true, the hydrogen lines being extremely faint. In the radiation from the cathode spot the hydrogen lines are missing, but several members of the subordinate series of sodium can be distinguished. Another interesting feature of the last spectrogram is the absence of any continuous spectrum, so in this case, at any rate, the temperature must be comparatively low with no indication of an incandescence state. In addition to the Balmer lines in the cathode glow there are many lines belonging to the secondary spectrum of hydrogen. Mercury lines are also present, the mercury vapour coming from the gauge.

These results indicate that the cathode vapour, under the conditions of the experiments, does not entirely sustain the cathode arc near the cathode region except at the cathode spot, so it is evident that this spot is all-important in the theory of the arc. The cathode fall for mercury has already been measured by different investigators, but preliminary attempts by the author

to measure it for sodium and potassium have not yet been successful. If the values for other metals, however, are any guide, it seems that the value for sodium should be in the neighbourhood of 5·1 volts, the ionization potential of this element. The potential difference across the sodium arc in the above experiments was round about 10 volts, and it was found that the current could be rapidly varied between 3 and 8 amperes without any measurable change in this voltage—at least to within 0·1 volt— although the intensity of the light increased with the current. Thus we may assume that the positive ion current increases as the current increases, and this suggests an apparent increase in the efficiency of the ionization process with current. Such an increase might arise because the cross-section of the arc stream is proportional to the current passing, and this may explain the fact that the voltage across the electrodes remains constant as the current is varied.

Currents of the order used in these experiments, 4–10 amperes, do not seem sufficiently large to provide the high cathode current density, viz., 1000 amperes per square centimetre, required if the "strong field" theory of the cold cathode is to hold, but the actual size of the cathode spot is unknown and cannot be estimated with any degree of accuracy from photographs. Mackeown * found that the electric field at which current begins to appear from a cold tungsten wire in a vacuum is variable, being very much lower for the case of a surface contaminated by impurities than for a clean surface that has been conditioned. Moreover, the current increases extremely rapidly as the field is increased beyond that necessary to produce the first perceptible current. Evidence deduced by Stern, Gossling, and Fowler † also shows that the current densities are extremely high, though the emitting areas are very small. Whether the same conditions result in the case of the arc is, of course, uncertain ; even if they do, the emitting spots may be so small, and so scattered about, that a very large gross positive ion current will be needed to maintain a high average field. In any case,

* Phys. Rev. xxxiv. p. 611 (1929).
† *Loc. cit.*

the total positive ion current required for an arc in which electrons are pulled out by a high field is at least as large as that required for an arc in which electrons are emitted thermionically from a cathode maintained at a high temperature ; quite possibly the positive ion current must be much larger for the " high field " arc.

Now although the cathode fall at the sodium electrode is unknown, it must be less than 10 volts and is probably in the neighbourhood of 5 volts. The anode fall, also unknown, is likely to be still smaller. In spite of these low potential falls hydrogen lines appear in the spectrograms. The ionization potential of the hydrogen atom is 13·5 volts and that of the hydrogen molecule still higher, viz., 16·2 volts, both greater than the total potential difference between the electrodes, so it is evident that an electron emerging from the cathode fall of this arc cannot have an energy equal to, or greater than, the ionizing potential of hydrogen. The hydrogen ions must be produced in some other manner as, for example, by a cumulative process. The ionization is probably caused in two stages, the electron energy being very close to the value necessary to produce metastable atoms and to ionize them when formed. We know that, unlike ionization by a single impact, these processes have a high probability when the energy of the impacting electron is only slightly in excess of the minimum energy required for the process. But experiments with low voltage arcs have proved that the favourable conditions for arcs to operate by such cumulative ionization are large current density and vapour-pressure of at least the order of 1 mm. of mercury. It would seem at first sight that this pressure is far beyond that of the hydrogen gas present in the arc, but hydrogen is nearly always occluded in metals, and makes its appearance when the pressure is lowered, particularly if any type of electrical discharge is passing. Thus in the present experiments we should expect this gas to be emitted from the cathode, and its partial pressure at the place of emission may well have a value consistent with the results obtained.

In conclusion, it was found that the rate of evaporation of the cathode metal was small, and this fact, together with the presence of the hydrogen lines, supports the " high field " theory of cold cathode arcs.

LXXVIII. *Notices respecting New Books.*

Recent Advances in Physics (Non-atomic). By F. H. Newman. [Pp. 378+57 illustrations.] (J. & A. Churchill. Price 15*s.*)

THE title of this useful book is misleading in the sense that a considerable part of it is in the true sense "atomic"—but that is a small and unimportant criticism.

Opening with a brief and very slight sketch of the wave nature of matter in the light of recent work, statistical mechanics is next given a chapter of some thirty pages. In this chapter summaries are given of a number of the better known applications of statistical theory—for example, the electron theory of metals (Fermi-Dirac), susceptibility of metals, contact potential difference, thermionics.

A chapter on general properties of matter embraces naturally a pretty wide range of topics, including, of course, High pressure effects, High vacua, Surface tension, and Viscosity.

Acoustics is given a chapter to itself—and deserves it, in view of the rapid extension of our knowledge in this interesting field recently.

In a long chapter on Electromagnetic Radiations such diverse (non-atomic!) topics are dealt with as the Ionization of the Upper Atmosphere, Infra-red Spectra, the Raman Effect, X-rays in refraction and scattering, and Cosmic Rays: a formidable list to dismiss so successfully in less than eighty pages.

Magnetism receives fair attention in a relatively long and coherent chapter, while under the head of Electricity a last chapter deals in a general manner amongst other things with Atmospheric Electricity, Ions and Electrolysis, and Super-conductivity.

In a book which covers such wide fields in so small a compass it should not really be inevitable that references to early pioneer work should often be absent—but no doubt the author, giving as he does Bibliographies at the end of each chapter, may expect the reader himself to repair such deficiencies.

The author in his preface states: "As the literature has been freely utilised, it is hoped that adequate credit has been accorded at the appropriate places in the text." It seems, nevertheless, rather a pity to the reviewer that the acknowledged means of indicating more precisely the source of tables and diagrams in particular have not been more fully used.

The book is printed and generally got up in excellent style, and should serve a useful purpose.

Photoelectric Phenomena. By A. Ll. Hughes and L. A. DuBridge. [Pp. xii+531, many figures in text.] (McGraw-Hill Publishing Company, Ltd. Price $5.)

A new book on Photoelectricity was badly needed in view of the very rapid rate of growth of our knowledge of this subject within

the last few years, and it is gratifying to see that one. The aim of this book is well set out in the preface, and, like all books of its kind, the intention is to provide a pretty complete summary of experimental methods and results—together with the associated theories,—the whole being coherent and plentifully supplied with the appropriate references. In this particular book it is realized that it may "serve as a guide to the fundamental physical principles which underlie the engineering and commercial applications."

After a short introductory chapter of a few pages the authors plunge at once into their subject by dealing with the fundamental laws of photoelectricity, the threshold, and the energy of photoelectrons. There is then a useful chapter on Theories of Photoelectric emission, in which the theories associated with the names of Einstein, Thomson, Richardson, Sommerfeld, Fermi-Dirac, Wentzel, Fowler, and others are associated. Although the authors hesitated, apparently, to include this chapter, it is a most important and very useful part of their concerted effort, and the book would have been much less valuable had it been omitted.

Chapters follow on Ionization of Gases by Ultraviolet Light, Photoconductivity, Photoelectric Effects of X-rays, and then a particularly valuable one on Photoelectric Technique. Few authors are more competent to deal with this topic than Messrs. Hughes and DuBridge, and they have risen to the occasion with real success.

Chapters dealing with photoelectric technique and applications seem a little strange in their simplicity after the complexities of the preceding chapters, but they are not really so out of place as might at first sight appear.

The name and subject indexes are well done, and the general appearance of the book is of a high standard.

OBITUARY NOTICE.

Mr. William Francis, who for nearly forty years was closely associated with the fortunes of the 'Philosophical Magazine,' died at his home in Eastbourne on Tuesday, August 16. The elder son of Dr. William Francis, he was born at Richmond on November 29, 1863, and on account of delicate health received his early education from a tutor. He entered King's College, London, October 1892, in preparation for the Science degree of the London University, but was not able to complete his course of studies, his services being required on the staff in Red Lion Court.

From 1894 to the beginning of 1904, when his father died, William Francis rendered valuable assistance in the conduct of this Journal. His name first appeared on the cover of the 'Philosophical Magazine' twenty-eight years ago. During the seven years from 1904 to 1911 Dr. Joly and he were the only editors: on the appearance of the twenty-first volume of the Sixth Series, in 1911, the names of Sir Oliver Lodge, Sir J. J. Thomson, and Prof. Carey Foster were added. Perhaps the most important and valuable piece of work in connexion with the 'Philosophical Magazine' for which William Francis was solely responsible was the compilation of the Author Index to the complete Sixth Series, 1901–1925, with an Appendix for the years 1926–1930 of the Seventh Series, where references are given to more than five thousand papers which had been contributed during those thirty years. He was a very old member of the Physical and Linnean Societies, and continued to take a keen interest in the advances of modern science.

For the greater part of his life Mr. Francis had been a sufferer from asthma, and during the last four or five years he suffered from attacks of bronchitis and heart trouble which confined him to his home for weeks together. A year ago he was obliged to go into a nursing home for an operation: although confined to bed from that time, he bore his painful illness with calmness and fortitude, and often recalled his happy association with the members of the staff of the 'Philosopical Magazine.' Men of science from all parts of the world who visited him in Red Lion Court will remember his kindly courtesy and gracious character. To those who knew him well his loss is deeply regretted; his personal integrity and straightforward character endeared him to his friends, and to them he leaves the stimulating memory of a disinterested and unselfish life.

[*The Editors do not hold themselves responsible for the views expressed by their correspondents.*]

Falling-plate photograph of the oscillatory discharge, illustrating its instantaneous and intermittent character.

Fig. 1.

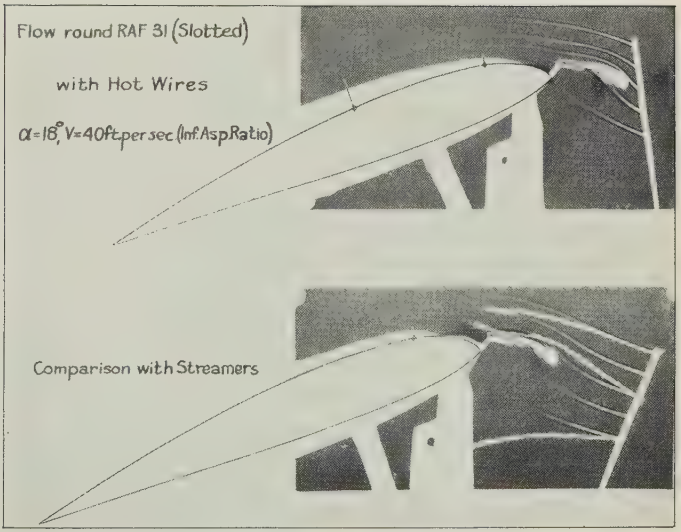

Flow round slotted aerofoil obtained with hot wires.

FIG. 2 (*a*).

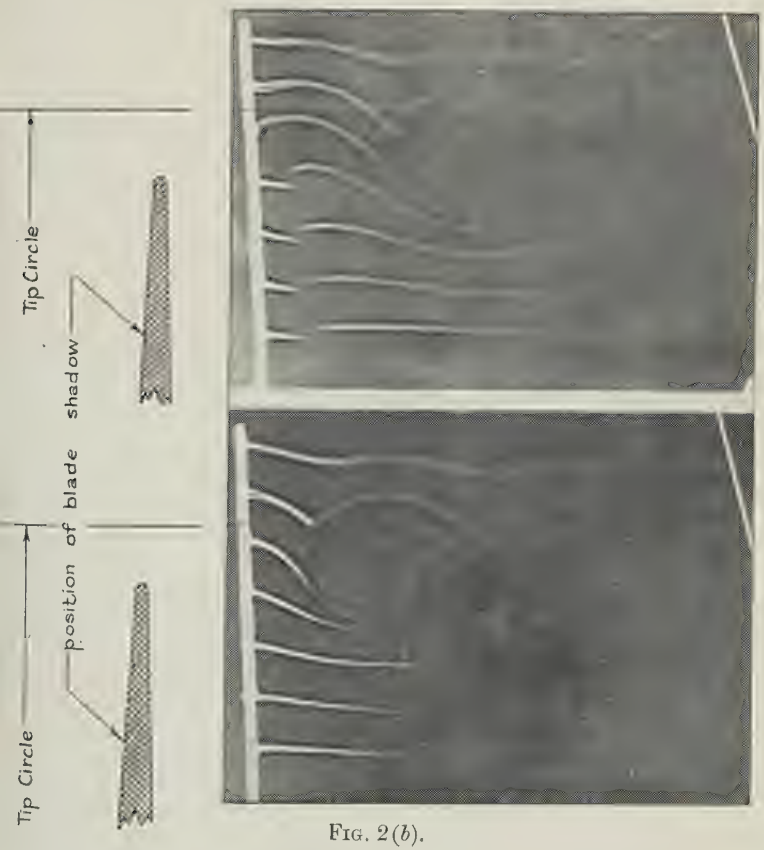

FIG. 2 (*b*).

Hot Wire Shadowgraphs of Flow behind Air-screw.

Figs. (*a*) and (*b*) differ in phase by 45°
Wind speed, V = 14·5 ft. per second.
Rotational speed of screw, $n = 24$ revs. per second.

$$\frac{V}{nD} = 0{\cdot}37.$$

Fig. 3 (*a*).

Photographs of sparks with 2, 3, and 5 mauve flames. Approximately 1 second exposure; frequency of sparks approx. 600 per second.

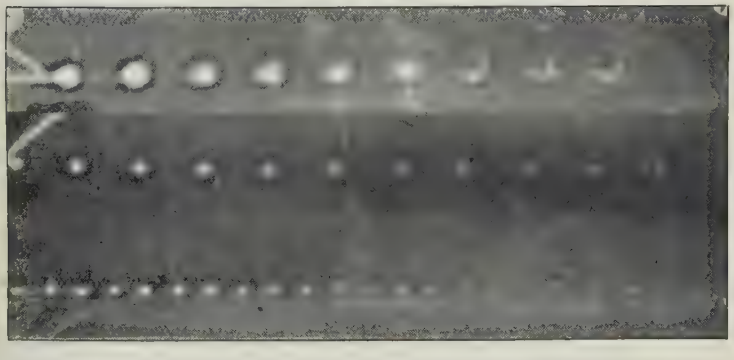

Fig. 3 (*b*).

Fig. 3 (*c*).

Fig. 3 (*a*).

Shadowgraphs of spark streams.

(*b*) and (*c*). Spark frequency about 650 per sec. Air speed V = 26 ft./sec.
(*d*). Spark frequency about 1300 per sec. One spark per $\frac{1}{2}$ cycle A.C.

Fig. 4.

Four spark gaps in parallel. Spark frequency about 600 per second.

Fig. 5 (*a*).

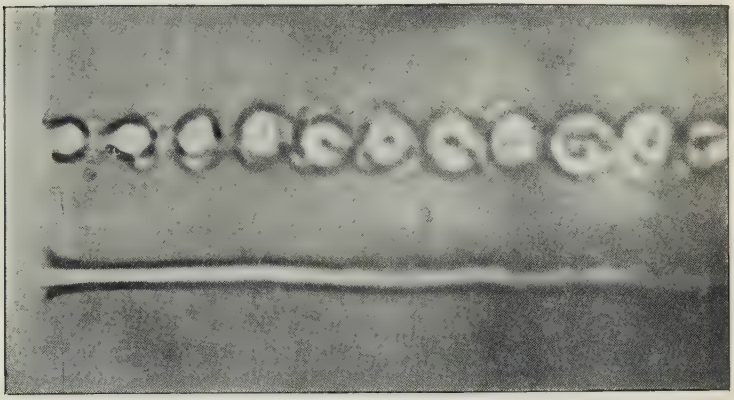

Flow in 14″ jet used for air-screw tests with sparks.
Above: Spark shadow.
Below: Hot wire shadow.
Wind speed V=12·6 ft. per sec.

Fig. 5 (*b*).

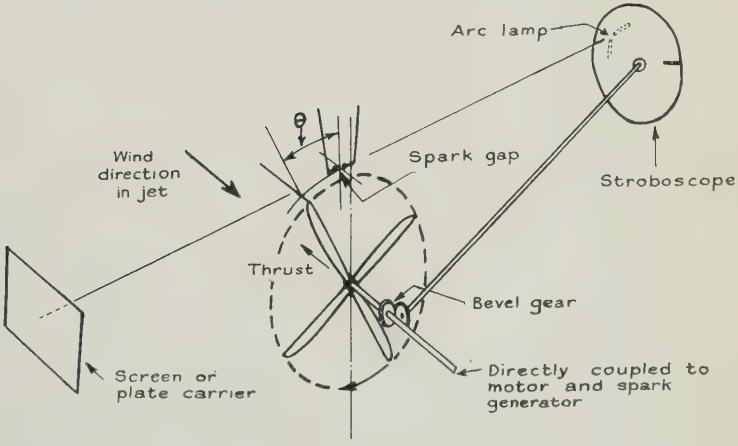

Spark shadows behind air-screw.

Sketch of apparatus, showing position of spark gap relative to the screw.

Fig. 6 (*a*).

Tip vortex just forming after the blade has cut across the spark-stream.

Fig. 6 (*b*).

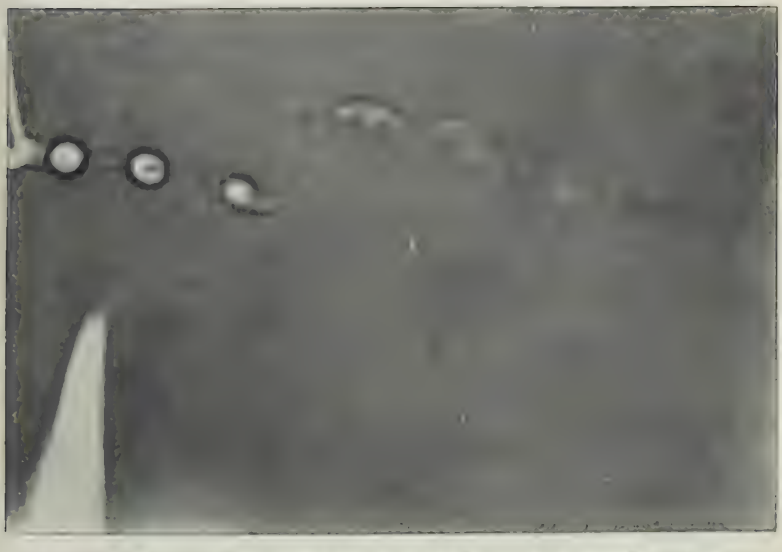

Appearance of tip vortex when blade has advanced about 30° further on.

Spark shadows behind air-screw.

Frequency of sparks 500 per second.
V = 13·5 ft./sec. Rotational speed 25 revs./sec.

Fig. 7 (a).

Flow near boundary of slip-stream ; $\theta = 45°$.

Fig. 7 (b).

Flow near boundary of slip-stream ; $\theta = 30°$.

Spark shadows behind air-screw.
Exposure 1/6000 second.

Fig. 8 (*a*).

Flow near boundary of slip-stream ; $\theta = 3^{\circ}$.

Fig. 8 (*b*).

Flow near boundary of slip-stream ; $\theta = 2^{\circ}$.

Comparison between records of hot wire and spark shadows.
Exposure 1/6000 second.

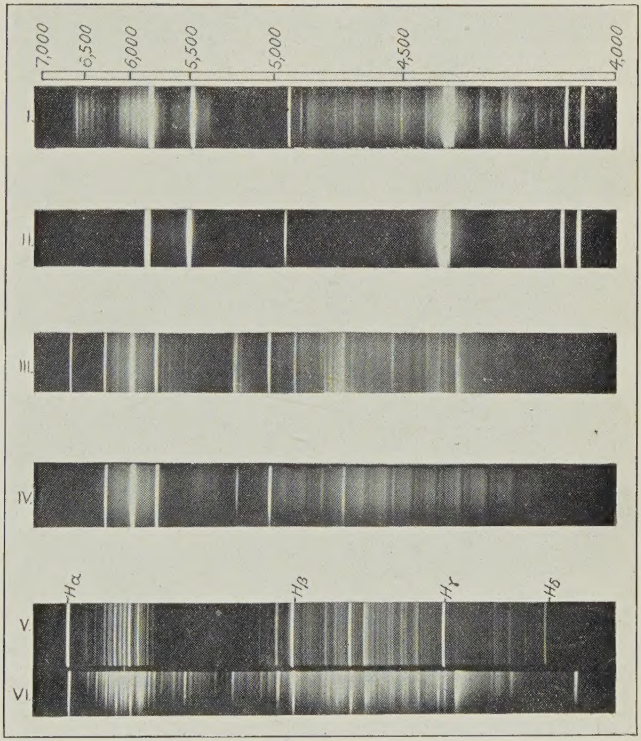

Spectra of Arc between different Metallic Electrodes.

I. Mercury. Arc started.
II. Mercury. Arc passing for some time.
III. Sodium. Arc started.
IV. Sodium. Arc passing for some time.
V. Hydrogen. Electrical discharge.
VI. Potassium. Arc.

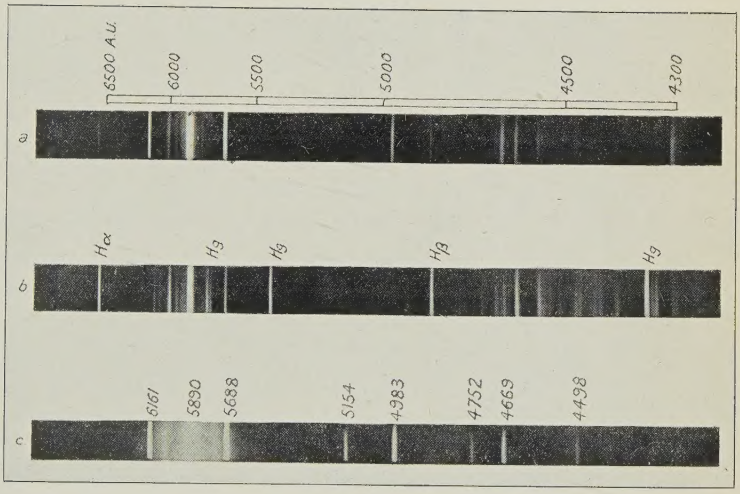

The sodium arc.
a. Anode glow.
b. Cathode glow.
c. Cathode spot.